Hydrogeological modeling of Northern Ireland drumlins in three dimensions

A Thesis

Submitted to the College of Graduate Studies and Research

In Partial Fulfillment of the Requirements

for the

Degree of Master of Science

in the Department of Civil Engineering

University of Saskatchewan

Saskatoon

by

Keely Kulpa

PERMISSION TO USE

The author has agreed that the library, University of Saskatchewan, may make this thesis freely available for inspection. Moreover, the author has agreed that permission for extensive copying of this thesis for scholarly purposes may be granted by professors who supervised the thesis work recorded herein or, in their absence, by the head of the Department or the Dean of the College in which the thesis work was done. It is understood that due recognition will be given to the author of this thesis and to the University of Saskatchewan in any use of the material in this thesis. Copying or publication or any other use of the thesis for financial gain without approval by the University of Saskatchewan and the author's written permission is prohibited.

Requests for permission to copy or to make any other use of material in this thesis in whole or part should be addressed to:

Head of Department of Civil Engineering

University of Saskatchewan

Engineering Building

57 Campus Drive

Saskatoon, Saskatchewan

Canada, S7N 5A9

ABSTRACT

The need to renew and expand civil infrastructure, combined with an increased acknowledgement of a changing climate, has highlighted the need to incorporate the influence of climatic factors into the design of infrastructure. In geotechnical engineering, this includes understanding how climate influences the performance of slopes associated with engineered cuttings in pre- existing natural landforms. This understanding extends to both hydrological and hydrogeological conditions, both of which are often analyzed using numerical modeling of surface water and groundwater.

Climate change predictions for Northern Ireland indicate that the amount and intensity of rainfall and extreme weather events will increase. This has raised concerns regarding the stability of existing engineered cut-slopes and the design of future highway and railway infrastructure. Recent studies have indicated that there is a link between pore pressure cycles and softening of slope structures, especially in clay rich materials typical of glacial till drumlins in Northern Ireland. These pore pressure fluctuations are caused by seasonal changes in the rate of recharge which then propagate through the deeper hydrogeologic system. As a consequence, the design of these cuttings requires that the hydrogeological response of these landforms to seasonal climate variations be incorporated into geotechnical designs.

Two dimensional hydrogeological simulations are typically used in engineering practice. The main objective of this study was to evaluate the sensitivity of these simulations to dimensionality (two- and three-dimensions). The primary focus was on steady state groundwater flow within two drumlins with large slope cuts. Two- and three-dimensional groundwater models were developed using available information for a highway and a railway study site. The performance of each of these models was then compared to field monitoring from each site. A series of sensitivity studies were undertaken to evaluate the influence of key material properties and boundary conditions.

Estimated recharge rates were found to range from 21 to 31 mm year^{-1} for both the railway (Craigmore) and highway (Loughbrickland) study sites. The hydraulic head distribution at the Craigmore site was similar for both dimensional simulations with a "best-fit" recharge rate of 50 to 60 mm year^{-1}. At the Loughbrickland site, similar hydraulic head distributions with the "best-fit" recharge rate of 80 mm year^{-1} were reached in both dimensions.

Overall, the research completed here emphasized the importance of gathering appropriate data prior to conducting development of hydrogeological models. As more data is made available, the overall complexity of the system can be better understood. As the complexity of the problem increases, the requirements for understanding the hydrogeological system in all three-dimensions becomes more important.

ACKNOWLEDGEMENTS

There are many people that I would like to acknowledge and thank for the completion of this research. My supervisor Dr. S. Lee Barbour has been a large help in guiding me and helping me at times of difficulty in the research. I'd also like to thank Dr. David Hughes, Michael McLernon, Claire McLernon and Laura Carse for all of their help in Belfast, Northern Ireland. Michael and Laura were especially helping in the field and the laboratory, as well as continuing the field monitoring while I was back at the University of Saskatchewan completing course work. Thank you to O'Kane Consultants and the Natural Sciences and Engineering Council of Research Canada (NSERC) for their funding and for the training to allow me to complete my research.

Lastly, thank you to my very supportive and understanding family. My family was always there to help me and encourage me to complete my research. To my husband, Justin, for making sure I was motivated to finish even when it felt like the end was never going to come!

TABLE OF CONTENTS

LIST OF TABLES

LIST OF FIGURES

1.0 INTRODUCTION

It is becoming increasingly important to incorporate the potential impact of climate cycles into the design of civil infrastructure. In the case of geotechnical engineering, this requires an evaluation of the impact of changing climatic conditions on hydrological and hydrogeological conditions. In many cases, these evaluations are facilitated through the application of numerical models of the surface and groundwater hydrology.

According to current climate change predictions developed by the Scotland and Northern Ireland Forum for Environmental Research (2002), Northern Ireland will undergo an increase in the level and intensity of rainfall and extreme weather events. Clay rich soils in Northern Ireland often undergo rapid rises in the water table and the development of saturated conditions during heavy rainfall. Thus, the stability and serviceability of geotechnical infrastructure, including road and railway embankments and cuttings, is currently being re-evaluated in light of this climate change. Areas of particular concern have been engineered cuttings in clay slopes, including glacial till drumlins, where studies of long-term stability have been undertaken to identify potential mechanisms causing instability as a result of climate change (Dixon and Brook, 2007).

Many of these studies have shown that there is a relationship between the stability of a slope and pore pressure fluctuations arising from seasonal climate cycles. This is particularly true for soils with a high percentage of clay materials (Hughes et al., 2007). The pore-pressure cycles appear to result in strain softening (i.e. weakening) of the soil which leads to instability (Ng and Shi, 1998, Picarelli et al., 2004, Potts et al., 1997 and Davies et al., 2008). An understanding of the magnitude and frequency of fluctuations in pore water pressure are required to accurately evaluate factors of safety against slope instability (Smethurst et. al., 2006).

The transient, hydrogeological flow systems associated with these pore-pressure fluctuations can be simulated with existing numerical models. One- or two-dimensional models are most commonly used to simulate the water flow dynamics within the soil in response to climatic conditions. However, glacial till drumlins are inherently three- dimensional structures due to their genesis and geometry. This three-dimensionality is often further complicated by the

geometry of the underlying bedrock geology and the orientation of the cut slope. As a result, it is not evident whether a simpler two- dimensional representation of the flow system is sufficient to capture these pore- pressure transients within glacial till drumlins or if more complex three-dimensional modeling is required. In conventional practice, these analyses have been undertaken only in two-dimensions.

Previous studies have attempted to evaluate how the inclusion of the third dimension influences simulations of groundwater flow and whether the increased cost and effort to characterize and simulate three-dimensional flow systems is warranted (Freeze, 1971, Segol, 1977, Frind and Verge, 1978), etc.). Freeze (1971) was one of the first to publish a three-dimensional, transient, finite-difference model for variably saturated conditions and a heterogeneous aquifer. Other studies have been completed to determine the importance of this third dimension, including work completed by Segol (1977), Frind and Verge (1978), Reissenauer et al. (1982) and Davis and Segol (1985). These have included research conducted using both the finite-difference and the finite- element methods (Huyakorn et al., 1986). More research has also been conducted to link the importance of the third dimension to slope stability analysis, such as Leach and Herbert (1982), Lam and Fredlund (1993), Griffiths and Marquez (2007) and Xie et al. (2006). This link will not be studied within this thesis, but should be considered as a next step in analyzing the effect of the third dimension on stability modeling.

1.1 Research Objectives

The overall goal of this thesis is to determine the influence of dimensionality (two- or three-dimensions) on steady state simulations of groundwater flow through glacial till drumlins in Northern Ireland which have been altered by the construction of a cut slope. This research will be undertaken by:

- developing two- and three-dimensional hydrogeological models that are based on field studies completed on site;
- comparing the performance of the two- and three-dimensional simulations to field observations at each site; and

- comparing the responses of the three-dimensional simulations in sensitivity studies of material properties and recharge rates.

The hydrogeological systems will be simulated under steady-state flow conditions. The transient conditions were considered out of scope of this research.

Two- and three-dimensional, steady-state flow models have been developed based on field characterization and are calibrated to monitoring data captured at the two field sites. The flow systems are compared in terms of the distribution of head (or pressure) and the water flow (recharge) through the drumlin as simulated using each model. A comparison between each simulation will consider water movement within the drumlin system as it relates to hydrogeology (i.e. pore pressure dynamics and water table fluctuations). Once developed, these models can then be utilized to evaluate difference in pore-pressure dynamics associated with seasonal changes in water balance.

By gaining an understanding of the hydrogeological response of drumlins and slopes to climate patterns, geotechnical engineers can more reliably undertake risk-based assessments of the performance and long term maintenance needs of these slopes. This understanding is important to engineers worldwide, as there is a potential danger to public safety, as well as an increasing cost to repair and replace roads and railways, where these failures occur.

2.0 LITERATURE REVIEW

A numerical hydrogeological model is a conceptual model that has been parameterized with the appropriate properties, boundary conditions and initial conditions (Fetter, 2001). Conceptual frameworks for groundwater flow systems have been discussed by Winter (2001) and Devito et al. (2005) in the context of Hydrological Landscape Units (HLU). These conceptual frameworks present a hierarchy of factors (Figure 2.1) that help characterize a landscape hydrogeologically. The fully characterized HLU can then be used to interpret hydrological processes that generally occur within similar HLUs or may be unique for a specific landscape (Winter, 2001).

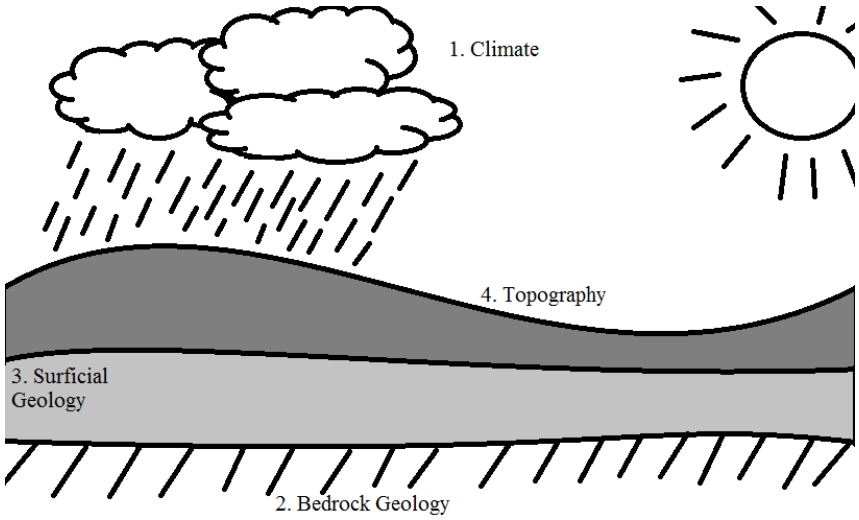

Figure 2.1 Factors used to characterize a hydrogeological landscape.

One of the primary factors in this hierarchy is the control that climate exerts at a regional scale encompassing the HLU, as well as at a local scale directly linked to the HLU itself. This factor includes the regional precipitation and evapotranspiration for that region, which define the limits or constraints of the water balance that are placed on the HLU and vadose zone. This water balance also has an impact on the overall water storage within the vadose zone and the potential for the growth of various vegetation types. The dominant direction of groundwater flow can also be influenced by climatic variations and stresses that might take place on the HLU, along with other influencing factors (Devito et al., 2005).

A second factor in developing a conceptual model of an HLU is the geology of the site. By understanding the hydraulic characteristics of the soil layers and bedrock, such as the hydraulic conductivity and lithology, the regional hydrogeological structure can be determined. This factor can have an impact on the regional, intermediate and local groundwater flow systems that may be present in the HLU, as well as the water table configuration. Differences between bedrock geology on a broad scale should also be understood, so that interactions or relationships between different geological structures can be considered (Devito et al., 2005).

Variations in the surficial geology are also important to include in the conceptual framework. The heterogeneity, lithology, structure, soil depth, texture and overall hydraulic properties are all factors that have an impact on the overall hydrogeological system. These factors vary across the local to regional scale and should be determined for each bedrock geological unit and HLU. These factors will have an impact on the location of recharge and discharge zones, as well as overall rates of infiltration and water storage in the vadose zone (Devito et al., 2005).

One of the most obvious factors on the definition of HLUs is topography. The topographical controls on groundwater flow have been studied for many years, including research conducted by Hubbert (1940), Toth (1963), Freeze and Witherspoon (1967), Haitjema and Mitchell-Bruker (2005), Glesson and Manning (2008) and Gleeson et al. (2011). This factor has an impact on the distribution of recharge and discharge areas, as well as the rates and direction of flow across the HLU and overall landscape (Devito et al., 2005).

This hierarchy of factors will be presented with particular reference to Northern Ireland on a regional scale and County Down on a more local scale. The climatic controls will be described, with information regarding average precipitation and evapotranspiration. The overall bedrock geology will be discussed and associated hydraulic properties found in previous research will be presented. The surficial geology will also be introduced, along with the overall hydraulic properties and origin of the typical geological structures found in Northern Ireland. A brief review of previous studies into the effect of dimensionality on hydrogeological and slope stability modeling will also be provided to give context to the present work.

2.1 Irish Climate

Northern Ireland has a temperate maritime climate, due to its proximity to the Atlantic Ocean, with an average annual evapotranspiration 400 to 500 mm $year^{-1}$ (Fitzsimmons and Misstear, 2006). The average temperature for Northern Ireland ranges from 5.2°C to 10.0°C depending on the altitude and proximity to the sea to the area of study (Figure 2.2). In the area of specific interest for this research (southeastern section), the average annual temperature ranges from approximately 8.2°C to 10.0°C. In the summer months, this temperature range increases to approximately 13.6°C to 15.4°C. In the winter, however, the temperature decreases to approximately 4.0°C to 6.5°C (Met Office, 2011).

The average annual rainfall for areas within Northern Ireland ranges from 700 to 2,200 mm $year^{-1}$, depending on altitude and proximity to water bodies (Figure 2.3). In the area of the current study, the precipitation ranges from approximately 900 to 1,300 mm $year^{-1}$. The season with the highest precipitation is the winter, with 250 to 400 mm occurring in these areas. The other 650 to 900 mm of precipitation is spread out equally throughout the remaining seasons. Snowfall in Northern Ireland is rare, so snow days are variable depending on the year and altitude. Some years have no snow days, while other years may have snow days for up to one month (Met Office, 2011).

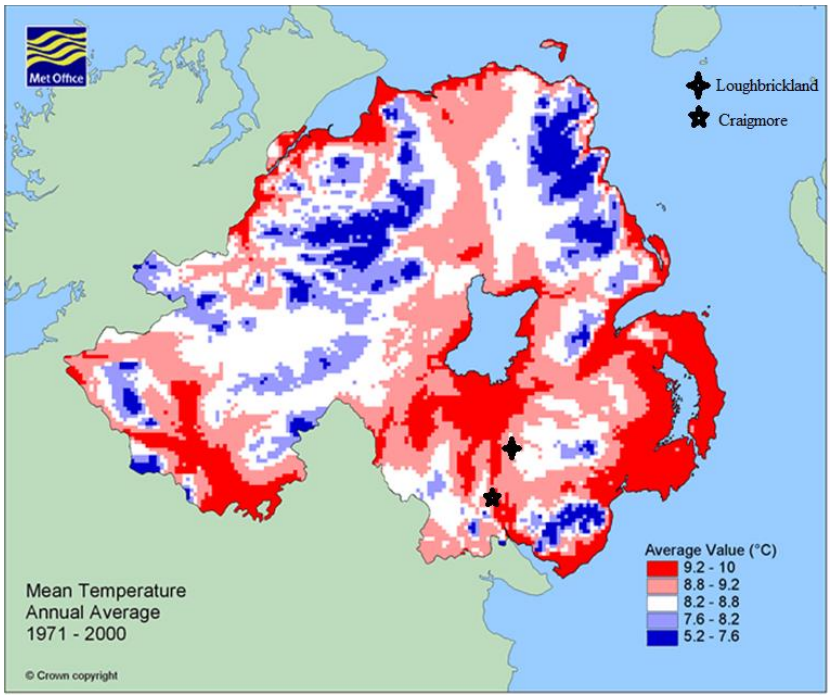

Figure 2.2 Average annual temperature for Northern Ireland from 1971 to 2000 (Source: MetOffice, 2011 (Contains public sector information licensed under the Open Government Licence v1.0)).

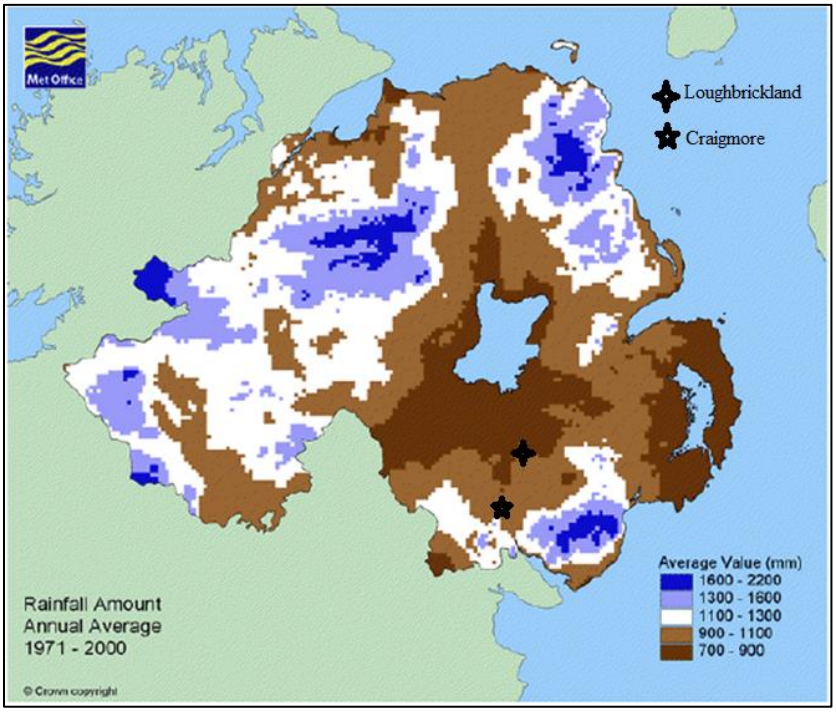

Figure 2.3 Average annual rainfall for Northern Ireland from 1971 to 2000 (Source: MetOffice, 2011 (Contains public sector information licensed under the Open Government Licence v1.0)).

2.2 Bedrock Geology of Northern Ireland

Northern Ireland is geologically diverse, containing every geological system from the Neoproterozoic to the Quaternary, excluding the Cambrian (Doran, 1992). The primary geology in the areas of the study sites is the Ordovician-Silurian shale that is considered to be approximately 416 to 443 million years old, with intrusive granitic plutons with an age of approximately 425 million years in the area surrounding Newry, County Down. The research areas are located on what is known as the Southern-Uplands-Down-Longford terrane that extends from the northern portion of the Republic of Ireland, through southern Northern Ireland and into the southern portion of Scotland (Figure 2.4). There are approximately 20 fault-defined tracts that are elongated parallel to strike from the northeast to the southwest within this terrain. This area becomes younger towards the northwest, indicating that the overall bedrock structure dips in this direction (Beamish et al., 2010).

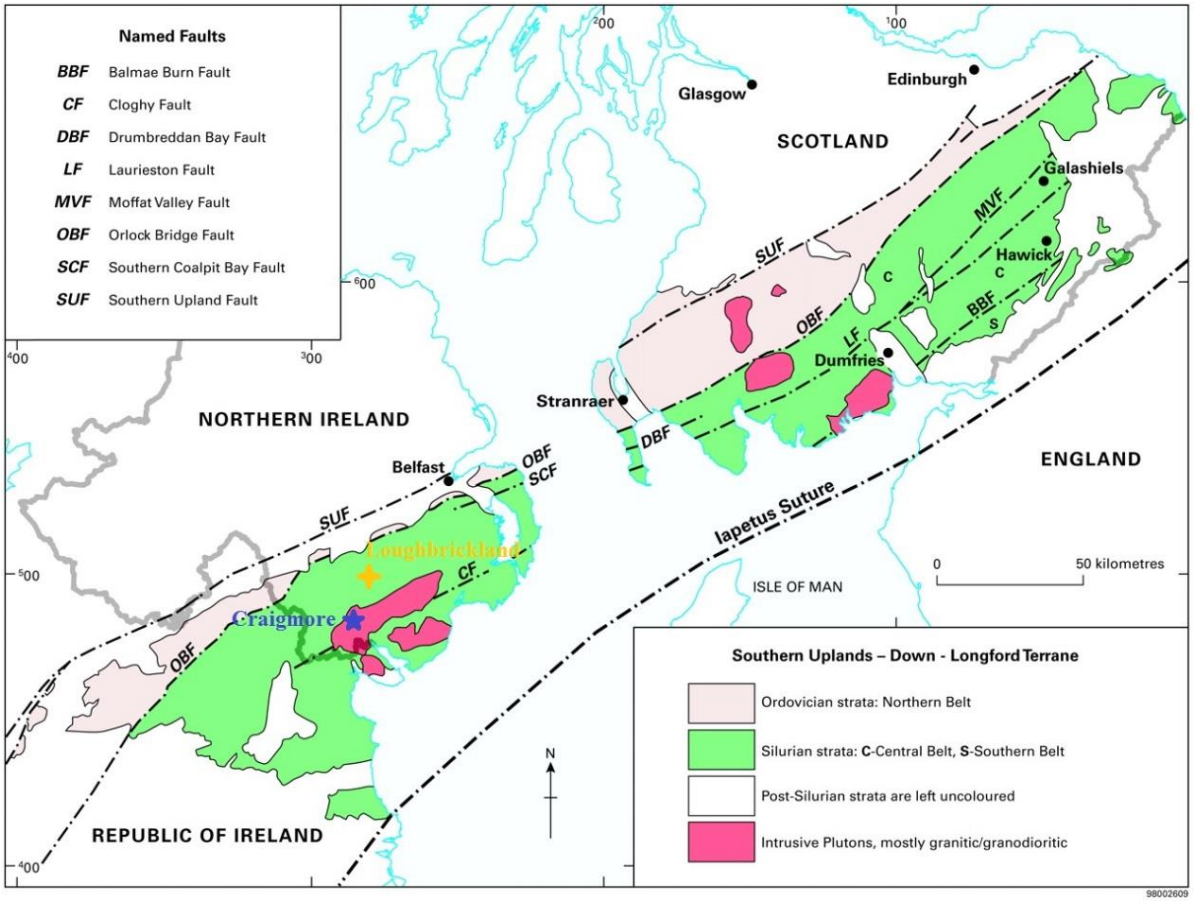

Figure 2.4 Southern-Uplands-Down-Longford terrane showing geological periods and faults (Beamish et al., 2010).

The bedrock geology of Northern Ireland is overlain by glacial deposits from two Pleistocene glacial advances; the Munsterian and the Midlandian. The glacial tills and drumlins in the research study area were typically formed during the Midlandian glaciations, which occurred approximately 75,000 to 10,000 years ago (Doran, 1992). This drumlin landscape is expected to have formed during the last re-advance of the glacier ice as it moved northwards and southwards from the Lough Neagh ice axis (Figure 2.5; Clarke, 2007).

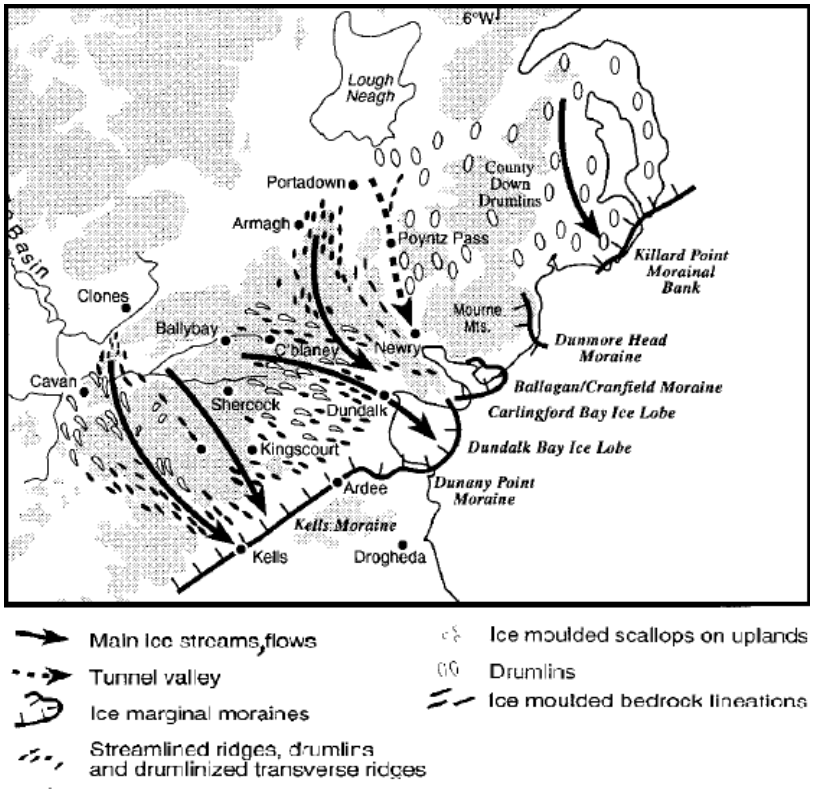

Figure 2.5 Ice flow and drumlin formation during the last re-advance of the ice southwards from the Lough Neagh ice axis (McCabe et al., 1999).

The drainage channel highlighted in Figure 2.6 developed during this last glaciation. The drumlin formations east of this channel are generally dominated by rock-core drumlins that are covered by a thin layer of lodgement till. The drumlins that are located west of this channel have ridged morphology with glacial till overlying the bedrock formations. Those drumlins that have formed along the drainage channel are predominantly have a sand-core (Dardis and McCabe, 1983). This drainage channel existed between the two main study sites of this research, with one of the drumlin sites located directly on the western border of the channel and the other to the east of the channel. The lodgement tills that overlay the bedrock in the areas of study are considered

clay that has been heavily overconsolidated by the weight of overlying ice during the glaciations. These tills are commonly referred to as "boulder clays" (Doran, 1992).

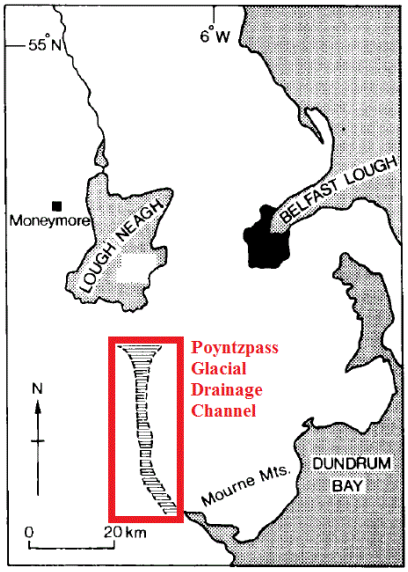

Figure 2.6 Location of Poyntz Pass glacial drainage channel, ending near Newry, County Down (Dardis and McCabe, 1983).

2.3 Characteristics of Glacial Till

Approximately 30% of the Earth was covered by ice during the Pleistocene period, making glacial deposits an important topic of study for geotechnical engineers. Glacial till is a material that is highly variable because of the dependence on the type of materials incorporated in the glacial ice, how the ice moves and transports the materials within the ice and the method in which the materials have been deposited. This large variation in the types of glacial till leads to a wide range in the geotechnical properties (Bell, 2002).

Geological surveys have determined that the glacial till commonly found in Northern Ireland is generally fairly thin, ranging in depth from approximately 5 to 20 m. These glacial tills are commonly defined as having "low" to "moderate" hydraulic conductivity in the range of 10^{-9} to 10^{-4} m s^{-1} based on field and laboratory testing (Fitzsimmons and Misstear, 2006). These tills are generally associated with surface-water-gley soils, related to the Gleysolic soils in Canada, which indicate permanent or intermediate water-logging of the upper soil zone (Fitzsimmons and Misstear, 2006).

The geotechnical index properties of these materials provide some insight into their genesis and behavior. Some of these properties include particle size distributions, Atterberg limits, bulk density, volumetric water content and specific gravity. As the nature of glacial till is dependent on the way it was deposited, there is a large variation in the particle size distributions. Till is generally defined as a mixture of clay, silt, sand, gravel and boulders that is poorly sorted due to the nature of the glacial movement and deposition (Hambrey, 1994). This makes it a difficult material to characterize for geotechnical engineers, as till is not a "textbook" material. Lodgement tills in particular, which includes the tills at the study sites, are generally composed of a high proportion of silt and clay because of the glacial abrasion and grinding typical in glaciated lowlands (Bell, 2002).

Bell (2002) conducted a study of three different sites located along the eastern coast of England to develop a database of geotechnical properties of lodgement till. The range of particle size distributions at Bell's three study locations were as follows: 15 – 64% sand, 18 – 54% silt and 12 – 55% clay sized particles. The ranges of plastic and liquid limits for these materials were from 9 – 26% and 19 – 53%, respectively. The coefficients of volume compressibility as measured in the laboratory ranged from 9.4×10^{-5} kPa^{-1} to 2.4×10^{-4} kPa^{-1}. These results suggested that the till materials in the three study areas had different sources, leading to a wide variation in the overall geotechnical properties. This emphasizes the importance of conducting site specific research to characterize the properties of the glacial till in a specific area of study to ensure that representative parameters are being used in a numerical model.

Grisak and Cherry (1975) measured properties of a glacial till in southeastern Manitoba. The Canadian glacial till was determined to have a clay-loam soil texture, similar to the study sites in this research. This glacial till was formed during the Wisconsin glaciation that began retreating approximately 12,000 years ago. The hydraulic conductivity, as determined by consolidation testing, was measured to be approximately 6.0×10^{-11} m s^{-1} with a standard deviation of 3.7×10^{-11} m s^{-1}. Hydraulic conductivity estimates of the glacial till, however, were estimated to be approximately 1.8×10^{-9} m s^{-1} using numerical modeling, indicating the presence of fractures. These hydraulic conductivity values were compared by Grisak and Cherry (1975) to other Canadian glacial till samples taken from the Interior Plains Region. The hydraulic

conductivity values ranged from 5.8 x 10^{-11} m s^{-1} to 2.8 x 10^{-11} m s^{-1} for the Saskatchewan and Alberta glacial tills, respectively, based on laboratory consolidation test data.

The specific storage (as calculated from measured compressibility) of the intergranular portion of the tills was also estimated from time-consolidation test results and ranged from 9.9 x 10^{-3} m^{-1} to 1.1 x 10^{-2} m^{-1}, which would have an equivalent compressibility of approximately 1.0 x 10^{-3} kPa^{-1} to 1.1 x 10^{-3} kPa^{-1}, for the Manitoba and Saskatchewan tills, respectively. The specific storage for the fractured sections of the tills was calculated to be approximately 3.0 x 10^{-5} m^{-1}, with an equivalent compressibility of approximately 3.1 x 10^{-6} kPa^{-1}. The liquid limits for the Manitoba tills ranged from 22% to 39%, with a void ratio ranging from 0.38 to 0.68 (Grisak and Cherry, 1975).

In a study to compare laboratory and field testing hydraulic conductivity results, van der Kamp (2001) indicated that laboratory results often obtain hydraulic conductivity results that are different than those obtained in the field. His study involved two sites in Saskatchewan prairie, where the glacial till thickness ranged from approximately 18 m and 70 m at the Dalmeny and Warman study locations. Laboratory testing at both sites gave matrix hydraulic conductivity values ranging from 10^{-11} m s^{-1} to 10^{-10} m s^{-1}. Large scale testing conducted *in situ* gave much higher hydraulic conductivity values for the glacial tills at each of these sites. For example, at the Dalmeny site, slug tests, piezometer pumping tests and seepage from a small pond all indicated a bulk hydraulic conductivity of 10^{-8} m s^{-1}. At Warman, however, slug tests, downward propagation of annual pressure fluctuations and flow into a large cavity indicated bulk hydraulic conductivity similar to the matrix hydraulic conductivity at depths greater than 8 m. At depths closer to surface, much higher values of hydraulic conductivity were reached of approximately 10^{-9} to 10^{-8} m s^{-1} (van der Kamp, 2001). These studies highlight the range of glacial till geotechnical properties that can be obtained from either field or laboratory testing and the dependence on the location, deposition type and presence of fractures.

Weathering of glacial till over time can also lead to changes in the overall geotechnical properties associated with these materials. In a study conducted by Eyles and Sladen (1981), the weathering profiles of glacial till in Northumberland, England were tested to determine the impact of weathering on stratigraphy and geotechnical properties. The lodgement till had been

divided into zones depending on the degree of alteration from the parent material. These zones include an unweathered till that is generally dark grey (Zone 1), the introduction of selective oxidation along fissures that generally are located along the coast in till cliffs (Zone 2), the transition into an oxidized till where the matrix colour has changed to a dark or red brown with increasing clay content (Zone 3) and a final stage of weathering where the till has a prismatic structure with the presence of gleying and is leached of primary carbonates (Zone 4) (Eyles and Sladen, 1981).

The geotechnical properties of the tills from each of the zones were compared including particle size distribution, Atterberg limits, water content and drained/undrained shear strength. The particle size distributions were combined for each zone and plotted on a ternary plot (Figure 2.7). Bulk density ranged from 2.15 to 2.30 g cm^{-3} for Zone 1 and 1.90 to 2.20 g cm^{-3} for Zones 3 and 4. The liquid limit and plastic limit for Zone 1 ranged from 25 to 40% and 12 to 20%, respectively. For Zones 3 and 4, however, the liquid limit and plastic limit ranged from 35 to 60% and 15 to 25% due to increased weathering. This research was completed to demonstrate the importance of understanding the method of deposition of lodgement tills, as well as consider the potential post-deposition weathering processes that may have taken place to develop the geotechnical properties experienced in specific locations with lodgement till (Eyles and Sladen, 1981).

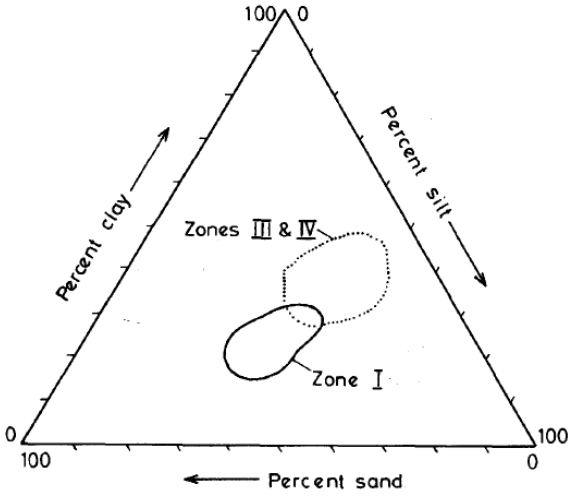

Figure 2.7 Particle size distribution clusters for lodgement till weathering Zone 1 and Zones 3 and 4 (Eyles and Sladen, 1981).

2.4 Hydrogeology of Northern Ireland Drumlins

As discussed by Cai and Ugai (2004), some of the important elements to consider in numerical modeling of pore-water pressure dynamics in slopes include hydraulic characteristics (hydraulic conductivity and compressibility) and water storage in near surface soils (depth to water table, field capacity or specific yield). Other elements that should be included are the other components of the water balance at the ground surface and the hydrogeological controls at depth within the drumlin.

The stability of slopes in these deposits will be sensitive to variations in pore-water pressure in response to climatic variability. Various studies have been completed which have discussed this link between slope stability and pore-pressure dynamics created by climatic variability (Hughes et al., 2007; Cai and Ugai, 2004; Premchitt et al., 1986). Seasonal fluctuations in the water table have been shown to cause cyclic pore-pressure responses within clay till slopes. The changes in pore-water pressures between wet and dry seasons can result in strain softening and ultimately progressive failure of slopes (Ng and Shi, 1998, Picarelli et al., 2004, Potts et al., 1997 and Davies et al., 2008). This highlights the importance of understanding the hydrogeological system prior to conducting slope stability analyses.

The seasonal fluctuations in the water table are, in turn, caused by seasonal changes in the water balance at the ground surface in response to climatic conditions. This availability of water for recharge, in combination with the relatively low hydraulic conductivity of the glacial till, results in a high water table. Even when the deposits are strongly under-drained, the water table within these glacial deposits is generally within 10 m of the soil surface (Fitzsimmons and Misstear, 2006). Preferential flow can also impact groundwater recharge and water table fluctuations. A field site in Shropshire, United Kingdom was used to understand the saturated and unsaturated hydraulic processes that contribute to groundwater recharge of a till deposit (Cuthbert et al., 2010). The results suggested that summer rainfall events caused water table fluctuations even when high suctions occur in the upper soil profile. Given the low hydraulic conductivity of the till at the site, it was concluded that preferential flow must be a mechanism of groundwater recharge. Even thin tills (less than 6 m in depth) are capable of restricting the amount of water recharging underlying aquifers (Cuthbert et al., 2010).

Changes in the water table elevation may also be caused by lateral drainage within the upper layers. In a study by Bonell (1972) on Holderness boulder clays, it was determined that vertical percolation through the till layers could not be the only mechanism for changes in the water levels of wells within the water table zone. Monitoring of piezometric data and rainfall events during times of low or non-existent soil moisture deficit was used to demonstrate rapid increases in water well levels (within a few hours). Following the rainfall event, the water levels took much longer periods of time (up to several days) to return to previous water levels if no more rainfall events occurred. This suggested that another mechanism, such as lateral drainage and movement of water from a perched water table in the upper soil profile (i.e. A horizon), must be involved in the water level fluctuations experienced in the wells (Bonell, 1972).

Vegetation on the slopes can also have an impact on these cyclic pore-water pressures experienced in the surficial soil layers. In the temperate climate of the United Kingdom and Ireland, the wettest season (winter) typically occurs when there is the lowest water demand from plants; while the highest water demand occurs during the drier summer period. This generally causes a seasonal change in the water content experienced within the vadose zone, and also causes shrinking and swelling of clay soils (Andrei, 2000).

Smethurst et al. (2006) conducted a study on a highway cutting on the A34 Newbury bypass in Southern England to further research the impact of vegetation on seasonal pore-pressure cycles. They studied the water uptake from grass and herb vegetation on the 20 m thick London clay during the summer months. They found that the vadose zone suction levels did not reach low enough levels to prevent the high water contents associated with slope failures during high rainfall events in the winter and spring. The study did indicate, however, that the grassy vegetation reduced the number and duration of events associated with critical water contents connected to failures following heavy rainfall. Vegetation was also found to cause a pattern of large cyclic variations in effective stress within the vadose zone up to a depth of 1.0 m between winter and summer (Smethurst et al., 2006).

2.5 Hydrogeological Modeling

Numerical modeling has been used as a tool to interpret hydrogeological behaviour at many sites around the world for many years. In general, these simulations have been conducted in one- or two-dimensions, with an increasing interest in the third dimension. Freeze (1971) was one of the first researchers to develop a three-dimensional finite-difference simulation of a variably saturated system. Since Freeze, there have been an increasing number of numerical methods used for the analysis of groundwater flow. Frind and Verge (1978), for example, developed three-dimensional models of a hypothetical and real aquifer system to determine what the extra cost of developing a three-dimensional simulation would be as compared to a two-dimensional simulation. They concluded that the use of the two-dimensional scenario is possible if the natural system is quite simple. However, as the complexity of the study domain increases or higher accuracy results are needed, a three-dimensional method is preferred. They concluded that as the complexity of the physical three-dimensional system increases, for example, through the addition of more boundary conditions or more heterogeneous materials, the application of a two-dimensional system became less valid.

Bakr et al. (1978) compared one and three dimensional confined flow models and concluded that there is a significant reduction in the variance in hydraulic head measurements in three-dimensions when compared to a simple simulation with only one-dimension. The one-dimensional system had to use an artificial value of hydraulic conductivity to obtain a "realistic" simulation of the groundwater system. The three-dimensional system, however, was able to use more realistic hydraulic conductivity functions, since the three-dimensional distribution of hydraulic heads does not have to be averaged or integrated into a two-dimensional domain. The use of the three-dimensional model in variably saturated and heterogeneous systems is therefore considered more realistic, as the hydraulic conductivity functions measured for the actual system can be used.

A two-dimensional analysis of a similar system to that used by Bakr et al. (1978) was also developed by Mizell et al. (1982). Similar to the study above, the head variances were reduced in the two-dimensional simulation when compared to the one-dimensional model. The head variances were still slightly larger in two-dimensions, however, when compared to the

three-dimensional system. Overall, the three-dimensional system was still considered to be more realistic than the two-dimensional system, especially where extra flow paths were open for water to by-pass sections of lower conductivity, as experienced in the real system. The two-dimensional system, however, was able to show similar results to the three-dimensional system and *in situ* data.

Given past research, it has been shown that in many cases where simulations of natural hydrogeological systems are developed, including the third dimension is preferred. This is especially true if the formation holds complex geological or hydrogeological properties. In the case of groundwater flow in Northern Ireland drumlins, there is generally a relatively thin layer of glacial till to consider. To determine the level of detail required for determining groundwater response to climate in these formations, the dimensionality effects will be studied in this research.

3.0 MATERIALS AND METHODS

The development of a numerical model of groundwater flow requires a characterization of the geology (geometry and region definition) and the measurement or estimation of appropriate boundary conditions and material properties. The methods utilized in this study included geological characterization based on existing site information as well as borehole drilling, field and laboratory testing, and estimates of field parameters based on the interpretation of monitoring data. In some cases, the required material properties could not be evaluated directly and had to be estimated from literature sources. The following section discusses the methods in which this data was collected and a description of how it was incorporated into the numerical models developed in this study.

3.1 Study Sites

Two study sites were chosen for the hydrogeological analysis conducted in this research. These sites are both located in County Down, Northern Ireland. Although the sites are both glacial drumlins, each site has unique conditions requiring site-specific field or laboratory testing and model calibration. This sub-section will provide a description of each site along with a short description of the methods used to characterize each site. This will be followed by an overview of the methods used to develop the two-dimensional and three-dimensional conceptual models.

Drilling, instrumentation and field testing at the two study sites was undertaken as a joint effort by three different students (including the author) as part of their own research studies. Two of the students are Ph.D. students from Queen's University of Belfast (QUB): M. McLernon is studying the effect of pore-pressure transients on slope stability; L. Carse is studying the effect of cyclic pore pressure on strain softening following cutting excavation.

The field and laboratory work completed as part of this research was undertaken primarily during the summers of 2009 and 2010. During this time, the author was involved in monitoring of the standpipes, conducting slug tests, calibration and installation of the EnviroScan water content sensors and tensiometers, conducting surface hydraulic conductivity testing,

pedological soil classification, installation and monitoring of the shallow wells, and general site maintenance as required at both of the sites, as well as a third site utilized by the QUB.

Laboratory work completed by the author consisted of the measurement of gravimetric water content and dry and bulk density. All other monitoring installation, data collection and laboratory testing was completed by QUB Ph.D. students and is presented here only as required for the model development. Some information for the Loughbrickland site was also obtained from previous research undertaken by Clarke (2007), as part of his Ph.D. research at QUB. This included pore pressure monitoring and modeling prior to the Loughbrickland excavation.

3.1.1 Craigmore, Newry, County Down

The primary study site is the Craigmore railway cutting located north of Newry, County Down (Figure 3.1). The bedrock geology of this area differs from the typical Ordovician-Silurian Shale generally present in the southern half of Northern Ireland. The Newry Igneous Complex is located along a northeast to southwest strike and comprises a granitic batholith that intruded the Silurian Shale approximately c. 425 Ma ago. This complex consists of three granitic plutons, where the center pluton is located below the Craigmore cutting (Baxter, 2008).

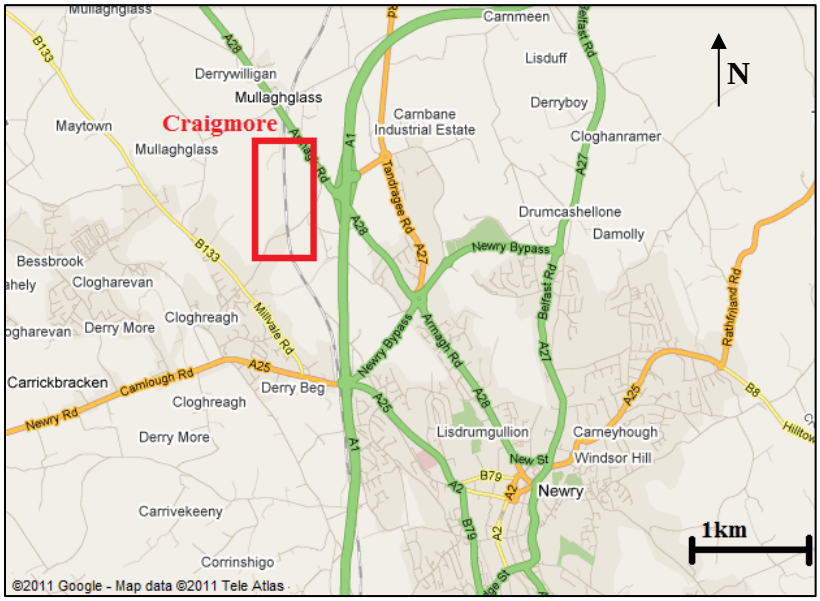

Figure 3.1 Location of Craigmore railway cutting north of Newry, County Down (Source: Google, 2011).

The Craigmore cutting was constructed in the 1850's by the Northern Ireland Railway (NIR) and is approximately 160 years old. The embankment is 17 m high with a slope of approximately 35 degrees. The cutting was excavated through the center of the drumlin and exposes two different layers of glacial till. The presence of two till layers is typical in the region and is supported by evidence from field measurements and physical attributes along the cutting slope. One unique characteristic of this cutting is the more sandy nature of the upper 1.0 m of the soil profile near the crest. This sandy material could have been created during the deposition of the Poyntzpass glacial drainage channel. The study site is located along the western border of what is thought to be the location of this channel (see Figure 2.6) (Dardis and McCabe, 1983).

The site is instrumented at four borehole locations with standpipes installed in both till units and in the upper weathered bedrock zone. Borehole 1 (BH1), Borehole 2 (BH2) and Borehole 3 (BH3) were installed during field work conducted by the Northern Ireland Geotechnical Engineering Branch (Department of Finance and Personnel) and QUB Ph.D. students between November 2007 and February 2008. The boreholes were installed on January 17th and 18th, 2010 using a heavy percussive drilling rig and are approximately 200 mm in diameter. All boreholes were drilled to the weathered bedrock zone at depths of 16.1 m, 10.5 m and 12.5 m for BH1, BH2 and BH3, respectively.

At BH1, three standpipes, BH1-1, BH1-2 and BH1-3, were installed at depths of 5.6 m, 10.7 m and 16.1 m, with screens of BH1-1 and BH1-2 located within the glacial till and BH1-3 in the weather bedrock zone. Screen lengths were 1.4 m, 1.8 m and 1.4 m for BH1-1, BH1-2 and BH1-3, respectively. At BH3, three standpipes, BH3-1, BH3- 2 and BH3-3, were installed with screens in the till at depths of 5.0 m (BH3-1) and 8.6 m (BH3-2) and in the weathered bedrock at 12.5 m (BH3-3). Screen lengths at BH3 were 1.4 m for all standpipes. Both BH1 and BH3 had gravel packs with lengths ranging from 1.4 to 1.8 m installed around the screens with seals created by bentonite pellets between each gravel pack. BH2 also had gravel packs and bentonite pellets forming seals with one standpipe screen located in the till at a depth of 5.8 m (BH2-1) and another in the weathered bedrock zone at a depth of 10.5 m (BH2-2). Screen lengths were 1.9 m and 2.5 m for BH2-1 and BH2-2, respectively.

Undisturbed U100 samples were taken at 1.5 m depth increments during borehole excavation. The QUB PhD students also took disturbed till samples from the soil materials that were excavated during drilling for classification and index testing (Hughes et al., 2008). The standpipes within BH1 have been monitored most frequently since they are most accessible. Less monitoring data is available from BH2 and BH3 due to limitations in site access.

Borehole 4 (BH4) was installed on October 19, 2010 by Geotechnical and Environmental Services and the QUB PhD students. This borehole (and instrumentation) was used to determine water levels and bedrock depths at the toe of the cutting near the railway track. This borehole was also installed using percussion drilling, but had a diameter of 106 mm. Three standpipes were installed with depths of 2.8 m, 2.9 m and 1.5 m for BH4A, BH4B and BH4C, respectively. The standpipe screens were 1.0 m in length for BH4A and BH4B, while BH4C had a length of 0.8 m.

Gravel packs were installed for the length around the screen intervals, similar to the other boreholes, with a bentonite seal above the gravel packs. Borehole details for all of the above installation are presented in McLernon (2014). Barometric pressure was removed from the 'absolute' pressure transducers used for monitoring the above boreholes. Further information on data corrected for barometric pressure using Skempton's B-bar can be found in Carse (2014). Laboratory testing on field samples was undertaken by Ph.D. students McLernon and Carse and included water contents, liquid limits, plastic limits and undrained triaxial compression tests. Further information on testing related to the conceptual model development will be included in subsequent sections.

Two EnviroScans to monitor volumetric water content in the upper 1.0 m of the soil profile were installed at the crest (ES02) and toe (ES01) of the slope. Shallow wells (SW-ES01 and SW-ES02) were also installed at these locations in August 2009 to gather information on the potential formation of shallow or perched water tables within the soil zone above the glacial till. SW-ES01 was installed near ES01 at the toe of the slope and had a depth of 0.8 m with a screen located from 0.5 m to 0.7 m. SW-ES02 was installed near ES02 at the crest of the slope at a depth of 0.7 m with a screen located from 0.4 m to 0.6 m. Monitoring at these shallows wells did not begin until October 2009. In July 2010, four tensiometers were installed along the slope to

help evaluate shallow water flow dynamics and to determine the relationship between the water content and suction of the upper material within the shallow vadose zone (Table 3.1). All monitoring locations are shown in the site plan presented in Figure 3.2.

Table 3.1 Details on tensiometer installations along the Craigmore slope embankment.

Tensiometer ID	Depth to Tip (mBGL)	Location
T50ES01	0.55	Slope toe
T80ES01	0.85	
T50ES02	0.55	Slope Crest
T80ES02	0.85	

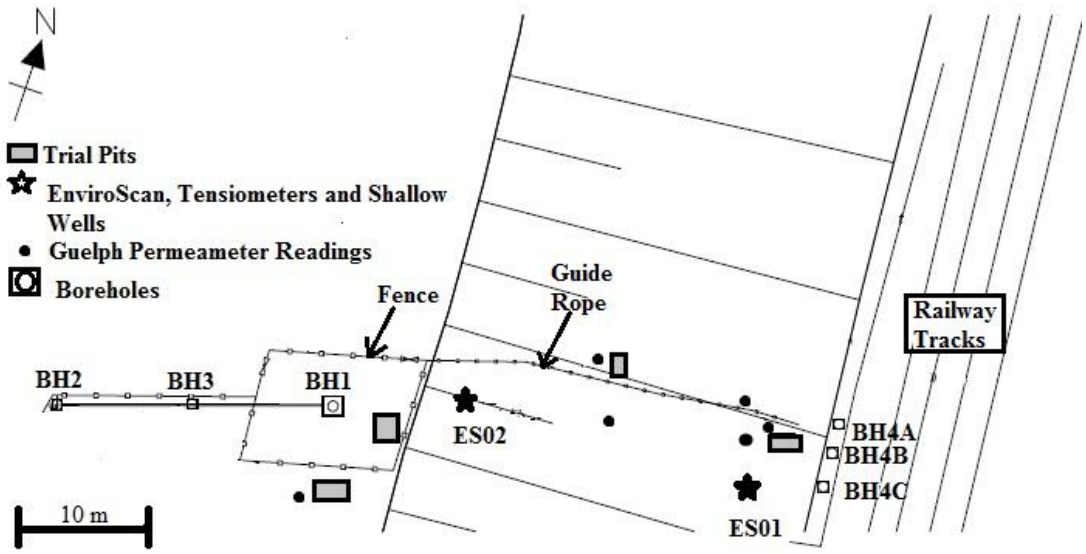

Figure 3.2 Monitoring equipment along the Craigmore railway cutting (McLernon, 2014).

Meteorological data was collected at the crest of the Craigmore slope to enable a comparison to be made to meteorological data gathered at a nearby governmental meteorological monitoring site. Collection of meteorological data at the Craigmore site started in 2009, but errors in the meteorological equipment required that new equipment be installed. Data collection from this new equipment began in August 2010. The QUB researchers were granted access to the British Atmospheric Data Center (BADC) to help fill in gaps in the meteorological data and provide access to historical meteorological data. BADC has a number of weather stations located in the geographic region. Because of the unreliable data at Craigmore and the lack of

equipment at Loughbrickland, data from the BADC will be used to characterize the climate at each site. Data from the BADC sites includes solar radiation, rainfall, wind speed, air temperature and relative humidity on an hourly and daily basis. All monitoring and meteorological data used in this research will be discussed in Section 4.0 of this thesis.

3.1.2 Loughbrickland, County Down

The Loughbrickland highway cutting is located just south of Loughbrickland, County Down (Figure 3.3). This cutting is located on the Silurian Shale structure that is dominant in the area. The glacial deposits are similar to those at Craigmore, but with less sandy materials. As described in previous sections, this area is located east of the Poyntzpass glacial drainage channel, which is considered to be dominated by rock drumlins (Dardis and McCabe, 1983). This drumlin appears to also be comprised of two glacial till layers, with the underlying till exhibiting a hydraulic conductivity one magnitude lower than the upper till (Clarke, 2007). More information will be given on these two glacial till hydrogeological properties in Section 4.

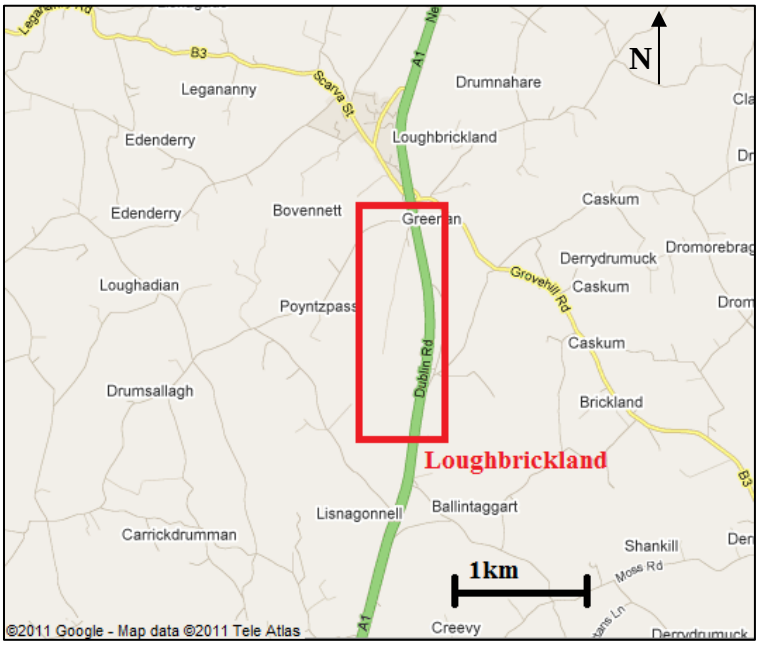

Figure 3.3 Location of Loughbrickland highway cutting near Loughbrickland, County Down (Source: Google, 2011).

The highway cutting at this site was constructed as part of the twinning of the A1 highway from Belfast to Dublin, Republic of Ireland. This cutting went through a portion of the drumlin (Figure 3.4) and was completed in 2004 after undergoing some preliminary monitoring by Clarke (2007) as part of his PhD research. This research included the monitoring of pore water pressures using standpipes installed at various depths along a transect across the original drumlin, perpendicular to the cutting alignment. The standpipes were installed in four boreholes and were located with screens within the two till layers and in the weathered bedrock zone (Figure 3.5). Two of these boreholes (BH1 and BH2) were still being monitored as part of this year. Three boreholes have been installed following cutting construction: BH3A is located along the toe of the slope; BH5A is located along the bench at mid-slope; and BH2A is located along the crest of the cutting near BH2.

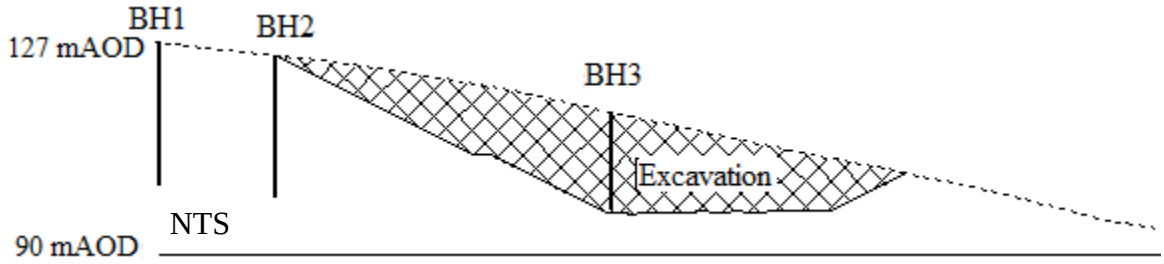

Figure 3.4 Excavation through portion of the drumlin with pre-excavation boreholes indicated (Clarke, 2007).

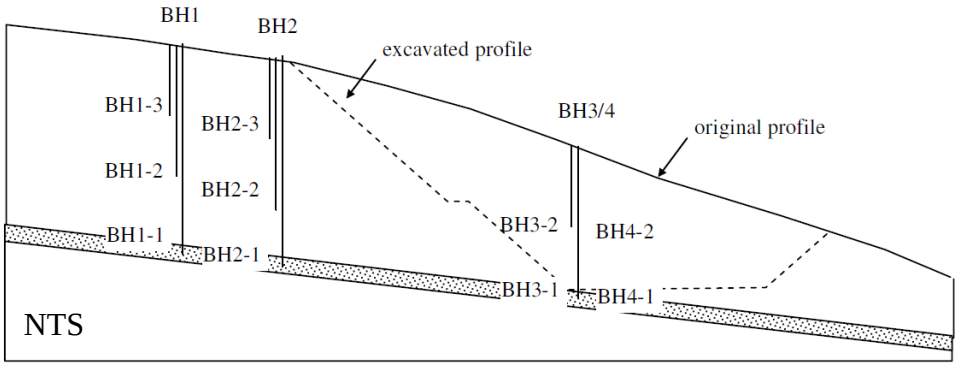

Figure 3.5 Borehole locations used in Clarke (2007) research prior to construction of Loughbrickland cutting embankment (Source: Clarke, 2007).

BH1 and BH2 were installed using light percussion drilling. The standpipe diameter was 200 mm and penetrated the bedrock at each location. Disturbed samples were used for

classification purposes, while undisturbed U100 samples were taken for laboratory testing. Standpipes (50 mm in diameter) were installed in each of the boreholes at varying depths to monitor pore pressures in each of the tills and at the bedrock surface (Clarke, 2007). BH1, BH2 and BH2A all have three standpipes in each of the boreholes. BH1-1, BH1-2 and BH1-3 are installed at depths of 9.7 m, 17.2 m and 24.4 m with screen lengths of 4.2 m, 2.0 m and 1.7 m, respectively. BH1-1 has a grout mix surrounding the screen zone, while the other two standpipes have gravel packs. BH2-1, BH2-2 and BH2-3 were installed at depths of 9.8 m, 17.1 m and 24.6 m with screen levels of 4.3 m, 6.0 m and 1.5 m, respectively. The two upper standpipes (BH2-1 and BH2-2) have a grout mix surrounding the screens, while BH2-3 has a gravel pack. Both boreholes have bentonite seals between each of the gravel and grout mix packs.

Additional boreholes were installed by the Northern Ireland Geotechnical Engineering Branch (Department of Finance and Personnel) and the QUB PhD students. BH3A and BH5 were installed using rotary core drilling (IDECO Rotary Percussive drill rig) while BH2A was installed using percussion drilling similar to BH1 and BH2. BH3A has two standpipes installed to depths of 0.8 m (BH3A-1) and 3.0 m (BH3A-2). The screen length of BH3A-1 covers the entire depth of the standpipe, while BH3A-2 has a screen length of 1.3 m. BH5 also has two standpipes, with depths of 6.3 m (BH5-1) and 11.5 m (BH5-2) and screen lengths of 1.1 m and 1.2 m. BH2A-1, BH2A-2 and BH2A-3 are installed at depths of 8.0 m, 15.7 m and 22.7 m with screen lengths of 1.7 m, 1.3 m and 1.4 m, respectively. All of these standpipes have gravel packs surrounding the screens with bentonite seals surrounding the packs, with the exception of BH3A-1 which is screened over nearly its entire length. All of the boreholes used for the installation of three standpipes were 200 mm in diameter while boreholes used to install only one or two standpipes were 150 mm in diameter. Sample recovery for these holes was similar to that used for BH1 and BH2. Details for all boreholes are provided in McLernon (2014).

The highway cutting is approximately 25 meters high with a slope of 26º. During construction, flowing artesian conditions developed at the toe of the slope (near BH3-1 of Figure 3.5), causing a localized slope failure. Stabilization of the cutting was undertaken by installing a drain along the toe of the slope that extended to the surface of the weathered bedrock zone (Carse et al., 2009). Drainage of the weathered bedrock surface was anticipated to be effective

in reducing the pore pressures at the toe of the slope. Information gathered by Clarke (2007) will be summarized in Section 4.0, including hydraulic conductivity test results, Atterberg Limits, particle size distributions, soil bulk density estimates, soil water characteristic curves and pressure monitoring data.

Two sets of EnviroScan water content monitoring sensors were installed on the crest and along the upper slope above the berm of the cutting to an approximate depth of 0.9 m. These sensors were installed in July 2010, along with three shallow wells to monitor the development of shallow water tables above the upper till. The shallow wells were installed on the crest near ES01 (SW-ES01), along the slope above the berm (SW01) and along the slope below the berm (SW02). A shallow well was also installed near ES02, but monitoring had not started during the development of this thesis. SW-ES01 was installed at a depth of 0.7 m with a screen located from 0.5 m to 0.7 m below the ground surface. SW01 and SW02, as well as the shallow well near ES02, were all installed to a depth of 0.6 m with screens located at depths of 0.3 m to 0.5 m. A detailed site plan showing the location of monitoring equipment can be seen in Figure 3.6.

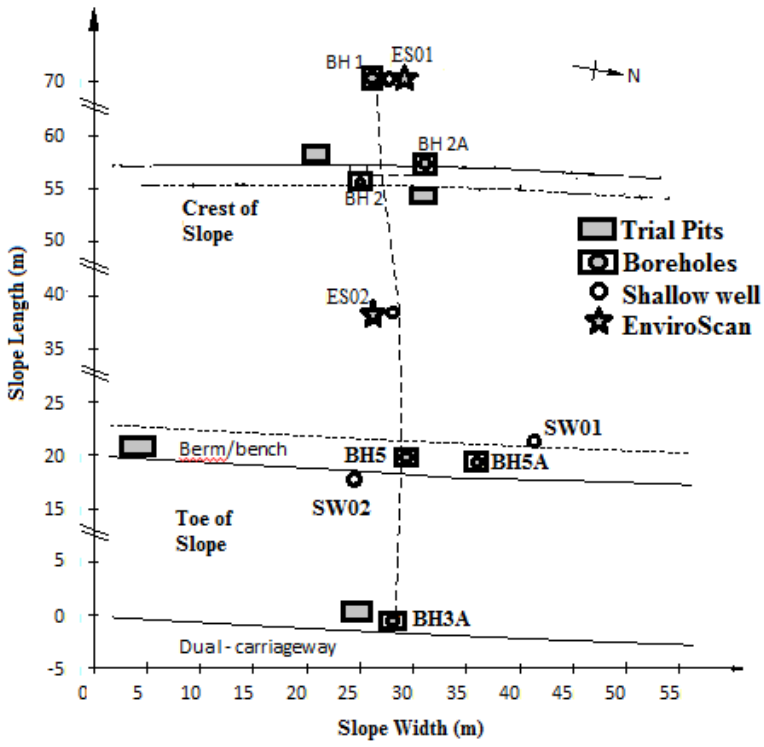

Figure 3.6 Monitoring equipment located along the slope of Loughbrickland excavation (McLernon, 2014).

3.1.3 Soil Testing

Various testing was completed at each of the sites to help develop a representative conceptual model prior to the development of the two- and three- dimensional models. Testing conducted at each location included hydraulic conductivity testing, such as slug tests and Guelph Permeameter tests, and general soil classification. Results from these tests and observations, along with other laboratory testing discussed in the following subsection, were compiled for each site to develop a representative material properties database.

Falling and rising head tests for hydraulic conductivity were conducted on the standpipes at each site. Falling head tests were conducted by adding 2 to 5 m of water to the standpipe and monitoring the water level changes with a level logger. Rising head tests were conducted in a similar manner but by rapidly lowering the water level in the standpipes by 2 to 5 m. The results from the falling or rising head tests in the glacial till were interpreted using the Hvorslev method (Hvorslev, 1951). The tests conducted on standpipe wells installed into the weathered bedrock at Craigmore could not be analyzed with the Hvorslev method since the geometry of flow into the screen from the weather bedrock zone was primarily horizontal. Calculated methods exist for dealing with confined aquifer slug testing, including Cooper-Bredehoeft-Papadopulos (Cooper et al., 1967; Papadopulos and Cooper, 1967; Papadopulos et al., 1973). The test results, however, were interpreted by simulating the field tests using a transient axisymmetric finite element seepage model (SEEP/W) assuming that flow occurred through a 1.0 m thick weathered bedrock zone. This allowed flexibility for the potential of draining conditions to be included in the analysis of the slug tests within the weathered bedrock zone.

The model domain was approximately 100 m in radius and it was assumed that the initial equipotential surface was defined by the monitoring data prior to the test and was spatially constant. A boundary condition was then applied at the location of the standpipe screen in which the applied head was a function of the total inflow into the screen interval. The hydraulic conductivity and compressibility of the weathered bedrock and overlying till were then varied to obtain a visual “best-fit” to the test data. The resultant transmissivity and compressibility were used in the calibration of the models for the site.

The falling head tests completed on the weathered bedrock at the Loughbrickland site could not be used due to errors in the borehole installations which resulted in unreliable data. The presence of the toe drain has also had an impact on the groundwater table within the bedrock. The standpipes that have screens located within the weathered bedrock near the toe of the cutting may be influenced by the toe drain. As the weathered bedrock zone has a higher transmissivity, flow from the lower slope to the toe drains will influence measurements taken at the standpipes. This could also prevent water from pooling in the standpipes for a period long enough to obtain a reading during the slug tests. It is also suspected that the standpipe installations on the crest of the slope were not allowed to properly seal, allowing a connection between standpipes at different elevations, decreasing the reliability of any data within the standpipes. This is evident in the hydraulic head measurements shown in Section 4.0.

A Guelph Permeameter was used in the summer of 2009 to conduct hydraulic conductivity testing of the upper 1 m of soil along the slope cutting and crest (Figure 3.7). This method is similar to a steady state flow test at a small scale. The tip of the Guelph Permeameter is lowered into an augered hole that ranges from 0.15 to 1.0 m in depth. The diameter of the augered hole is approximately 0.06 m. For deeper tests (greater than 0.5 m), holes were dug using shovels until 0.5 m and then augered to the desired depth to allow the Guelph Permeameter to sit flush at the bottom of the augered hole. In high clay materials, a brush was used to reduce potential smearing along the walls of the hole prior to starting the test. This was not required for holes augered in materials with higher sand content. The air inlet tube was then raised 0.05 m to create a ponded height of water of 0.05 m within the augered well. Measurements of flow rates with time were then taken at various time steps until a steady rate could be determined (approximately 6 time steps were used to determine this rate).

Once steady state conditions under the first applied head were measured, the ponded water level in the well was then set to a height of approximately 0.1 m and the test was repeated. Each steady flow rate was then used in an equation given by Soil Moisture Equipment Corp. (2010) to determine the hydraulic conductivity of the soil. In cases in which the hydraulic conductivity was lower (e.g. at greater depths within the till), the inner reservoir of the Guelph Permeameter was used to determine the steady flow rates for each well head height. Equations

from the Guelph Permeameter Operating Instructions given by Soil Moisture Equipment Corp. (2010) were used and are based on standard literature (Elrick and Reynolds, 1986 and Elrick et al., 1989).

Figure 3.7 Image showing the setup and use of a Guelph Permeameter in the field at Craigmore site.

Soil classification was undertaken during excavation of the soil pits at each site. Visual characteristics of the A and B horizons above the glacial till C horizon were used in conducting this analysis. Visual characteristics that were noted include colour change within the materials, layer thickness of the A and B horizons, as well as any notable characteristics such as mottling were included in this analysis. Results of the soil classification findings are found in Section 4.0.

3.1.4 Laboratory Testing

Laboratory testing was completed on soil samples taken from the site for water content and bulk density from which volumetric water content and porosity was calculated (assuming a particle density of 2.65 g cm^{-3}). Additional laboratory testing on samples retrieved from each site was conducted by the QUB PhD students (McLernon, 2014 and Carse, 2014). This testing included Atterberg limits, particle size distributions, bulk density and gravimetric water content as well as shear strength testing. Laboratory data relevant to the hydrogeological modeling in this research will be reported in Section 4.0.

Soil pits dug at each of the sites also allow undisturbed soil samples to be collected from the wall of the pits. These were collected using small rings with a volume of 51.9 cm^3. The rings were placed along the wall of the soil pit and hammered in using a small sledge hammer. A small piece of cylindrical plastic tubing was used to transfer load from the hammer to the ring to prevent compaction of the soil. These soil rings were then weighed in the laboratory and oven-dried. The weight of the dry and wet samples, along with the volume of the ring, was then used to determine volumetric water content using standard methods. The volume and weight of the samples were also used to calculate dry bulk density, porosity and void ratio using standard methods.

The EnviroScan sensors were calibrated in the laboratory using the procedure recommended by Sentek Technologies (Sentek Pty Ltd, 2001). This procedure involves the collection of bulk soil samples from the field for each of the representative materials in which the sensors are installed. This material was oven dried and placed into a container large enough to allow the installation of an access tube for the EnviroScan sensors while providing at least 10 cm of material surrounding the access tube. The soil was packed to a similar dry density as in the field. Prior to calibrating the sensors with soil, the sensors were tested in air and in water to define upper and lower bounds of water content for the calibration. These counts were then used with the soil counts to determine the soil calibration curve:

$$y = \frac{(\text{Air Count} - \text{Field Count})}{(\text{Air Count} - \text{Water Count})} \tag{3.1}$$

Soil counts were obtained over a range of volumetric water contents. First, the sensor was calibrated using a dry soil sample created by oven drying the entire bulk sample. Water was then added to the bulk soil samples to create a range of water contents. The water content sensor was lowered into each representative soil sample until three measurements were taken at each depth and for each prepared water content. Samples were then removed from the bulk soil by using a ring and hammer similar to processes described for field measurements. Samples were then weighed and oven-dried to determine the density and volumetric water content reached within the laboratory pails. This process was repeated for three to four water contents representing a range of saturation levels. Once the final sample was taken at a high saturation,

readings for each of the water contents were converted to scaled frequencies and were plotted against water content to develop a regression equation as outlined by an example given by the calibration manual (Sentek Pty Ltd, 2001) (Figure 3.8). Constants from the regression equation where entered into the EnviroScan program, along with the air and water counts, to directly obtain volumetric water contents from each sensor reading in the field using the appropriate equation for the particular soil type. The regression equation was:

$$y = A\theta^B + C \tag{3.2}$$

where A, B and C are constants, y is the scaled frequency and θ is the volumetric water content measured in the laboratory.

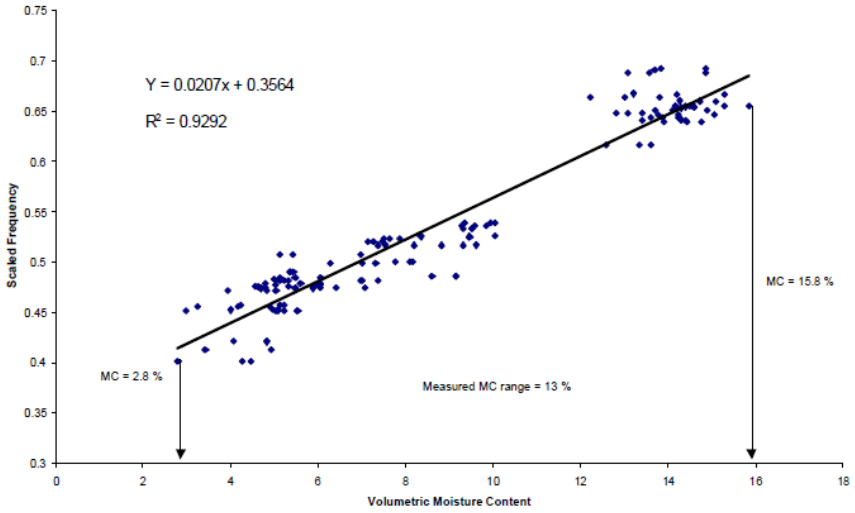

Figure 3.8 Example of the scaled frequency versus volumetric water content curve, with regression equation (Sentek Pty Ltd, 2001).

3.1.5 Seismic Refraction Surveys

Seismic refraction surveys were completed by the author and fellow PhD students from QUB along a number of transects at each study site to help define the bedrock topography. These were completed using 24 geophones spaced between 3 to 5 m apart, depending on the anticipated depth to bedrock. Seismic surveys were undertaken along ten transects at each study site, as shown in Figure 3.9 and Figure 3.10. A sledge hammer and metal plate placed on the soil surface near every other geophone was used as the energy source. Two additional hits were

completed approximately 10 m from each end of the transect line. The raw data from these surveys was sent to Optim Software & Data Solutions, for data reduction using the tomography method (Pullammanappallil and Louie, 1994).

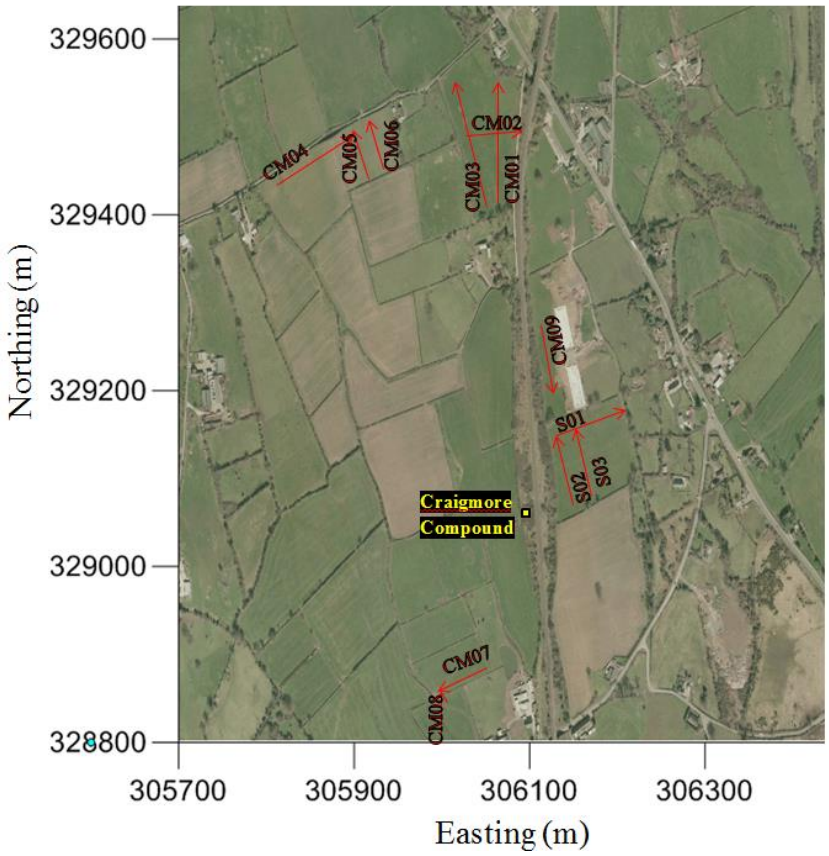

Figure 3.9 Seismic refraction survey transects (marked as red lines) at the Craigmore study site.

The tomography results were used to determine approximate depths to bedrock for each transect. These depths were then imported into Golden Software's Surfer© software, where all data points and borehole logs were used to interpolate the bedrock topography. Bedrock outcrops, where present, were also used in the interpolation to ensure reasonable elevations were being used. In areas where no transects or outcrops exist, an approximate depth of bedrock was given to ensure that the interpolation did not exceed the ground surface elevation.

Carse (2014) also developed an estimate of soil stiffness (i.e. compressibility) based on the seismic velocities measured through each material at each site. Details of these analyses are

documented in Carse (2014) and will not be described in this thesis. Methods used of estimating compressibility are described in Section 3.2.4. Results of all tomography sections are presented in Appendix A.

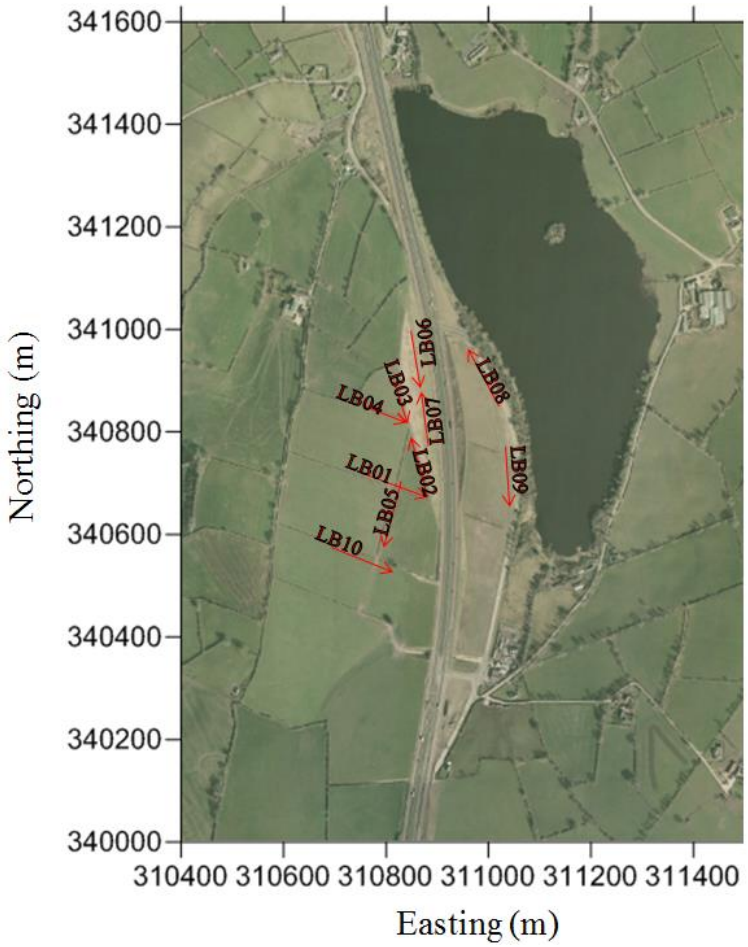

Figure 3.10 Seismic refraction survey transects (marked as red lines) at Loughbrickland study site.

3.2 Model Development

Three-dimensional models were developed for each site based on conceptual models created for each. These conceptual models were developed using the information gathered from literature review, field testing and laboratory testing, as described in previous sections. Two-dimensional models were then extracted from the three-dimensional models along cross-sections roughly perpendicular to the road or railway cuttings. Only one two-dimensional cross-section

was used at each site. This allowed all the known borehole data to be incorporated into the simulation and calibration, but also was consistent with conventional practice of using a two-dimensional groundwater model to develop an interpretation of pore-pressure conditions for use in slope stability analyses.

The modeling software that was used to develop both the three-dimensional and two-dimensional models was Feflow. Feflow is a groundwater flow and contaminant transport modeling software that can be used to develop both three- and two-dimensional models in both the saturated and unsaturated scenarios (DHI-WASY, 2011).

3.2.1 Model Geometry

Information on surface water bodies and borehole water levels at the bedrock surface were used to develop a groundwater level contour map. This groundwater contour map was an interpolation of all water level data at each site to help identify flow directions and define potential recharge and discharge areas. Once developed, the water level contours, along with a surface elevation map, were used to define groundwater divides and constant hydraulic head boundary conditions which provided the basis for establishing the areal extent for the models. Additional borehole data, available from the Northern Ireland Railway and the Geological Survey of Northern Ireland, were also added to this interpolation for completeness. Where contours could not be estimated in a reasonable matter, surface elevation was used to help estimate bedrock depth. The highest elevations of drumlins or lowest points of valleys were assumed to be groundwater divides.

The layers within the three-dimensional model were selected using the depths and thicknesses of the various geological units. The upper active soil zone was represented by a 0.5 m layer, with another 1.0 m layer to provide a transition zone representative of a weathered B or C horizon as was typically seen in the field. This was underlain by 2 layers representing the upper and lower glacial till units. The lowest layer of the model was assigned to be the weathered bedrock underlain by the surface of the un-weathered bedrock, which was assumed to be a lower zero flux boundary. A transition layer was also included above this weathered

bedrock zone to represent the transition from the till to the weathered bedrock. This was considered reasonable, as the presence of large boulders and macropores would change the hydrogeological behaviour of material between the glacial till and bedrock.

The glacial till sections were subsequently separated into a number of layers. In areas where soil was shallow (i.e. bedrock was within 5.0 m of the soil surface), the layer elevations were adjusted so that the lowest model boundary was at least 5.0 m below the surface. The elements within the mesh for each layer were then assigned appropriate material properties based on geology and elevation to ensure that the weathered bedrock reached the appropriate depth estimated by the seismic refraction surveys, without model convergence becoming an issue. This was completed to assist with convergence of the three-dimensional model since convergence problems are more likely to occur when many layers are used over a very small depth. Feflow does not have the ability for "black box" or "deleted" elements in certain layers of the mesh, so all layers must extend the entire model domain, making it difficult to accurately simulate rapid changes in the bedrock such as outcrops.

The two-dimensional models were extracted from the three-dimensional models as transects of unit depth (into the page) and as a result used the same geometry, material properties and boundary conditions as the three-dimensional model. The locations of the far left and right boundaries were located based on the presence of bedrock outcrops for Craigmore and groundwater divides for Loughbrickland. The layer elevations for each material type were then imported into the two-dimensional mesh to ensure that the same layer elevations were being used. The elements of the two-dimensional mesh were then assigned appropriate material properties to match those found in the three-dimensional models. This was completed to ensure that proper comparison could be conducted between each model scenario.

3.2.2 Mesh Development

The three-dimensional mesh used for each of the models consisted of triangular elements of various sizes. The mesh was refined to smaller element sizes near points of interest, such as along the cutting or along the cross-sections used to develop the two-dimensional models. Nodal

spacing ranged from approximately 35 m in areas far from the cross-section of interest to 1.0 m along the cutting cross-section. A total of 14, 426 nodes per slice (upper boundary of each layer) were used in the Craigmore model and 19,342 nodes per slice in the Loughbrickland model. The Feflow triangle mesh generator was used for the three-dimensional models and the T-mesh generator was used for the two-dimensional models. The Triangle mesh generator was used due to its ability to handle complex meshing geometries with points and lines added to the geometry. As the lines of the cross section and borehole points were being added to the mesh, it was determined that this mesh generator would create the smoothest mesh with less element size errors (DHI-WASY, 2011).

Nodal spacing of the two-dimensional models ranged from 0.1 m to 3.0 m along the cross-sections, with the smallest elements located along the shallower layers taken from the 3-D model. A total of 4,317 nodes were used in the Craigmore cross-section and 10,779 nodes for Loughbrickland. As the two-dimensional mesh only included lines along the layers imported from the three-dimensional models, it was determined that the T-mesh would develop a reasonable mesh. The mesh of the two-dimensional model; however, had to be refined more than the three-dimensional mesh to ensure convergence. This refinement was not completed in the three-dimensional mesh as it would make the three-dimensional model more complex and the comparison would become more difficult and time-consuming, whereas this refinement was required for the two-dimensional model to simulate results without convergence issues. One of the purposes of this study was to evaluate whether the two-dimensional modelling conventionally undertaken in support of slope stability analyses are applicable at these sites, consequently, simpler model development methods were used as much as possible.

3.2.3 Boundary Conditions

The boundary conditions for each of the three-dimensional models were determined using the groundwater contour maps, surface water bodies and elevation highs and lows, as described above. No flow boundary conditions were placed on areas where flow was not expected to pass the model geometry, such as at groundwater divides. In areas where surface water bodies were present, a constant head boundary condition was applied and the hydraulic head was set to equal

the elevation (pressure is 0 kPa). When a groundwater contour was used to determine a model boundary, a constant head boundary condition equal to that contour was applied to the weathered bedrock surface layer along that geometry boundary. The bottom boundary of each model was assumed to be the surface of an un-weathered bedrock zone and was assigned as a no flow boundary.

A recharge condition was applied in the three-dimensional models to the surface layer using the Feflow *in/out flow* parameter in the material properties section. The recharge input was estimated using water balance calculations for each of the sites, as discussed in Section 3.2.5. For the steady-state models, an annual recharge estimate was applied to the surface. The magnitude of this recharge was then varied by 10 mm $year^{-1}$ until a "best-fit" model could be reached for each of the cases. In areas where seepage was expected, a seepage face boundary condition was applied to the surface layer. These seepage face boundary conditions allow seepage to occur when the hydraulic head at the surface layer is equal to the elevation (pressure equals 0 kPa). This boundary condition prevents infiltration of water into these nodes, which may not always be realistic, but is a limitation of the software.

The same boundary conditions were used for the two-dimensional simulations as those presented for the three-dimensional scenarios above. The only difference that exists between each model is the boundary condition used to apply recharge at the surface layer. In the two-dimensional case, the model is developed in a cross-section view instead of a planar view. To ensure that the recharge was applied in a similar matter, the *sink/source* boundary condition was applied to the first layer of elements representing layer 1 in the cross-section. The surface nodes were then applied with the same seepage face boundary condition that was applied in the three-dimensional model.

3.2.4 Material Properties

A material properties database was developed for each of the study sites to ensure that all input parameters for the simulations was available, either through literature review, laboratory work or field testing. Some of these parameters included hydraulic conductivity, soil water

characteristic curves (SWCCs) and porosity. The hydraulic conductivity parameters were estimated using *in situ* test results, as explained above. Porosity values were estimated based on measurements from field samples and then used to help estimate SWCCs.

The Van Genuchten method was used to determine the SWCCs for each material type. The parameter fitting software that is a part of the Feflow modeling package was used to help determine each parameter for the Van Genuchten equation in Feflow. This software requires that a relationship between saturation and matric suction be input prior to obtaining a "best-fit" of Van Genuchten parameters. The resultant parameters were then entered into Feflow on individual elements of the model mesh representing each material type. SWCC for Loughbrickland were taken from previous research by Clarke (2007) and current research being undertaken by McLernon (2014). The Craigmore SWCC for the glacial till and surface materials were estimated based on soil index properties. The Van Genuchten equation was used to develop these curves and is given by:

$$S = \frac{1}{\left[1+(\psi/a)^b\right]^c} \tag{3.3}$$

where S is the saturation, ψ is the matric suction (kPa) and a, b and c are constants, defined by:

$$a = 0.0015(WPI)^3 + 0.1028(WPI)^2 + 0.5871(WPI) + 11.813 \tag{3.4}$$

$$b = 0.00011(WPI)^2 - 0.01358(WPI) + 1.76987 \tag{3.5}$$

$$c = -5 \times 10^{-6}(WPI)^2 - 0.00014(WPI) + 0.14175 \tag{3.6}$$

where WPI is the weighted plasticity index of the soil (%) using the amount of soil passing through the #200 U.S. Standard Sieve (decimal) and the plasticity index (%). This method was based on research by Ganjian et al. (2007). The WPI is defined by:

$$WPI = Material\ passing\ \#200\ Sieve \times Plasticity\ Index \tag{3.7}$$

The SWCC for the weathered bedrock zone at Craigmore could not be estimated because of the lack of access to material. To ensure that a curve was still available, the Feflow default curve was used, which is similar to an SWCC of a coarse sand material with a low porosity.

This was deemed reasonable as it was anticipated that the weathered bedrock zone would remain saturated.

3.2.5 Water Balance and Recharge Estimation

A simple, one-dimensional water balance calculation was developed for the study sites to estimate recharge into the groundwater. The water balance equation was written as follows:

$$\Delta S = P - AET - RO - R \tag{3.8}$$

where ΔS is the change in water storage of the vadose zone (mm), P is the measured precipitation (mm), AET is the actual evapotranspiration (mm), RO is the runoff (mm) and R is the recharge (mm).

Potential evapotranspiration (PET) was calculated using the FAO Penman and Monteith combination method (Allen et al., 1998):

$$PET = \frac{0.408\Delta(R_n - G) + \gamma^{900}/_{T+273} u_2 (e_s - e_a)}{\Delta + \gamma(1 + 0.34u_2))} \tag{3.9}$$

where Δ is defined in:

$$\Delta = \frac{2508.3}{(T+237.3)^2} \cdot \exp\left(\frac{17.3 \cdot T}{T+237.3}\right) \tag{3.10}$$

R_n is the net solar radiation (MJ m^{-2} d^{-1}), G is the soil heat flux density (assumed to be 0 MJ m^{-2} d^{-1} for daily estimations), γ is the psychometric constant (kPa K^{-1}), T is the air temperature (ºC), u_2 is the wind speed (m s^{-1}), e_s is the saturated vapour pressure, given by:

$$e_s = e^* = 0.611 * exp\left(\frac{17.3+T}{T+237.3}\right) \tag{3.11}$$

where RH is the relative humidity (%) and e_a is the actual vapour pressure:

$$e_a = RH \cdot e^* \tag{3.12}$$

All equations above are given by Dingman (2002).

As only solar radiation (MJ m^{-2} d^{-1}) was available from the BADC database, the net solar radiation was determined using methods given by the Allen et al. (1998). This method involves the calculation of the extraterrestrial radiation and net longwave and shortwave radiation. The extraterrestrial radiation can be estimated using:

$$R_a = \frac{24(60)}{\pi} G_{sc} d_r (\omega_s \sin(\varphi) \sin(\delta) + \cos(\varphi) \cos(\delta) \sin(\omega_s)) \quad (3.13)$$

where R_a is extraterrestrial radiation (MJ m^{-2} d^{-1}),G_{sc} is the solar constant (0.0820 MJ m-2 min^{-1}), d_r is the inverse relative distance Earth-Sun, ω_s is the sunset hour angle, φ is the latitude (radians) and δ is the solar decimation. The net longwave radiation is calculated by:

$$R_{nl} = \sigma \left(\frac{T_{maxK}^4 + T_{minK}^4}{2}\right) \left(0.34 - 0.14\sqrt{e_a}\right) \left(1.35 \frac{R_s}{R_{so}} - 0.35\right) \quad (3.14)$$

where R_{nl} is the net outgoing longwave radiation (MJ m^{-2} d^{-1}), σ is the Stefan-Boltmann constant (4.903 x 10-9 MJ K^{-4} m^{-2} d^{-1}), T_{maxK} is the maximum daily absolute temperature (K), T_{minK} is the minimum daily absolute temperature (K), R_s is the solar radiation (MJ m^{-2} d^{-1}) and R_{so} is the clear-sky radiation. The net shortwave calculation is as follows:

$$R_{ns} = (1 - a) R_s \quad (3.15)$$

where R_{ns} is the net incoming shortwave radiation (MJ m^{-2} d^{-1}) and a is the albedo (assumed to be 0.23 for grass reference crop). The inverse relative distance Earth-Sun required above can be determined using the following equation:

$$d_r = 1 + 0.033 \cos\left(\frac{2\pi}{365} J\right) \quad (3.16)$$

where J is the number of the day in the year, where January 1st is J = 1. The sunset hour angle and solar decimation are determined by:

$$\omega_s = \arccos[-\tan(\varphi) \tan(\delta)] \quad (3.17)$$

$$\delta = 0.409 \sin\left(\frac{2\pi}{365}J - 1.39\right) \quad (3.18)$$

The clear-sky radiation can also be calculated by:

$$R_{so} = (0.75 + 2e^{-5}z)R_a \quad (3.19)$$

where z is the station elevation above sea level (m) (Allen et al., 1998). Finally, the net radiation can be determined by the following simple equation:

$$R_n = R_{ns} - R_{nl} \quad (3.20)$$

AET was then taken as a proportion of PET based on a relative water content within the rooting zone defined as follows:

$$\theta_{rel} = \frac{(\theta - \theta_{pwp})}{(\theta_{fc} - \theta_{pwp})} \quad (3.21)$$

where θ_{rel} is the relative water content, θ is the actual water content, θ_{pwp} if the permanent wilting point and θ_{fc} is the field capacity. The permanent wilting point and field capacity were estimated using the SWCC curves and vadose zone water content monitoring given by the EnviroScan equipment. Daily AET was calculated by multiplying the relative water content by the PET value (Dingman, 2002). If the water content of the vadose zone reached saturation, a runoff (RO) function was then turned on to remove excess water until the water content was brought back down below the saturated water content. Precipitation was applied at a daily rate (mm day^{-1}) and was calculated by summing the hourly precipitation measurements given by the BADC database.

The STELLA software package (ISEE Systems, 2011) was used to develop a system dynamics model showing the water content dynamics of the upper vadose zone and the recharge into the upper till soil profile. Seepage from the upper till into the lower till was also incorporated into the model simulation to allow the upper till water table to be simulated. This was completed to ensure that an accurate representation of the potential saturation of the upper till, shutting down the movement of water into the till and creating a water table within the vadose zone.

An average weighted soil water content within the rooting zone and the upper till was estimated by dividing the total volume of water in each zone by the total volume based on the water content measurements from the EnviroScan monitoring. The total volume of water at saturation was calculated using the porosity of each soil type and multiplying it by the volume of each soil zone. The volume and porosity of the lower till zone was not included, as it was assumed to be far enough from the rooting zone to have no effect on the overall recharge rate into the upper till.

Recharge into the underlying glacial till layer was assumed to occur only when the rooting zone was above field capacity. The recharge rate was calculated by a function of the hydraulic conductivity and overall head gradient of the glacial till. Recharge was then accumulated on a daily basis in STELLA and summed at the end of the simulation year to determine the annual recharge rate.

At the end of each simulation, the change in water volume was used to update the water content within the rooting zone. These water contents were compared to field data from the EnviroScans at the crest of each site slope for calibration. The "best-fit" models were determined using all data in the following model verification equations:

$$\mathrm{RMSE} = \sqrt{\frac{\sum_{i-1}^{n}(O-P)^2}{n}} \tag{3.22}$$

where RMSE is the root mean square error, O is the observed or actual hydraulic head (m), P is the predicted or simulated hydraulic head (m) and n is the number of observations. The RMSE value closest to zero would indicate the "best" model.

$$\mathrm{MARE} = \frac{1}{n} \times \sum \left(\frac{|O-P|}{O}\right) \tag{3.23}$$

where MARE is the mean absolute relative error, where the value closest to zero would also indicate the "best" model (Dawson et al., 2007).

$$\mathrm{R} = \frac{\sum(O-\bar{O})(P-\bar{P})}{[\sum(O-\bar{O})^2]^{0.5}[\sum(P-\bar{P})^2]^{0.5}} \tag{3.24}$$

where R is the Pearson's product-moment correlation coefficient, $\bar{O}$ is the mean observed or actual hydraulic head (m) and $\bar{P}$ is the mean predicted or simulated hydraulic head (m). The model with an R nearest to 1 would be considered the "best" calibration.

$$E = 1 - \frac{\sum(O-P)^2}{\sum(O-\bar{O})^2} \quad (3.25)$$

where E is the coefficient of efficiency and where a result of 1 would indicate the "perfect" model and a negative score indicates the model is not at all representative.

$$d = 1 - \frac{\sum(O-P)^2}{\sum(|P-\bar{O}|+|O-\bar{O}|)^2} \quad (3.26)$$

where d is the index of agreement, where the "best" model would be indicated by the result nearest 1 (Legates and McCabe Jr., 1999). The "best-fit" water balance was determined based on the simulation that was able to reach water storage fluctuations that obtained the most "perfect" score for the highest number of calibration equations (Equations 3.22 to 3.26). This "best-fit" was then used to simulate the water balance of a "wet", "average" and "dry" year to determine the reasonableness of the recharge being used in the "best-fit" steady state groundwater flow models. As AET is considered to occur at a similar rate each year because of the expectation that AET=PET for most years, only precipitation will be used to determine each of the "wet", "average" and "dry" years.

3.3 Hydrogeological Model Calibration/Verification Parameters

The model calibration equations RMSE, MARE, R, E and d (equations 3.22 to 3.26) were also used to determine the "best-fit" steady state simulations for both the three-dimensional and two-dimensional hydrogeological scenarios. The observed or actual heads used in these equations were determined using the average water level of the standpipes at each site that are currently undergoing monitoring. Standpipes reaching bedrock along the crest of the Loughbrickland cutting (BH1, BH2 and BH2A) were not used in the calibration methods, as these standpipes have been plugged and monitoring has not been undergoing since installation.

The resultant recharge parameters used in each of the "best-fit" simulations were also compared to the water balance recharge estimates to ensure that a reasonable value was being used.

3.4 Steady-State Simulations – Base Model

Steady state simulations were developed to create a base model for each of the simulations. These simulations were developed using the model calibration/verification factors described above to ensure a reasonable conceptual model was being used. The models were first developed using a saturated system, where the unsaturated Van Genuchten parameters were not used, to allow for a simple conceptual model to be developed. Once these models were determined to provide a reasonable simulation of the flow system the model was made more complex by adding the unsaturated material properties to the simulation. These models were subjected to the calibration/verification procedures described above until a "best-fit" model was developed. These "best-fit" models were then subjected to more complex testing through sensitivity analyses described below.

3.5 Sensitivity Analyses

To understand the importance of the estimated simulation parameters on the flow system, a series of sensitivity analyses were completed. The sensitivity analyses were primarily used on the three-dimensional models to indicate the reasonableness of the parameters used in each model. The two-dimensional models were subjected to only the base scenarios to help compare them to the three-dimensional models.

The three-dimensional models were subjected to three sensitivity analyses, separate from the two-dimensional simulations. One of these analyses included varying the transmissivity of the bedrock. The hydraulic heads simulated in each of the transmissivity models were compared to the average observed hydraulic heads in the field. The observed versus simulated hydraulic head distributions for each simulation were then plotted against the various values of transmissivity used in this analysis to show the reasonableness of the final value used for the

bedrock transmissivity in the three-dimensional model. The evaluation equations were also used to determine the "fit" of the transmissivity values used in the sensitivity analysis.

The "best-fit" three-dimensional, base models were then used to determine the impact of varying the hydraulic conductivity on the surface and glacial till layers on recharge rates. As different ratios of recharge to hydraulic conductivity can result in similar head distributions, this analysis was used to show the appropriateness of the final material properties applied to the base model. Further sensitivity of the simulation to the hydraulic conductivity values used within the domain was completed. Similar to the bedrock transmissivity models, results of this analysis was plotted with the observed versus simulated hydraulic head distributions, as well as evaluated using the evaluation equations described above. These plots were then used in the analysis of varying material properties of the upper and lower glacial till layers individually in the three-dimensional models.

The three-dimensional models were then subjected to one more sensitivity analysis to help with the comparison and analysis of each. In this analysis the influence of bedrock topographic "roughness" on the overall groundwater model was evaluated. The "roughness" was considered to be the presence of convex and concave surfaces in the bedrock topography, as found in the seismic refraction surveys completed at each site. The weathered bedrock zone was kept at a constant depth for these analyses. Further analysis could be completed on the effect of varying depths of the weathered zone between the glacial till and bedrock on the overall groundwater system.

A "smooth" bedrock surface was developed for each of the sites by simplifying the interpolation to include only a few points from each of the seismic refraction transects and the borehole data. The overall mesh size was changed to a coarser nodal spacing when interpolating the bedrock data. While doing this, the borehole depths were kept in the interpolation, while the seismic refraction surveys along the drumlin were given less priority. This allowed the bedrock topography to show less "bumps". These "smooth" elevations were then applied to the three-dimensional models to analyze the changes in the overall groundwater system. Table 3.2 summarizes each of the model scenarios applied to each dimensional model and site.

Table 3.2 Model scenarios applied to each site and dimensional model, including the appropriate results section in brackets.

Model Scenario	Simulation Applied to*			
	CM2-D	CM3-D	LB2-D	LB3-D
Base Case	√ (5.1.3)	√ (5.1.3)	√ (5.2.2)	√ (5.2.2)
Recharge Rate versus Hydraulic Conductivity		√ (5.1.4)		√ (5.2.3)
Bedrock Transmissivity		√ (5.1.4)		√ (5.2.3)
Presence of mid-slope "bench"				√ (5.2.3)
"Rough" vs. "Smooth" Bedrock surface		√ (5.1.4)		√ (5.2.3)

* where CM = Craigmore, LB = Loughbrickland, 2-D = two-dimensional simulation and 3-D = three-dimensional simulation.

4.0 RESULTS AND DISCUSSION – FIELD TESTING AND MONITORING DATA

The laboratory and in situ test results from each site are discussed in this section. The Craigmore site will be discussed first, with information on standpipe installations, monitoring equipment data and testing for material properties (in situ and laboratory). Similar information will also be provided for the Loughbrickland site in the following sub-section. All of the data following in this section has been used to develop the three- dimensional and two-dimensional models for each site. Results of each of the models will be discussed further in Section 5.0.

4.1 Craigmore Railway Cutting

The Craigmore railway cutting was considered to be the primary study site as this site was the older of the two sites, continues to require ongoing monitoring and maintenance by NIR, and has undergone a number of shallow slips along the embankment.

4.1.1 Site Geology

As described in previous sections, the Craigmore site is located on a granitic pluton that is located along the southern portion of Northern Ireland. The glacial till overlying the bedrock appears to be from two different depositional periods. As seen in the borehole logs (McLernon, 2014), the drumlin has a stiff glacial till overlain by approximately 5 – 8 m of a glacial till with a higher sand and gravel content.

Figure 4.1 shows a conceptual diagram of a geological cross section of the Craigmore cutting. Excavation of the cutting would have stripped away the upper sandy glacial till and the underlying glacial till would have been exposed to the atmosphere. A new topsoil profile developed along the exposed surface of these tills and this profile will be described further in the laboratory results section below. Samples were taken from each of these materials along the

cutting to further understand the geotechnical properties associated with each.

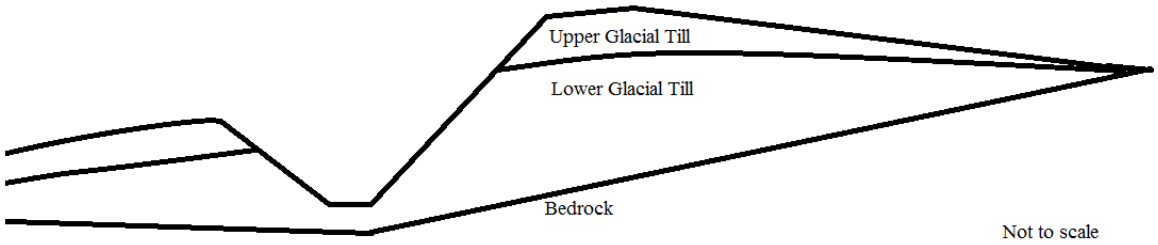

Figure 4.1 Cross section of the geological stratigraphy at the Craigmore railway site (approximately 250 m in length).

4.1.2 Laboratory Results

Particle size distributions were determined by the researchers at Queen's University Belfast (Carse, 2014) using standard hydrometer and sieve methods. Results of these analyses are shown in Figure 4.2. Particle size distributions were further analyzed using the soil triangle method, where the plots of sand, silt and clay percentages were plotted on the soil triangle (Figure 4.3). This plot indicates that the soil type is dominantly a sandy loam, with some samples having lower sand or higher clay content, thus becoming a sandy clay loam or loam. The depth of the samples ranged from approximately 0 to 10 m.

Soil classification exercises conducted at the site were used to determine the appropriate layering of materials on site, as well as to compare with the types of soils described from the particle size analysis completed above. All soils were found to have mottles within the upper 0.6 m of the soil profile. This characteristic is indicative of the soil being saturated intermittently throughout the year, which is expected of the area. Other soil surveys completed near the study sites have shown that surface-water-gley soils are one of the dominant soil types in the area (Cruikshank, 1997). The presence of these mottles show that soil profiles along the cuttings of each site would also be considered surface-water gley soils.

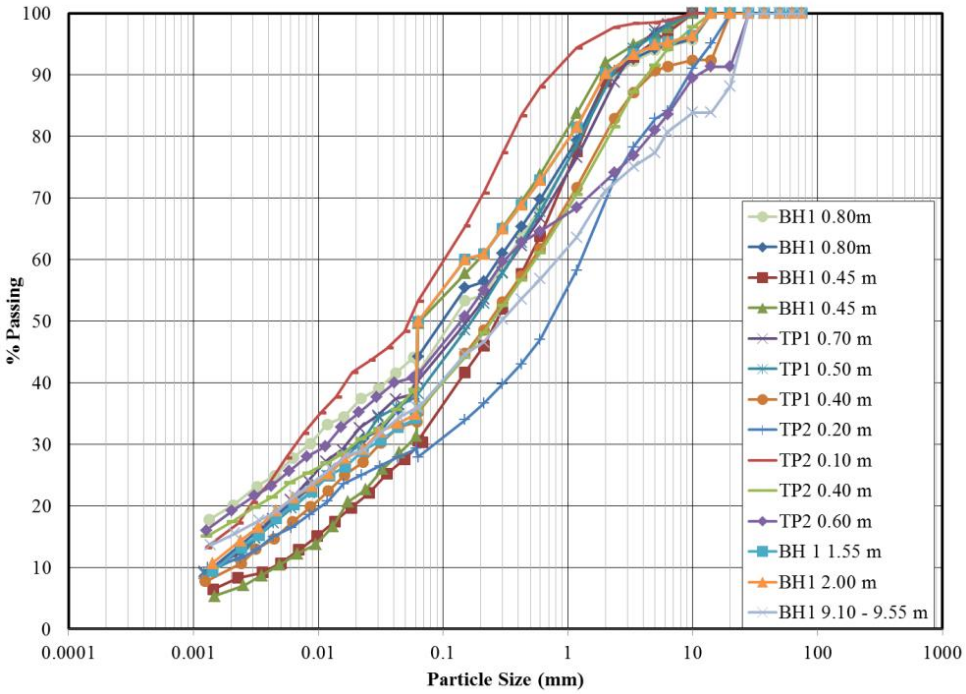

Figure 4.2 Particle size distribution of soil samples taken from the upper 10 m at Craigmore.

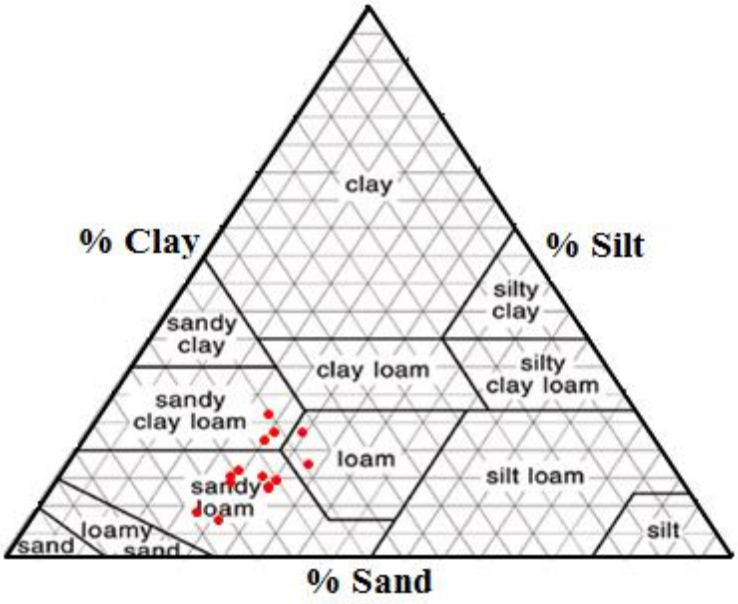

Figure 4.3 Soil texture triangle with samples taken from Craigmore site in upper 10 m of soil (Source of Triangle: Graham and Midgley, 2000).

The depth of the A horizon at the Craigmore site varied from 0.3 m to 0.6 m and was greatest at the crest of the cuttings. Along the toe, the A and B horizons were much shallower, and may be indicative of the natural A and B horizons being stripped away during the excavation and reflect the development of new A and B horizons because of weathering of the exposed

slope. The presence of vegetation along the slope of the cuttings suggests that new A and B horizons are being developed (Figure 4.4).

a)  b) 

Figure 4.4 Images showing one of the soil pits dug at the Craigmore site at the crest (a) and along the cutting (b).

Dry density values (Tables 4.1 and 4.2) indicate that the soil becomes more compact with increasing depth. Dry density values were used to calculate porosity and void ratio, assuming that the soils were saturated. A thick layer of sandy glacial till overlies the lower glacial till at the crest of the cutting. This can be seen in the different void ratios and densities in the upper 0.5 m of ES02. The void ratios calculated for each of the EnviroScans are comparable to other loam tills that have higher clay fractions. Laboratory tests completed by Grisak and Cherry (1974) show a range in void ratios from 0.38 to 0.68 for a clay loam till with an approximate hydraulic conductivity of 1.80×10^{-9} m s^{-1}. The higher values of void ratio are near the surface of the profile as expected for soils which have undergone weathering and are composed of higher organic contents associated with the root zone. In a study completed by Aimrun et al. (2004), the void ratio of the topsoil ranged from 0.40 to 2.08. Although the soil described by Grisak and Cherry (1974) and Aimrun et al. (2004) generally have higher clay fractions then what was experienced at the site, the wide range in void ratios can be expected to occur in topsoil material.

Table 4.1 Dry densities, porosities and void ratios of samples taken from Craigmore during EnviroScan installations (where particle density is assumed to be 2.65 g cm^{-3}).

Depth (m)	ES01 (toe of cutting)			ES02 (crest of cutting)		
	Dry Density ($g\ cm^{-3}$)	Porosity (%)	Void Ratio	Dry Density ($g\ cm^{-3}$)	Porosity (%)	Void Ratio
0.1	1.35	49.1	0.96	0.84	68.3	2.15
0.2	1.57	40.8	0.69	1.37	48.3	0.93
0.3	1.61	39.3	0.65	1.54	41.9	0.72
0.4	1.94	26.8	0.37	1.36	48.7	0.95
0.5	1.9	28.3	0.39	1.7	35.9	0.56
0.6	-	-	-	1.65	37.7	0.61
0.7	2.04	23.0	0.30	1.64	38.1	0.62
0.8	-	-	-	1.76	33.6	0.51
0.9	2.14	19.3	0.24	1.78	32.8	0.49

Table 4.2 Atterberg limits of samples taken from Craigmore (Borehole 1).

Depth (m)	Liquid Limit (%)	Plastic Limit (%)	Plasticity Index
1.95 – 2.00	31.50	15.27	16.23
6.50 – 6.55	31.60	15.40	16.20
11.00 – 11.05	32.20	16.92	15.28
13.90 – 13.95	-	16.26	-
15.40 – 15.45	30.50	13.94	16.56

Source: M. McLernon and L. Carse (2011)

Samples collected at a depth of 0.1 m in ES02 included large amounts of organic matter associated with the roots of long grasses that are dominant in the area. This causes a decrease in the overall bulk density of the soil, which will increase the values of porosity and void ratio. This high amount of organic matter in the soil sample also made it difficult to collect an undisturbed sample. Values of porosity calculated for samples retrieved from upper 0.1 m of the profile during installation of the EnviroScans (ES01 and ES02) indicate that the upper soil material has a much higher porosity than seen at greater depths. The dense vegetation on site

described above would increase the porosity of the soil by increasing the sizes of macropores and root spaces.

The liquid and plastic limits determined in the laboratory program (Table 4.2 and Figure 4.5) are similar to those measured for other glacial clay tills around the world. Milligan (1976) reported a range of liquid and plastic limits for glacial clay till samples taken from locations in Canada (Alberta and Ontario) and Scotland. Liquid limits ranged from 28% in eastern Canadian and Scottish glacial tills to 30% in western Canadian glacial tills. Plastic limits for these samples ranged from 14% in Canadian glacial tills to 20% in Scottish tills. Grisak and Cherry (1975) also reported liquid limits of 22-30% for glacial tills taken from southeastern Manitoba. The water contents of the samples taken are typically below or similar to the plastic limit, indicative of over- consolidated soils like glacial tills. The plasticity index for the glacial till samples taken from the Craigmore site are considered to be low to medium plasticity, with a group name of clayey sand (ASTM Standard D2487, 2000). The plasticity index, combined with the particle size distribution analysis (Figure 4.2), was used to determine the engineering classification of the soil found at the Craigmore site. It was determined that the soils of the upper 2.0 m at Craigmore are considered to be silty sand.

Soil-water characteristic curves were estimated using the WPI van Genuchten method described in Section 3.2.1.4 using the measured particle size distributions (Figure 4.6). A single SWCC was used to represent the surface soils within the upper 0.5 m of the model, while the till SWCC was applied to the remaining till layers. The bedrock SWCC was given default values by Feflow, as this material is expected to remain saturated. The SWCC curves give an approximate air entry value (AEV) of 9 kPa, 12 kPa and 0.15 kPa for the surface, glacial till and weathered bedrock zones, respectively. A porosity of 0.45 for the surface materials was considered reasonable, given the porosity estimates found during laboratory analysis seen above. A porosity of 0.35 was assigned to the glacial till, which was based on soil sample analyses obtained from Queen's University Belfast (McLernon, 2014). A porosity of 0.10 was assumed for the weathered bedrock based on research completed by Irfan and Dearman (1978), where granite bedrock weathering patterns were studied.

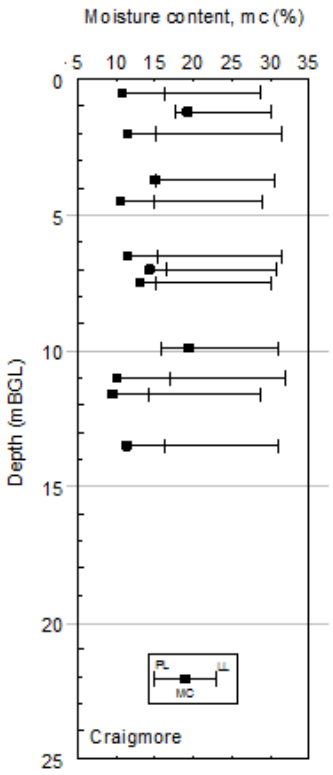

Figure 4.5 Water content, liquid limit and plastic limit versus depth for the Craigmore site (Carse, 2014).

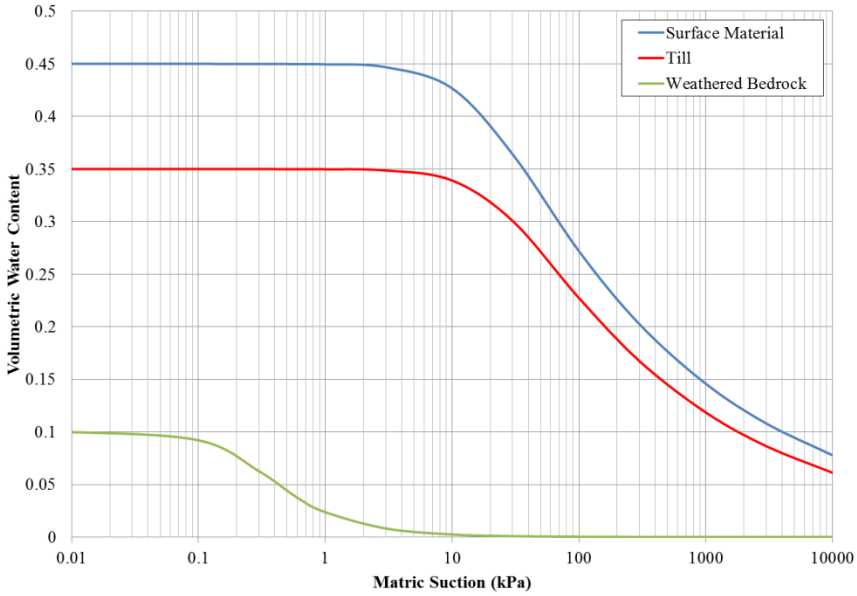

Figure 4.6 Soil water characteristic curves estimated using particle size distribution samples taken *in situ*.

4.1.3 Climate Conditions

The BADC database was used to collect meteorological data from 1960 to 2010 to help develop a climate database that would be usable in water balance analyses. The precipitation from the Armagh database for the year of 1960 to 2010 was analyzed to determine the average annual precipitation rate for Northern Ireland (Figure 4.7). The weather station is located approximately 18 km northwest of the Glenanne precipitation station used for the precipitation data at the sites (Figure 4.8). This frequency analysis shows that the average annual precipitation rate is approximately 820 mm year^{-1}. Extreme values show that "wet" years can have up to 1070 mm year^{-1} and "dry" years as little as 590 mm year^{-1}. The standard deviation of this data was determined to be approximately 94 mm.

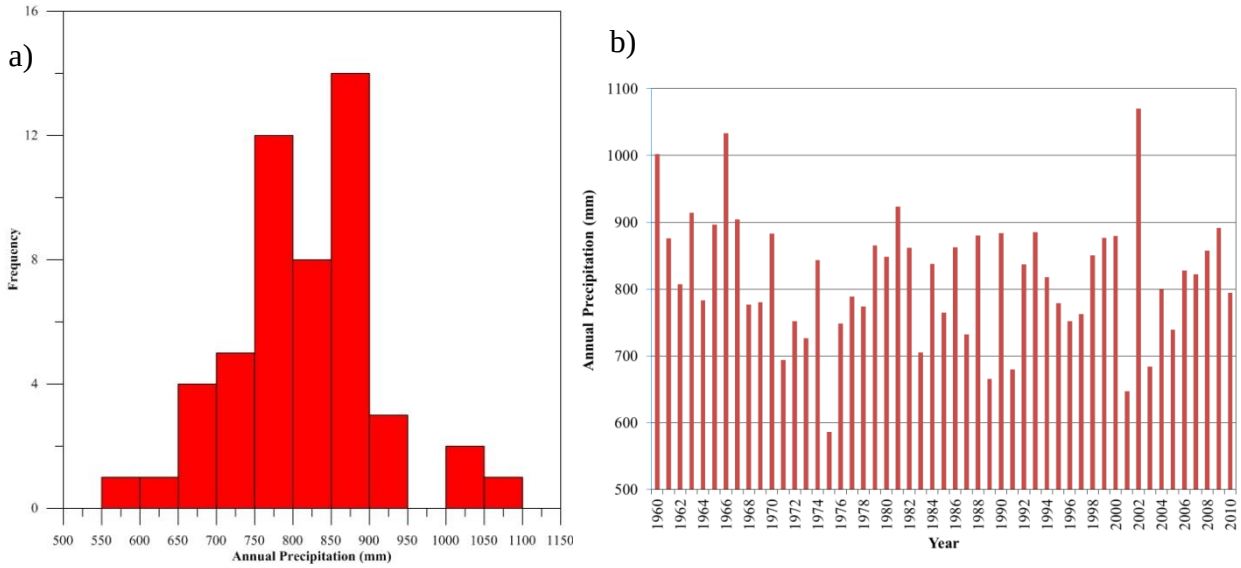

Figure 4.7 Frequency of annual precipitation from 1960 to 2010 (a), with annual precipitation rates for each year (b).

Other collected data include solar radiation, wind speed, relative humidity and maximum, minimum and average air temperature. This data was collected only for those years that were used in the water balance estimation, as shown in Section 5.1.1 (1975, 1994, 2002 and 2009). The station which this data was taken from is located near Aldergrove (source #1450), which is west of Belfast, County Antrim (Figure 4.8). This meteorological station is the only one in Northern Ireland which measures all parameters required for the water balance estimations.

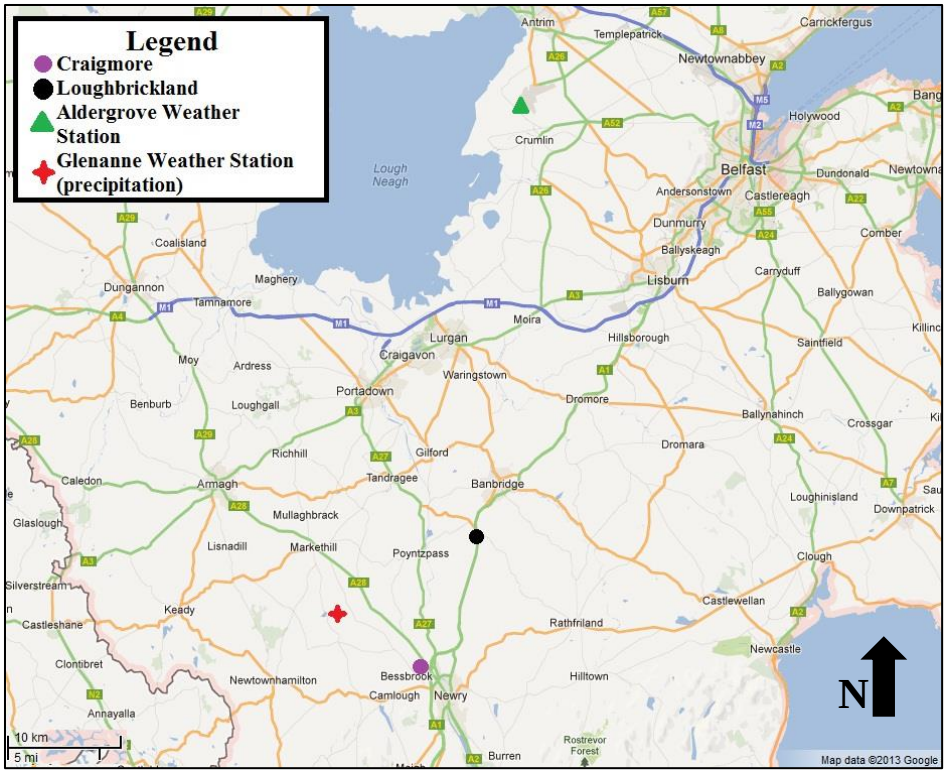

Figure 4.8 Location of the Aldergrove and Glenanne meteorological stations in relation to the location of the study sites (Source: Google, 2011).

4.1.4 Soil Conditions Monitoring

The monitoring periods for each measurement outlined in the Materials and Methods chapter (Section 3.1.1) vary depending on the type of installation, but generally start in early 2009 and are still being monitor. The data reported in this thesis is up to the last data collection sent to the author in April 2011. Further data may be available by students Carse (2014) and McLernon (2014) by the conclusion of their research programs.

Two EnviroScans were installed at the Craigmore study site in 2009 to conduct preliminary measurements of water content. These sensors were not operated very long due to problems with calibration and sensor malfunction. Calibration of the sensors was undertaken during July to August 2010 and the sensors were reintroduced into the field at Craigmore. Monitoring has been ongoing since August 2010, although there is one period of data missing because of technical difficulties in mid-August. The final calibration constants that were

developed based on the laboratory calibration procedure provided by Sentek Pty Ltd (2001) are summarized in Appendix B.

Data collected from the EnviroScan located at the toe of the slope (ES01) is presented in Figure 4.9. This monitoring data shows that the water content of the soil profile remains relatively high, near saturation throughout the year. This is not unexpected given the location of the sensor and the wet conditions in Northern Ireland. The maximum water contents recorded within the profile indicate that the actual porosities in the field may be as high as 0.58 in the upper 0.1 m and as low as 0.37 for the soil below 0.5 m. These values are slightly higher than expected, but could represent the effect of rooting associated with the dense vegetation that exists along the soil surface. The presence of macropores or small fractures within the glacial till may also allow more water to be present within the upper 1.0 m of the soil profile. The quick response time of the sensors in the upper 0.3 m of the profile could be an error resulting from installation. During installation, the dense vegetation and higher conductivity till layer made it difficult to install the EnviroScan access tube. This may have caused some space to form between the tube and the surrounding soil, which would allow water to pool here before draining into the surrounding soil. This would cause a false saturation reading that disappears quickly as the water drains into the soil profile. Other erroneous readings may come from railway traffic causing vibrations to create false saturation.

To further analyze the influence of climate on the water content of the upper 1.0 m of soil at ES01, a tornado plot was developed (Figure 4.10). The plots show the soil water content at different seasons, with three plots surrounding an event of rain that occurred on site on December 27, 2010. The total rain experienced for the site was approximately 16 mm on December 26, 2010 and 18 mm on December 27, 2010. As shown in the tornado plot, the water content on December 26, 2010 showed the lowest water content profile for the dates shown. This is changed quickly on December 27, 2010 during the rainfall events, where the highest water contents are experienced. The total change in water storage in the upper 1.0 m given by ES01 at Craigmore was an increase of 42 mm between December 25 and December 28. This value is larger than the total measured rainfall (34 mm), but this could be a result of runoff pooling near the location of the EnviroScan.

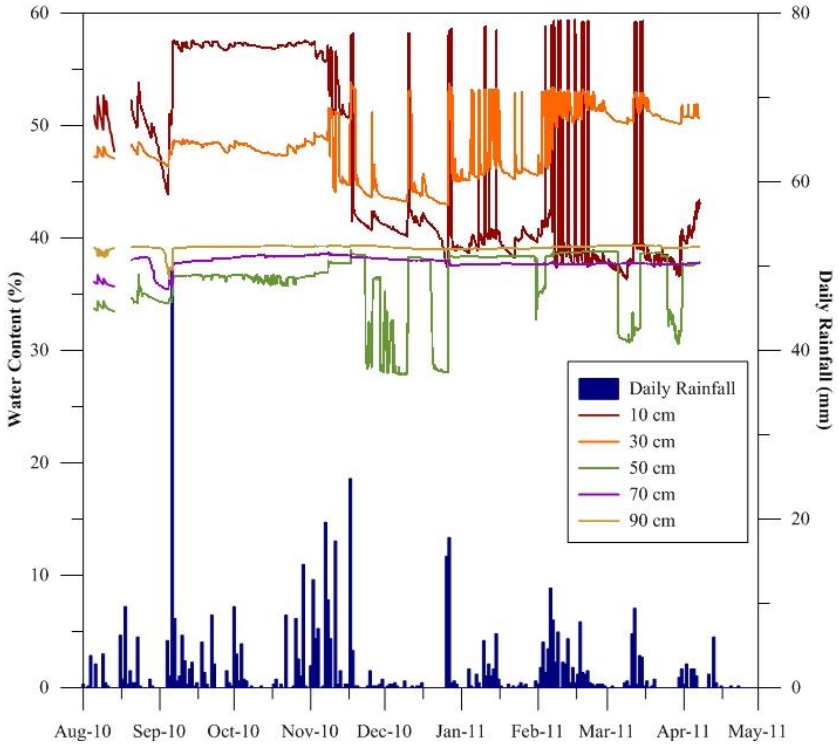

Figure 4.9 Water content measurements at the toe of the slope cutting at Craigmore (ES01).

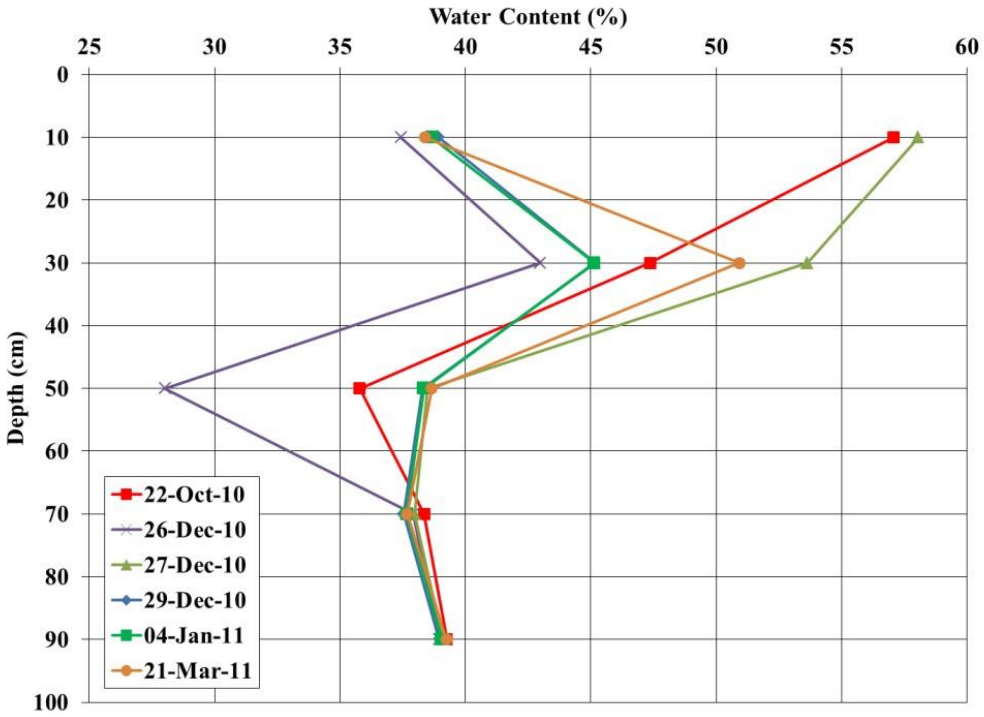

Figure 4.10 Tornado plot of water content along the upper 1.0 m of soil at ES01.

By December 29, 2010, the water content of the profile decreases as the water is slowly draining from the profile to return to the original water content. October also shows another profile with increased water content because of various rainfall events occurring around that date. The upper profile saturates and dries during rainfall events, while the lower sensors (< 0.5 m depth) show a much smaller change in the water content. This could be a result of the lower hydraulic conductivity of the upper till as it becomes less weathered. This could also be indicative of a layer that remains relatively saturated throughout the year, decreasing the impact of rainfall events at that depth. This was also evident above in Figure 4.9 where the water content was fairly static and did not exhibit drastic responses to climatic changes.

The second Craigmore EnviroScan is located near the crest (ES02). Monitoring data collected at this location can be seen in Figure 4.11. The data collected from this location along the upper slope of the cutting indicates that the range of porosity values are different than observed at the toe. In Figure 4.11, the maximum water content appears to be approximately 0.20 in the upper 0.1 m and increases with depth, which could indicate that the upper zone did not receive enough water to saturate the system. The upper soil zone in this area also has a higher sand content than what is observed at the toe, which will have a definite impact on the overall porosity of the material and how fast water drains through the profile. Sand generally has a lower porosity then soils with higher clay or silt fractions. As one moves deeper into the soil profile, the porosity becomes more indicative of a soil material with a lower sand fraction. This can also be seen in samples taken from the sites shown in the particle size distributions above. However, this low observed water content might also be related to installation problems in which there are air gaps between the access tube and the adjacent soil.

The spikes of the water content at ES02 are less drastic when compared to ES01, especially during what appear to be lower water content periods at ES01. As the water content drops in the upper 0.5 m, the occurrence of precipitation causes a drastic rise and fall in the water contents around the sensors. This could be an effect of fracturing or air pockets surrounding the EnviroScan sensors causing water to move more rapidly through the profile. Given the higher clay content near the toe of the slope, there could also be cracking allowing for faster preferential flow in the soil zones of lower water contents. The sensor at 0.7 m for ES02 also shows some

more drastic changes in water content. These may also be a result of air gaps between the access tube and soil contact, as there was some difficulty at this depth during installation. The presence of a rock is suspected at this depth, which would increase the presence of macropores, causing some unrealistic jumps in the values as well.

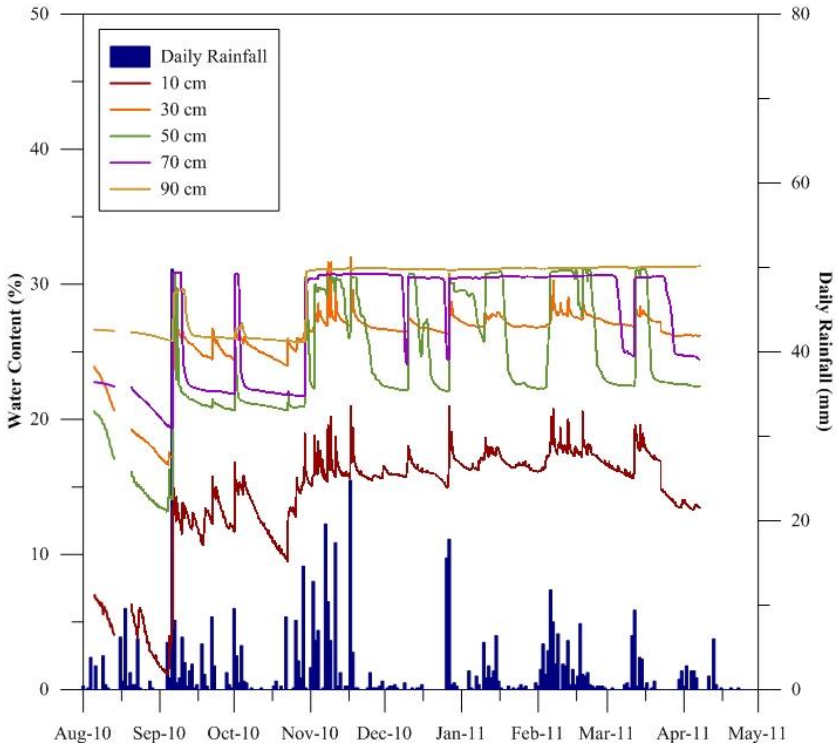

Figure 4.11 Water content measurements at the crest of the slope cutting at Craigmore (ES02).

To further analyze the impact of climatic conditions on the upper 1.0 m soil profile, a tornado plot was developed given the same dates shown for ES01 above (Figure 4.12). This tornado plot shows a slightly different pattern then what was seen at ES01. The entire soil profile shows large increases in water content during the rainfall event that occurred on December 26 and December 27, 2010. An increase of 19 mm in the water storage of the upper 1.0 m was experienced at this location, indicating that some rainfall may have not infiltrated into the profile and instead acted as runoff. The upper soil sensors (> 0.5 m) indicate faster drainage than those at greater depths. This may be indicative of water draining into the lower soil profile, decreasing the speed at which the water content lowers. Also, the decrease of the root mass of vegetation in depths greater than 0.2 m would decrease the presence of macropores, thus decreasing the

hydraulic conductivity experienced in the soil profile. As the water drains from the weathered zone in the upper 0.5 m, the lower soil profile remains saturated for a longer period of time.

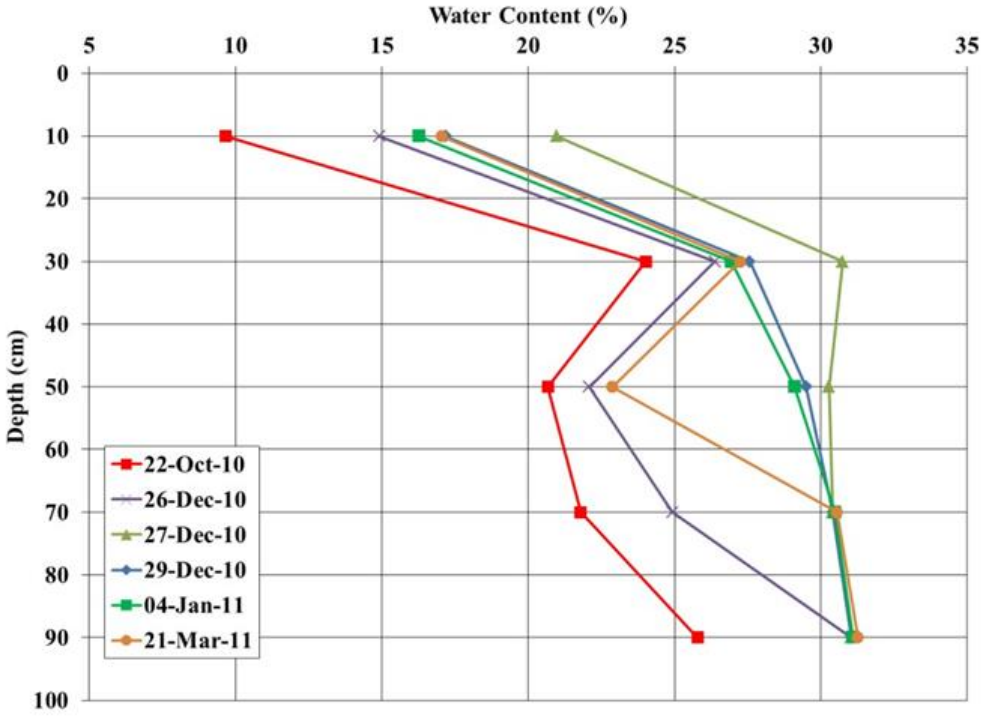

Figure 4.12 Tornado plot of water content along the upper 1.0 m soil profile at ES02.

Four tensiometers were installed along the cutting slope to measure the matric suction within the upper 1.0 m of the soil surface. The tensiometers were installed in July 2010 and have been monitored since that time. One section of data is missing in November 2010, where the batteries of the Datahog datalogger connected to the tensiometers went down. Two of the tensiometers were installed near ES02 at the crest of the cutting, while two were installed along the toe near ES01. The depths of the tensiometers at each location reach approximately 0.5 m and 0.8 m.

The monitoring data in Figure 4.13 shows that the soil profile at the toe of the slope tends to be more saturated than the upper slope. The upper slope tensiometers also show a larger fluctuation during the summer months of monitoring. As this area tends to have a higher sand content in the upper 1.0 m of the soil profile, it would be expected that climate would have a stronger influence on the overall matric suction. Given that the tensiometers at the toe are

generally located in an area where discharge is expected to occur, this area will generally have a higher saturation than the crest where recharge is occurring. The increased clay/silt content of the upper 1.0 m profile at the lower slope would also decrease the climatic impact on the water content because of the soils ability to retain water for longer periods of time.

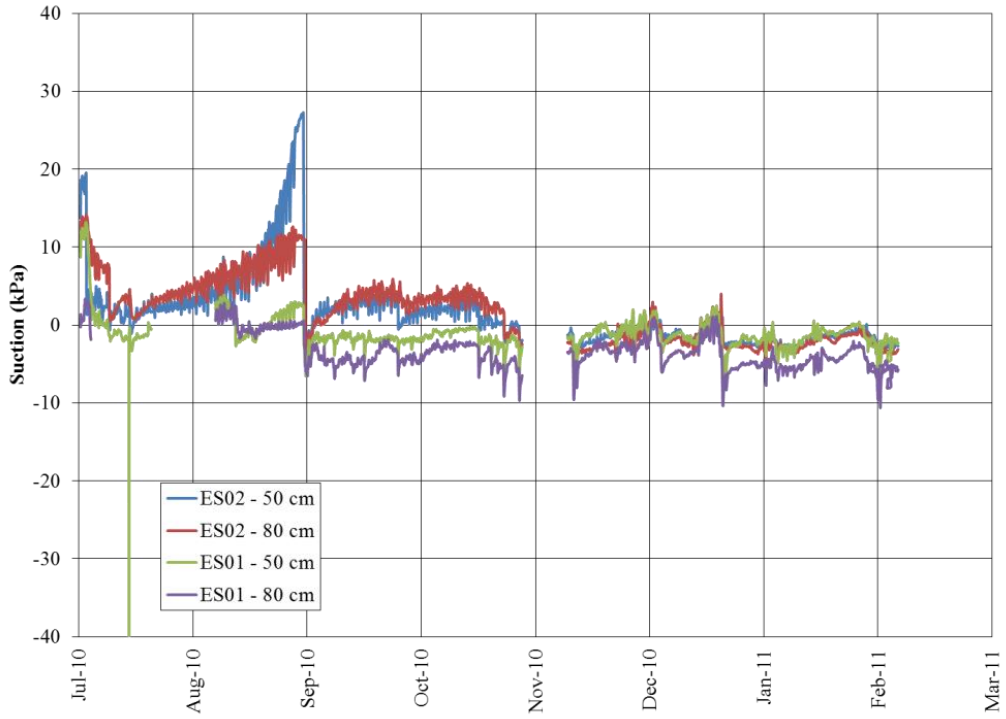

Figure 4.13 Matric suction monitoring at Craigmore near the crest (ES02) and toe (ES01) of the cutting.

Two shallow water wells were installed near the EnviroScans on the crest (ES02) and toe (ES01) of the cutting slope. These shallow water wells were installed within the upper 1.0 m of the soil surface to monitor the potential existence of a shallow water table above the surface of the upper till. Monitoring at the crest of the slope began in January 2010, while monitoring at the toe began in October 2009. Barometric pressure was removed from the 'absolute' data to obtain the 'gauge' pressure data and then converted to hydraulic heads for each location. The wells do not have packers and were not grouted, but were simply placed in an augered hole. The hole had the same width of the standpipes used, so the water level could be monitored simply to determine if a shallow water table was present.

Using depths from a nearby trial pit, the approximately till surface was approximately only 0.1 m below the ground surface. The water level data in Figure 4.14 shows that the near surface zone contains a high enough water content to maintain a water level of at least 0.3 m throughout the year. During times of rainfall, the water increases and sometimes rises above the elevation of the ground. This would be expected at a location where discharge is expected to occur. Also, it appears that the water level trend changes closer to spring, where the base water level increases from approximately 0.3 m to 0.5 m.

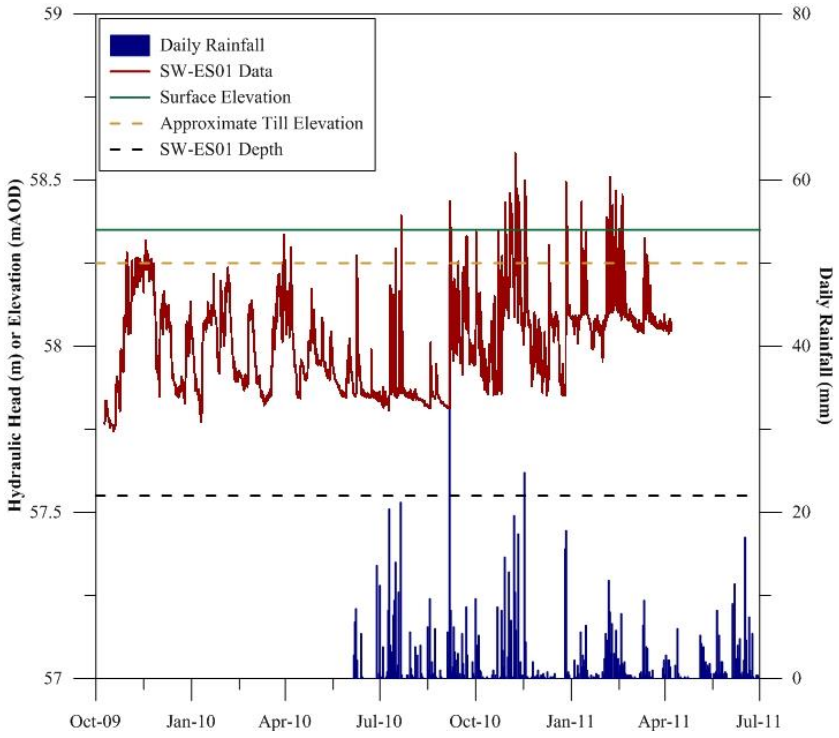

Figure 4.14 Shallow water levels monitored at the toe of the slope near ES01.

At the crest of the slope, the shallow well (SW-ES02) was installed into the sandy upper till to a depth of 0.7 m. The top of the C horizon, expected to be the unweathered upper till, was approximately 0.4 m below the surface using data from a nearby trial pit. Water levels show a different pattern than what was seen at the toe of the slope. As seen in Figure 4.15, the water levels were generally below the till surface. The water level also usually drained from the well quickly after rainfall events, which is expected since the well is located in a recharge zone.

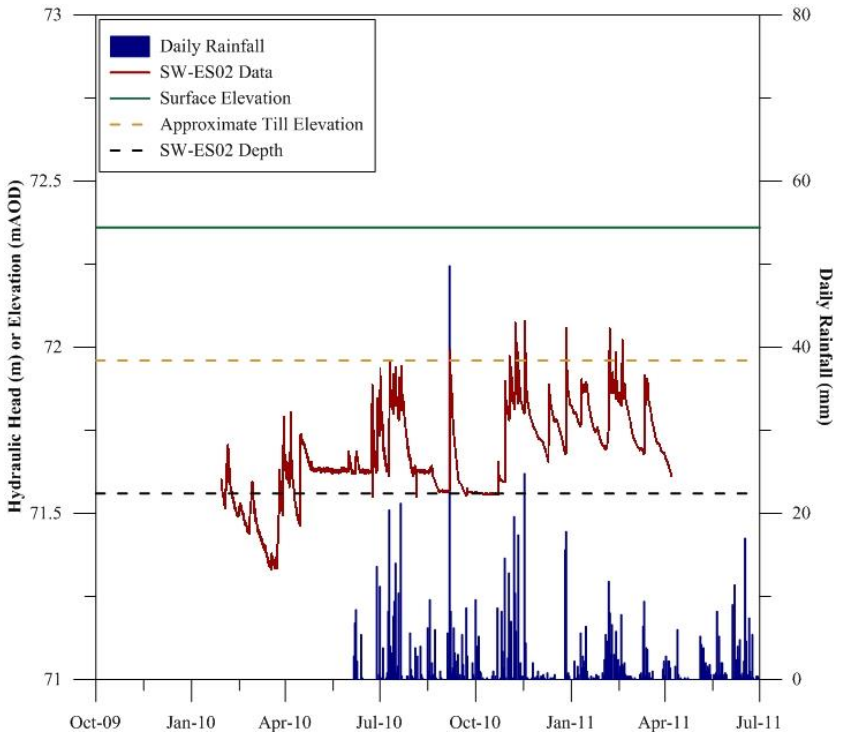

Figure 4.15 Shallow water levels monitored at the crest of the slope near ES02.

Water levels were also measured within each of the standpipes in BH1 for the duration of the monitoring program for this research. The standpipes at BH2 and BH3 were not available during this time due to unforeseen access limitations. Water level monitoring at BH4 began in October 2010 in two of the standpipes that were installed (BH4A and BH4C). Data collected from each of these monitoring programs are shown in Figure 4.16 for BH1 and Figure 4.17 for BH4.

The heads in Figure 4.16 indicate that there are strong downward gradients in the vicinity of BH1 with vertical gradients of close to unity between the mid-level standpipe and the bedrock. The water level response within the upper till at BH1 appears to be directly connected to recharge events at surface. Rises and falls also occur at the middle and bedrock depths, but are much more subdued. The low hydraulic conductivity of the lower till decreases the speed that water can reach the middle standpipe. This would also increase the potential for lateral movement of water in the upper vadose and till zones. Lateral drainage at the bedrock surface may also have some effect on the bedrock standpipe, limiting the range of pore-pressure

fluctuations. The mechanisms controlling these transients are explored in more detail by McClernon (2014).

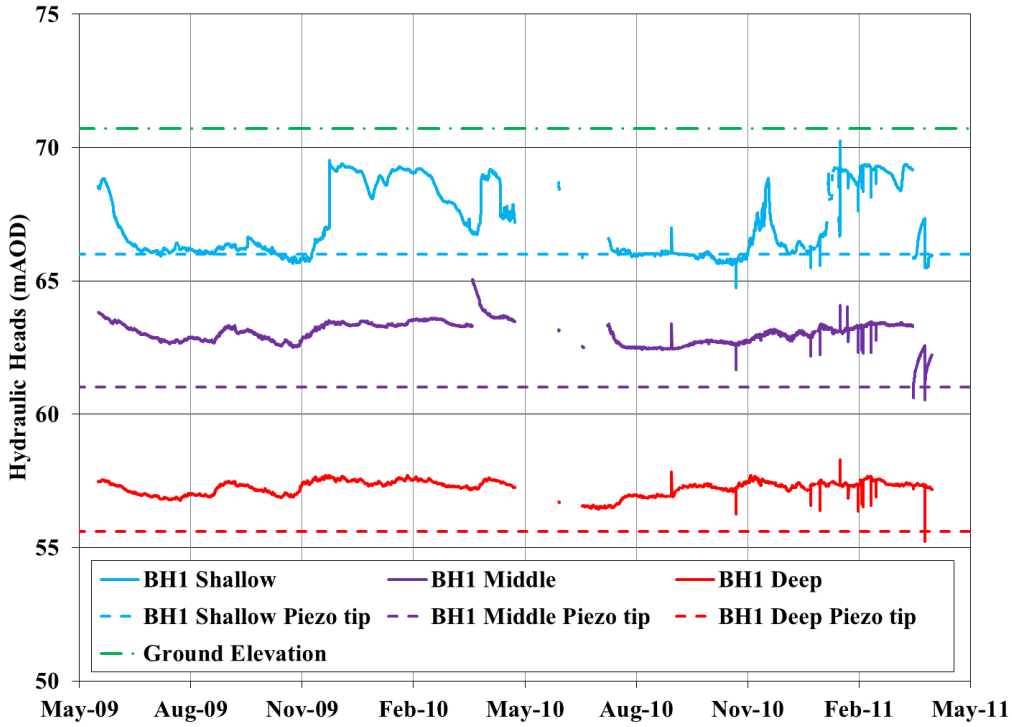

Figure 4.16 Water level monitoring from Craigmore at BH1 from May 2009 to April 2011.

Monitoring conducted at the toe of the slope in BH4A and BH4C shows that water flow is moving from the weathered bedrock towards the surface, such that the heads within BH4C located deeper within the bedrock exceed the heads observed in BH4A. As this area is a discharge zone, the water levels become higher as you move into the weathered bedrock zone from the glacial till. Water was not seen discharging at the site of the shallow well installations, however, because of the thick layer of gravel fill that was laid for the construction of the railway tracks.

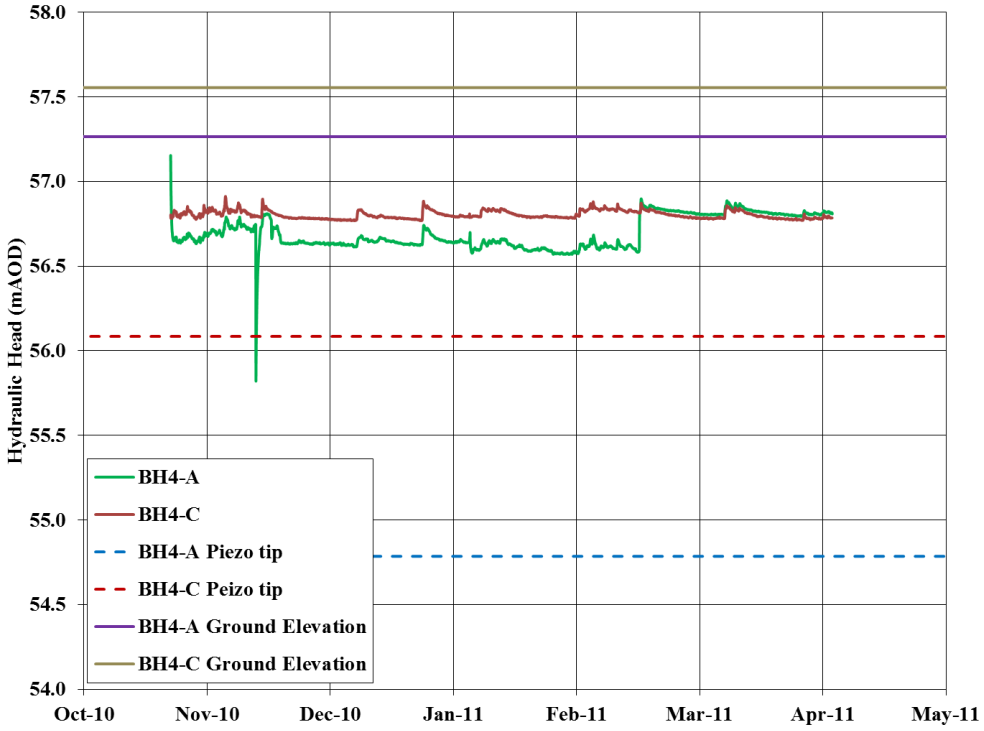

Figure 4.17 Water level monitoring from Craigmore at BH4A and C from October 2010 to April 2011.

4.1.5 Hydraulic Conductivity

Hydraulic conductivity parameters were estimated using slug tests and Guelph Permeameter tests completed in the field. The results of these tests were compiled and compared to develop an estimate of the hydraulic conductivity of the site soil materials. The Guelph Permeameter was used primarily on the upper weathered zone, also considered the vadose zone, and was not used past a maximum depth of 1.0 m. Slug testing was undertaken on each of the standpipes in BH1. These standpipes are located in the upper till, lower till and weathered bedrock zones.

The Guelph Permeameter was used along the Craigmore cutting to a maximum depth of 1.0 m. These tests were conducted along the crest, mid-slope and toe of the slope cutting to get an idea of the changes in hydraulic conductivity and material properties that may exist along the cutting. A total of 11 tests were completed at Craigmore, three at the crest, three at mid-slope

and five at the toe. The final results of these tests can be seen in Figure 4.18. The measured hydraulic conductivity within the 1.0 m profiles along the slope cutting ranged from 1.0 x 10^{-5} m s^{-1} to 1.0 x 10^{-9} m s^{-1}.

The range of hydraulic conductivity within the upper 1.0 m zone was determined to be between 1 x 10^{-8} m s^{-1} and 1 x 10^{-6} m s^{-1}. This was chosen based on the range of hydraulic conductivity values that were shown in Figure 4.18. This range was then used to determine a reasonable hydraulic conductivity in the groundwater flow models for the vadose zone. One layer was used to represent this zone, with another layer underlying it to represent the weathered zone that exists between the vadose zone and the upper till layer.

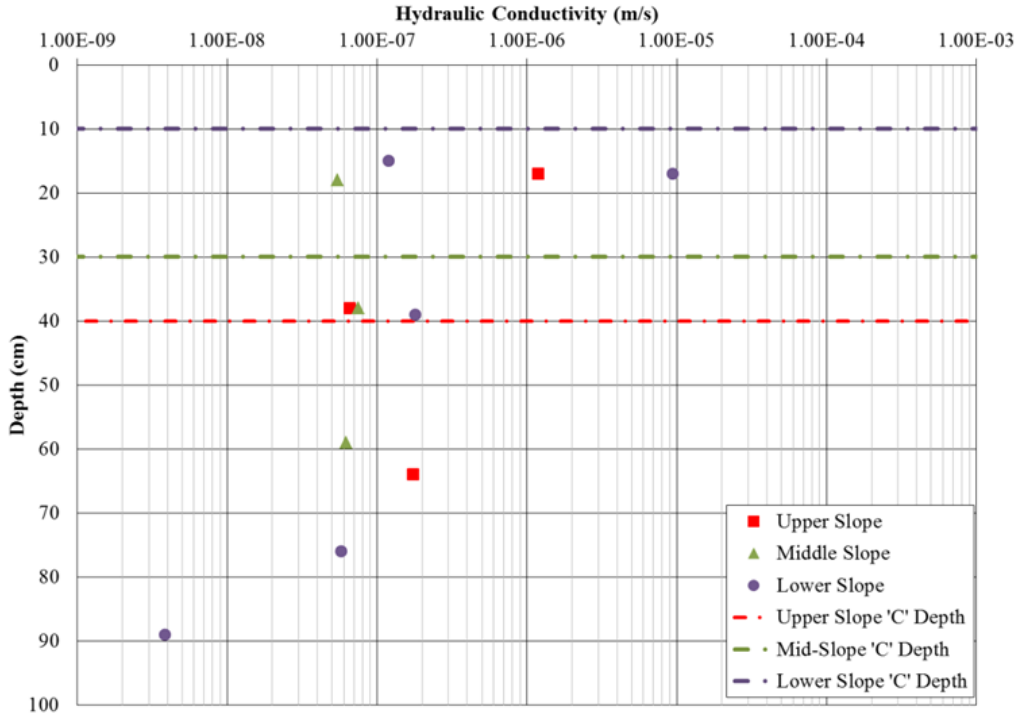

Figure 4.18 Guelph Permeameter measurements of Hydraulic conductivity for the upper 1.0 m of the Craigmore study site, with a soil profile of a trial pit dug at the crest of the slope (near ES02).

Slug tests were conducted during the first two years of monitoring and were interpreted using the Hvorslev method. Slug tests within the weathered bedrock zone were interpreted through simulation using SEEP/W due to the geometric constraints created by the geometry of the thin weathered bedrock surface. It is important to note, however, that in this case the

interpretation is essentially that of the bedrock transmissivity rather than the hydraulic conductivity itself. The simulations of the Craigmore bedrock transmissivity modeling will be presented in Section 5.1.2.

The range of hydraulic conductivity values for the glacial till was from 7.62 x 10^{-9} m s^{-1} to 7.46 x 10^{-10} m s^{-1}. The glacial till in Northern Ireland is known to have a "low" to "moderate" hydraulic conductivity, ranging from 10^{-4} m s^{-1} to 10^{-9} m s^{-1} (Fitzsimmons and Misstear, 2006). The overall trends of the Guelph Permeameter results seen above (Figure 4.18) tend to be consistent with this range, with the hydraulic conductivity near 1 x 10^{-9} m s^{-1} at depth. The results from the slug tests completed on BH1 and BH3 also appear to lie in the lower range of these values. The test results are summarized in Table 4.3 for each of the slug tests completed on site. These results were used to determine the appropriate hydraulic conductivity values of the upper and lower tills in the conceptual model discussed in Section 5.1.

Table 4.3 Results of the Hvorslev analysis of slug tests completed on BH1 standpipes in the upper and lower glacial till.

Material Type	**Hydraulic Conductivity** (x 10^{-9} m s^{-1})					
	BH1-a	BH1-b	BH3-a	BH1-c	BH1-d	BH1-e
Upper Till	1.02	1.31	3.74	-	-	-
Lower Till	-	-	-	0.788	1.45	0.746

4.1.6 Seismic Refraction Survey Results

The seismic refraction surveys were undertaken to characterize the bedrock topography for use in the three-dimensional models. The analysis of the raw data was conducted by Optim Software & Data Solutions. The final results of the analysis were imported into Golden Software's Surfer program and the bedrock topography was interpolated. Adjustments were made to the interpolation to ensure that bedrock outcrops were not being interpolated at locations

where they were known not to exist. The final bedrock surface, along with those inputs for the interpolation that exist within the three-dimensional model boundaries, can be seen in Figure 4.19. The overall surface elevation can be seen in Figure 4.20, where the dip in the overall elevation is seen to the east of the drumlin, where the Poyntzpass glacial drainage channel would have had an impact on the drumlin formation at the study site

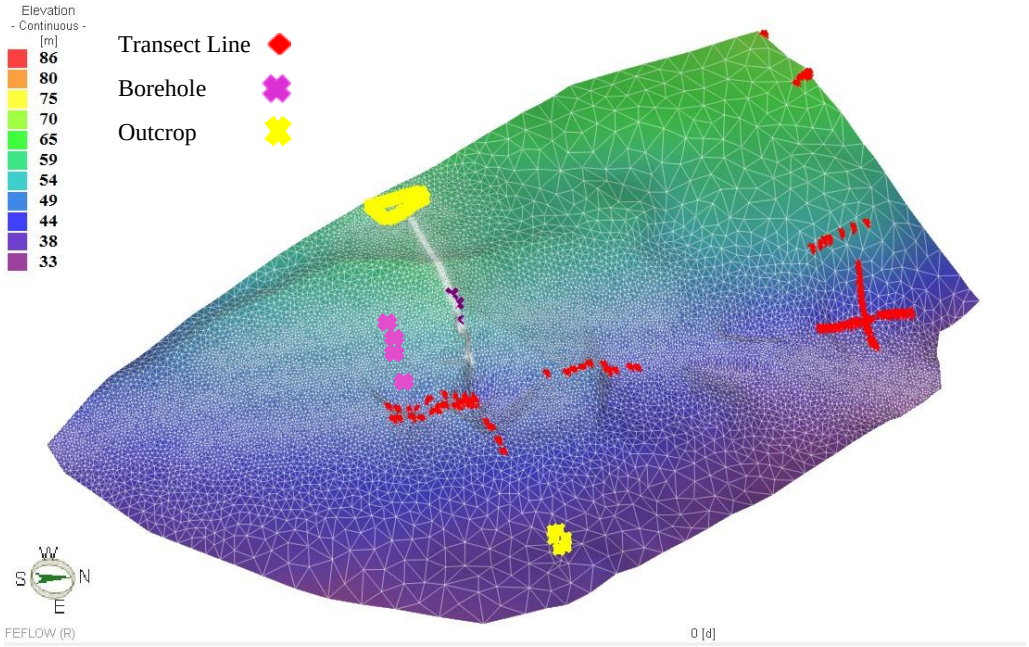

Figure 4.19 Final bedrock surface used in the Craigmore three-dimensional model geometry, interpolated using bedrock outcrop, borehole and seismic refraction survey data.

The overall direction of the dip within the bedrock is unclear as the site is located on the granitic pluton present near Newry, County Down. The dip of the bedrock structure of the pluton as depicted in Figure 4.19 appears to be south east. This is the opposite of what is seen in the Ordovician-Silurian Shale, which can be expected since intrusive plutons do not tend to follow the same dip as the underlying geology. As the granitic pluton was formed by magma intruding through a shale fault, the overall bedrock structure is not expected to match that of the shale. Final tomography results obtained for the seismic refraction surveys can be seen in Appendix A.

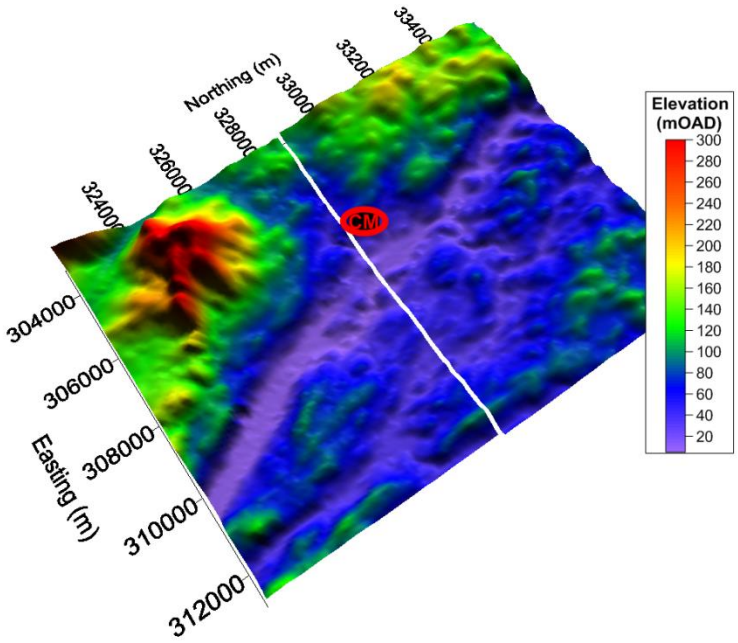

Figure 4.20 Surface elevation of area surrounding Craigmore study site (Land and Property Services (Northern Ireland), 2012).

4.2 Loughbrickland Highway Cutting

The Loughbrickland highway cutting is the secondary site for this research. Prior to construction in 2004, Clarke (2007) collected field and laboratory data relating to the glacial tills and water levels present prior to the construction of the drumlin cutting. Following construction, Clarke continued to collect some data, as well as begin the initial monitoring that is present on site. Since Clarke (2007), monitoring has continued at Loughbrickland, including the addition of more monitoring wells and other equipment. All data used in this research was collected using both Clarke (2007) results and recent monitoring and testing programs.

4.2.1 Site Geology

The Loughbrickland site is located on the Ordovician-Silurian shale typical of the area. The glacial till within this drumlin consists of two layers; however, they differ from the till layers observed at Craigmore. The brown sandy layer at Craigmore is not present at Loughbrickland. Instead, a stiff grey layer exists overlying a stiffer dark grey layer.

Figure 4.21 shows a conceptual geological cross section at the Loughbrickland cutting. Similar to Craigmore, the construction of the cutting exposed underlying layers of glacial till, leading to the development of a thin weathered soil zone along the surface of the slope. Samples were analyzed from along the cutting, as well as from the material taken from the original drumlin, as discussed in Section 4.2.2.

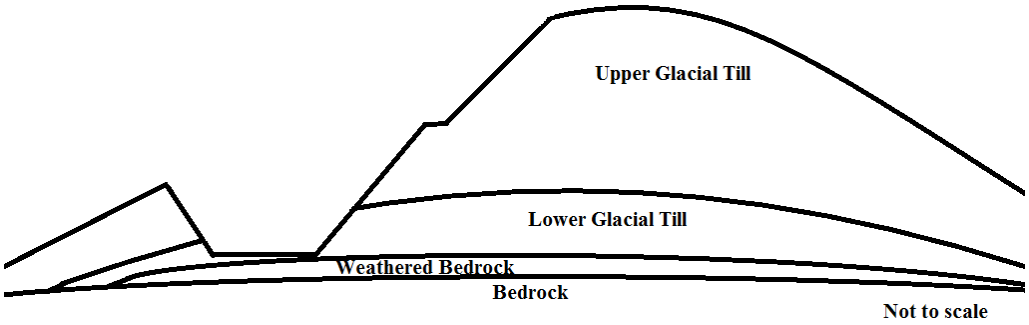

Figure 4.21 Cross section of the geological stratigraphy at the Loughbrickland highway site (approximately 300 m in length).

4.2.2 Laboratory Results

Particle size distributions on samples taken from the site were measured by Carse (2014) (Figure 4.22) and have a similar distribution to those found at Craigmore. These distributions were analyzed further by entering the proportions of sand, silt and clay into the soil texture triangle (Figure 4.23). This analysis indicates that the Loughbrickland glacial till tends to have higher clay fractions than those experienced at Craigmore. The dominant soil type would still be considered to be loam, but some sandy clay loam lenses may exist. In general, the Loughbrickland glacial till has less sand than the Craigmore glacial till, especially within the upper vadose zone. This may be an effect of the Poyntzpass glacial drainage channel that was located along the Craigmore drumlin. Loughbrickland did not have a large glacial drainage channel associated with its formation, decreasing the amount of sand fractions in the deposit.

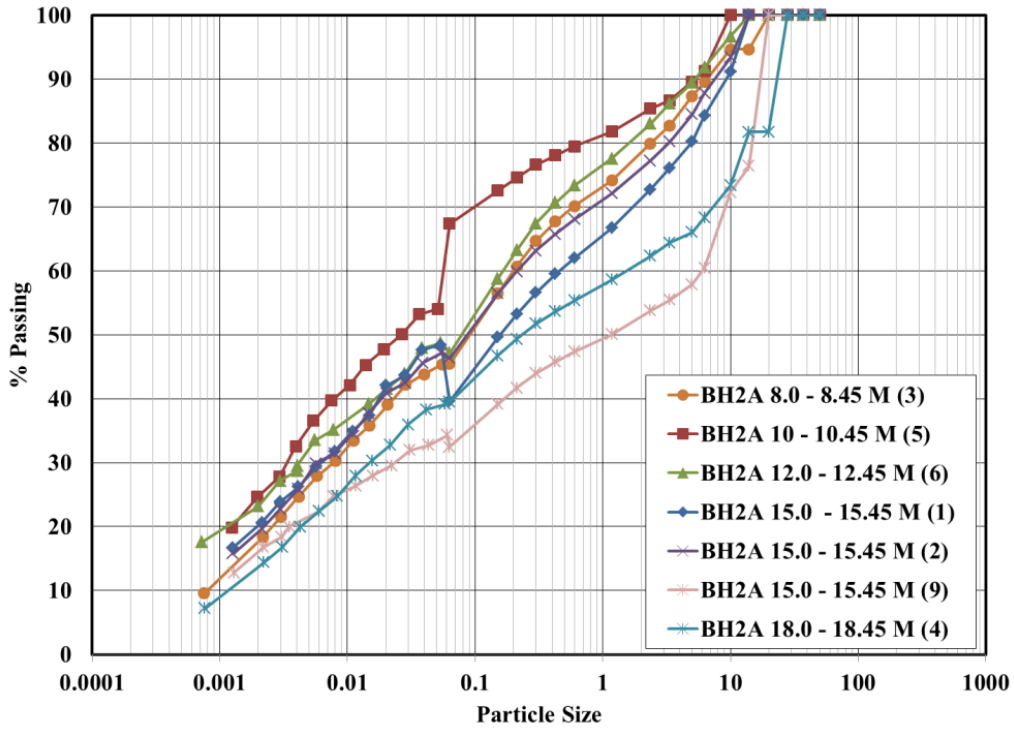

Figure 4.22 Particle size distributions obtained for samples taken from Loughbrickland study site.

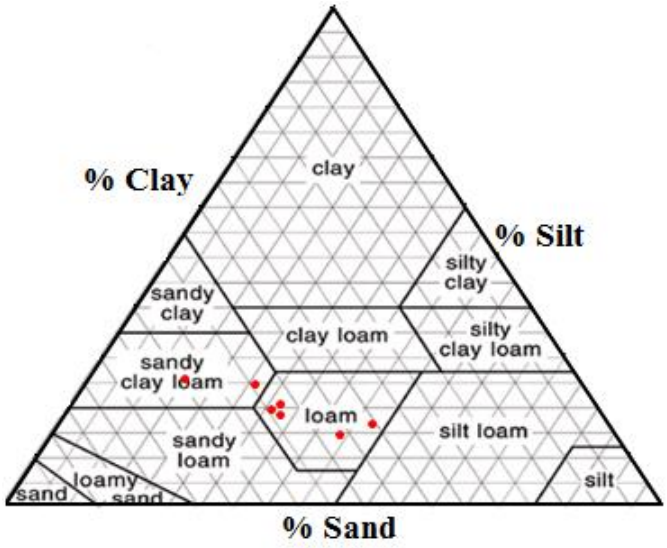

Figure 4.23 Soil texture triangle with samples taken from Loughbrickland site between 8 to 20m depth (Source of Triangle: Graham and Midgley, 2000).

Soil classification exercises completed at Loughbrickland determined that the surficial soils at Loughbrickland are similar to those at Craigmore. There were mottles present within the

soil pits completed along this embankment within the upper 0.6 m of the soil surface. Small rocks were very common in this section as well, but the surface- water gley soil description would still apply. Slight differences in the colour and texture of the soil existed in the Loughbrickland cutting, where less sand is present and a grey hue is located closer to the surface of the profiles, as shown in Figure 4.24.

Figure 4.24 Images showing one of the soil pits dug at the Loughbrickland site along the slope.

Many laboratory tests were completed on the Loughbrickland till by Clarke (2007) and were utilized in this research. Material properties that were adopted from this research include the specific gravity, void ratio, porosity and unit weight (Table 4.4). The porosity values given by Clarke (2007) have a large range, without depth being indicated by Clarke. It is expected that the porosity decreases with depth, as this was also seen in the Craigmore laboratory analyses. A porosity of 0.27 was used for glacial till below the active (soil) zone, as this value was the approximate average value of porosity reported by Clarke (2007). This value is reasonable considering the large range of porosities that have been reported for glacial till.

Table 4.4 Soil properties measured at Loughbrickland prior to construction of the embankment (Source: Clarke, 2007).

Soil Property	Estimated Range
Specific gravity	2.65
Void ratio	0.22 - 0.54
Porosity, (%)	18.0 - 35.0
Unit weight (kN m^{-3})	21.5 – 22.7

Other tests that were completed by Clarke (2007) included the measurement of in situ water content and liquid and plastic limits of samples taken from the field (Figure 4.25). Water content of the samples taken directly from the site ranged from approximately 8% to 29%, including outliers. Overall, the water content through the entire profile of glacial till was between 10% and 16%. The average liquid and plastic limits were 37.4% and 19.6%, respectively (Clarke, 2007). Like samples taken from Craigmore, these plastic and liquid limits fall within the range specified for glacial till samples taken from around the world. Also similarly to Craigmore, the water content is typically below or at the same level as the plastic limits, indicative of over-consolidated soils.

The porosity values measured by Clarke (2007) were used to establish the saturated water content for the estimate of the soil-water characteristic curves for each of the materials. The surface material was considered to have the highest porosity, so the saturated water content was estimated to be 40%. The glacial till was estimated to have a saturated volumetric water content of 27%, which is within the range of porosity values reported by Clarke (2007). The weathered bedrock was assumed to be similar to the bedrock at Craigmore, so the same saturated water content was used. All of these curves were estimated using information from Clarke (2007) (Figure 4.26).

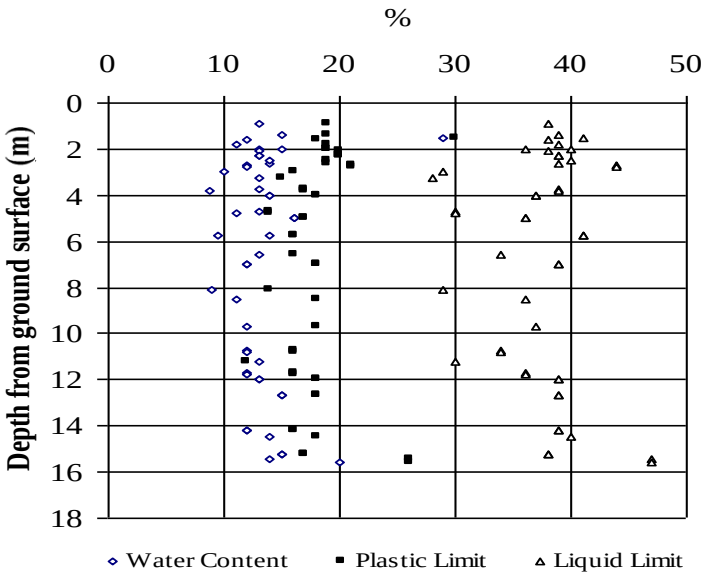

Figure 4.25 Atterberg limits versus depth for Loughbrickland samples taken from BH1 and BH2 (Source: Clarke, 2007).

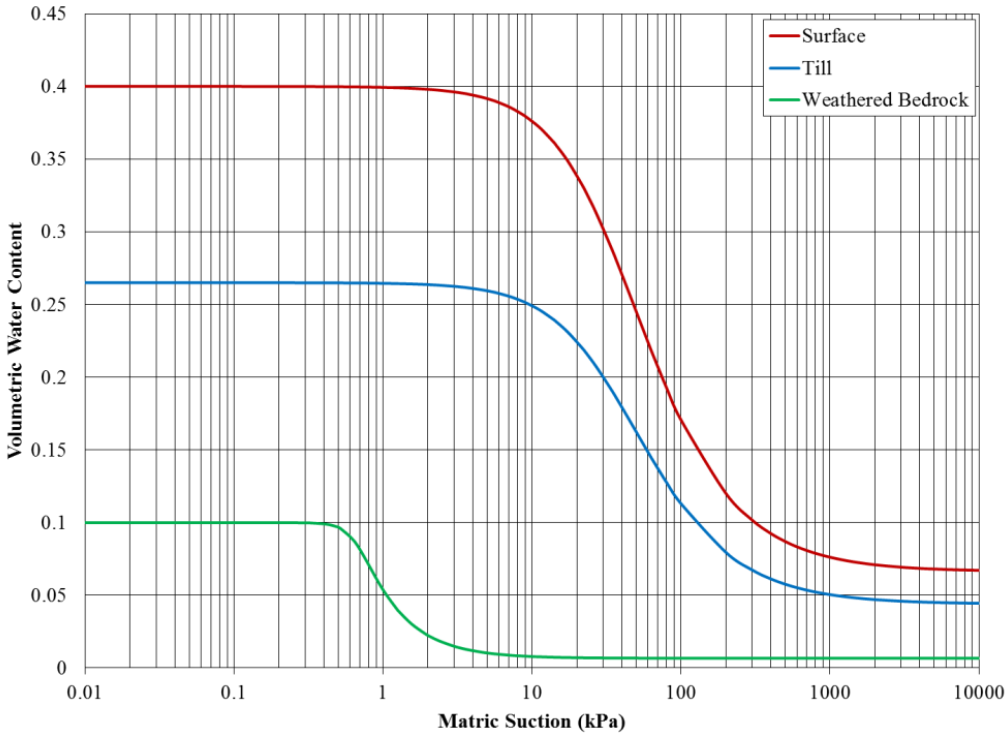

Figure 4.26 Soil-water characteristic curves estimated using information gathered from Clarke (2007).

4.2.3 Climate Conditions

Climate conditions were determined using the BADC databases as described previously for Craigmore since Loughbrickland does not have a meteorological station. The same climatic conditions (BADC's Aldergrove and Glenanne stations) were used at Lougbrickland as for Craigmore in order to estimate potential evapotranspiration. As the two study sites are both in County Down, weather conditions are not expected to change dramatically. Loughbrickland, however, has a slight difference in the overall elevation, so further research could be conducted when in situ weather monitoring is available.

4.2.4 Soil Monitoring

The monitoring located along the Loughbrickland cutting embankment is similar to the monitoring at the Craigmore railway site. Monitoring is ongoing for vadose zone water content, shallow water levels in the vadose zone and water levels in the upper till, lower till and weathered bedrock zones. Hydraulic conductivity measurements were also conducted at this site in standpipes that were available for slug testing. As explained, some of the standpipes were deemed ineffective, so were not included in this analysis. These standpipes include those reaching the weathered bedrock zone at BH1, BH2 and BH2A. The standpipes reaching the weathered bedrock in BH3A and BH5 were included for comparison, but were typically dry following installation.

The two EnviroScans at Loughbrickland are located along the back of the crest and the top of the crest and have been monitoring water content response since August 2010. The sensors were calibrated within the laboratory using Loughbrickland soil materials prior to installation. The final calibration constants that were estimated using the laboratory calibration procedure provided by Sentek Pty Ltd (2001) can be seen in Appendix B.

The first EnviroScan that was installed at the Loughbrickland site is located near BH1 at the back of the crest of the drumlin slope (ES01). This EnviroScan was installed in August 2010 and monitoring started within the same month following installation of ES02 along the upper slope of the cutting near BH2. The monitoring data of ES01 shows that saturation appears to

occur at depth for majority of the year (Figure 4.27). This can be seen from the flat line representing water content at sensor depths 0.7 m and 0.9 m. The saturated water content at this depth appears to be approximately 43%. Above these sensors, the soil seems to reach saturation periodically throughout the year. This saturation, however, is short-lived, as the water content decreases as drainage occurs following rainfall events. The water content at all of the sensors to a depth of 0.5 m appears to have been increasing steadily since the time of installation. This may be indicative of a seasonal moisture pattern, but cannot be verified until a "dry" season is monitored. The potential saturated water contents for each depth appear to occur between 39 – 50% for this section of soil. Spikes in the data could be errors in the equipment due to spaces around the installation. A period of data was lost between February and March 2011, where the battery on site lost power, shutting down all equipment.

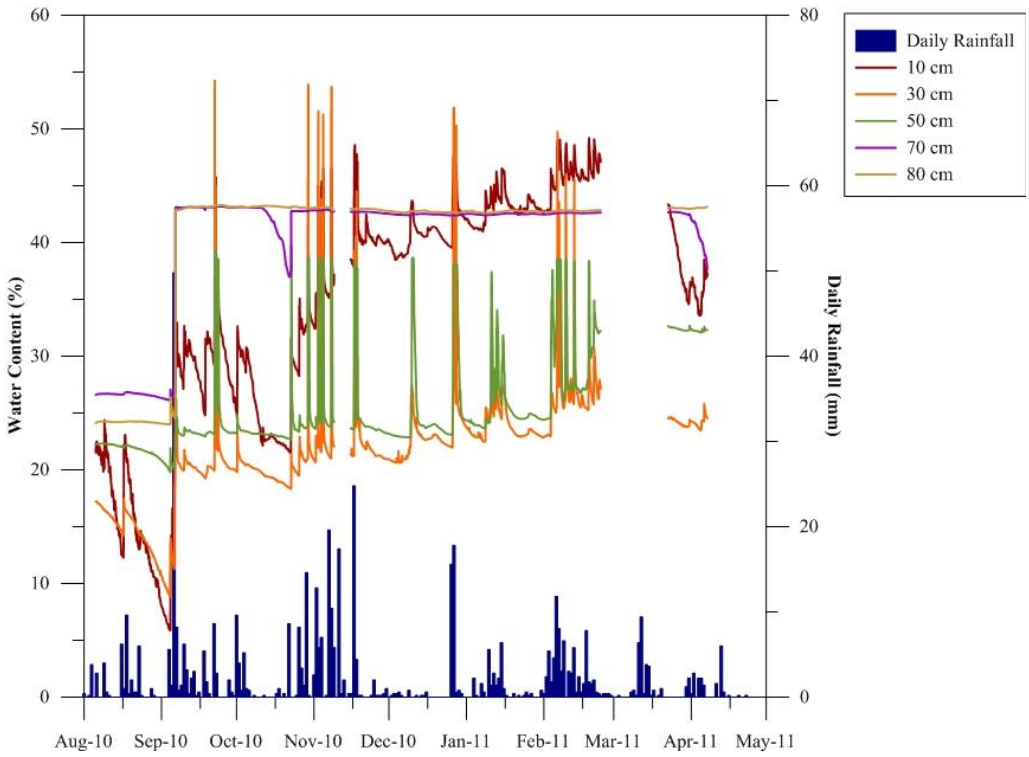

Figure 4.27 ES01 water content measurements in the vadose zone along the back of the crest of the excavation near BH1.

As was completed for the EnviroScans at Craigmore, the water content data was further analyzed by developing tornado plots for the same dates (Figure 4.28). As seen in the graph, the soil at depth (0.8 m sensor) appears to stay saturated throughout the year. As the soil becomes

shallower, the water content appears to be varying in response to climatic conditions. Following rainfall on December 26, 2010 (16 mm) December 27, 2010 (18 mm), the change in water storage increases by 33 mm, which is only 1 mm less than the expected rainfall measured at Craigmore. Following these rainfall events, the water appears to be removed rather quickly from the upper soil zone, indicated by the decreasing water contents on December 29, 2010. The water is removed very quickly from the sensor at a depth of 0.3 m, which may be indicative of lateral flow or the uptake by grass roots in the area. The upper 0.1 m lost water at a slower rate, which may due to continuing rainfall or ponded water along the soil surface in the thick grassy vegetation or increased storage by the organic material at the surface.

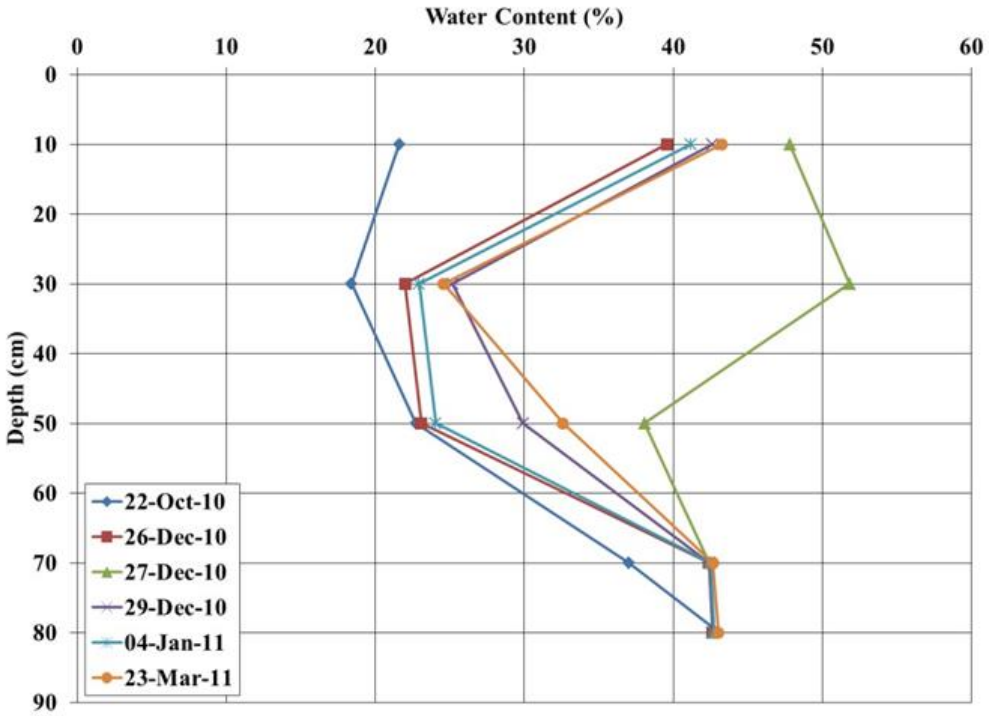

Figure 4.28 Tornado plot of water content at each depth at ES01 at Loughbrickland.

Monitoring data collected at ES02 along the upper slope can be seen in Figure 4.29. These sensors show that the soil profile at this location appears to reach saturation more frequently than ES01. For this soil profile, that saturated water content appears to be only 31% for the upper "A" horizon. The porosity then appears to increase at 0.3 m, where the saturation level is approximately 55%. The saturated water content then decreases with depth, moving

down to 52% at 0.7 m. The water content at depths of 0.5 m and 0.7 m drop away from saturation around November 2010, but remain steady for the remainder of the monitoring period. An increase in the porosity appears to occur at depths greater than 50 cm, which may be explained by the clay inclusions that were seen in the glacial till during excavation, which may increase the potential porosity of the material near the EnviroScan (Clarke, 2007). Another potential explanation could be the presence of rocks or space between the EnviroScan and the glacial till, causing water to pool near the EnviroScan until it is able to drain. This may explain the more dramatic decrease in water content following periods of saturation.

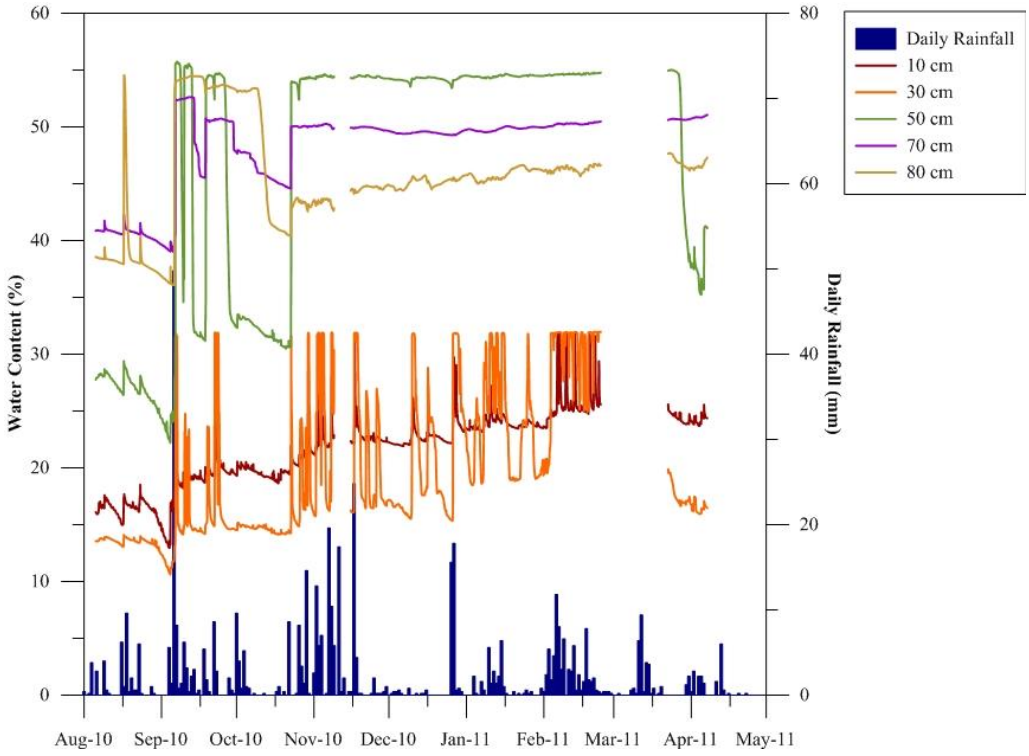

Figure 4.29 ES02 water content measurements in the vadose zone along the crest of the excavation near BH2.

A tornado plot in Figure 4.30 gives the water contents for each depth for the same dates used above. This tornado plot shows that the water contents at this location do not appear to respond as much to changes in climatic conditions as was experienced at the crest of the drumlin. Following the rainfall events on December 26 and 27, 2010, there is an increase in water content within the upper 0.2 m of the profile, however, there is very little change in water content at depths greater than 0.3 m. This would indicate that the soil remains fairly saturated throughout

the year at depths greater than this sensor, which was also seen in Figure 4.29. The more significant response to climatic conditions in the upper 0.2 m would be a result of the presence of roots from the grassy vegetation, as well as the increased weathering of the upper A and B horizons, increasing potential macropores. A total change in water storage along the entire profile, however, was 24 mm, which indicates the potential of runoff occurring along this upper portion of slope, decreasing the amount of rainfall infiltrating the profile.

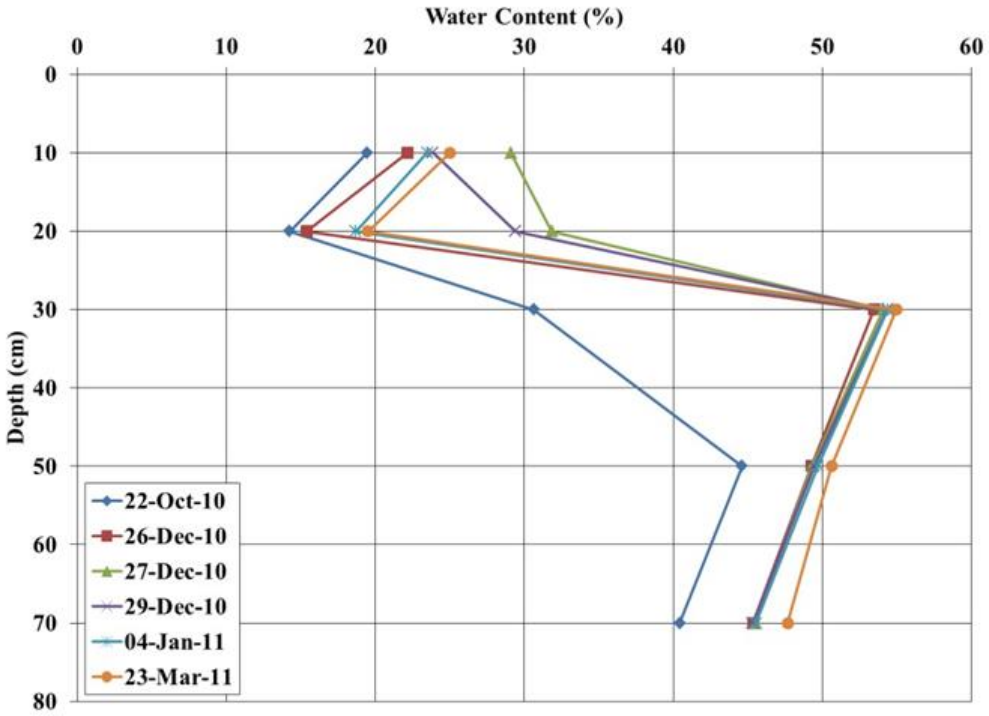

Figure 4.30 Tornado plot of water content at each depth for ES02 at Loughbrickland.

Shallow well installations conducted at Loughbrickland during the summer months of 2010 were monitored using a level logger installed in the tube in August 2010. This monitoring continued March 2011 (Figure 4.31). The barometric pressure was fully removed from the monitoring data, as the level logger was an absolute pressure transducer. The data shows that the water level remains approximately 0.2 m above the bottom of the pipe, with many rapid spikes to near the surface elevation of the tube. These spikes are expected to occur during rainfall events, as the hydraulic conductivity of the upper soil zone is expected to be one or two magnitudes

higher than the underlying glacial till. The water levels increase to a level that is approximately the same as the till surface in October 2010 and remain near that surface for the remainder of the monitoring period, indicating that the till appears to remain fairly saturated throughout the year. This is similar to what was seen at 0.6 m to 0.7 m depths in the EnviroScan installation of Figure 4.27.

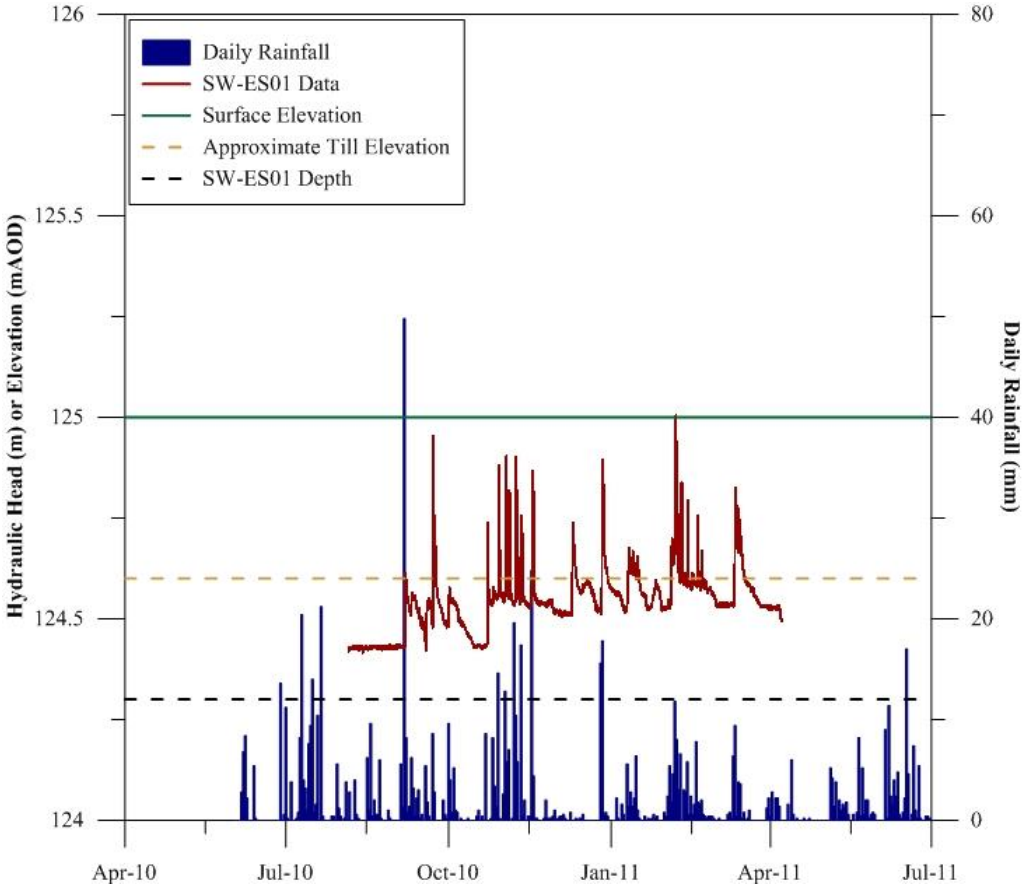

Figure 4.31 Shallow water table monitoring data near ES01 at Loughbrickland from August 2010 to April 2011.

Two more shallow wells have been monitored since April (SW01) and June (SW02) of 2010. These wells are located near the "bench" of the slope cutting (at mid- slope). One of these shallow wells is approximately 3.0 m upslope from the bench (SW01), while the other is approximately 3.0 m downslope from the bench (SW02). The monitoring data for each of these wells can be seen in Figure 4.32. This data has had the barometric pressure removed, similarly to SWES01, as they were not sealed into the installation tubes.

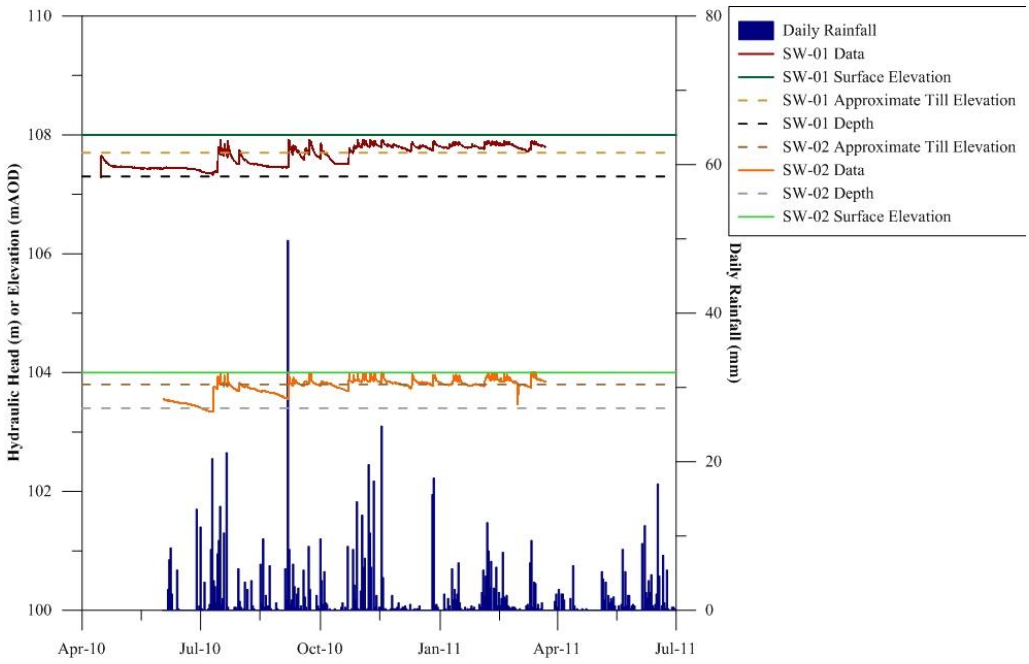

Figure 4.32 Shallow water table monitoring data near BH5 along the Loughbrickland bench from August 2010 to April 2011.

The data is similar to that seen along the back crest of the cutting (SWES01). Spikes occur at times that the study site is expected to be undergoing rainfall events. The difference between the two locations, however, is the magnitude of these spikes. SW01 and SW02 have smaller responses to the rainfall events; however, the water table remains closer to the surface than SWES01. This could be an effect of the material types in the vadose zone. The soil near ES01 has regularly been treated to seeding and harvesting by the owner of the land. Along the cutting, the grassland vegetation is not harvested or seeded, but left to grow naturally every season. Hydraulic conductivity measurements would also indicate the potential changes in material type between the crest and mid-slope positions of the cutting, as discussed below. Water is expected to infiltrate slower at the mid-slope position and saturation is likely to occur more frequently than along the crest. Both of these locations are located down-slope from ES02 and near areas where vegetation types are indicative of more saturated conditions.

Borehole water level monitoring has been conducted at the Loughbrickland site since prior to construction. In this section, only monitoring conducted after construction will be studied as a part of this research.

The monitoring data from BH1 has remained relatively steady near 122 mAOD and 116.5 mAOD at BH1-1 and BH1-2 for the entire monitoring period (Figure 4.33). The spikes and dips during June/July 2010 reflect the recovery following slug tests completed on each standpipe. Some small fluctuations in the water level data exist around these dates, showing that some response to climatic conditions does occur. These fluctuations are much smaller than what was experienced in the shallow wells. This is expected as the glacial till has a much lower hydraulic conductivity and would experience less influence by climatic conditions than the shallow wells. Data from both standpipes follow a very similar pattern even though they are located at different depths. When looking at the data on a much smaller time scale, it can be noted that there is a slight delay in the lower till water level fluctuations as compared to the upper till measurements. This indicates that there is a connection between the upper and lower tills. The periods of missing data occur during times that slug testing was conducted on the wells.

Water level monitoring along the crest of the cutting involved two boreholes with three standpipes each. As discussed earlier, the standpipes reaching bedrock have not been used in this analysis, as they are deemed to be unreliable. For BH2, the upper till and lower till standpipes show similar patterns as BH1 (Figure 4.34). Each standpipe shows a similar pattern to the other, with a slight delay existing in the lower till as compared to the upper till. This would be indicative, again, of a connection between the upper and lower till recharge rates. The delay experienced in the lower till will be a result of a longer path for the water to move, as well as a lower hydraulic conductivity level. The patterns in the lower till in this case are also of a smaller magnitude than in the upper till. This shows that the response to weather conditions and recharge is slower in the lower till than the upper till. The water level monitoring at BH2A has recently been determined to be unreliable, as the water levels between each standpipe have become equal (Figure 4.35). It has been determined that a loss of seal between standpipes must have occurred. This may have been a result of an error in the installation of the borehole, where the bentonite between each standpipe depth did not provide a proper seal. Data from prior to loss

of reliable data in the upper till standpipe will be used for calibration purposes in the models. Again, large spikes in the data of both Figure 4.34 and Figure 4.35 are created by slug testing completed on site.

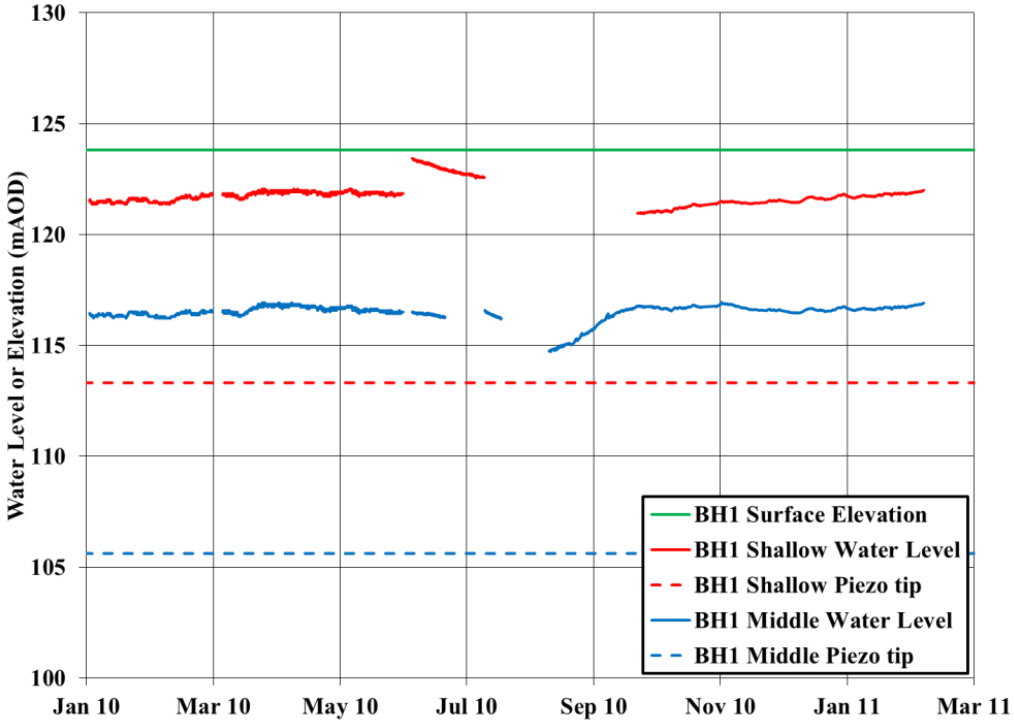

Figure 4.33 Water level monitoring collected from BH1 at the Loughbrickland study site.

A level logger has been installed in each of the standpipes located at BH5 and the standpipe that reaches the weathered bedrock zone for BH3A at the toe of the cutting (Figure 4.36). These level loggers have shown changes in water levels even though they have remained dry during all manual dips of each standpipe. As these standpipes are also not sealed, they are exposed to the full barometric pressure experienced on the site. The inability for the water levels to be determined in each standpipe has been expected to be a result of the drain installation along the toe at the weathered bedrock zone, as water would be removed via the drain instead of pooling within the weathered bedrock zone. Errors in the installation practice may have also occurred, causing the seal within the borehole between each standpipe to be lost, similar to the occurrence in BH2A. The "dry" water level indicated by the level loggers has been included in the calibration process of the model development to determine if the simulation also develops these "dry" conditions.

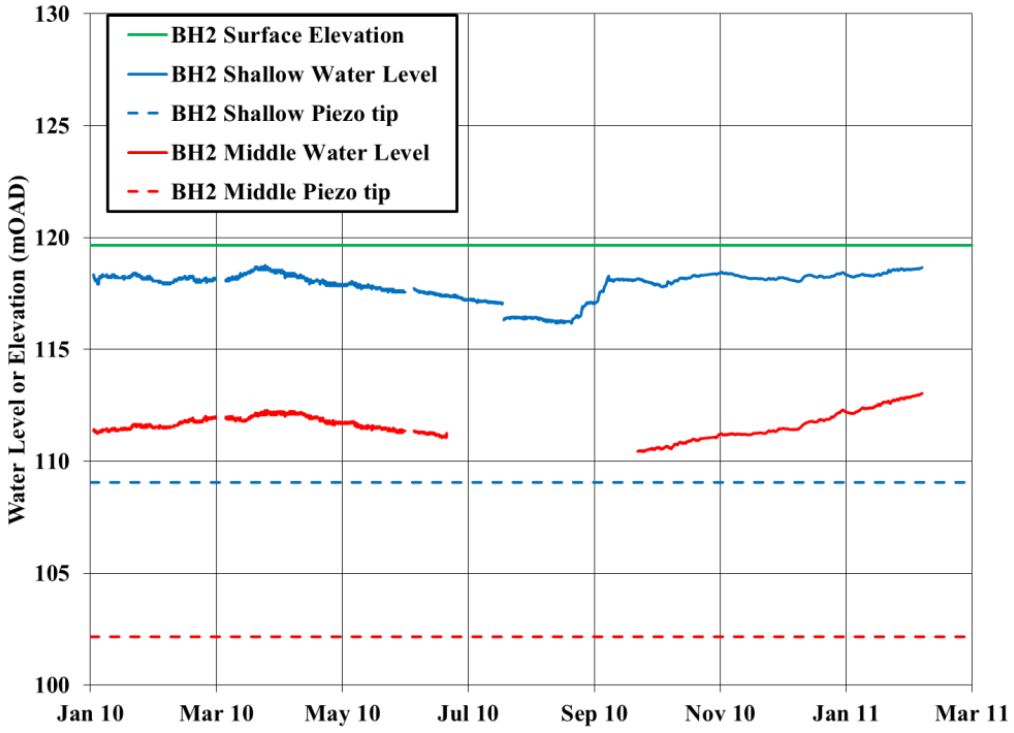

Figure 4.34 Water level monitoring collected from BH2 at the Loughbrickland study site.

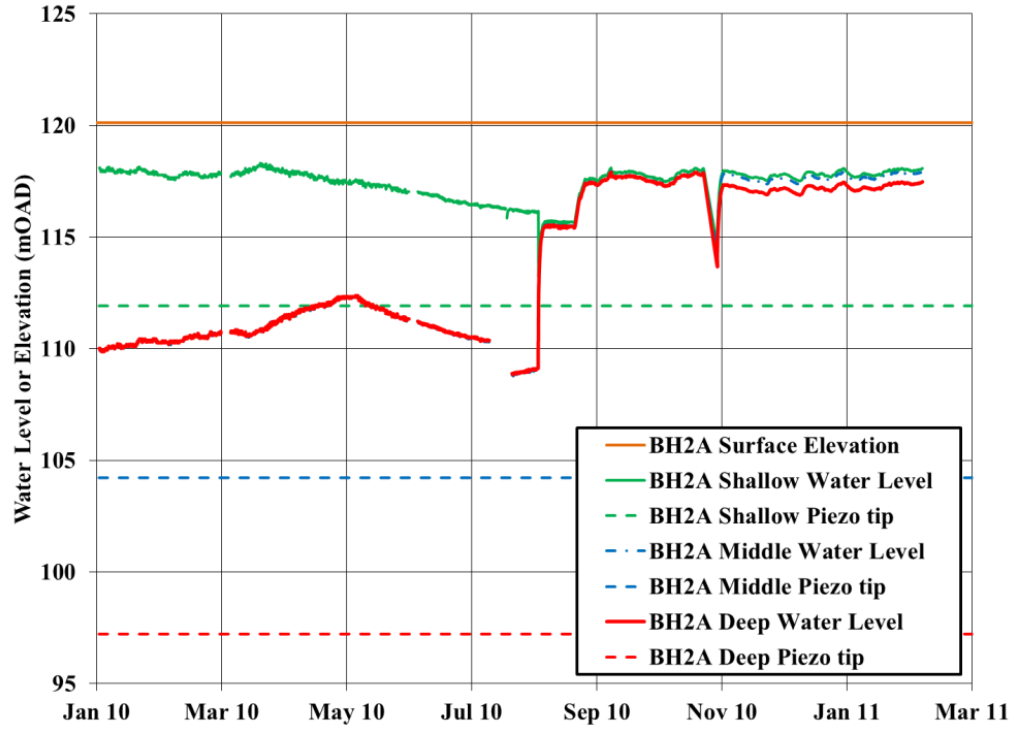

Figure 4.35 Water level monitoring collected from BH2A at the Loughbrickland study site.

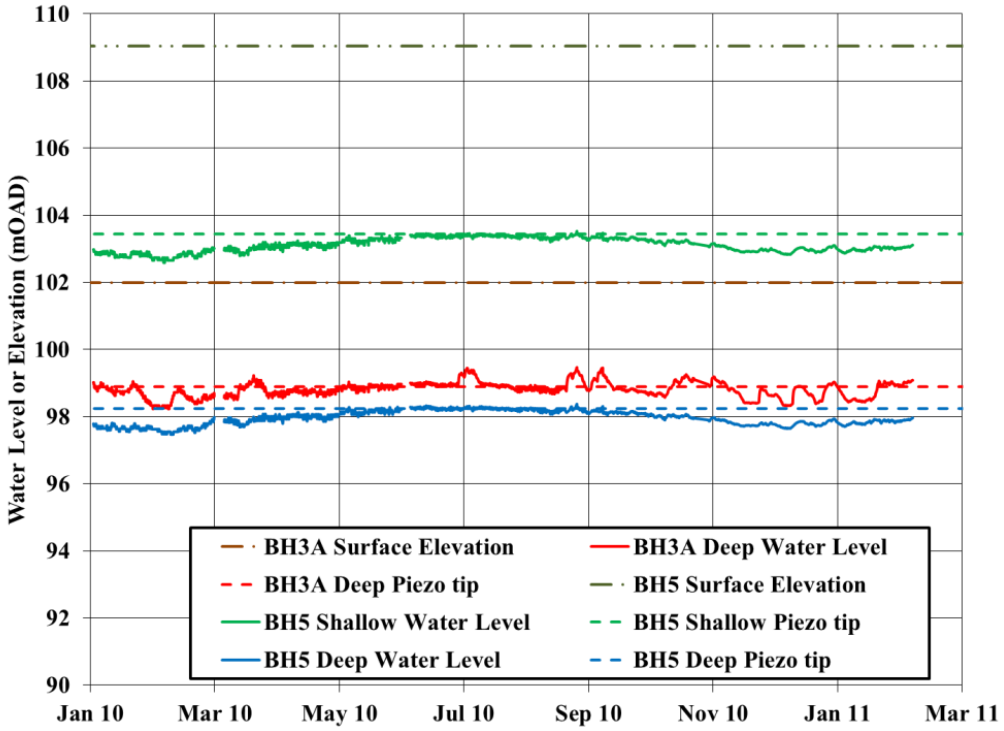

Figure 4.36 Water level monitoring collected from BH3A and BH5 at the Loughbrickland study site.

4.2.5 Hydraulic Conductivity

Hydraulic conductivity estimates were conducted at the site using the Guelph Permeameter and slug tests on boreholes available on the site. The boreholes reaching the weathered bedrock were not included in this analysis, as tests completed on them were unreliable. The hydraulic conductivity for the weathered bedrock zone was estimated using the values obtained from Clarke (2007), as tests were completed on the weathered bedrock zone prior to construction of the highway cutting. Comparisons were also made to estimates given by Clarke (2007) for the upper and lower till hydraulic conductivities.

The Guelph Permeameter was also used at the Loughbrickland excavation to obtain estimates of the hydraulic conductivity of the vadose zone. These tests were completed in the same manner that was applied at the Craigmore site, with tests being completed within the upper 1.0 m. A total of twelve tests were completed on site, with eight above 0.5 m depth and four

between 0.5 m and 0.8 m. The tests were completed along the upper slope, the middle tier ("bench") and the lower slope. The results of all tests can be seen in Figure 4.37 for all sections of the embankment. The average hydraulic conductivity of materials 9.0 x 10^{-5} m s^{-1} to 2.5 x 10^{-9} m s^{-1}, with the hydraulic conductivity values generally decreasing as depth increases. As surface material can be highly variable, the large range is to be expected and will be caused by presence of vegetation and macropores developed by insects.

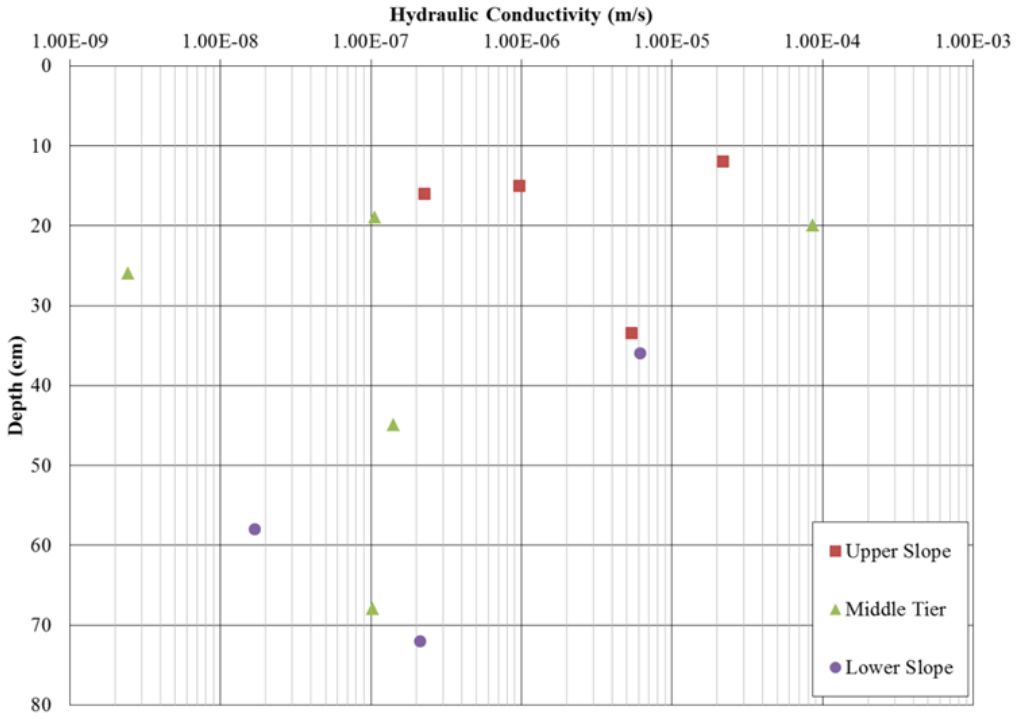

Figure 4.37 Hydraulic conductivities of the upper 1.0 m soil profile at Loughbrickland using the Guelph Permeameter.

The final range of hydraulic conductivity for the upper 1.0 m zone water determined to be within 1.0 x 10^{-8} m s^{-1} and 1.0 x 10^{-6} m s^{-1}. As seen in the figure, seven of the twelve tests fall within this range, with some more extreme values present in the upper 0.5 m. This range was used to develop the initial material properties of the groundwater flow models to ensure that a representative hydraulic conductivity was being used in the upper 1.0 m zone.

Slug tests that were completed in the boreholes in the field were analyzed using the Hvorslev method to determine the range in hydraulic conductivity for each of the glacial till

materials. The standpipes that extended into the upper and lower tills were the only slug tests that were considered reliable and used in this analysis. A total of six slug tests were completed during the field programs in 2009 and 2010, with three in the upper till zone and three in the lower till zone (Table 4.5). Some of the slug tests were conducted by removing a "slug" of water via pumping at a fast rate and then allowing the water to rise. Others were completed by adding a "slug" of water and monitoring the rate at which the water fell.

Table 4.5 Results of the Hvorslev analysis of slug tests completed on BH1, BH2 and BH2A standpipes in the upper and lower glacial till.

Material Type	**Hydraulic Conductivity** ($\times 10^{-9}$ m s^{-1})					
	BH1-a	BH1-b	BH2-a	BH2-b	BH2-c	BH2A-a
Upper Till	1.37	-	73.27	-	-	0.19
Lower Till	-	0.34	-	0.38	0.21	-

The range in hydraulic conductivity for the upper till was 7.3 x 10^{-8} to 1.9 x 10^{-10} m s^{-1}, which also matches the trend shown in the Guelph Permeameter readings where the hydraulic conductivity at depth falls around 1.0 x 10^{-7} to 1.0 x 10^{-8} m s^{-1}. The range in hydraulic conductivity for the lower till, however, was from 3.8 x 10-10 to 2.1 x 10^{-10} m s^{-1}. The values of hydraulic conductivity obtained by Clarke (2007) using slug tests were 2.0 x 10^{-9} to 1.3 x 10^{-9} m s^{-1} for the upper till, and 2.7 x 10^{-9} to 6.5 x 10^{-10} m s^{-1} for the lower till. As the standpipes reaching the weathered bedrock zone were considered unreliable or were plugged during the time of the slug tests, the values obtained through the Hvorslev method by Clarke (2007) were used for the development of the conceptual groundwater models. This range was from 9.6 x 10^{-6} to 2.9 x 10^{-7} m s^{-1}.

4.2.6 Seismic Refraction Survey Results

Seismic refraction surveys were completed along the drumlin on each side of the highway excavation to help define the bedrock topography. The topography of the bedrock past

this drumlin was estimated using surface elevations, as this area is expected to have an overall structure that mimics the surface topography (Figure 4.38). This area is located along the Ordovician-Silurian shale that is present in most of County Down. The overall structure is said to dip to the northwest, which cannot be seen well in this image. The overall structure along the Loughbrickland drumlin is relatively similar to the overall topography of the surface. If a larger geometry could be studied with further seismic refraction surveys, the overall bedrock structure may be seen to dip to the northeast as expected. As a topographic low occurs along the eastern edge of the geometry (the Lough), and a valley and drumlin were used along the eastern boundary, the overall bedrock structure is more difficult to predict (Figure 4.39).

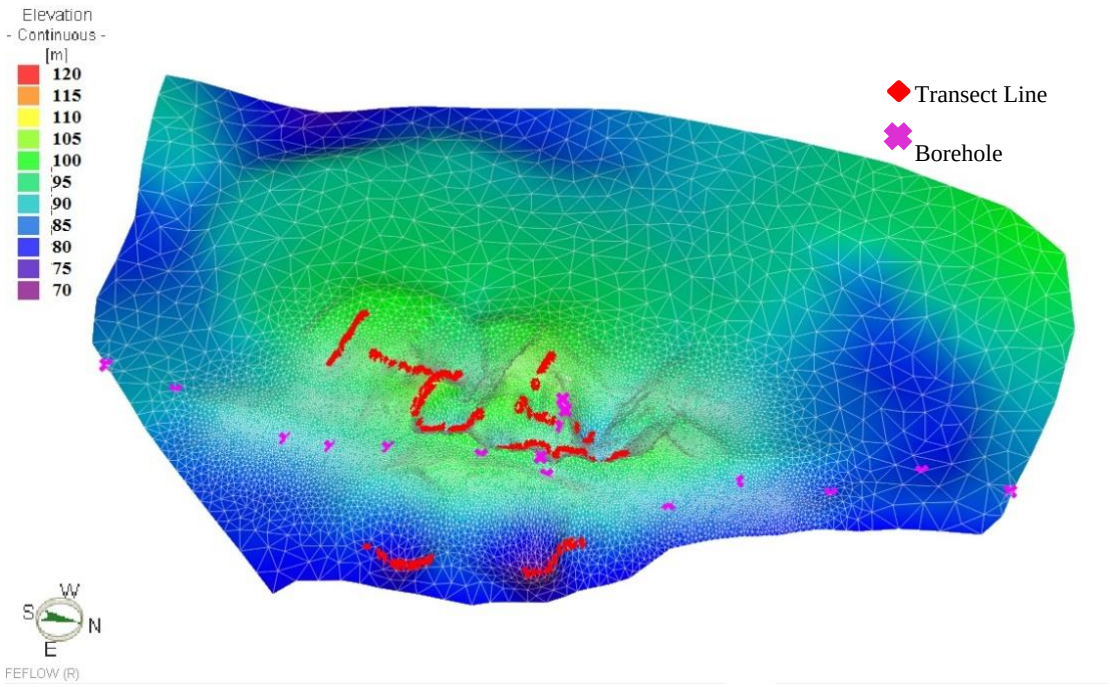

Figure 4.38 Final bedrock surface elevations from interpolation using seismic refraction survey and borehole data.

The surface elevations show that the overall ground surface dips towards the northwest, indicating that the surface mimics this overall structure of the bedrock. Many highs and lows in elevation, however, occur along the surface, which may indicate some variability in both the bedrock topography and depth of glacial till. The final bedrock surface was imported into the

three-dimensional groundwater models for development of the base condition simulation. The variability in the bedrock topography shows that there are many concave and convex formations in the bedrock, which is not apparent when the surface is estimated using borehole elevations alone. Final results of the tomography analysis of the seismic refraction surveys can be seen in Appendix A.

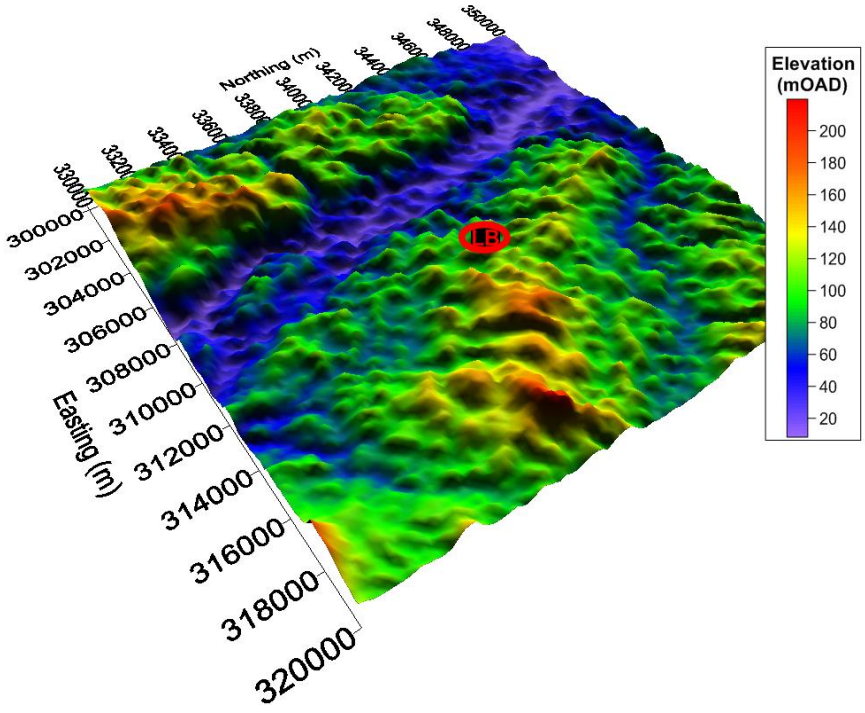

Figure 4.39 Surface elevations for larger area surrounding Loughbrickland drumlin study site (Land and Property Services (Northern Ireland, 2012)).

5.0 RESULTS AND DISCUSSION – MODEL RESULTS

This section outlines the results of each of the steps taken in the development, calibration and analysis of the two- and three-dimensional models. As Craigmore was considered the primary site, all results pertaining to the model development and analysis at this site are outlined first, followed by a parallel discussion for the Loughbrickland site. Each section outlines the results of the steady-state simulations followed by sensitivity analyses.

5.1 Craigmore Railway Cutting

Annual recharge rates are required as an upper boundary condition in the numerical models and were developed based on an annual water balance estimate. The water balance estimations are described first, showing the "best-fit" result which was used later as the base case for the simulations. The two- and three-dimensional groundwater flow simulations were then developed using site data as described in Section 4.0. Each simulation was developed as a steady-state, saturated model first, and was then incrementally made more complex so as to establish the effect that various inputs had on performance.

5.1.1 Water Balance Estimation Results

Meteorological data collected from the BADC climate database were used as inputs to the water balance developed in STELLA. The BADC data, including precipitation, radiation, temperature, relative humidity, etc., was used in the water balance to calculate AET, PET, runoff and recharge into the upper till. The water storage volume measurements from ES02, located at the crest of the Craigmore cutting, were used to develop an estimate of the stored water volume within the active zone (e.g. rooting zone) which could be compared to the water storage volume calculated using in the STELLA simulation. Material properties used for each of these simulations are summarized in Table 5.1. These properties were determined by first using the

estimated permanent wilting point, field capacity and saturated water content (estimated porosity) properties obtained from the SWCC for the surface material. These limiting water contents were then varied slightly to determine if water storage volume patterns that were more similar to the EnviroScan measurements could be calculated (Figure 5.1). The stored water volume within the rooting zone was represented by the weighted average water content, calculated by taking the volume of the water in the rooting zone and dividing it by the rooting zone depth. The "best-fit" water balance model was determined using RMSE, MARE, R, E and d (Equations 3.22 to 3.26); similar to what was conducted during the development and calibration of the two-dimensional and three-dimensional groundwater flow models. The results of this calibration process are presented in Table 5.2.

Table 5.1 Material properties used in the water balance simulations to determine the "best-fit" model.

Simulation	**Porosity**	**Field Capacity**	**Permanent Wilting Point**
Run 1	0.45	0.36	0.13
Run 2	0.30	0.25	0.11
Run 3	0.25	0.15	0.10
Run 4	0.27	0.22	0.11
Run 5	0.25	0.20	0.13

Table 5.2 Calibration results to determine the "best-fit" water balance model with bold italics indicating the "best" model.

Simulation Properties	**Evaluation Method**				
	Run 1	Run 2	Run 3	Run 4	Run 5
RMSE	0.19	0.06	***0.02***	0.04	0.03
MARE	0.46	0.20	***0.08***	0.13	0.09
R	***0.83***	0.82	***0.83***	0.80	0.80
E	-37.1	-2.57	***0.47***	-0.54	0.36
d	0.12	0.93	***0.99***	0.97	***0.99***

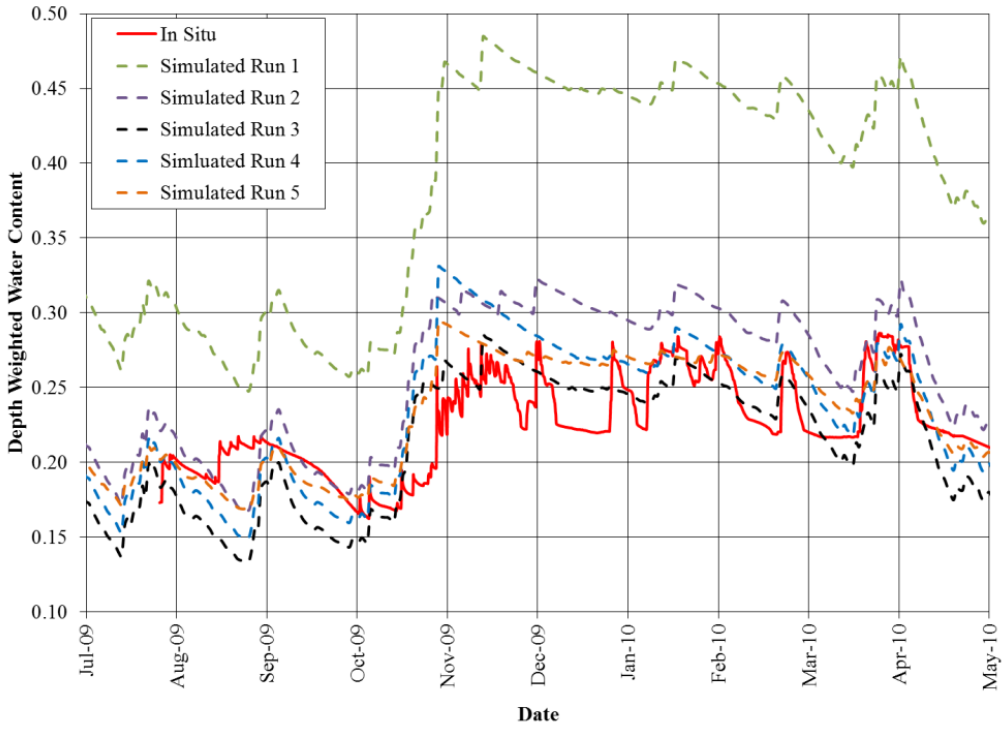

Figure 5.1 Comparison of depth weighted water content in the upper active zone with the average depth weighted water content from ES02 on the crest of Craigmore slope.

The hydraulic conductivity of the upper and lower tills is used in the simulation and it was found that the hydraulic conductivity of the upper till had an important influence on the water balance since it acted to limit the drainage of water from the active zone. The hydraulic conductivity values were set to match the values used in the groundwater flow simulations, which were based primarily on the results from the Hvorslev tests conducted on monitoring wells (see Section 4.1.5.2). The upper till was assigned a hydraulic conductivity of 1×10^{-9} m s^{-1}, while the lower till was assigned a value of 1×10^{-10} m s^{-1}.

The initial water balance was conducted using an active zone depth of 0.5 m as this was the general rooting depth observed at the site; however, this depth was varied as part of the sensitivity analysis. The resultant weighted average water contents for this sensitivity analysis can be seen in Figure 5.2. It was difficult to simulate the drastic spikes in the storage values during the simulation. These are likely associated with rapid filling of macrpores, particularly following conditions in which antecedent infiltration as elevated saturation levels within the soil matrix. At slope (crest or toe) locations this is further complicated by any lateral flow that might

occur as runoff or interflow. The equations described in Section 3.2.5 for obtaining the 'best-fit' simulated results were used to again determine the depth that gave the most accurate simulation results (Table 5.3). The depths of the active zone that were used as a part of this sensitivity analysis were 0.5 m, 0.8 m, 1.0 m, 0.9 m and 0.6 m for Run 3-1, 3-2, 3-3, 3-4 and 3-5, respectively.

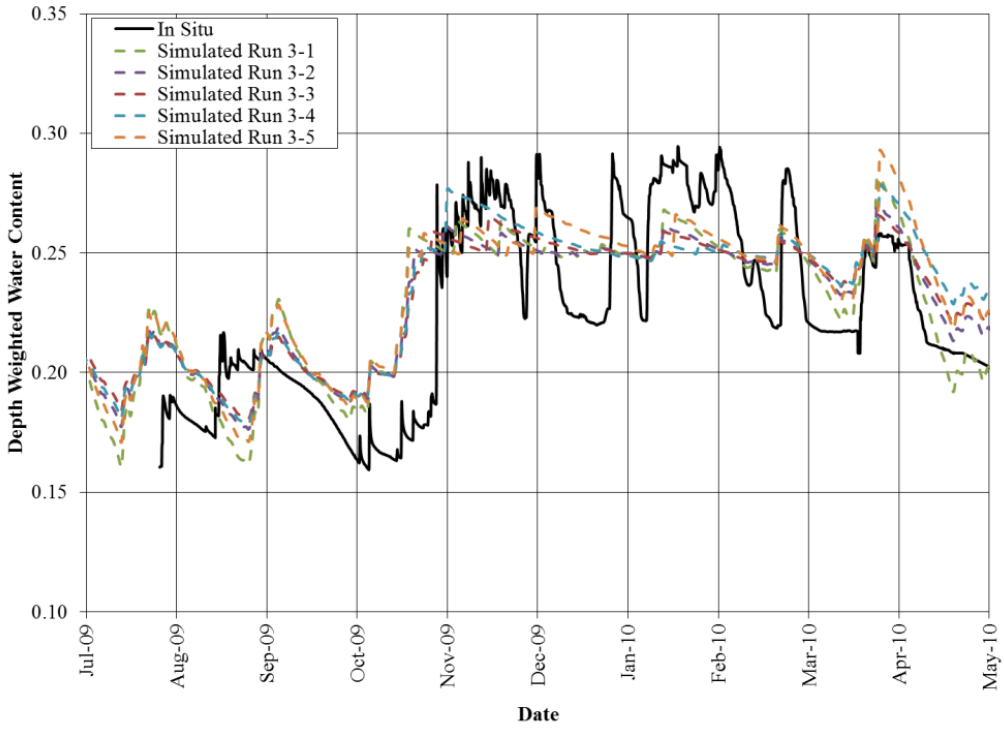

Figure 5.2 Sensitivity analysis results showing the influence of the active zone depth on average water content in the water balance model.

Table 5.3 Evaluation method results to determine the "best-fit" depth for the active zone, with the "best-fit" is in bold italics.

Evaluation Method	**Depth of Active zone (m)**				
	0.5	*0.8*	*1.0*	*0.9*	*0.6*
RMSE	2.29×10^{-2}	2.15×10^{-2}	***2.14×10^{-2}***	2.30×10^{-2}	2.40×10^{-2}
MARE	7.69×10^{-2}	***7.47×10^{-2}***	7.56×10^{-2}	8.12×10^{-2}	8.17×10^{-2}
E	0.83	***0.84***	***0.84***	0.82	0.82
R	0.47	***0.54***	***0.54***	0.47	0.42
d	***0.99***	***0.99***	***0.99***	***0.99***	***0.99***

The water content data taken from ES02 at Craigmore was only available from July 2009 to July 2010. In order to obtain annual estimates of recharge for use in the groundwater flow models, the frequency analysis of the BADC weather data (Section 4.1.3) was used to determine an appropriate range of recharge rates based on a range of precipitation values. The above "best-fit" properties were then used in the STELLA model to simulate estimated recharge rates under four different atmospheric scenarios. This analysis involved the use of the BADC meteorological data (radiation, wind speed, temperature, relative humidity and rainfall) from the Aldergrove weather station for periods of "high", "low" and "average" annual precipitation, given that the potential evaporation is relatively constant regardless of the year being considered (ranging from 450 to 600 mm $year^{-1}$). The years that were used are 1975, 1994 and 2002, where the annual precipitation was 694 mm, 884 mm and 1094 mm, respectively. The study year (2009) was also included in the analysis to obtain an estimate of recharge for the site (Figure 5.3).

The cumulative PET, AET, runoff and recharge was also included in the analysis for each of the study years. The "best-fit" water balance model used for this analysis was Run 3-3, where the active zone was 1.0 m deep, the porosity was 0.25, the field capacity was 0.15 and the permanent wilting point was 0.10. The results of the 1975, 1994 and 2002 water balance analyses are shown in Figure 5.4, Figure 5.5 and Figure 5.6, respectively. The annual water balance components are summarized in Table 5.4.

Table 5.4 Cumulative values of hydrologic parameters determined in water balance model with estimated annual rates for each study year.

Year	Precipitation	PET	AET	Runoff	Recharge	ΔS
	(mm)					
1975	694	635	463	141	21	70
1994	884	530	480	307	25	74
2002	1094	511	509	485	31	69
2009	976	447	436	446	25	71

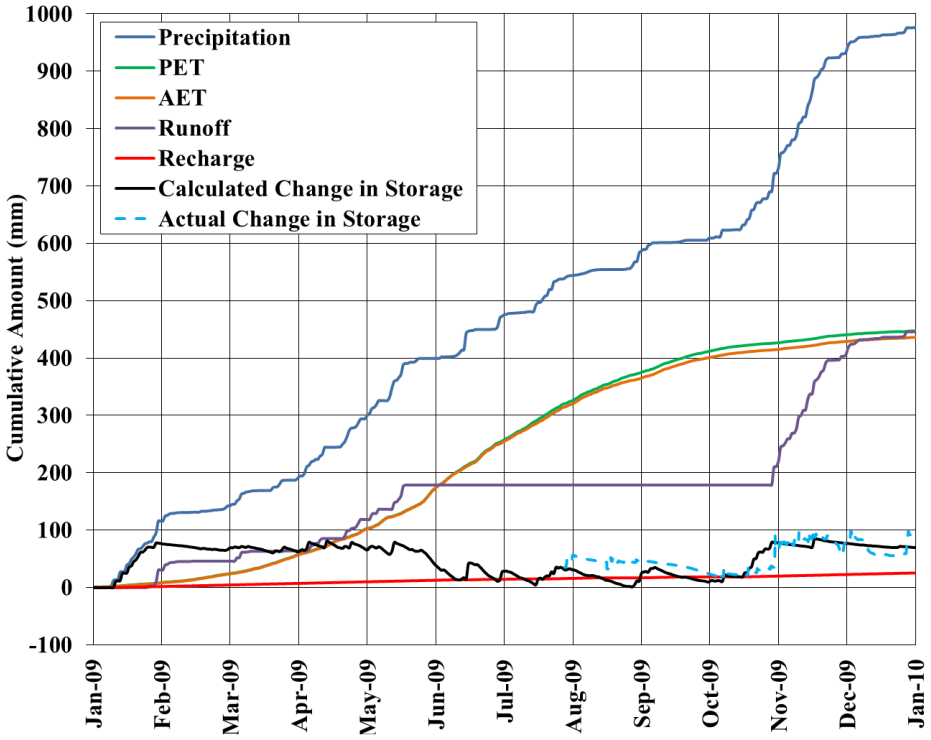

Figure 5.3 Final water balance developed for Craigmore for the full year of 2009.

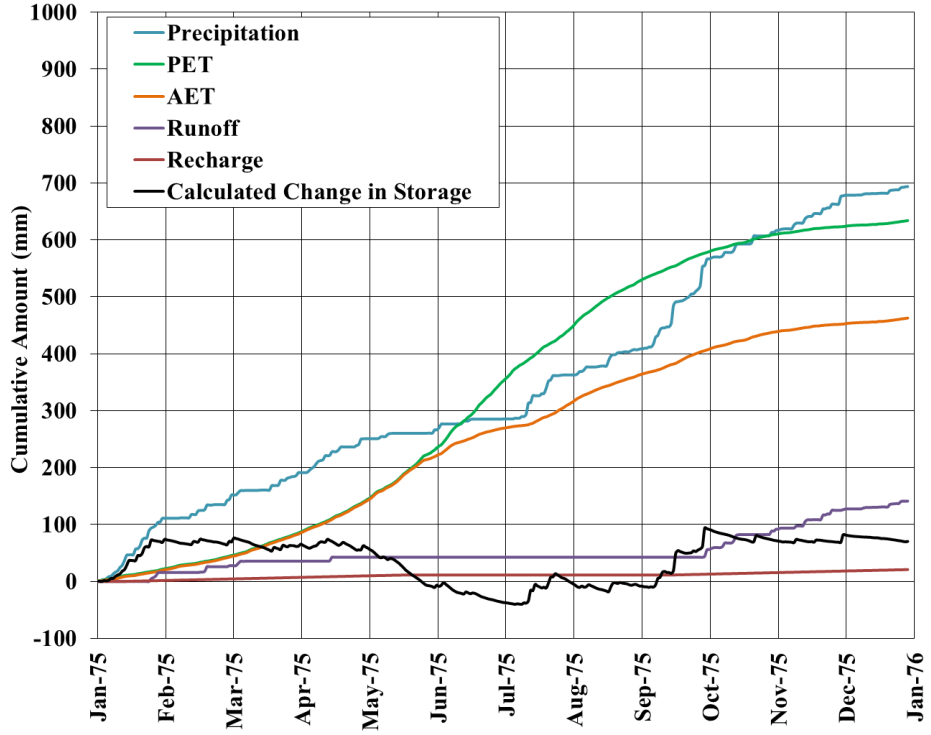

Figure 5.4 Final water balance developed for Craigmore for the full year of 1975.

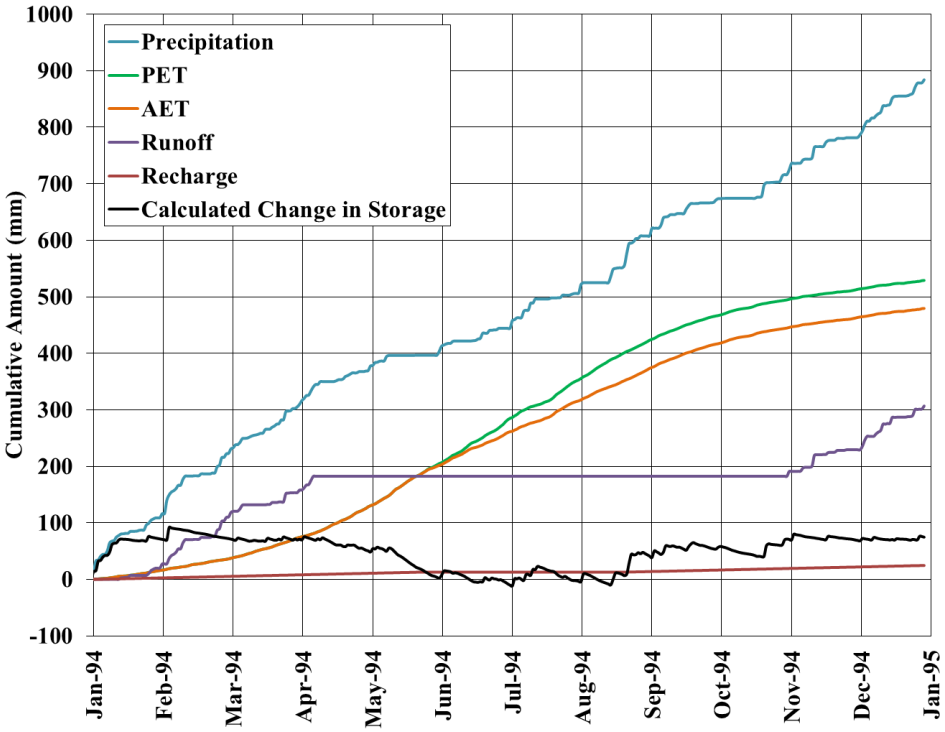

Figure 5.5 Final water balance developed for Craigmore for the full year of 1994.

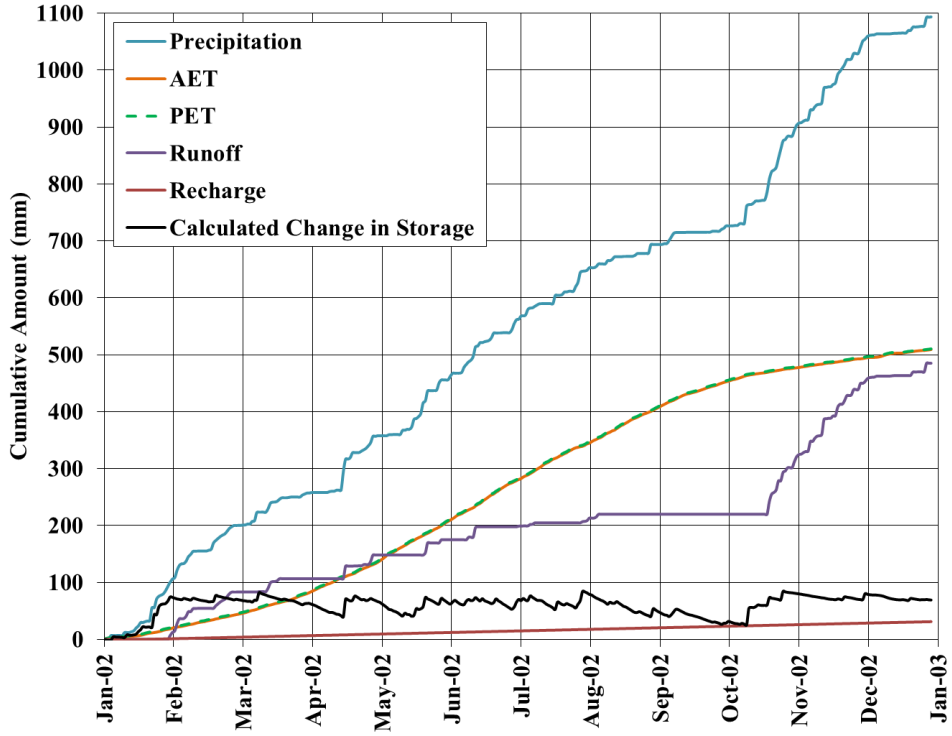

Figure 5.6 Final water balance developed for Craigmore for the full year of 2002.

Overall, the water balance estimates are consistent with previous research on water balances in Northern Ireland. The PET in 1975 was considered to be high, but the final AET estimate fell within the average 400 to 500 mm $year^{-1}$ range typical for annual AET (Fitzsimmons and Misstear, 2006). This is likely because of lack of precipitation available for AET to remove, so water was being removed from storage. The AET estimate for 2002 was slightly higher than this range, but allows all other estimates to be within reasonable parameters given the higher rate of rainfall.

The water balance analysis shows that recharge at this site could be expected to range from approximately 20 mm $year^{-1}$ to 30 mm $year^{-1}$. The hydraulic conductivity of the upper glacial till provides an upper limit to the annual recharge rates. For example, a soil with a hydraulic conductivity of 1 x 10^{-9} m s^{-1} would allow a maximum rate of recharge of approximately 32 mm $year^{-1}$ under a unit gradient. Annual recharge rates may drop below this upper value as a result of seasonal moisture deficits in which the average water content within the active zone falls below the field capacity.

5.1.2 Bedrock Transmissivity Modeling

The results from the slug tests completed on the standpipes located in the weathered bedrock zone were analyzed using an axisymmetric transient flow simulation using GeoStudio's SEEP/W program. The simulations of each slug test assumed that there was a 1 m depth of weathered bedrock extended laterally to a radius of at least 100 m with an overlying glacial till layer of 10 m. A constant head boundary condition was set on the upper till boundary to ensure that the till layer stayed saturated. The slug test was simulated using a hydraulic head versus volume boundary condition at the screen which represented the change in the head in the standpipe as a function of the water volumes entering or exiting the screen. These models were used to simulate the well response for a range of hydraulic conductivity and soil compressibility values. The results were then plotted against the actual slug tests completed in the field to select a "best-fit" to the measured data based on visual comparison. A total of three slug tests, one for each borehole location, were simulated in this manner. The results of the simulations are included in Figure 5.7 for BH1, Figure 5.8 for BH2 and Figure 5.9 for BH3.

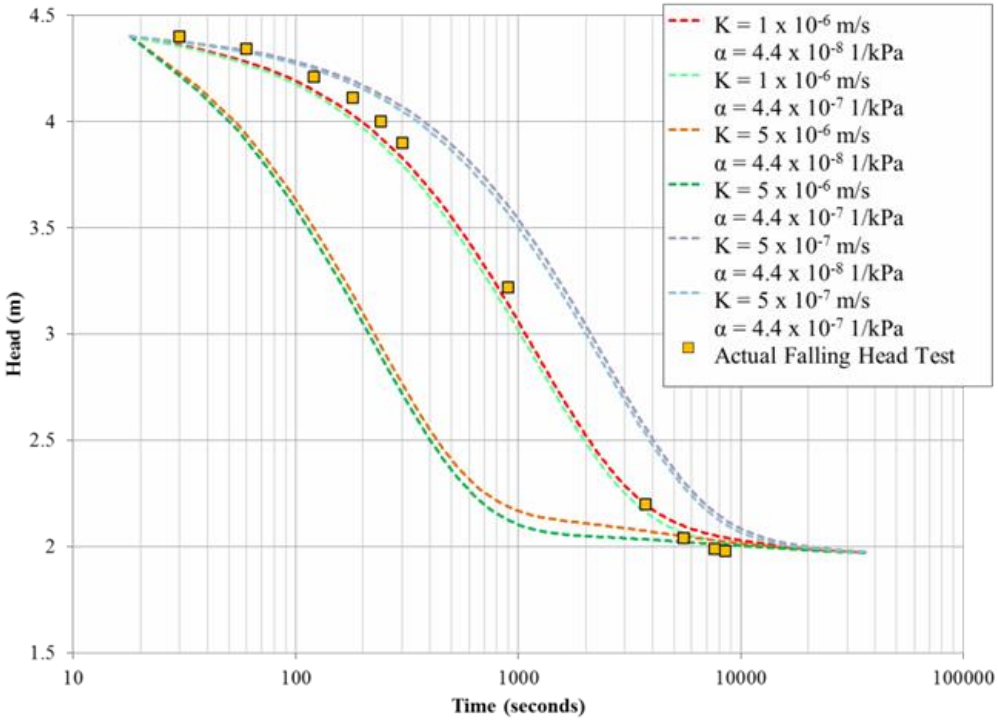

Figure 5.7 Estimation of bedrock hydraulic conductivity using 2-D model simulation results versus actual field falling/rising head analyses at BH1.

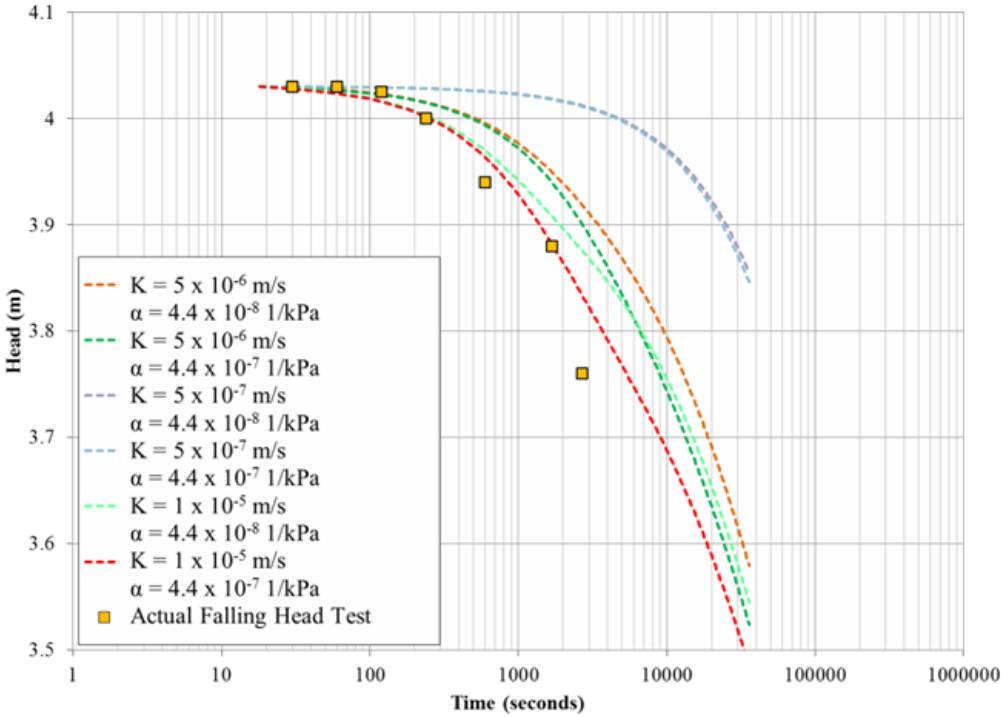

Figure 5.8 Estimation of bedrock hydraulic conductivity using 2-D model simulation results versus actual field falling/rising head analyses at BH2.

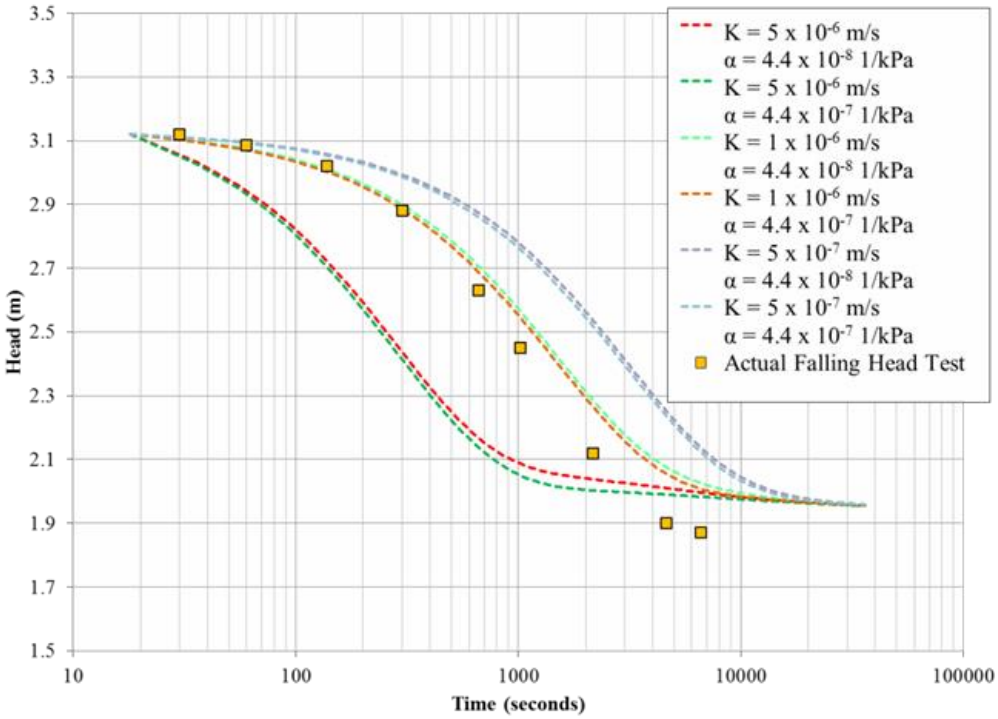

Figure 5.9 Estimation of bedrock hydraulic conductivity using 2-D model simulation results versus actual field falling/rising head analyses at BH3.

The range of hydraulic conductivity from the analysis is from 1 x 10^{-6} m s^{-1} to 1 x 10^{-5} m s^{-1} with little sensitivity of the simulations to soil compressibility. The fit between measured and simulated recovery for the slug test completed on BH2 was not as good as for the other two tests. This could be due to differences in the depth of weathering at the different locations. Errors could also have been made by those conducting the tests, leading to measurements of water levels being inaccurate. Given the similarities between the tests completed at BH1 and BH3, the value that has been deemed appropriate for the purpose of the groundwater flow modeling is a transmissivity between 1 x 10^{-5} m^2 s^{-1} and 1 x 10^{-6} m^2 s^{-1}. Further analysis of the "best-fit" transmissivity values will be conducted in the three-dimensional model simulations.

5.1.3 Steady-State Hydrogeological Simulations

Steady-state simulations were developed for each of the model cases used to compare the two-dimensional and three-dimensional simulations. Saturated models were developed first and

used to determine an appropriate range of material properties for the variably saturated model simulations. The unsaturated models were then developed and are explained in detail within this section. The base case for the three-dimensional model will be described first, as this model was used for the basis of all other simulations. Each of the two-dimensional models that are included in the comparison will then be described followed by the sensitivity analyses.

In order to ensure that an appropriate geometry was used in the development of the conceptual model, a water level map was developed (Figure 5.10). This map was interpolated from known points of water levels in Golden Software's Surfer program. Data was taken from borehole standpipes and surface water areas, such as creeks, ponds and lakes. The final water level map was then used to decide on the final areal extent of the model domain. The lateral boundaries were located using locations of assumed groundwater divides, such as the location of surface water bodies and the location of topographic high or low points (i.e. the center of drumlins or valleys). One of the geometric boundaries that did not fall onto either of these categories was a location along which a constant head boundary was assumed (east boundary) from the water level map. Other no-flow boundaries were assumed to exist along lines perpendicular to the head contours.

The model elements were assigned the material properties given in Table 5.5, with two areas of bedrock outcrop where bedrock material properties extended to the surface. These areas were included in the first layer of the model geometry by assigning the relevant properties to the appropriate elements located within the boundaries of these bedrock outcrops. The elements within layers 2 to 12 were then assigned based on the interpolation of the bedrock topography described above and estimated depths of the upper and lower tills based on information gathered from standpipe installations. The bedrock layer was interpolated based on the estimated bedrock elevations determined by the tomography method described in the previous section, with an estimated depth of 0.5 m for the weathered bedrock zone. The impact on the weathered bedrock zone depth and potential variability in depth was not included in the scope of this research, but further research should be conducted to determine this impact on overall hydrogeology.

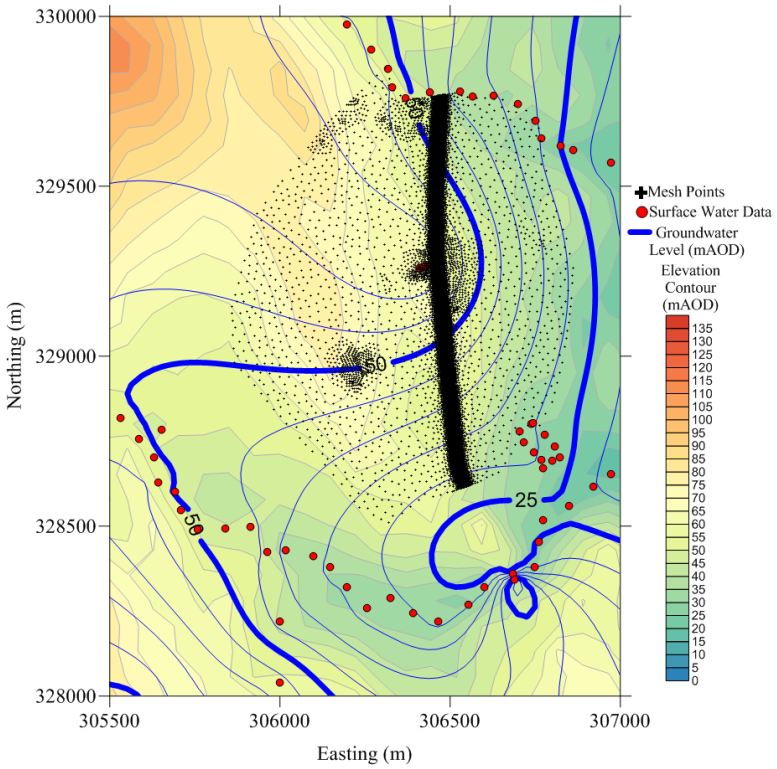

Figure 5.10 The groundwater contour map developed for the Craigmore railway cutting using surface water and borehole water level data.

Table 5.5 Material properties used in development of the three- and two-dimensional models estimated using laboratory/field data (with some bedrock materials in upper layers where bedrock outcrops occur).

Material	**Layer(s) (depth (m))**	**Hydraulic Conductivity**	**Porosity**
		m s^{-1}	
Surficial Layer	1 (0.5)	3 x 10^{-7}	0.45
Root/Weathered Zone	2 (1.0)	1 x 10^{-8}	0.40
Upper Till	3 – 6 (up to 5)	1 x 10^{-9}	0.35
Lower Till	7 – 10 (up to 5)	1 x 10^{-10}	0.35
Till/Weathered Bedrock Interface	11 (0.2)	1 x 10^{-8}	0.35
Weathered Bedrock	12 (0.3)	1 x 10^{-6}	0.10*

*weathered bedrock effective porosity given by: Irfan and Dearman (1978).

The final material properties that have been used in each of the models were considered reasonable given the ranges of soil properties determined in the laboratory or from in situ measurements in Section 4.1. Transition layers were included between layers which had a hydraulic conductivity contrast of more than three orders of magnitude to ensure convergence in the Feflow model. These layers included the 1.0 m transition zone between the weathered/root zone and upper till in layer 2 and the lower glacial till to bedrock transition. It is anticipated that the surficial weathered zone extends past the 0.5 m that was assumed in the model. For example, it was evident in soil pits that were dug in the crest of the Craigmore cutting that the 'B' horizon extended to almost 1.0 m in depth. The interface layer between the weathered bedrock layer and the lower till was assumed to have the properties of a mixture of the glacial till and weathered bedrock and was assigned a depth of only 0.2 m.

Figure 5.11 shows the model geometry in relation to the Craigmore cutting. A constant head boundary condition was applied along the most northerly boundary to represent the approximate heads along the creek. Seepage face conditions were applied to the surface nodes of the model to allow seepage to occur in low lying areas and along slopes of the drumlins. These seepage face conditions were applied to the entire surface of the domain to ensure that pressure could not reach unrealistic levels within the glacial tills. The resultant hydraulic head boundary conditions were then checked for each simulation to ensure that areas of suspected recharge were not included as a seepage face.

Recharge was applied to the entire surface layer of the model domain using the in/out flow from top parameter in Feflow. The seepage face boundary condition in Feflow does not allow infiltration at nodes where this boundary condition is set, indicating a potential limitation to the Feflow model. As discharge is generally expected to occur whenever the area is saturated, which is common at this site, this limitation is not expected to have any major impact on the overall model results. Areas of expected recharge are primarily located in areas of higher elevation, whereas seepage points were primarily expected at locations of low elevation or near bedrock outcrops. Figure 5.12 shows a visualization of the three-dimensional topography covering the model domain.

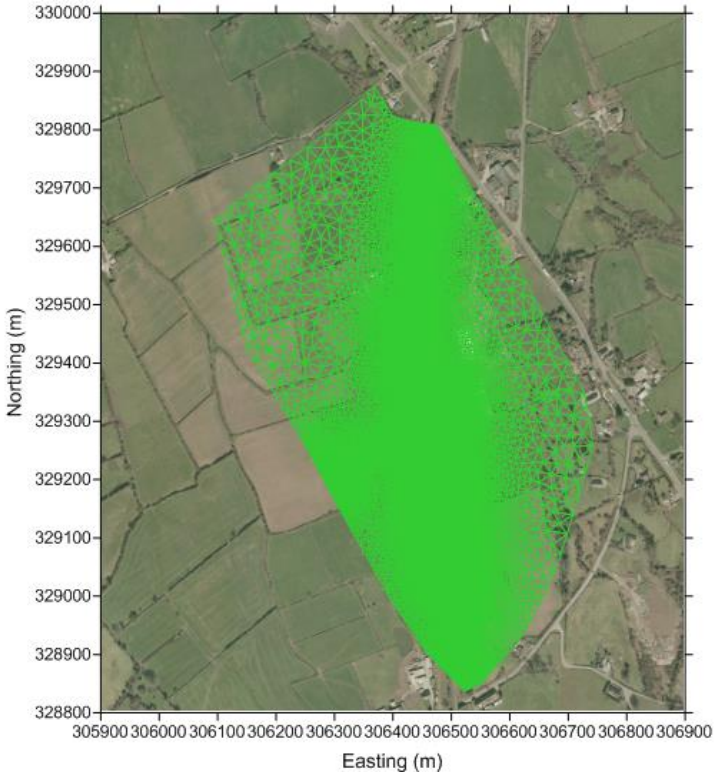

Figure 5.11 Geometry and mesh of 3-dimensional model for Craigmore site.

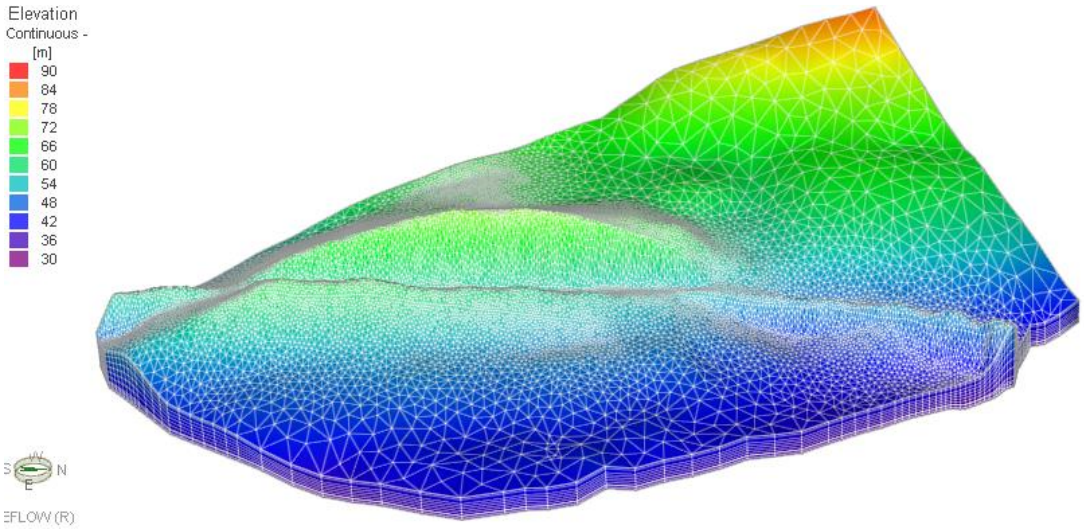

Figure 5.12 View of the entire three-dimensional Craigmore model geometry with elevation head (note: a vertical exaggeration of 5 was applied to give a better visual representation of the topographic variations at the site).

The model was evaluated based on the average hydraulic head measurements within individual boreholes. The average hydraulic heads used in this analysis can be seen in Table 5.6.

These heads were determined by taking the average pressure readings from the level loggers for the monitoring year of interest and adding the estimated elevation of the level logger. Screen levels of the standpipes were also taken into consideration when looking at the final "best-fit" results of the hydraulic head gradients, as well as the high and low hydraulic head data measured at each location. All borehole data shown in Table 5.6 can also be seen in Figure 5.13. The actual elevations for the top of the boreholes were not surveyed at the time of this research, so a topographic map was used to estimate these depths. Given the small amount of data for BH2 and BH3, estimates of average water levels are based on old data from when the standpipe monitoring was automated as well as more recent manual measurements. Standpipe screen levels are also given in Table 5.6.

Table 5.6 Average hydraulic heads taken from standpipe monitoring at the Craigmore study site for the 2009 study period.

Borehole	Standpipe	Average Hydraulic Head	Hydraulic Head High	Hydraulic Head Low	Standpipe Screen Elevations
		(m)			
1	Upper Till	67.1	69.5	65.7	64.8 – 66.2
	Lower Till	63.2	65.1	62.5	59.5 – 61.3
	Weathered Bedrock	57.2	57.7	56.8	54.4 – 55.8
2	Upper Till	66.5	67.0	65.2	63.2 – 65.1
	Weathered Bedrock	61.6	61.9	60.4	58.0 – 60.5
3	Upper Till	67.5	67.7	67.1	65.1 – 66.5
	Lower Till	67.5	67.7	67.0	61.1 – 62.5
	Weathered Bedrock	59.8	60.2	58.9	57.6 – 59.0
4C	Upper Till	56.8	56.9	56.8	56.1 – 56.9
4A	Weathered Bedrock	56.7	57.2	55.8	54.8 – 55.8

The values of applied recharge flux determined to produce the "best-fit" simulation for the assumed hydraulic conductivity values are summarized in Table 5.7. This value was around 60 mm year^{-1} based on the evaluation equations. Figure 5.14 also shows the observed versus

simulated hydraulic head distribution for the various recharge rates shown in Table 5.7. Both the table and figure show that a recharge rate near 60 mm year^{-1} appears to give the most realistic hydraulic head distribution. Figure 5.14 also highlights that a change in the recharge rates appears to have a larger influence on the overall hydraulic heads within the glacial till layers when compared to the weathered bedrock. In this plot, the weathered bedrock zones area located at or below the hydraulic head value of 62 mAOD. Given the small differences between models for small variations in recharge, further analysis of recharge versus hydraulic conductivity in the simulations was conducted and will be discussed in Section 5.1.7.2.

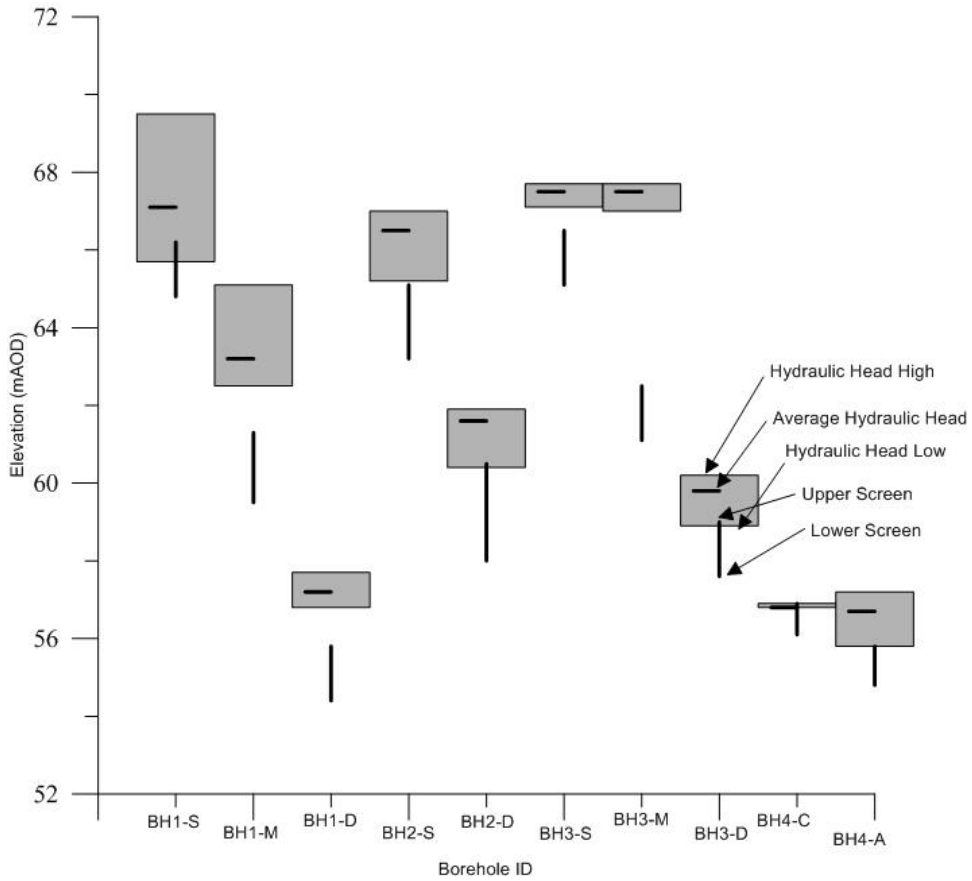

Figure 5.13 Borehole monitoring data summary showing upper and lower screen elevations and hydraulic head monitoring data for study period of 2009.

Table 5.7 Model evaluation methods used to determine "best-fit" recharge rate (***bold italics*** indicate "best" results).

Evaluation Method	Recharge Rate (mm year^{-1})			
	40	*50*	*60*	*70*
RMSE	1.30	1.12	***1.08***	1.11
MARE	1.66×10^{-2}	***1.38×10^{-2}***	1.41×10^{-2}	1.55×10^{-2}
E	0.91	0.93	***0.94***	***0.94***
R	***0.97***	***0.97***	***0.97***	***0.97***
d	0.97	***0.98***	***0.98***	***0.98***

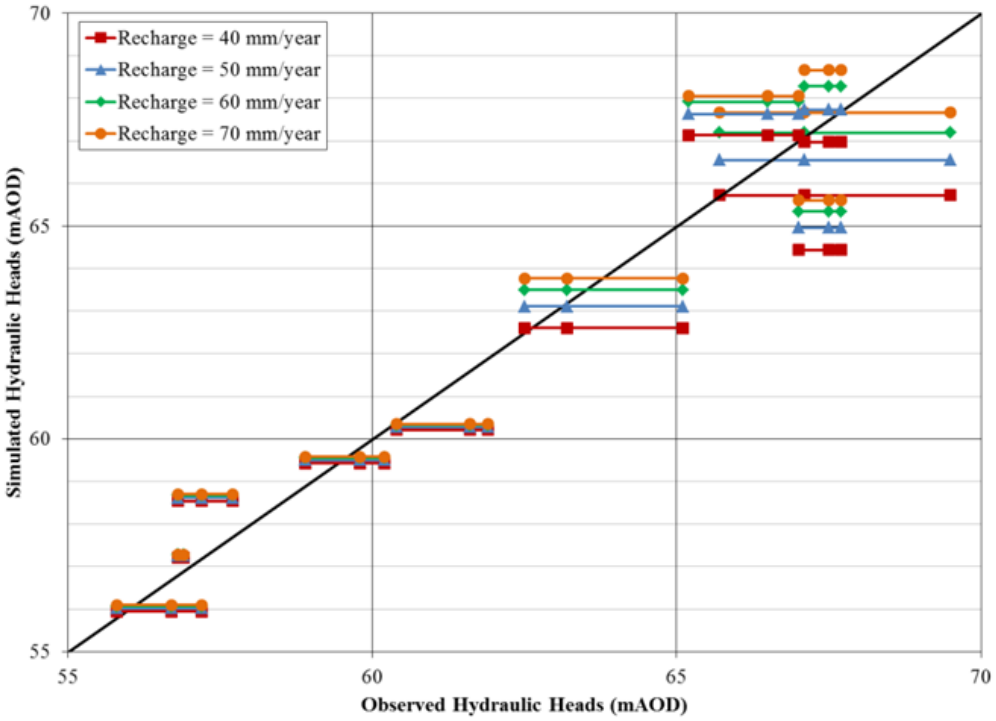

Figure 5.14 Simulated three-dimensional hydraulic head distributions given varying recharge rates versus observed hydraulic heads at Craigmore. Note that 3 values of 'observed hydraulic head' are provided at each borehole location (minimum, average and maximum).

The two-dimensional model cross-section was developed directly from the layer elevations in the three-dimensional model. The simulation cross-section was selected to coincide with a transect running through the locations of the boreholes along the crest of the cutting to allow for a better comparison of field measurements with simulated hydraulic heads. The far left and right geometric boundaries were chosen based on boundary conditions present in the three-

dimensional model and the bedrock outcrops on each side of the drumlin as geometric boundaries. In the three-dimensional model, the west bedrock outcrop has a small surface water pond that is currently being used by the producer that owns the field. The other bedrock outcrop on the east side of the geometry was assumed to have a seepage face boundary condition as the weathered bedrock that runs below the glacial till layers daylights in this location. Other boundary conditions that were applied include the seepage face boundaries along the slope cutting, as they were applied in the three-dimensional scenarios.

The recharge rates were varied using the same values that were used in the three-dimensional simulations. The "best-fit" was determined using the same evaluation methods as for the three-dimensional simulation (Table 5.8) and the simulated versus observed hydraulic head distribution is shown in Figure 5.15. The distribution of hydraulic heads is similar to those obtained in the three-dimensional simulation shown in Figure 5.14. The two-dimensional simulation gave similar results as the three-dimensional, with the "best-fit" recharge rate between 50 to 60 mm year^{-1}. It can also be noted that the weathered bedrock zone is not sensitive to the applied recharge rates, similar to what was experienced in the three-dimensional case.

Table 5.8 Evaluation results for each recharge rate used to determine the "best-fit" two-dimensional cross-section model (***bold italics*** indicate "best" results).

Evaluation Method	**Recharge Rate (mm year^{-1})**			
	40	*50*	*60*	*70*
RMSE	1.28	1.15	***1.14***	1.19
MARE	1.38×10^{-2}	***1.26×10^{-2}***	1.34×10^{-2}	1.52×10^{-2}
E	0.91	***0.93***	***0.93***	0.92
R	0.96	***0.97***	***0.97***	***0.97***
d	0.97	***0.98***	***0.98***	***0.98***

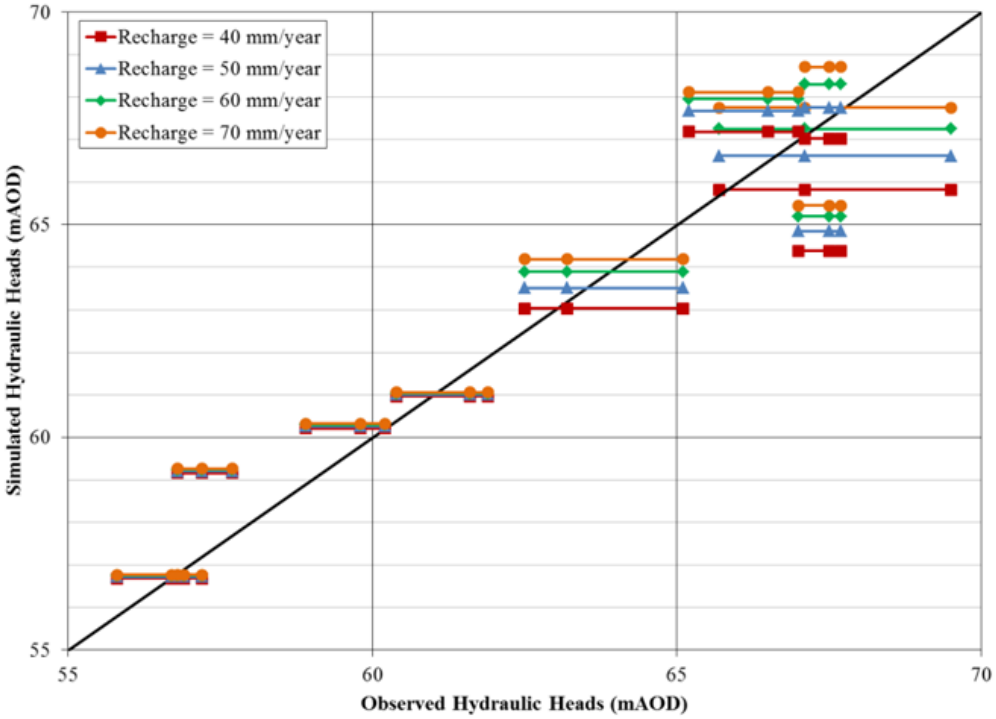

Figure 5.15 Simulated versus observed hydraulic head distributions for each recharge rate used at the Craigmore two-dimensional cross-section.

The simulated results were compared with the average field observations (Table 5.6) for each depth to obtain a "best-fit" steady-state groundwater flow model in both dimensions. The "best-fit" recharge rate of 50 to 60 mm year^{-1} was higher than the net percolation estimated for 2009 using the water balance model (25 mm year^{-1}). Other research that indicates there is a large range in potential recharge in glacial tills. Robins and Misstear (2000), for example, indicate that the general rule for recharge through a glacial till is 30% of rainfall. For this site, this would be a potential recharge rate of almost 300 mm year^{-1}. In a study completed by McConnville et al. (2001), however, the calculated recharge rate through a surface gley soil overlying glacial till was only 22 mm year^{-1}. The latter study was conducted using $\delta^{18}O$ profiles in various formations around the Belfast area to calculate recharge rates into the Enler Catchment. As seen in Figure 5.14 and Figure 5.15, the lowest observed heads would be better fitted using a much lower recharge rate, closer to that obtained from the water balance estimate.

The results of this "best-fit" analysis can be seen in Figures 5.16, 5.17, 5.18 and 5.19 for BH1, BH2, BH3 and BH4, respectively. As seen in the figures, this recharge rate results in a

hydraulic head distribution that would be acceptable given the screen lengths used for the average, high and low field observations. To ensure that the two layers of glacial till were required for the simulation, a test simulation was conducted with a single hydraulic conductivity assigned to both the upper and lower tills (1×10^{-9} m s^{-1}). Results of this analysis concluded that the slope change in the hydraulic head distribution that occurs at the upper and lower till interface could not be reached, thus concluding that a change in hydraulic conductivity of approximately one order of magnitude was required to represent the groundwater system accurately. Analyses from this evaluation was not included in the results of this thesis, but is noted to show that steps were taken to simplify the simulation; however in this case an accurate representation of the head distribution was not possible without including a lower hydraulic conductivity till layer at depth.

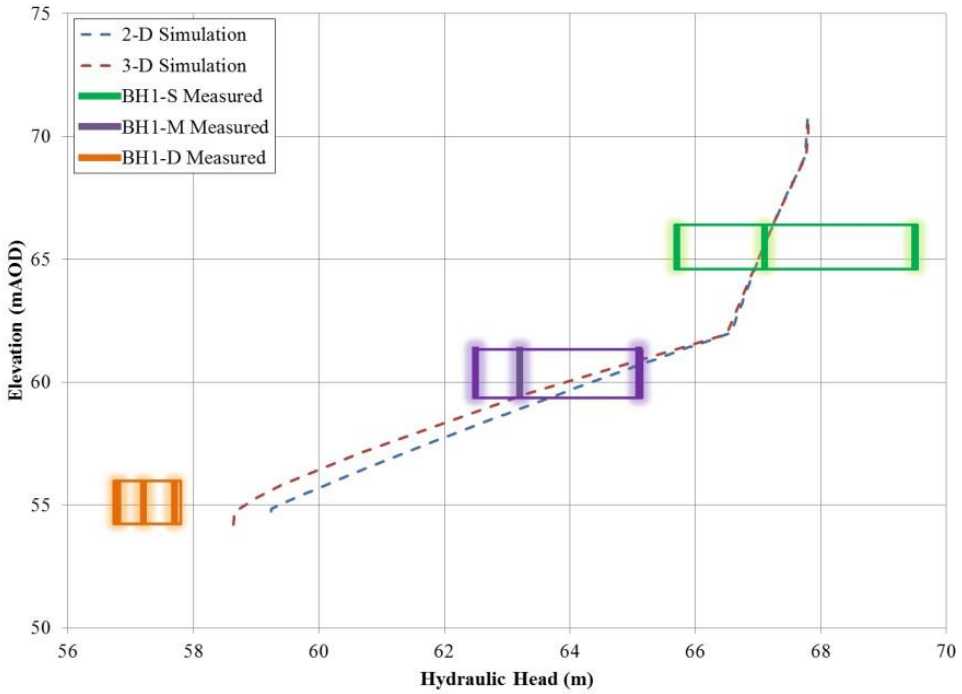

Figure 5.16 Hydraulic head measurements determined in the field and in the model simulation at BH1 (where S = upper till, M = lower till and D = weathered bedrock). Note that the box represents the zone of the screen with the observed minimum, average and maximum head measurements.

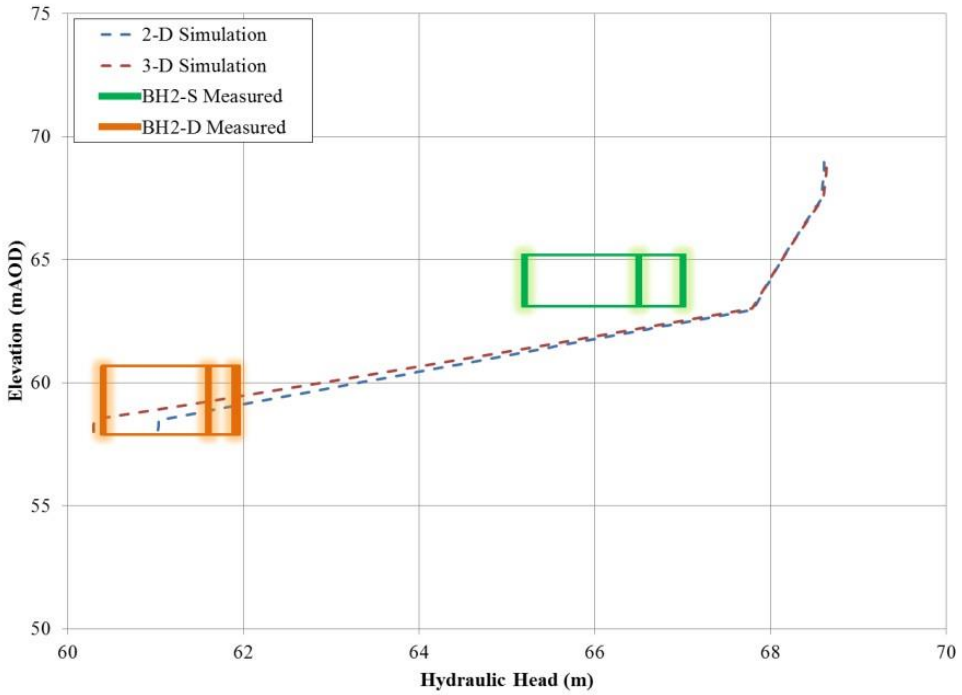

Figure 5.17 Hydraulic head measurements determined in the field and in the model simulation at BH2. Note that the box represents the zone of the screen with the observed minimum, average and maximum head measurements.

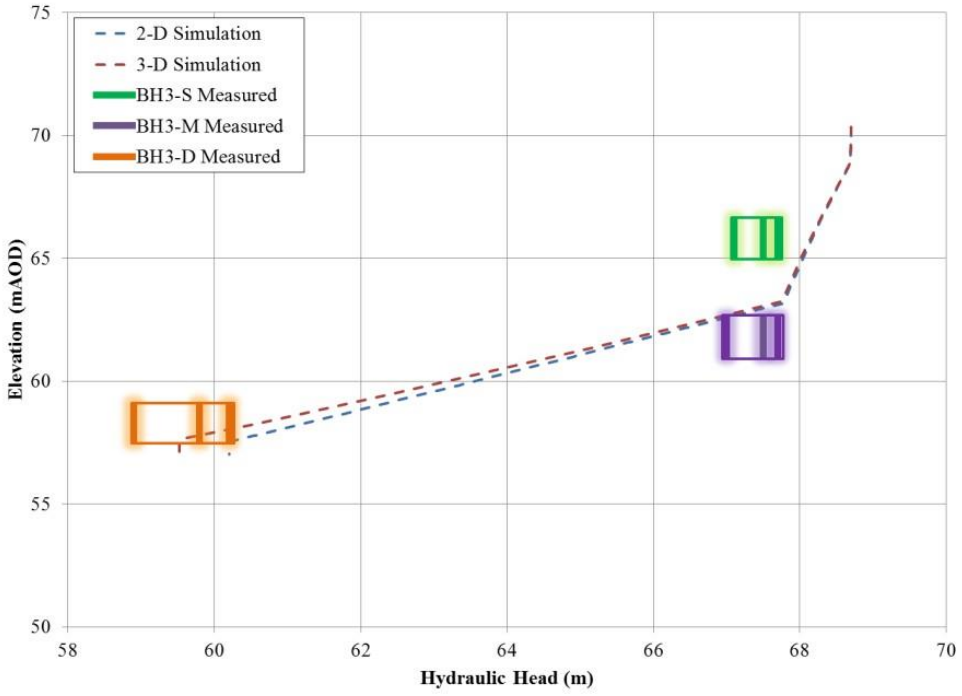

Figure 5.18 Hydraulic head measurements determined in the field and in the model simulation at BH3. Note that the box represents the zone of the screen with the observed minimum, average and maximum head measurements.

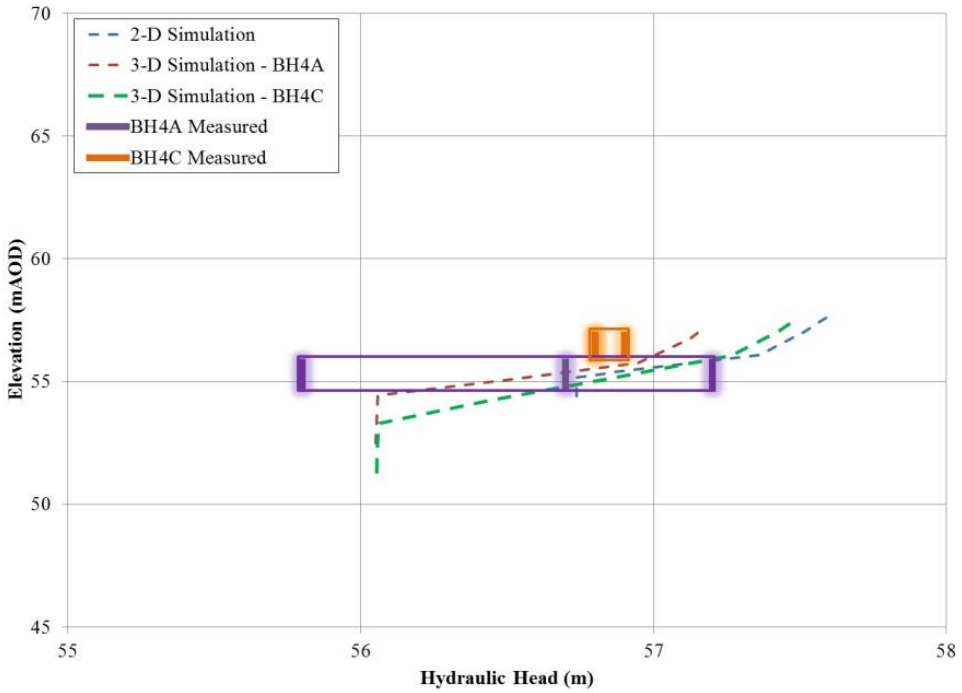

Figure 5.19 Hydraulic head measurements determined in the field and in the model simulation at BH4. Note that the box represents the zone of the screen with the observed minimum, average and maximum head measurements.

The lower vertical hydraulic gradient across the upper portion of the flow domain is of note, especially when looking at BH3. The slope between the middle and deep standpipes within each of the boreholes show that these screens must be located within a lower hydraulic conductivity soil, indicating the presence of a lower hydraulic conductivity glacial till overlying the weathered bedrock zone. The change in hydraulic conductivity by one magnitude between the upper and lower glacial tills appears to give a similar pattern in the simulation. When the hydraulic conductivity of the upper and lower till was set equal 1×10^{-9} m s^{-1}, the gradient loses the pattern seen in the field. This suggests that the slug tests conducted within the glacial tills may not have provided a representative sample of the two materials. Five of the six slug tests could only be performed on one of the boreholes (BH1) and more testing should be conducted on all boreholes to rule out testing errors in the slug test data. Given the different materials that were experienced during the construction of the boreholes, as well as during the soil classification exercises, the use of two glacial till layers with a difference in hydraulic conductivity by one magnitude is a realistic assumption.

Similar patterns of hydraulic head can be seen in the two-dimensional cross- section when compared to the three-dimensional system. The two-dimensional simulation generally showed higher heads in the weathered bedrock and lower till zones than in the three-dimensional simulations, especially in areas near or along discharge zones (BH4). This may be a factor of dimensionality, where the three-dimensional domain allows more water to flow away from those locations within the model domain. Note, the standpipes of BH4 were drilled as separate holes along the western side of railway instead of being clustered into one borehole, so the cross-section model passes through the center of the two standpipes representing BH4A and BH4C. This may lead to a slight change in the hydraulic head measurements based on in situ material properties and elevations. This would be considered a limitation of using standpipe data for calibration of a two-dimensional model when the data is collected perpendicular to the cross-section being used in the simulation. BH4A and BH4C measurements were still included in the analysis, however, so that data from the toe of the slope could be included in the model. This was completed to ensure that an approximate representation of the saturation at the toe of the slope could be captured. Further simulations should be conducted with more recent meteorological data, as these boreholes are a fairly recent addition to the monitoring data and may not be representative of the conditions during the monitoring period used for the simulation (2009).

The primary purpose of this model study was to compare the simulated groundwater flow system and pore-pressure (heads) along the same cross-section between two- and three-dimensions. Similar boundary conditions and elevations were used in each of the simulations to obtain as similar a representation as possible. These images were exported from Feflow for the three-dimensional and two-dimensional simulations using a recharge rate of 55 mm $year^{-1}$ (Figure 5.20).

The hydraulic head contours of both figures indicate that both dimensional simulations produced similar hydraulic head distributions within the area of interest (where the boreholes are present). Both dimensions indicate that there is a discharge zone where the water exists at the surface along the railway at the toe of the excavation, as well as on either side of the drumlin itself, where the bedrock outcrops exist. The distribution of hydraulic head within each of the

models are similar; however, it is important to note that the three-dimensional simulation extends past the two bedrock outcrops, which may allow water to flow past these points from the drumlin. As shown in the figure, however, a water table forms around the location of the outcrops that should allow for most water to be discharged at that point. The water budget analysis of the nodes along the cross section also shows that there appears to be a higher amount of water leaving the domain at these points instead of entering. Also, there may be an influence on the hydraulic head distribution and water balance of the three-dimensional model from the constant head boundary condition along the northern edge of the three- dimensional geometry that is not present in the two-dimensional simulation, as there is a small creek located there that is not present along the drumlin cross-section. Overall, the hydraulic head gradients and the water table position are very similar for both dimensional simulations.

The overall water budget over the cross-sections and model domains were obtained for the dimensional models by conducting a simple water budget within Feflow. The water leaving the model domain through seepage faces and constant head boundaries is compared to the total amount of water entering the cross-sectional domain. In both models, the cross-section is analyzed by gathering recharge data from the elements surrounding the nodes of the cross-section, while the discharge is measured from boundary conditions placed directly on the nodes. To ensure that this calculation was completed in a manner that is similar to those completed in the two- dimensional simulations, element sizes were manually adjusted along the line of the cross-section by using 1 m nodal spacing. By ensuring that these elements had a 1 m nodal spacing, the calculation of the total recharge would only be taken over a width of 1 m, as Feflow calculates the recharge and discharge based on half of each of the elements on either side of the line. The two-dimensional models calculate recharge and discharge by assuming a 1 m depth along the cross-section, allowing the comparison to be more alike. The results of the water budget calculations by Feflow are presented in Table 5.9.

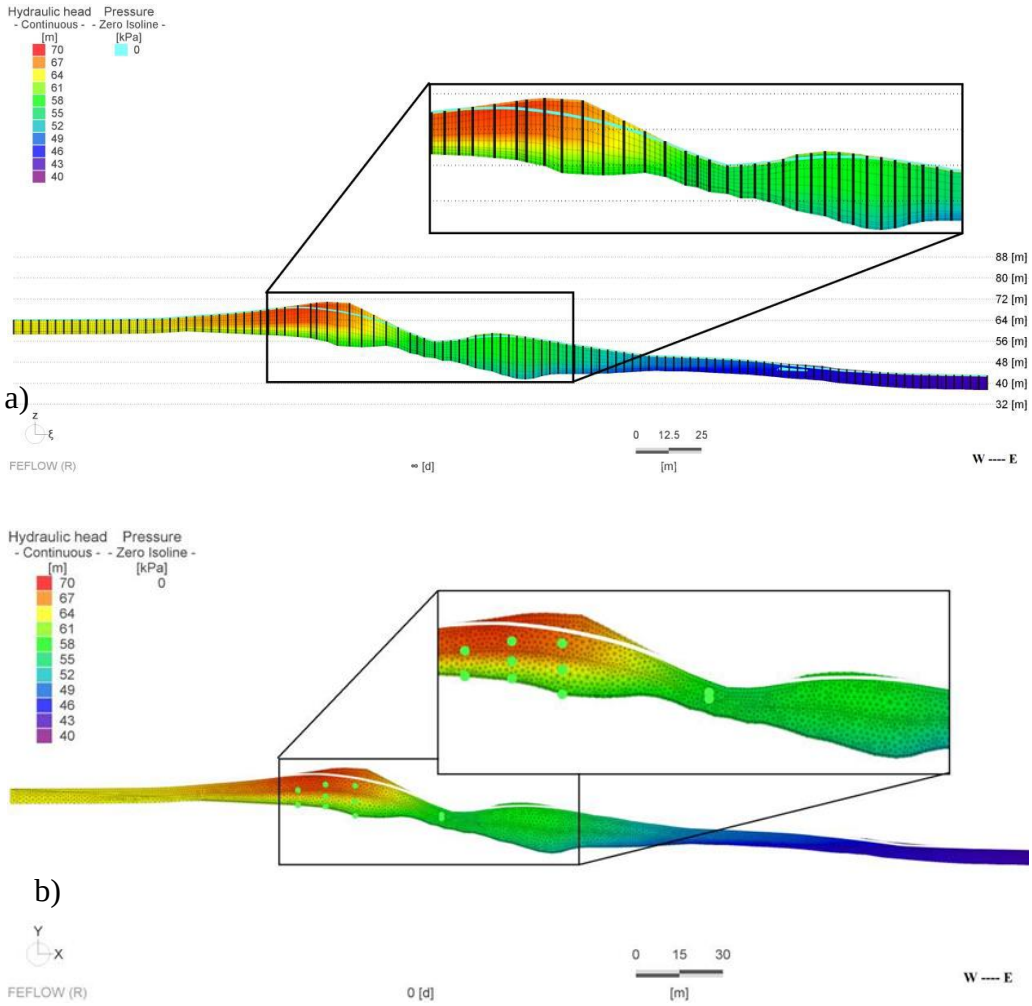

Figure 5.20 Hydraulic head distribution and water table level (zero pressure line) in the a) three- dimensional and b) two-dimensional cross-section (with approximate borehole "tips") Craigmore simulation.

As seen in Table 5.9, the overall water budget for both simulations was able to generate an acceptable balance. The total recharge rates calculated for the just the surface of the cross-sections show that the three-dimensional model allowed more total discharge than the two-dimensional simulation, resulting in a lower net recharge. This could be a result of the use of boundary conditions to represent seepage faces along the east and west boundaries of the two-dimensional model domain. These were added to ensure that the daylighting weathered bedrock zone could be accurately represented. As the nodes do not only exist directly on the surface of

the two-dimensional cross-section, water can leave the domain in areas other than the surface node, leading to a higher net recharge in the two-dimensional system.

Table 5.9 Comparison of applied unit flux rates to obtain similar hydraulic head gradients and resultant total recharge amounts in each of the two-dimensional and three-dimensional simulations.

Simulation (Software)	**Total Recharge (mm year^{-1})**	**Total Discharge (mm year^{-1})**	**Net (mm year^{-1})**
3-D (entire domain)	55.8	55.8	0
3-D (cross-section)	55.2	51.9	+3.4
2-D (entire domain)	55.1	55.1	0
2-D (surface only)	55.1	44.6	+10.4

5.1.4 Sensitivity Analyses

As described in the Materials and Methods section (Section 3.0), sensitivity analyses were completed on the base condition model to ensure that the "best-fit" material properties and recharge rates were used. Other sensitivity analyses were also completed to determine the overall influence of bedrock topographic variations completed on the three-dimensional model. The sensitivity analyses were not studied on the two-dimensional analysis, as this model was based on parameters used on the three-dimensional simulations to allow for proper comparison between each.

Hydraulic Conductivity versus Recharge Rate

The hydraulic conductivity values within a steady state model can generally be changed in proportion to a change in applied flux with substantively altering the distribution of hydraulic head. Consistent with steady state analyses, the hydraulic head distribution stays the same as long as the ratio of the recharge/hydraulic conductivity remains unchanged. For example, varying both the values of hydraulic conductivity and the applied flux rate by a factor of 3 (increase or decrease) indicated that the same head distribution as obtained for the base case

(which had an applied recharge rate of 60 mm year^{-1}) can be obtained for applied flux rates ranging from 20 mm year^{-1} to 180 mm year^{-1}. A change in hydraulic conductivity by a factor of 3 is not unreasonable and this highlights that the agreement between the water balance estimates and the steady state groundwater flow simulation estimates are in fact quite close. A decrease in the hydraulic conductivities by only a factor of 3 results in a "best-fit" recharge rate near the water balance estimate given in Section 5.1.1.

A sensitivity study was also undertaken on differences in hydraulic conductivity for the upper and lower tills, individually. These values were varied along with the recharge rates and were compared to the base condition. The hydraulic conductivity of the upper and lower tills was varied by a factor of 5 with the recharge rate held constant at 60 mm year^{-1} (the base condition "best-fit"). It is apparent that the hydraulic head distribution was sensitive to the value of the hydraulic conductivity of the upper till (Figure 5.21). As the hydraulic conductivity increased, a greater proportion of the recharging waters were diverted laterally within the upper till resulting in a decrease in the vertical flow into the lower till. The impact of changes in the hydraulic conductivity of the lower till was most apparent in the heads within the weathered bedrock zone. This would indicate that the aquifer recharge, and overall weathered bedrock flow system, is more significantly influenced by the lower till when compared to the upper till system. The hydraulic heads within the weathered bedrock zone increased as the hydraulic conductivity of the lower till increased causing more flow into the bedrock system.

Table 5.10 shows the "best-fit" results comparison for each of the analyses completed above with a fixed recharge rate of 60 mm year-1. The results indicate that the most significant "worst-fit" occurs when the hydraulic conductivity of the upper till is decreased or the lower till is increased, as this would be similar to a single layer of material without the contrasting conductivities of the two layers in the drumlin. Given the results of all of the analyses between the upper and lower till hydraulic conductivities, it would appear that the lower till has a more significant influence on the overall hydraulic head distribution, as indicated in Figure 5.21.

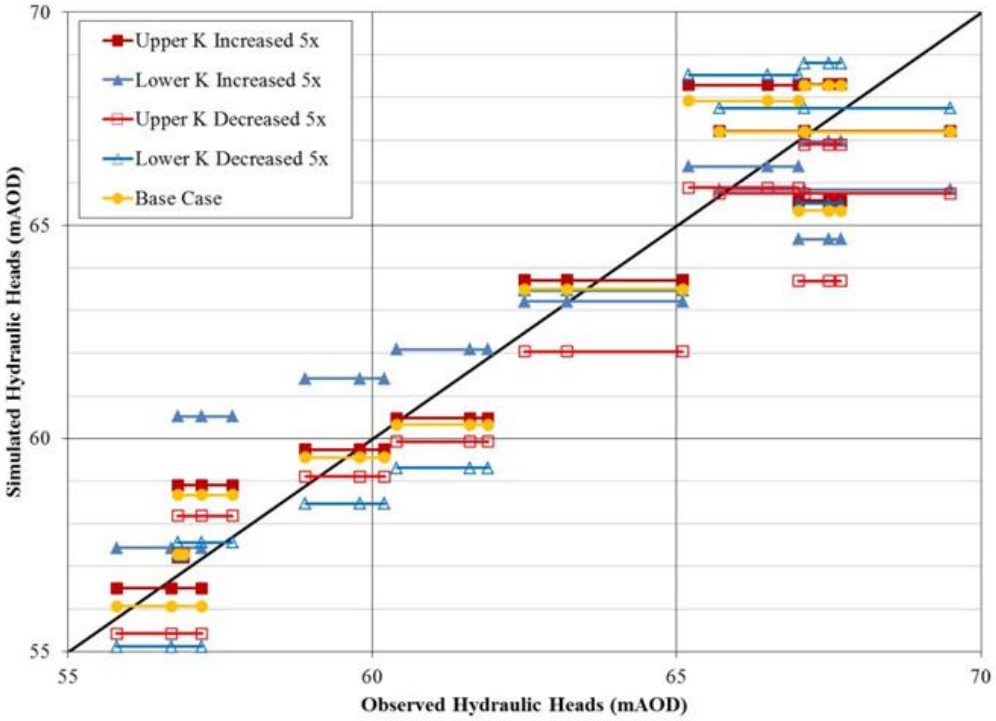

Figure 5.21 Sensitivity of the Craigmore three-dimensional simulation to hydraulic conductivity of the two glacial till layers. Note that 3 values of 'observed hydraulic head' are provided at each borehole location (minimum, average and maximum).

Table 5.10 **"B**est-fit" results as part of the hydraulic conductivity versus recharge analysis at Craigmore cross-section.

Model	Evaluation Method				
	RMSE	MARE	R	E	d
Base	***1.08***	1.41×10^{-2}	***0.97***	***0.94***	***0.99***
Upper Till K increase	1.10	$\boldsymbol{1.36 \times 10^{-2}}$	***0.97***	***0.94***	***0.98***
Upper Till K decrease	1.57	2.06×10^{-2}	0.96	0.87	0.97
Lower Till K increase	1.56	1.84×10^{-2}	0.96	0.87	0.96
Lower Till K decrease	1.42	1.96×10^{-2}	0.96	0.89	0.98

Bedrock Transmissivity

The sensitivity of the results to the transmissivity of the weathered bedrock was evaluated by comparing the head distribution for transmissivity values of 5 x 10^{-7} m^2 s^{-1} and 1 x 10^{-8} m^2 s^{-1}. The simulation was unable to converge if the transmissivity was increased higher than 5 x 10^{-7} m^2 s^{-1}. Figure 5.22 shows the results of the hydraulic head distributions for changes in the weathered bedrock transmissivity from 2 x 10^{-7} m^2 s^{-1} (base condition) to 5 x 10^{-7} m^2 s^{-1}, 1 x 10^{-7} m^2 s^{-1} and 5 x 10^{-8} m^2 s^{-1}. Table 5.11 shows the "best-fit" analysis of each of the transmissivities shown in the figure, indicating that the transmissivity of 2 x 10^{-7} m^2 s^{-1} is the "best-fit" of the analysis.

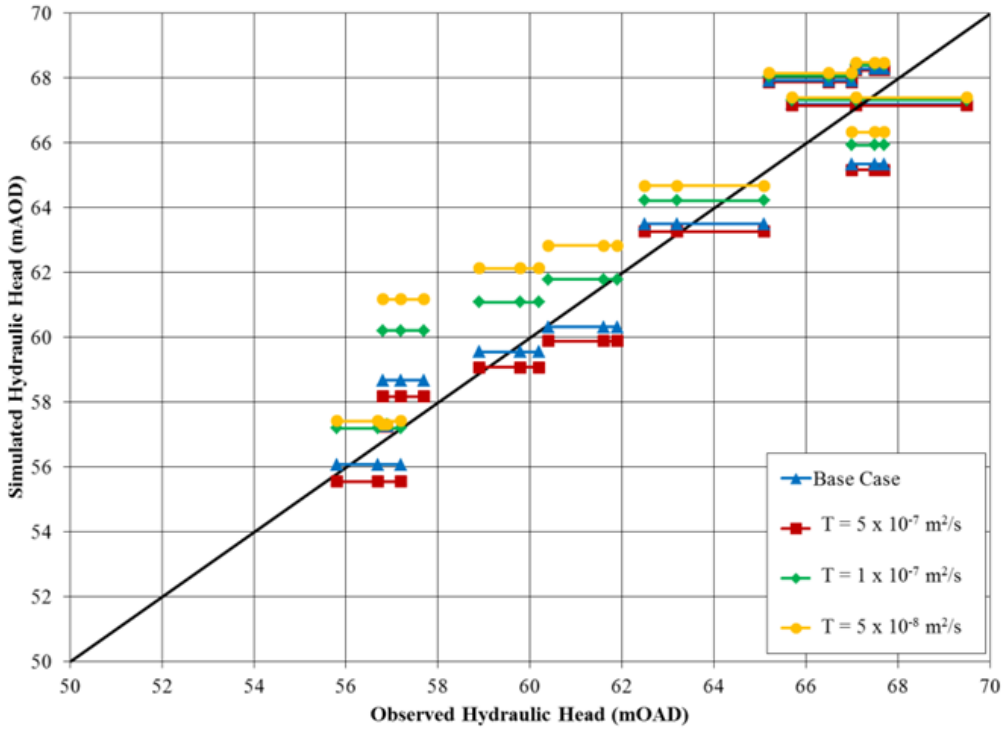

Figure 5.22 Hydraulic head distributions for each model of bedrock transmissivity in the three-dimensional simulations. Note that 3 values of 'observed hydraulic head' are provided at each borehole location (minimum, average and maximum).

Table 5.11 Evaluation results of the Craigmore weathered bedrock transmissivity analysis (bold italics indicate the "best-fit").

Evaluation Method	Transmissivity ($m^2 s^{-1}$)			
	5×10^{-7}	*2×10^{-7}*	*1×10^{-7}*	*5×10^{-8}*
RMSE	1.17	***1.08***	1.33	1.74
MARE	1.55×10^{-2}	***1.41×10^{-2}***	1.68×10^{-2}	2.25×10^{-2}
E	0.93	***0.94***	0.91	0.84
R	***0.97***	***0.97***	***0.97***	0.96
d	0.98	***0.99***	0.98	0.96

As the bedrock transmissivity was changed, the upper till hydraulic head measurements were not affected significantly. The lower till and weathered bedrock zones were impacted the most by the changes in transmissivity, which would be expected given the low conductivity of the lower till decreasing the interaction between the upper till and weathered bedrock zone. When comparing the base condition to the scenario in which the transmissivity was set to 5×10^{-8} $m^2 s^{-1}$, there is a change in hydraulic heads by as much as 1.5 to 2.5 m. The hydraulic heads within the upper till however, only change by less than 0.5 m. This indicates that most of the water movement through the upper vadose zone of the drumlin is not affected by the weathered bedrock transmissivity since the bedrock aquifer is free draining and is not fully confined near the discharge area. The heads within the weathered bedrock zone are sensitive to the assigned transmissivity, as this is where most of the water movement through the aquifer occurs.

"Smooth" versus "Rough" Bedrock

The analysis of the influence of the bedrock topography on the overall groundwater flow systems was conducted by "smoothing" out the bedrock layer. This was done to remove the large variability in the weathered bedrock zone surface elevations. The mesh for the base condition model was used when developing this model, so that the same boundary conditions, nodal spacing and material properties could be applied to each. Some of the details from the seismic refraction surveys were removed from the interpolation of the bedrock surface to allow less

refinement of the bedrock variability. The information obtained from the bedrock outcrops and borehole data were kept in the interpolation, along with some of estimated bedrock topography used in the base condition. Overall, the Craigmore cutting did not have a lot of variability in the original bedrock interpolation, as the seismic surveys were not available along the cutting itself. The areas where changes in bedrock are more prominent are within the other drumlins surrounding the cutting area (Figure 5.23).

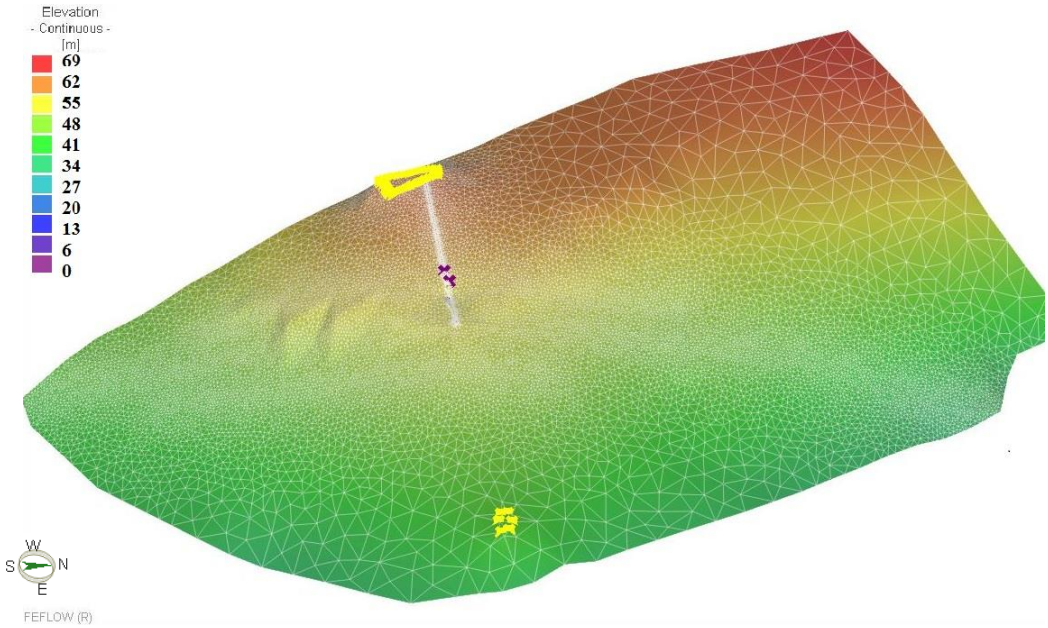

Figure 5.23 "Smooth" bedrock surface interpolated using only some outer boundaries obtained using the seismic refraction survey results and the bedrock outcrop and borehole elevations.

The interpolated "smooth" bedrock surface was then imported into the geometry of the base condition model. To ensure that the comparison is based on just bedrock topography alone, the material properties were all kept the same as the base condition models. Recharge rates were also kept the same at 55 mm year^{-1} for ease of comparison with the three- and two-dimensional "rough" simulations. The two-dimensional simulation was not included in this analysis.

The hydraulic head contours for the cross-section of the three-dimensional "smooth" model are given in Figure 5.24. This hydraulic head distribution is very similar to that obtained in the three-dimensional "rough" bedrock simulation. The only difference in hydraulic head

distribution can be seen in the right portion of the drumlin excavation. As this section has been flattened to remove the dips on that side of the drumlin, there is less space for water flow. Given the high water table, however, the head distributions are similar at similar elevations. Overall, the simulations in either the "smooth" or "rough" scenario appear to result in similar hydraulic head distributions given the same recharge rate.

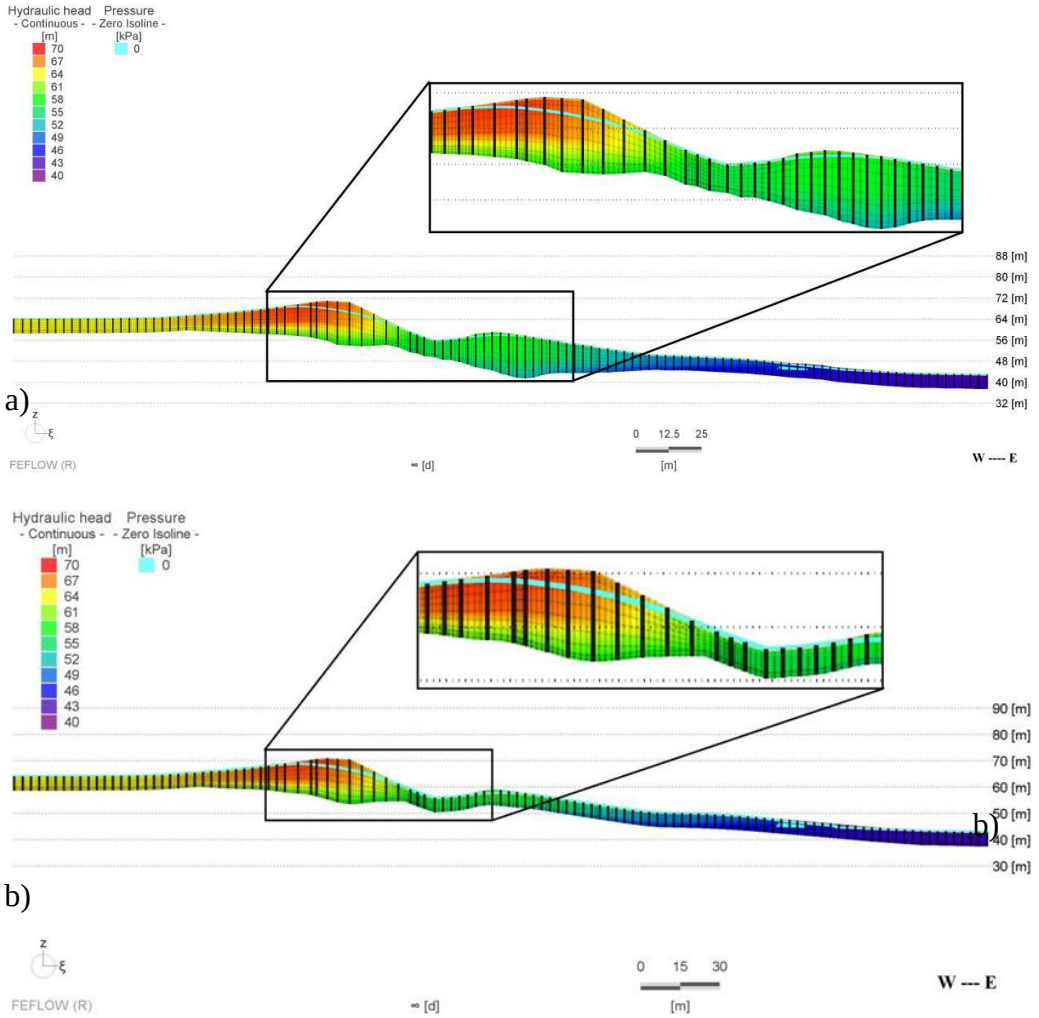

Figure 5.24 Hydraulic head distribution with water table (zero pressure line) in the three-dimensional Craigmore cross-section for the a) "rough" and b) "smooth" scenarios.

In order to analyze the differences between the simulations further, the recharge and discharge rates were calculated in Feflow using the budget analyzer tool (Table 5.12). The same recharge input of 55 mm year^{-1} was used for both models. In this scenario, the net recharge values are more similar than what was seen in the "rough" simulations above. There is less

discharge occurring in the "smooth" simulation when compared to the "rough" scenario. As seen in the cross-section (Figure 5.24), this could be resultant of the depth below the bedrock outcrops being much smaller than in the "rough" condition. As the exact depth of the tills up to these outcrops is not known, as well as the potential depth of weathering at these outcrops, either condition may exist.

Overall, the three-dimensional simulations did not differ significantly when the bedrock surface was changed from "rough" to "smooth". The overall impact of the bedrock topography refinement appears to have only a small influence on the overall groundwater flow system. Further analysis should be completed on the influence of the weathered bedrock thickness above the bedrock surface on overall hydraulic head distributions and modeling efficacy in both dimensions.

Table 5.12 Total recharge and discharge rates for each model given the unit flux rate applied to each "best-fit" simulation.

Simulation (Software)	**Total Recharge (mm year^{-1})**	**Total Discharge (mm year^{-1})**	**Net (mm year^{-1})**
"Smooth" (Entire Domain)	55.6	55.6	0
"Smooth" (Cross-Section)	55.1	42.5	+12.6
"Rough" (Entire Domain)	55.8	55.8	0
"Rough" (Cross-Section)	55.2	51.9	+3.4

5.2 Loughbrickland Highway Cutting

The model presentation for the Loughbrickland site will follow the same sequence as for the Craigmore site with initial recharge estimates based on a surface water balance followed by two- and three-dimensional simulations. The 'best-fit' model will then be tested through a set of sensitivity analyses.

5.2.1 Water Balance Estimation Results

The STELLA model described above was also used to simulate the water balance for this site. In order to make these estimations more site-specific, the material properties and depths were changed and a similar sensitivity analysis on these parameters was conducted as was done at Craigmore. The material properties of active zone were varied first to determine the "best-fit" material properties given the precipitation, estimated evapotranspiration and estimated runoff (Table 5.13). This "best-fit" was determined in the same manner as the Craigmore water balance, where the measured water content of the active zone for the EnviroScan located in the field along the crest of the drumlin was used for the calibration process (Figure 5.25).

Table 5.13 Material properties used in the water balance simulations to determine the "best-fit" model.

Simulation	Porosity	Field Capacity	Permanent Wilting Point
Run 1	0.30	0.20	0.10
Run 2	0.31	0.17	0.09
Run 3	0.32	0.18	0.10
Run 4	0.31	0.20	0.10

The "best-fit" material properties for the Loughbrickland water balance were determined to be a porosity of 0.31, field capacity water content of 0.17 and a permanent wilting point water content of 0.09 (Run 2). An initial depth of 0.6 m was used at the start of the analysis, as this value is further analyzed in the next step. Results of the evaluation methods can be seen in Table 5.14. Three of the five evaluation methods determined that this method was the "best-fit". The first simulation resulted in two of the methods naming it the "best-fit", given the initial data comparison prior to the spike in water content during August 2010. As the spikes in water content were never experienced in this model, the other evaluation methods did not consider it the "best". These spikes were difficult to mirror in the STELLA model, as the actual in situ properties cannot be matched perfectly given the "black box" technique used in the estimation method.

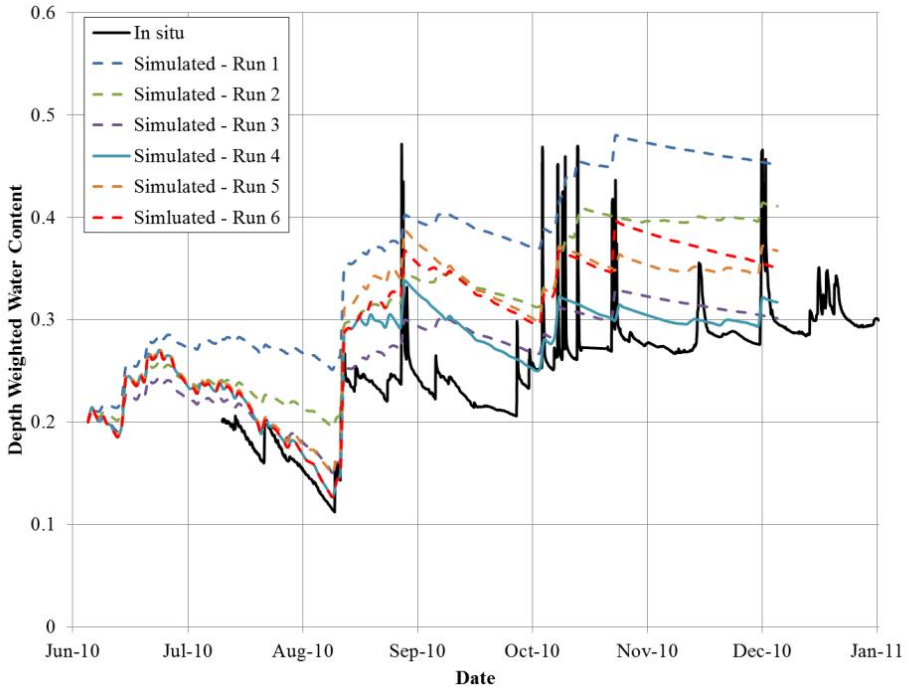

Figure 5.25 Comparison of calculated depth weighted water content in the upper active zone with the average water content from ES01 on the crest of Loughbrickland slope.

Table 5.14 Calibration results to determine the "best-fit" water balance model with bold italics indicating the "best" model.

Simulation Properties	**Evaluation Method**			
	Run 1	*Run 2*	*Run 3*	*Run 4*
RMSE	2.17×10^{-2}	***2.15×10^{-2}***	2.56×10^{-2}	2.30×10^{-2}
MARE	***5.51×10^{-2}***	5.88×10^{-2}	7.38×10^{-2}	6.74×10^{-2}
R	***0.95***	0.92	0.92	0.92
E	0.82	***0.83***	0.76	0.80
d	***1.00***	***1.00***	0.99	0.99

The "best-fit" water balance model determined above was further analyzed using varying depths of the active zone. This depth ranged from 0.5 m to 0.9 m, which is the range that is expected given visual observations of the soil profiles during the excavation of soil pits near the location of the EnviroScan. Each simulation was analyzed using the same evaluation methods as above, comparing the simulated changes in water content with the observed water content measurements (Figure 5.26). The final results of each evaluation method determined that the "best-fit" active zone depth was 0.8 m (Table 5.15). As the EnviroScan could only be installed to

this depth, it is estimated that the upper till interface is close to this depth. This "match" in the overall depth of the active zone indicates that a reasonable model has been developed.

Table 5.15 Evaluation method results to determine the "best-fit" depth for the active zone, with the "best-fit" is in bold italics.

Evaluation Method	**Depth of Active zone (m)**				
	0.5	*0.6*	*0.7*	*0.8*	*0.9*
RMSE	2.23×10^{-2}	2.56×10^{-2}	2.06×10^{-2}	***2.02*** $\times 10^{-2}$	2.05×10^{-2}
MARE	6.60×10^{-2}	5.88×10^{-2}	5.18×10^{-2}	***5.12*** $\times 10^{-2}$	5.45×10^{-2}
E	0.93	0.92	0.93	0.94	***0.95***
R	0.82	0.83	0.84	***0.85***	0.84
d	0.99	1.00	1.00	***1.00***	1.00

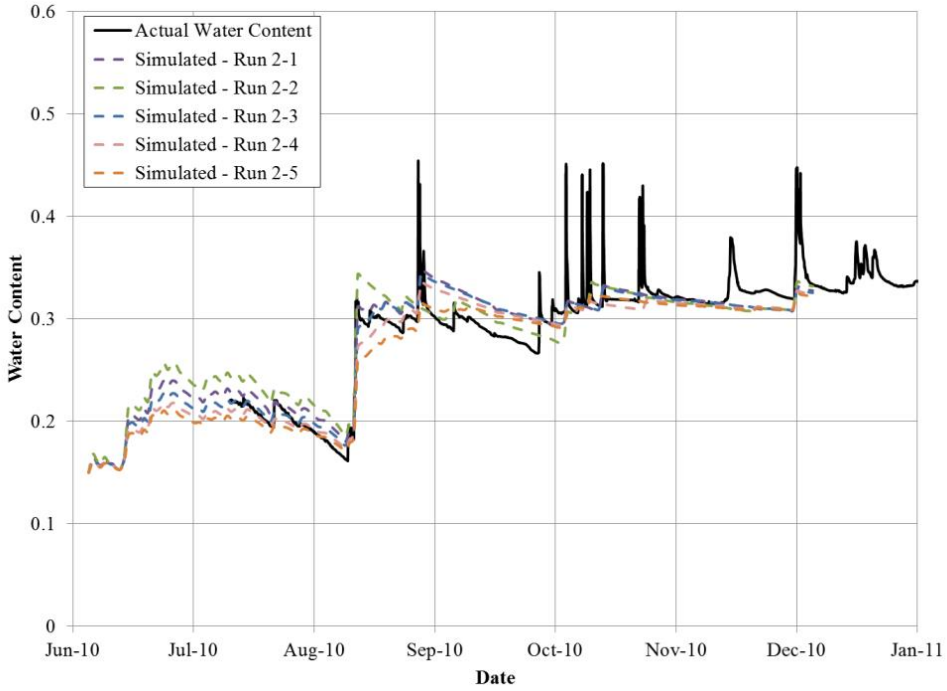

Figure 5.26 Sensitivity analysis results showing the influence of active zone soil depth used in the water balance model.

As the measurements of the EnviroScan did not commence until 2010, the year of 2010 was used for the initial estimation of recharge for the Loughbrickland site. The weather data was taken from the same meteorological station described above and was entered into the "best-fit"

water balance model developed in STELLA. The final water balance for 2010 can be seen in Figure 5.27. The same weather conditions for the "wet", "dry" and "average" years were also used to develop water balance estimations to get a good estimation of the potential annual recharge rates given varying annual precipitation rates. As conducted in the Craigmore water balance, the years 1975, 1994 and 2002 were used for the "dry", "average" and "wet" years. The results for each of the water balance simulations can be seen in Figure 5.28, Figure 5.29 and Figure 5.30 for 1975, 1994 and 2002, respectively. Final annual estimates for precipitation, potential and actual evapotranspiration, runoff and recharge can be seen in Table 5.16.

As seen in Table 5.16, differences exist between the estimated hydrologic parameters when compared to Craigmore. The AET estimate can differ, as the relative water content of the active zone will change given the new material properties and soil depth. Errors in the models must have occurred in the case of the calculation of PET, as the parameters for each were kept the same for each year as Craigmore. The reason for this error is unknown, as the same calculations and inputs were used. Overall, the water balance estimations suggest that the average recharge value is around 31 mm year^{-1}.

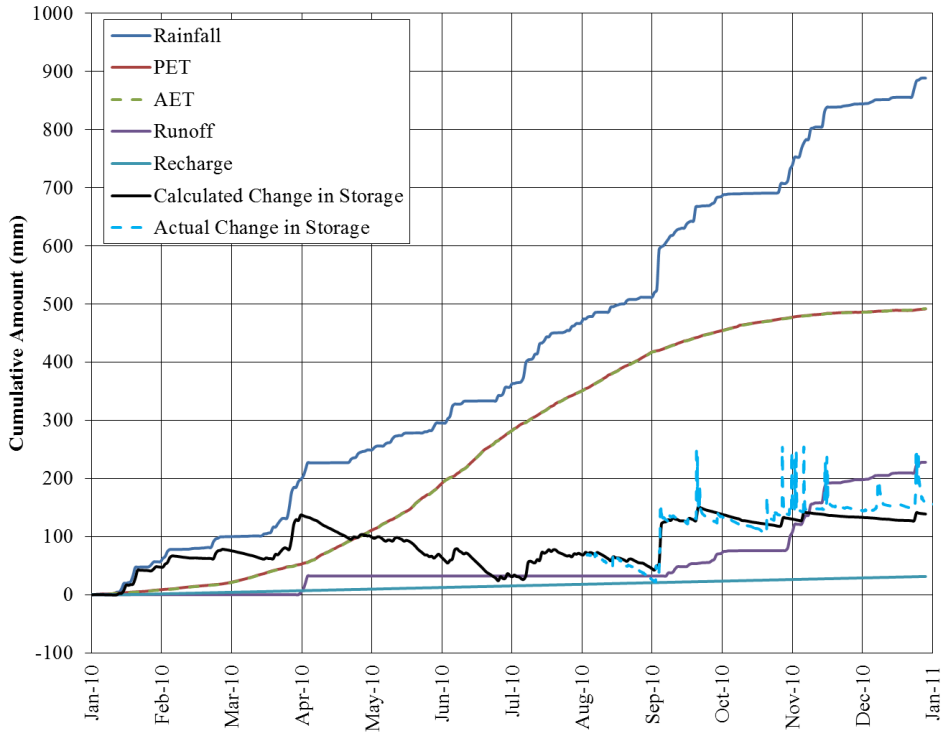

Figure 5.27 Final water balance developed for Loughbrickland for the full year of 2010.

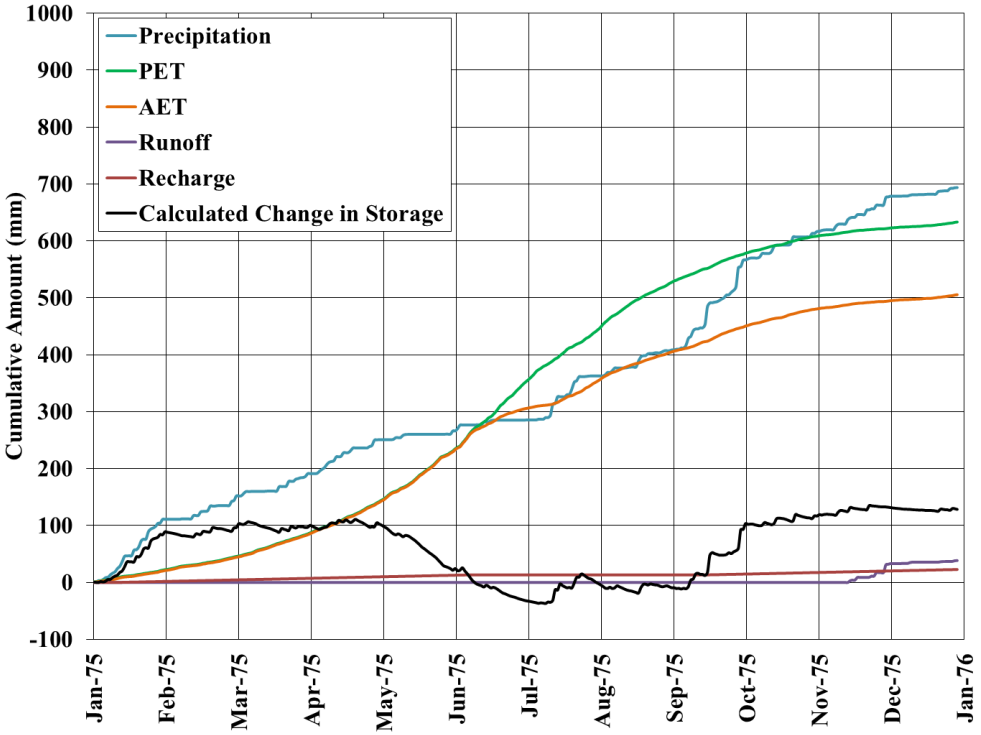

Figure 5.28 Final water balance developed for Loughbrickland for the full year of 1975.

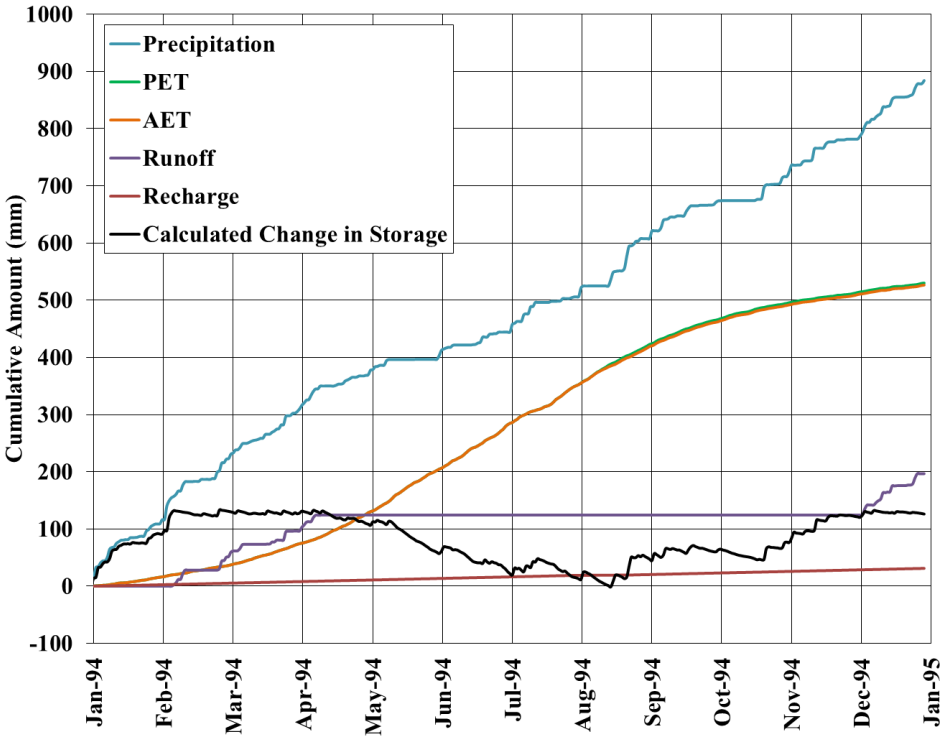

Figure 5.29 Final water balance developed for Loughbrickland for the full year of 1994.

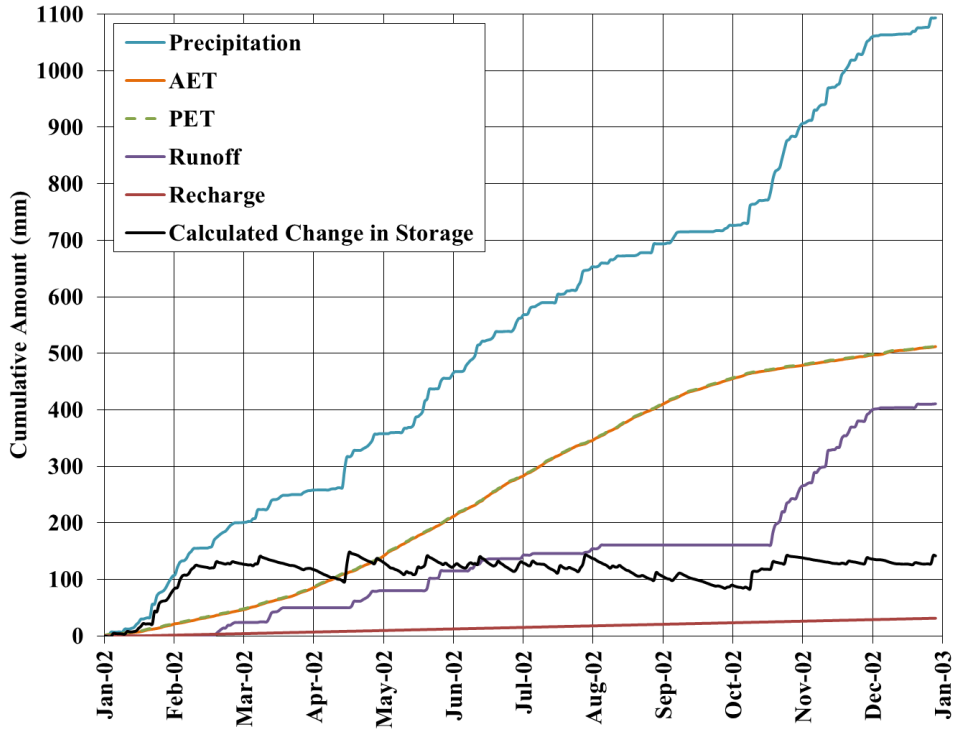

Figure 5.30 Final water balance developed for Loughbrickland for the full year of 2002.

Table 5.16 Cumulative values of hydrologic parameters determined in Loughbrickland water balance model with approximate annual numbers given based on rates.

Year	Precipitation	PET	AET	Runoff	Recharge	ΔS
			(mm year^{-1})			
1975	694	634	506	39	23	128
1994	884	531	527	197	31	131
2002	1094	514	512	411	31	141
2010	888	492	492	228	31	138

5.2.2 Steady-State Hydrogeological Simulations

Similar scenarios were developed for the Loughbrickland highway cutting as was completed in the Craigmore simulations. The initial three-dimensional base model was set up using field data and literature sources. Once this conceptual model was developed and determined "best-fit", a cross-section was chosen and simulated in two- dimensions. This scenario was developed with the same boundaries applied in the three-dimensional cross-section. Each of these simulations was then compared and underwent a series of sensitivity analyses. All

of the data compiled from these simulations were then analyzed to further understand the dimensional analyses and determine the most appropriate method for use in future research.

The conceptual three-dimensional model was developed using similar methods as described previously for the Craigmore simulations. A groundwater contour map was developed for the site using data obtained by borehole data and surface water bodies (Figure 5.31). The groundwater contour map, along with surface elevation files, was then used to determine appropriate geometry boundaries for the three-dimensional simulation. Model geometry boundaries were based on the locations of estimated groundwater contours and known water levels. The Lough on the east side of the drumlin provides a convenient constant head boundary condition. The northern boundary was developed using estimated groundwater divides along the topographic high of a nearby drumlin. The western boundary was chosen based on the contour map and was given a seepage face boundary condition given the area is known to be marsh- like. The southern boundary was placed along no flow boundaries that were perpendicular to contour lines, as well as along a portion of one of the interpolated contour lines. Boundary conditions were included on the weathered bedrock layer where drainage ditches were installed along the bench and the toe to ensure that water levels remained below the highway structure. This was included using a seepage face boundary condition given a specific hydraulic head along the area of the drainage ditches. The approximate location and length of the drains present along the toe and bench of the slope were estimated and included in the conceptual model based on information gathered by Clarke (2007).

Material properties that were used in the three-dimensional conceptual model were determined using ranges given by data collected in situ, from laboratory and by past research (Clarke, 2007). The "best-fit" material properties are outlined in Table 5.17. These values were varied to ensure that the "best-fit" model could be determined. The most realistic, simple conceptual model was then used to develop the "calibrated" models described below. The weathered bedrock to lower glacial till interface did not require a transition layer as was required for Craigmore. Convergence was reached without this layer, however, the vadose zone weathering layer was still required to be set at 1×10^{-8} m s^{-1}.

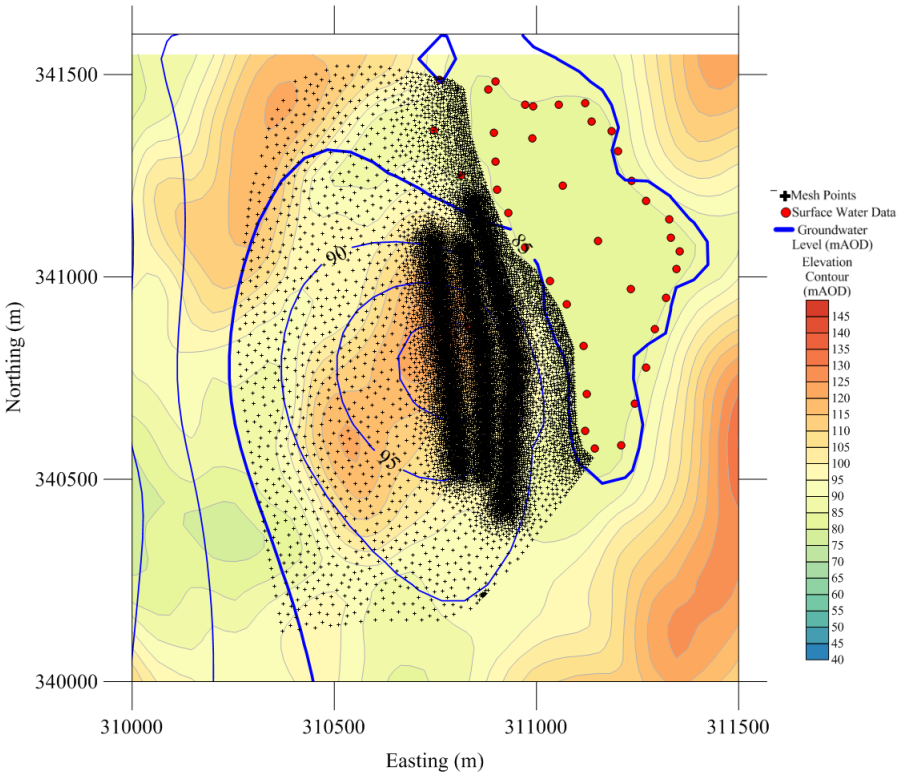

Figure 5.31 The groundwater contour map developed using known surface water levels and borehole water level data (where orange and yellow lines are roads).

Table 5.17 Material properties used in three-dimensional model estimated using laboratory/field data and information obtained from Clarke (2007).

Material	**Layer(s) (depth)**	**Hydraulic Conductivity** m s^{-1}	**Porosity**
Surficial Layer	1 (0.5 m)	1.5×10^{-6}	0.40
Root/Weathered Zone	2 (1.0 m)	1×10^{-8}	0.265
Upper Till	3 – 6 (up to 8 m)	1×10^{-9}	0.265
Lower Till	7 – 9 (up to 10 m)	1×10^{-10}	0.265
Till/Weathered Bedrock Interface	10 (0.2 m)	1×10^{-8}	0.265
Bedrock	11 (0.5 m)	1×10^{-7}	0.10

The final geometric domain used in the three-dimensional model can be seen in Figure 5.32. Other boundary conditions that were applied to the model other than those described above include seepage face conditions along the surface domain of the models. The in/out flow parameter in Feflow was also used to apply estimated recharge to the entire model domain. As there are no known bedrock outcrops or other surface water bodies within the model geometry,

no other boundary conditions were applied. The final three-dimensional surface elevation of the final simulation can be seen in Figure 5.33. The location of the valley and the other high topography zones of other surrounding drumlins can also be seen in this figure.

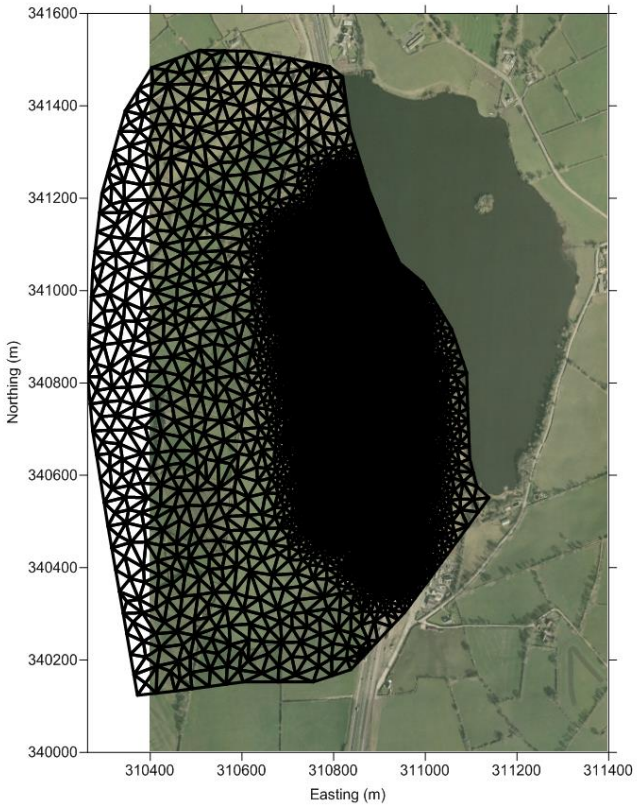

Figure 5.32 Geometry and mesh of 3-dimensional model for Loughbrickland site.

Simulated hydraulic heads were taken at similar depths as in the field boreholes. These simulated results were compared with the average field observations for each depth to ensure a "best-fit" steady-state groundwater flow model. The average annual hydraulic head measurements were taken from the monitoring data collected from each of the standpipes described earlier (Table 5.18). Figure 5.34 also shows borehole information, including hydraulic head seasonal highs, lows and screen elevations.

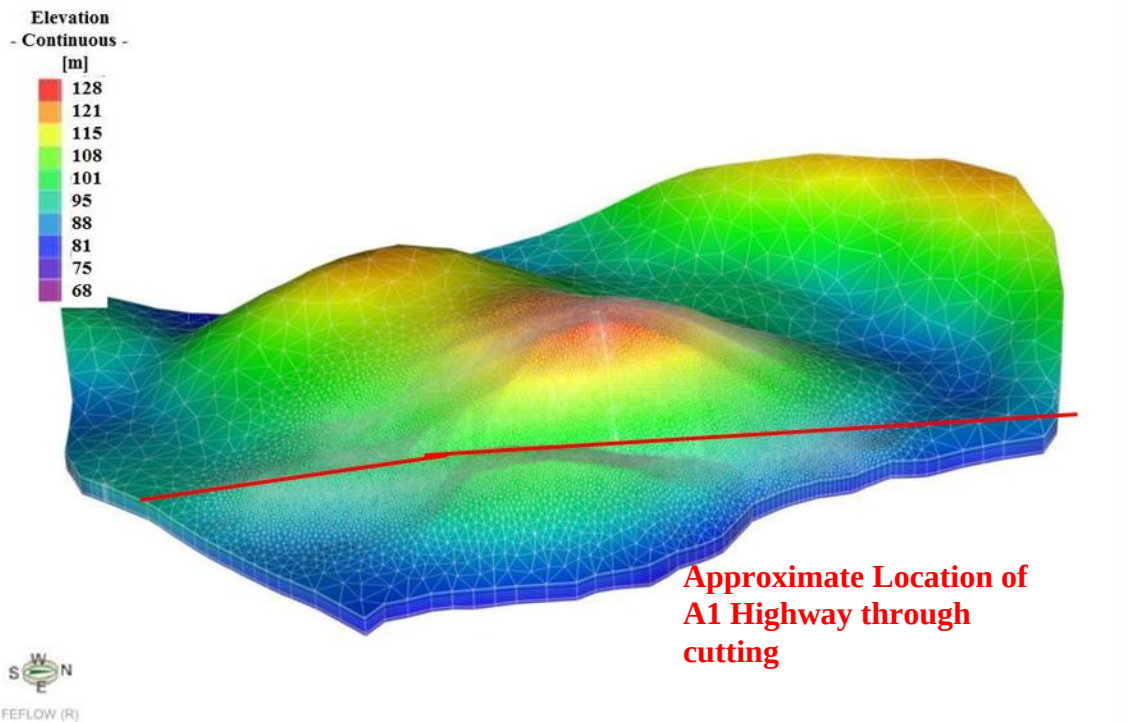

Figure 5.33 View of the entire 3-D Loughbrickland model geometry with elevation head (Note: a vertical exaggeration of 5 was applied to enhance the visual representation of the elevation).

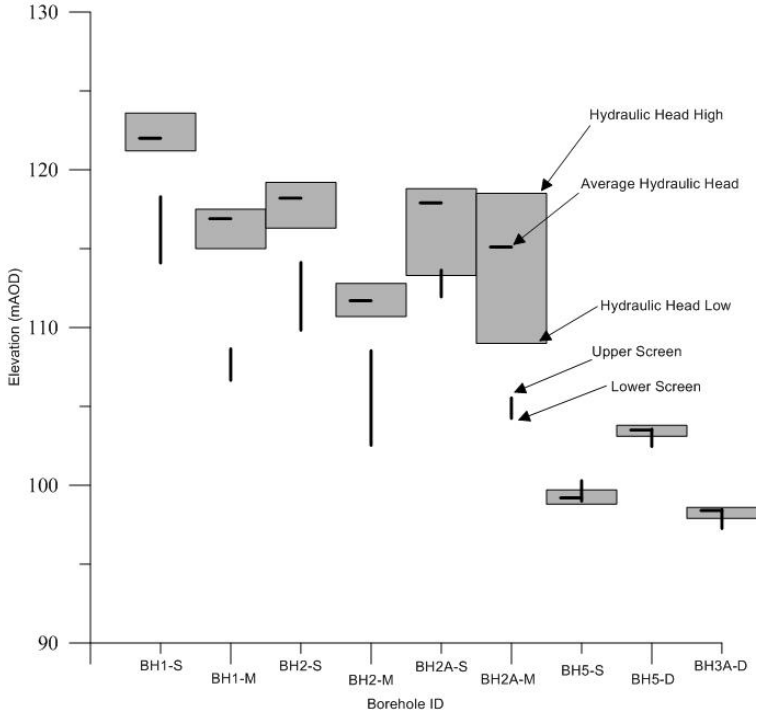

Figure 5.34 Borehole information including screen length and elevations and average, high and low hydraulic heads for the study period of 2010.

Table 5.18 Average hydraulic heads taken from standpipe monitoring at the Loughbrickland study site.

Borehole	Standpipe	Average Hydraulic Head	Hydraulic Head High	Hydraulic Head Low	Standpipe Screen Elevations
			(m)		
1	Upper Till	122.0	123.6	121.2	114.09 – 118.29
	Lower Till	116.9	117.5	115.0	106.65 – 108.65
2	Upper Till	118.2	119.2	116.3	109.83 – 114.13
	Lower Till	111.7	112.8	110.7	102.53 – 108.53
2A	Upper Till	117.9	118.8	113.3	111.94 – 113.64
	Lower Till	115.1	118.5	109.0	104.24 – 105.54
3A	Weathered Bedrock	99.2	99.7	98.8	98.99 – 100.29
5	Upper Till	103.5	103.8	103.1	102.46 – 103.56
	Weathered Bedrock	98.4	98.6	97.9	97.26 – 98.46

The "best-fit" recharge rate was determined to be around 80 mm year^{-1}. Other recharge rates were evaluated to determine this "best-fit", as can be seen in Table 5.19, by comparing simulated hydraulic head values to field hydraulic head measurements using five model evaluation methods. The final hydraulic head distributions, as compared to the field observations, can be seen in Figure 5.35. The evaluation methods described show that as the recharge rate is increased past 80 mm year^{-1}, the hydraulic head distribution continues to improve. However, as the recharge rate is increased past 80 mm year^{-1} the hydraulic head distribution approaches the maximum observed heads. Past this rate, the changes in hydraulic head decrease dramatically, indicating that any additional water applied to the model is simply being rejected without altering the head distribution (i.e. water table has risen to the surface of the model).

Table 5.19 Model evaluation methods used to determine "best-fit" infiltration rate (***bold italics*** indicate "best" results).

Evaluation Method	Recharge Rate (mm/year)				
	50	*60*	*70*	*80*	*90*
RMSE	3.25	2.15	1.61	1.37	***1.32***
MARE	$2.49x10^{-2}$	$1.75x10^{-2}$	$1.25x10^{-2}$	$1.02x10^{-2}$	***$0.94x10^{-2}$***
E	0.85	0.94	0.96	0.97	***0.98***
R	***0.99***	***0.99***	***0.99***	***0.99***	***0.99***
d	0.96	0.98	***0.99***	***0.99***	***0.99***

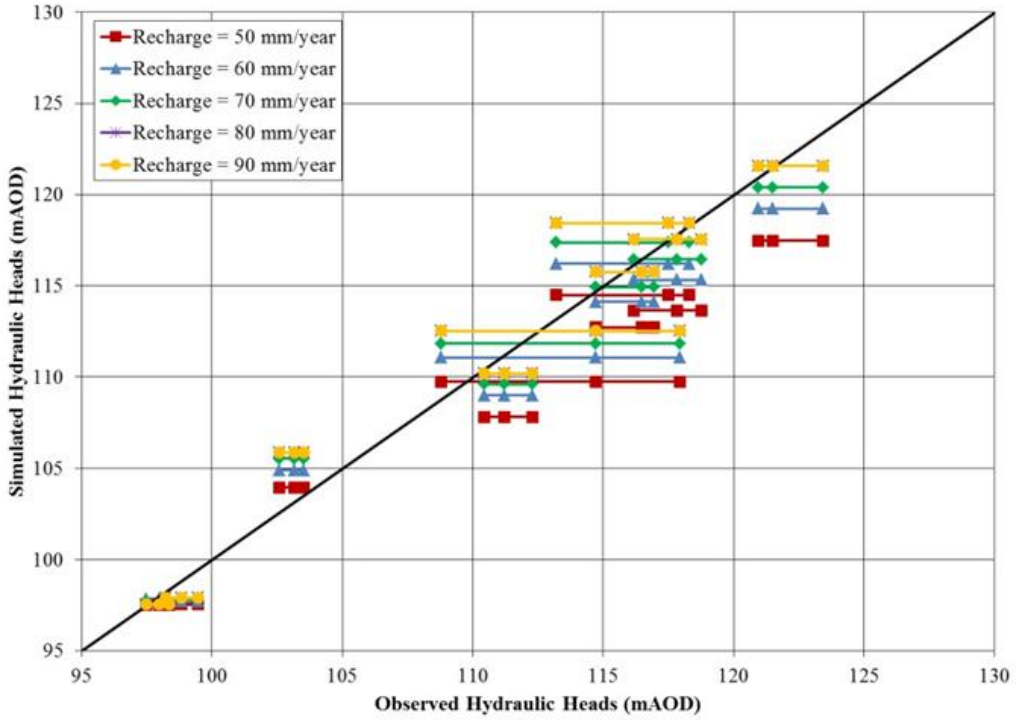

Figure 5.35 Simulated versus observed hydraulic head distributions for varying recharge rates at the Loughbrickland three-dimensional cross-section. Note that 3 values of 'observed hydraulic head' are provided at each borehole location (minimum, average and maximum).

The two-dimensional cross-section was developed using the same boundary conditions and material properties as the above three-dimensional base condition. A range of recharge rates was applied to the two-dimensional simulation to determine the "best-fit' recharge required to obtain a similar hydraulic head distribution as simulated above. Evaluation results indicate that

the recharge rate of 80 mm year^{-1} obtained the "best-fit" hydraulic head distributions (Table 5.20). This is similar to what was indicated in the three-dimensional analysis. Figure 5.36 indicates that the three- dimensional simulation has a higher sensitivity to the overall recharge rate than the two-dimensional simulation as shown by greater spread in simulated hydraulic heads. This is likely an impact of the Lough and marsh-like areas that are located on either side of the drumlin. These areas would add more constraints to the drumlins, increasing the impact of changing the recharge rate boundary condition. Also, given the three-dimensional system has more locations for water to flow, there could be more water being added to the cross-section from other areas as the recharge rate is increased.

Table 5.20 Model evaluation methods used to determine "best-fit" recharge rate (***bold italics*** indicate "best" results).

Evaluation Method	**Recharge Rate (mm/year)**				
	50	*60*	*70*	*80*	*90*
RMSE	2.03	1.42	1.13	***1.03***	1.04
MARE	1.66×10^{-2}	1.13×10^{-2}	0.88×10^{-2}	0.77×10^{-2}	$\boldsymbol{0.76 \times 10^{-2}}$
E	0.94	0.97	0.98	***0.99***	0.98
R	***0.99***	***0.99***	***0.99***	***0.99***	***0.99***
d	0.98	0.98	***1.00***	***1.00***	***1.00***

The final water balances for each of the three-dimensional and two-dimensional models can be seen in Table 5.21. A recharge rate of 80 mm year^{-1} was used in the three- and two-dimensional simulations to allow for a comparison between the different dimensional simulations. The recharge rates over the cross-sections were similar for both cases, which is expected given that this is a specified boundary condition. The major difference occurred in the total discharge along the cross-section surface, which was much smaller in the three-dimensional simulation. This could be caused by an increase in the flow of water to and from other areas within the three-dimensional model domain to the cross-section, decreasing the amount of discharge required along the cross-section. In the two-dimensional case, the same amount of water added to the domain must leave, where most of the water addition and removal occurs at the surface.

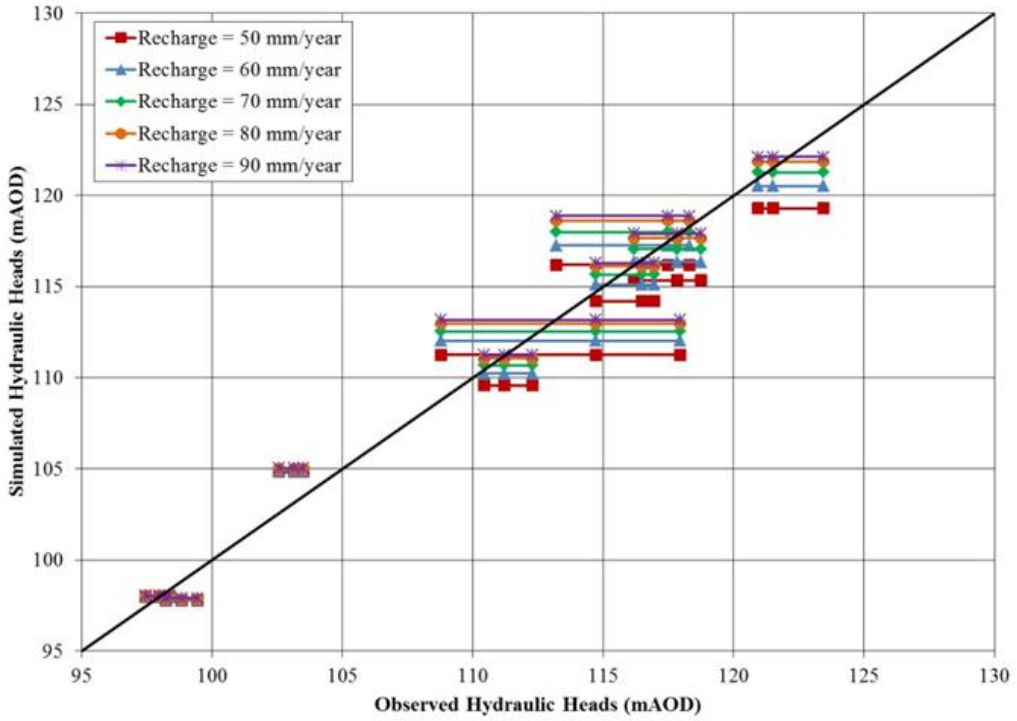

Figure 5.36 Simulated versus observed hydraulic head distributions for varying recharge rates at the Loughbrickland two-dimensional cross-section. Note that 3 values of 'observed hydraulic head' are provided at each borehole location (minimum, average and maximum).

Table 5.21 Comparison of the water balance calculated in each of the two- and three-dimensional simulations.

Simulation	Total Recharge (mm year^{-1})	Total Discharge (mm year^{-1})	Net (mm year^{-1})
3-D (Entire Domain)	80.2	80.2	0
3-D (Cross-section)	79.5	60.4	+19.1
2-D (Domain)	80.1	80.1	0
2-D (Surface only)	80.1	77.9	+2.1

The results of this "best-fit" analysis can be seen in Figure 5.37, Figure 5.38, Figure 5.39, Figure 5.40 and Figure 5.41 for BH1, BH2, BH2A, BH3A and BH5, respectively. The same overall gradient that was seen in the Craigmore simulations is also experienced in

Loughbrickland. The change in hydraulic conductivity between the upper and lower tills is made apparent when looking at the hydraulic gradient between each borehole standpipe. All of the boreholes outlined in the figures show this sudden change in the hydraulic gradient when the upper till and lower till interface is passed.

The *in situ* hydraulic head data for BH3A and BH5 have been included for comparison in Figures 5.40 and 5.41. This data does show the hydraulic heads are below the elevation of the dry standpipes, which is indicative of the toe drain having a strong influence on the overall hydraulic gradient along the slope cutting. The bottom of the standpipe screen was used as the hydraulic head measurement, which may be inaccurate as the exact location of the water body is unknown. The location of BH2A is not along the cross-section transect used for the two-dimensional domain. This borehole was included in the comparison, but does not indicate the exact elevation experienced in the field, therefore the hydraulic head distributions in the two-dimensional simulation may not be accurate. These standpipes were not included in the evaluation calculations of the two-dimensional simulations.

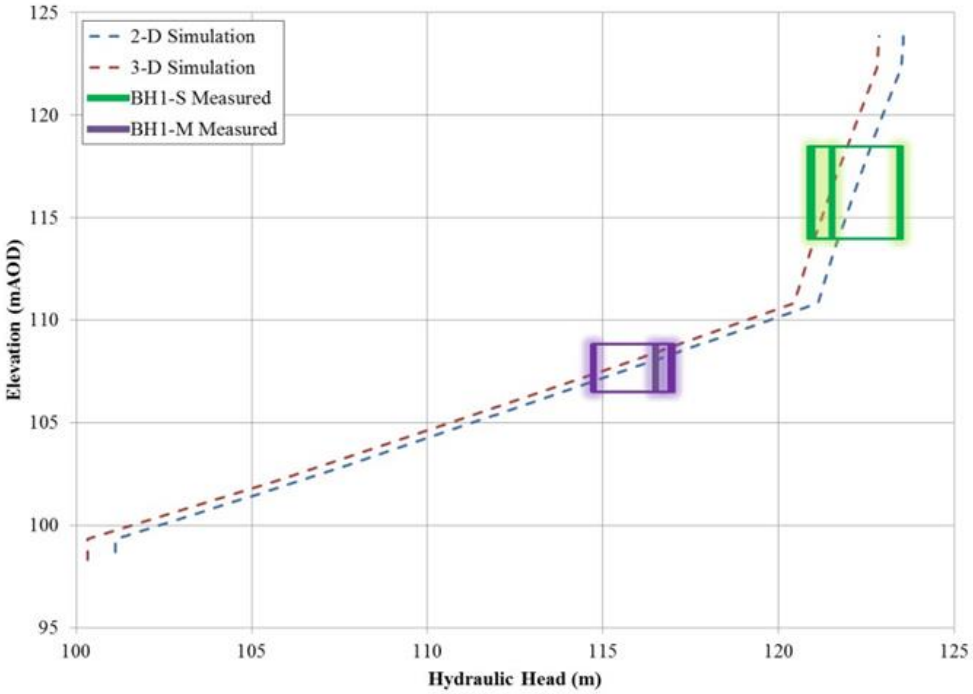

Figure 5.37 Hydraulic head measurements determined in the field and in the model simulation at BH1. Note that the box represents the zone of the screen with the observed minimum, average and maximum head measurements.

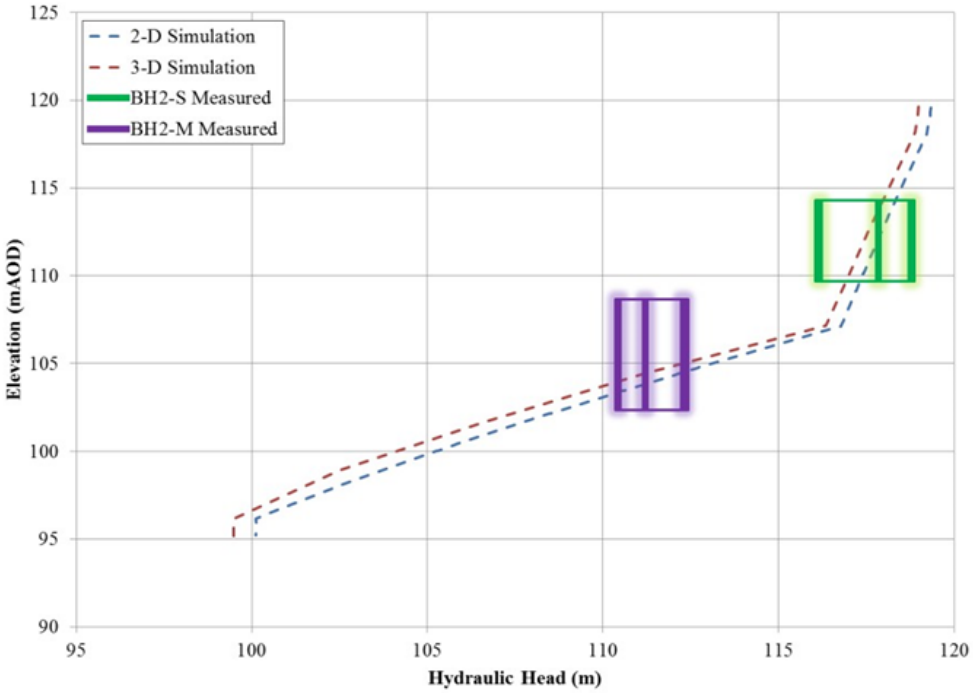

Figure 5.38 Hydraulic head measurements determined in the field and in the model simulation at BH2. Note that the box represents the zone of the screen with the observed minimum, average and maximum head measurements.

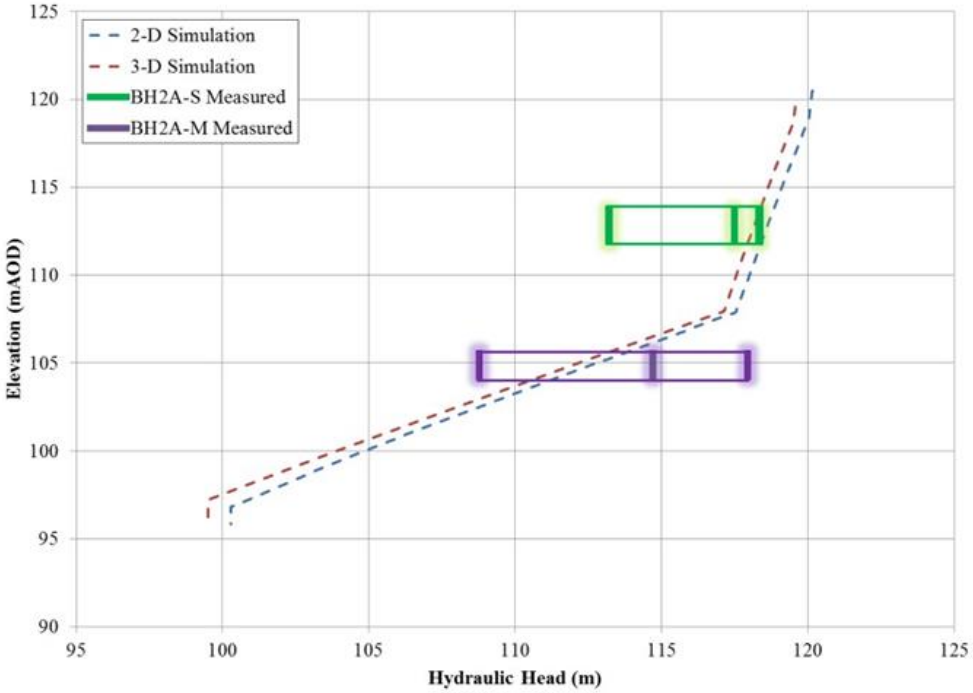

Figure 5.39 Hydraulic head measurements determined in the field and in the model simulation at BH2A. Note that the box represents the zone of the screen with the observed minimum, average and maximum head measurements. (Note: the 2-D cross- section did not land directly on the location of BH2A, so elevation data is slightly different than that experienced in the field).

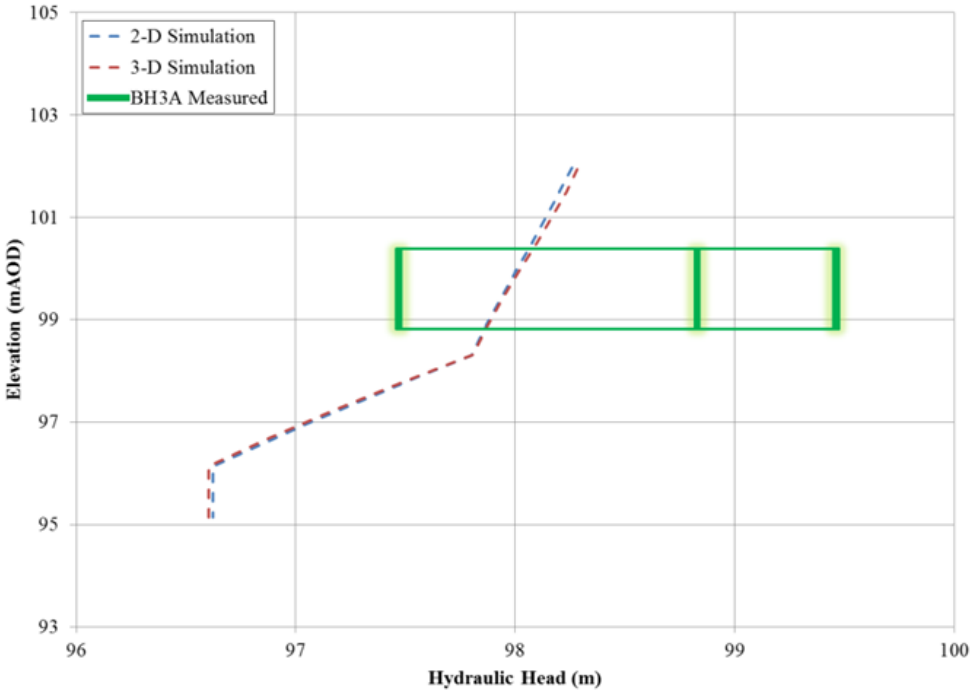

Figure 5.40 Hydraulic head measurements determined in the field and in the model simulation at BH3A. Note that the box represents the zone of the screen with the observed minimum, average and maximum head measurements.

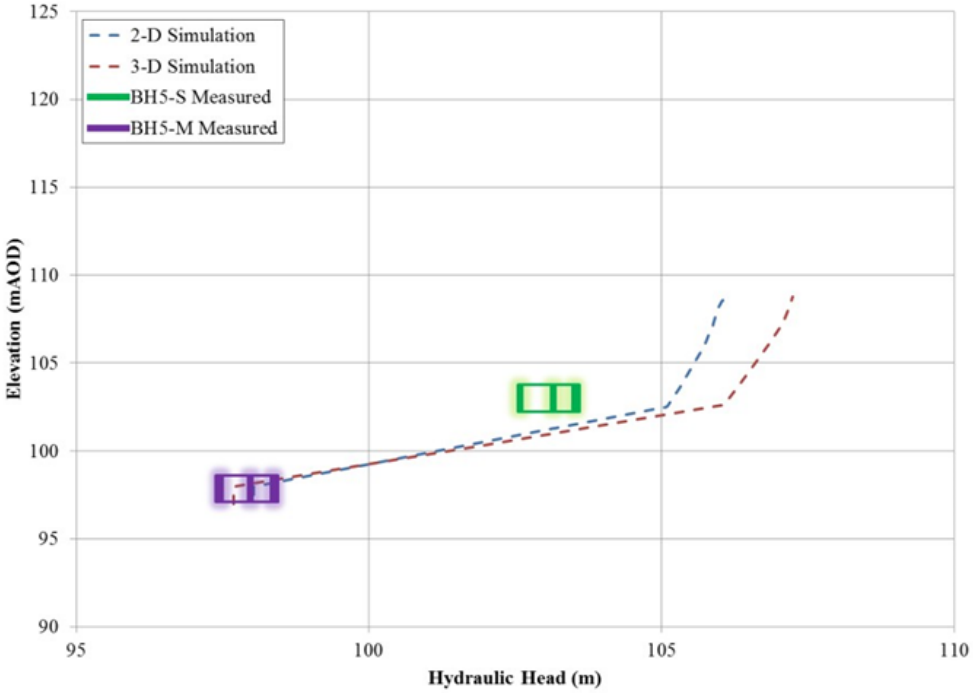

Figure 5.41 Hydraulic head measurements determined in the field and in the model simulation at BH5. Note that the box represents the zone of the screen with the observed minimum, average and maximum head measurements.

The results in Figures 5.37, 5.38, 5.39, 5.40 and 5.41 show that the three- and two-dimensional simulations were able to reach very similar representations of the drumlin at a recharge rate of 80 mm year^{-1}. Hydraulic head distributions fit well between the simulated and observed average hydraulic heads within the field at BH1, BH2, BH2A and BH5. At BH3A however, the heads were much lower than the observed values, which may be a result of using the screen elevations as the hydraulic head measurement. As the standpipe at this location remains dry year round, the actual water table elevation at this location is unknown. In the simulation, is the standpipe is located along the elevation of the toe drain, which is considered to be at the top of the weathered bedrock zone, as discussed above.

The hydraulic head contours along the same cross-section for the three- and two-dimensional models are shown in Figure 5.42(a) and Figure 5.42(b), respectively. The hydraulic head distributions of the three-dimensional system are similar with the primary difference between the two models related to the extent of drainage within the weathered bedrock zone. As shown in Figure 5.42, drainage of the bedrock surface creates larger zones of zero pressure below the crest of the drumlin, as well as below the bench of the slope. This is likely due to the ability of the three-dimensional model to move water in all three dimensions, while the two-dimensional simulation creates more pressure build up within the weathered bedrock at these two locations. Given the inability to use the standpipes that are located within the weathered bedrock zone along the crest of the slope, the natural conditions of the water table at this location are unknown. It is recommended that further boreholes are installed along the crest into the weathered bedrock zone to determine which simulation is more accurately representing the natural condition.

Overall, both scenarios were able to produce hydraulic head distributions that were similar to the field monitoring. The three-dimensional system had less discharge along the cross-section as when compared to the two-dimensional scenario. The hydraulic head distribution, however, was similar in both simulations, as well as the location of the water table.

It should be noted that the location of the “bench” along the western portion Loughbrickland cutting was not included in the elevation files provided. A simple comparison was completed where a “bench” was manually entered along the slope in the approximate

location according to engineered drawings. This presence of the bench did not appear to have any impact on the overall hydraulic gradients within either of the simulations, so was left out of this analysis. It was noted that this bench is located in an area where the water table does not reach the surface as well as where a drain is located 3 m below the surface, so it should not have a significant impact on the hydraulic head distributions seen above.

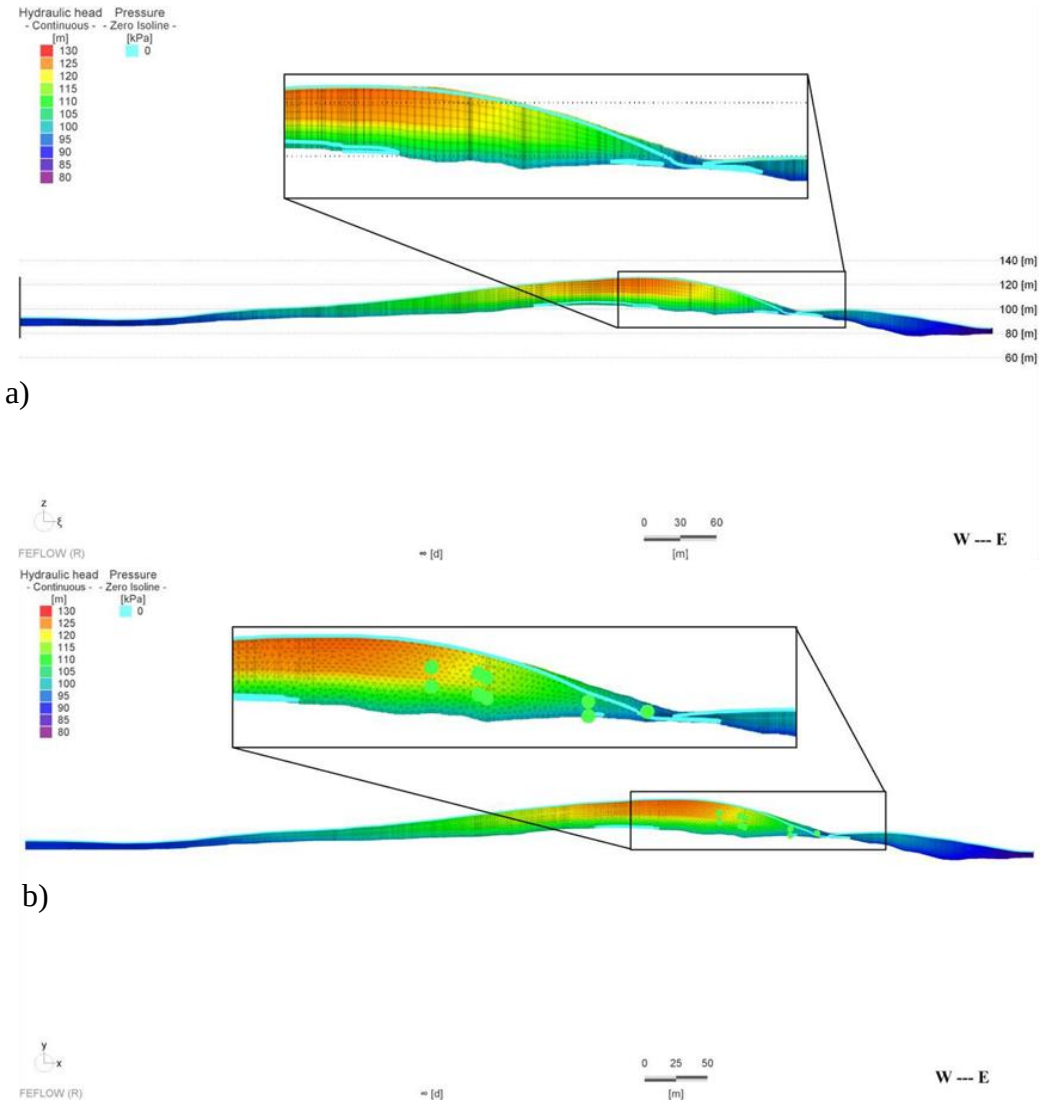

Figure 5.42 Hydraulic head distribution along the Loughbrickland cross-section in the (a) three-dimensional and (b) two-dimensional simulation. The water table is indicated in blue (where pressure head = 0 kPa).

5.2.3 Sensitivity Analyses

Sensitivity analyses similar to those conducted on the Craigmore simulations were completed on the Loughbrickland base condition models. The three-dimensional simulations underwent the sensitivity analyses on the bedrock transmissivity and the hydraulic conductivity versus recharge rate. Further analysis was also conducted on the influence of the bedrock "roughness" on the hydraulic head distributions throughout the soil systems. The two-dimensional simulations were not included in these analyses.

Hydraulic Conductivity versus Recharge Rate

A sensitivity analysis was completed on the Loughbrickland three-dimensional simulations to show that varying the recharge and hydraulic conductivity values can yield similar hydraulic head distributions as long as the recharge to hydraulic conductivity ratio remains the same as the base condition. As observed in the Craigmore simulations, the Loughbrickland simulation also gave the same head distributions when the hydraulic conductivity and recharge values of the base condition were varied by a factor of 3. This indicated that similar head distributions can be reached for recharge values of 27 mm $year^{-1}$ and 240 mm $year^{-1}$ as long as the hydraulic conductivity values were all varied by this same factor of 3.

A further sensitivity analysis was conducted on the hydraulic conductivity of the upper and lower till layers, as was completed at the Craigmore location. In this case, however, the model would not converge if the hydraulic conductivity of the lower till was lowered by a factor of 5, so only a factor of 2 was used (hydraulic conductivity of 5×10^{-11} m s^{-1}). As seen in Figure 5.43, the toe drain has a significant impact on the standpipe that is nearest to it (BH3A), so the hydraulic conductivity of both the upper and lower tills do not have a significant impact on the hydraulic heads at that location. At BH5, the hydraulic heads in the weathered bedrock zone (far left of the graph) only undergo large changes if the lower till hydraulic conductivity is increased. This would be resultant of the lower till acting as a confining layer between the weathered bedrock zone and the upper till. As these were the only two locations with reliable hydraulic head measurements in the weathered bedrock zone, it cannot be determined how the distributions

were influenced below the crest of the drumlin. It can be seen, however, that the lower till also has a more significant impact on the entire drumlin hydraulic head distribution as compared to the upper till. This is similar to what was experienced at the Craigmore site. As the hydraulic conductivity of the upper till is increased, the flow dynamics of the system are changed in a similar manner to what was observed at Craigmore, with an increase in the lateral flow and a decrease in the vertical flow, causing the hydraulic heads at each standpipe to actually increase instead of decrease. Overall, the Loughbrickland two layer system acts in a similar manner as the Craigmore simulation.

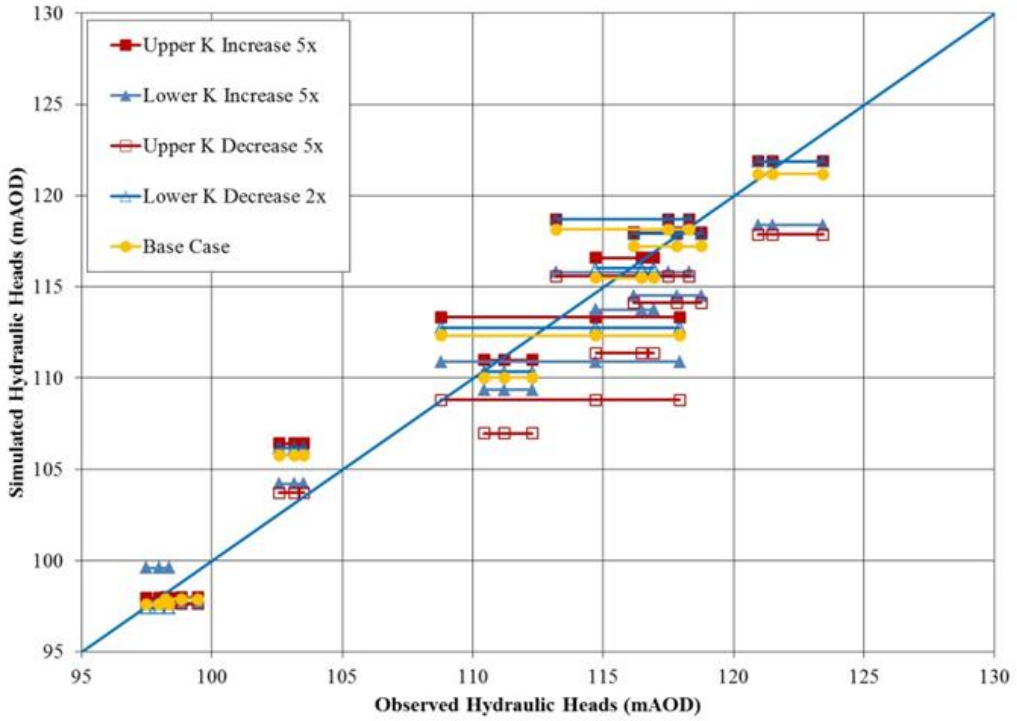

Figure 5.43 Hydraulic conductivity versus recharge analysis of the upper till at Loughbrickland.

The results of the evaluation equations given in Table 5.22 show that the most significant shift away from "best-fit" is when the hydraulic conductivity of the lower till is increased by a half an order of magnitude, as was seen at Craigmore. As the lower till is decreased, it appears to have less of an impact, but this would be a result of the change in hydraulic conductivity being smaller than was completed in the upper till. Given the results of all of the analysis between the upper and lower till hydraulic conductivities, it would appear that the lower till has a more

significant influence on the overall hydraulic head distribution and overall recharge, which is similar to what was seen at the Craigmore site (Section 5.1.4). As seen by the results, an increase in the upper till by a factor of 5 actually yields slightly better results than the base case. This is a result of the use of the average hydraulic heads as well as an indication of the maximum heads being reached, as the change in recharge rates at this hydraulic conductivity did not significantly change the head distributions.

Table 5.22 "Best-fit" results as part of the hydraulic conductivity versus recharge analysis at Loughbrickland cross-section.

Model	Evaluation Method				
	RMSE	MARE	R	E	D
Base	1.37	1.03×10^{-2}	***0.99***	0.97	***0.99***
Upper Till K increase	***1.29***	***0.76×10^{-2}***	***0.99***	***0.98***	***0.99***
Upper Till K decrease	3.53	2.68×10^{-2}	0.98	0.82	0.95
Lower Till K increase	2.46	2.04×10^{-2}	***0.99***	0.91	0.97
Lower Till K decrease	1.36	0.96×10^{-2}	***0.99***	0.97	***0.99***

Bedrock Transmissivity

The sensitivity of the three dimensional model results to changes in the bedrock transmissivity was analyzed by conducting a series of simulations using different transmissivity values for the weathered bedrock zone. The depth of this zone was kept the same for all simulations (1 m). The average hydraulic head values for each of the boreholes were taken from the steady-state base condition and used for evaluation in this analysis. The hydraulic head distributions were then plotted to allow for visual analysis (Figure 5.44). The results of the evaluation criteria were also given to indicate that the "best-fit" transmissivity value was used in the simulations above (Table 5.23). In this analysis, the transmissivity values ranged from 5×10^{-7} $m^2 s^{-1}$ (base case) to 5×10^{-10} $m^2 s^{-1}$. Figure 5.44 shows the resultant hydraulic head

distributions for transmissivities of 5 x 10^{-7} m^2 s^{-1}, 1 x 10^{-7} m^2 s^{-1} and 5 x 10^{-8} m^2 s^{-1}. Convergence could not be reached when the transmissivity was increased, so only results for decreasing the transmissivity are shown.

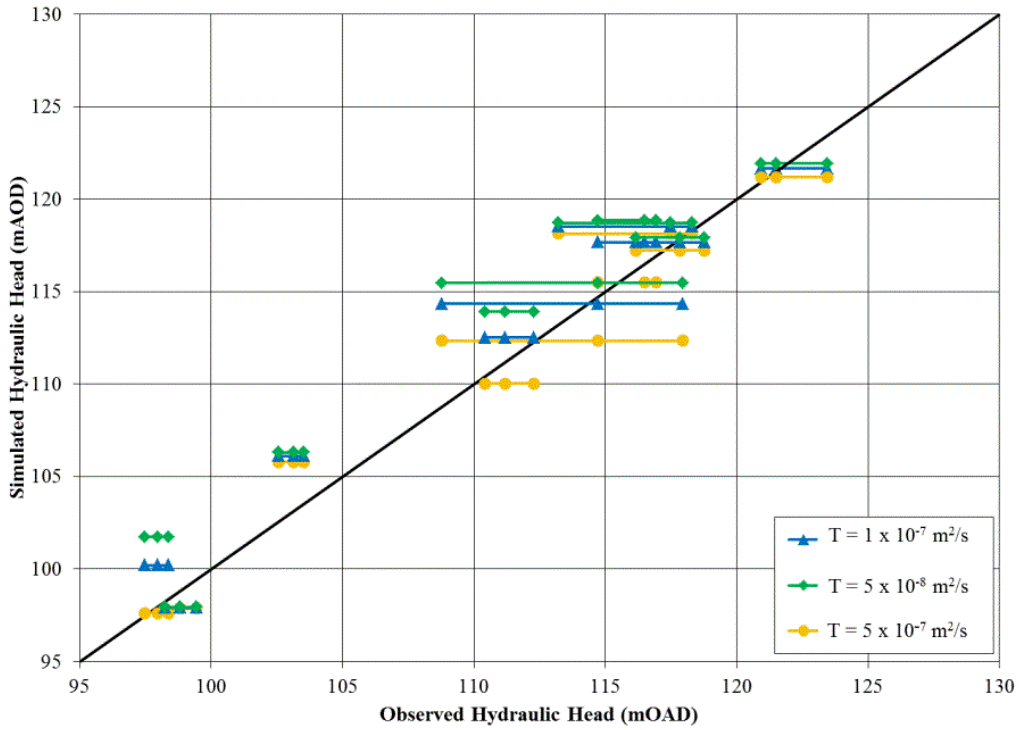

Figure 5.44 Hydraulic head distributions for each model of bedrock transmissivity in the Loughbrickland three-dimensional simulations. Note that 3 values of 'observed hydraulic head' are provided at each borehole location (minimum, average and maximum).

Table 5.23 Evaluation results of the Loughbrickland weathered bedrock transmissivity analysis (***bold italics*** indicate the "best-fit").

Evaluation Method	**Transmissivity (m^2 s^{-1})**		
	5.0 x 10^{-7}	*1.0 x 10^{-7}*	*5.0 x 10^{-8}*
RMSE	***1.37***	1.45	2.11
MARE	***1.03x10^{-2}***	1.06x10^{-2}	1.56x10^{-2}
E	***0.97***	***0.97***	0.94
R	***0.99***	***0.99***	0.98
d	***0.99***	***0.99***	0.98

As shown in the figure above, a decrease in the transmissivity of the weathered bedrock zone causes the hydraulic heads across the drumlin to increase. Where drains are present near BH5 and BH3A standpipes, there is little sensitivity to changes in transmissivity due to the control exerted by these constant head conditions. Table 5.23 also shows that the hydraulic head distribution reached during the base case simulation (transmissivity of 5×10^{-8} m^2 s^{-1}) gives the "best-fit" distribution out of all of the transmissivities used in this analysis. As the transmissivity of the weathered bedrock zone is decreased past the value of 5×10^{-9} m^2 s^{-1}, the change in the hydraulic head distribution decreases significantly. This would be a result of the model domain becoming more saturated and the lower weathered bedrock zone acting as an extension of the lower glacial till layer instead of as a separate aquifer below a confining layer. The confining properties of the lower till also ensure that the changes in transmissivity of the weathered bedrock zone do not have a large influence over the hydraulic head distributions in the upper till.

"Smooth" versus "Rough" Bedrock

The "smooth" simulation was developed in the same method that was used for the Craigmore "smooth" models. The borehole data as well as some of the overall bedrock surface from the "rough" models were used to develop a bedrock surface with less concave and convex sections (Figure 5.45). The Loughbrickland bedrock surface that was interpolated above for the base condition has more "rough" dips and bumps along the drumlin cross-section than that experienced along the Craigmore cutting. This would be a result of the availability of seismic transects directly along the drumlin excavation. The larger dips in the bedrock surface were kept; however, smaller scale "roughness" was removed.

The interpolated "smooth" bedrock surface was imported into the Loughbrickland three-dimensional geometry for comparison between the base condition and each of the dimensional models. The material properties that were used in the base condition were kept the same for each of the simulations for ease of comparison. The recharge rate was kept constant at 80 mm $year^{-1}$ for ease of comparison with the "rough" simulations. The results for each simulation are given below, with comparison between the "smooth" and "rough" simulations.

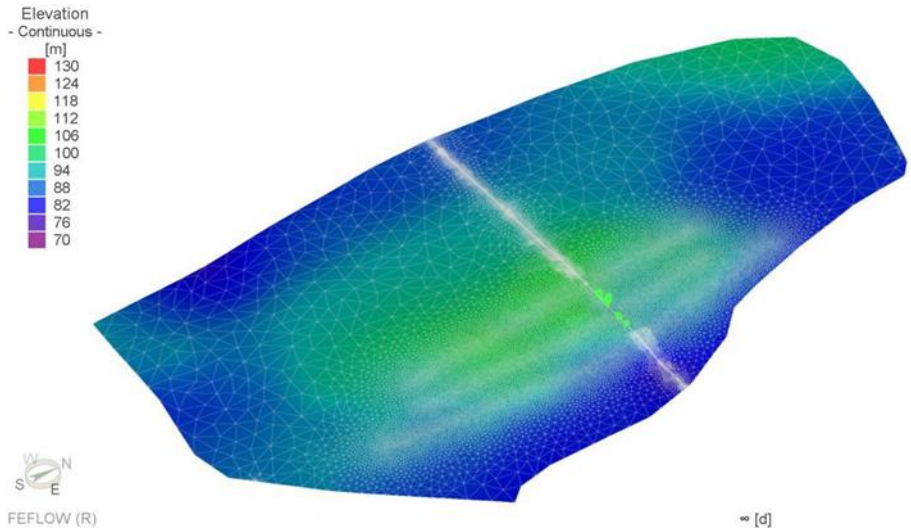

Figure 5.45 "Smooth" bedrock surface elevations determined using interpolation of borehole data (green circles) and surface elevations.

As conducted previously, the same hydraulic conductivity, porosity and SWCC as outlined for the base condition simulations were used in the "smooth" simulations. The hydraulic head distribution that was obtained from the analyses for the three- dimensional scenario is shown in Figure 5.46. The hydraulic head distribution of the "smooth" simulation is very similar to what was obtained in the "rough" scenario above. The most significant difference between the "rough" and "smooth" scenarios for three-dimensional scenarios is the location of the water table. There appears to be less drainage from the weathered bedrock zone in the "smooth" case, as there are less zones of zero pressure along the cutting. Monitoring along BH5 within the weathered bedrock zone indicates that some zero pressure should be present along the weathered bedrock zone below the bench. In this case, the "rough" simulation would be more accurate. Given the standpipes in the weathered bedrock below the crest of the cutting were not functioning, it is unknown if a zero pressure zone actually exists there. Further monitoring in this area should be installed to determine the actual parameters existing on the site.

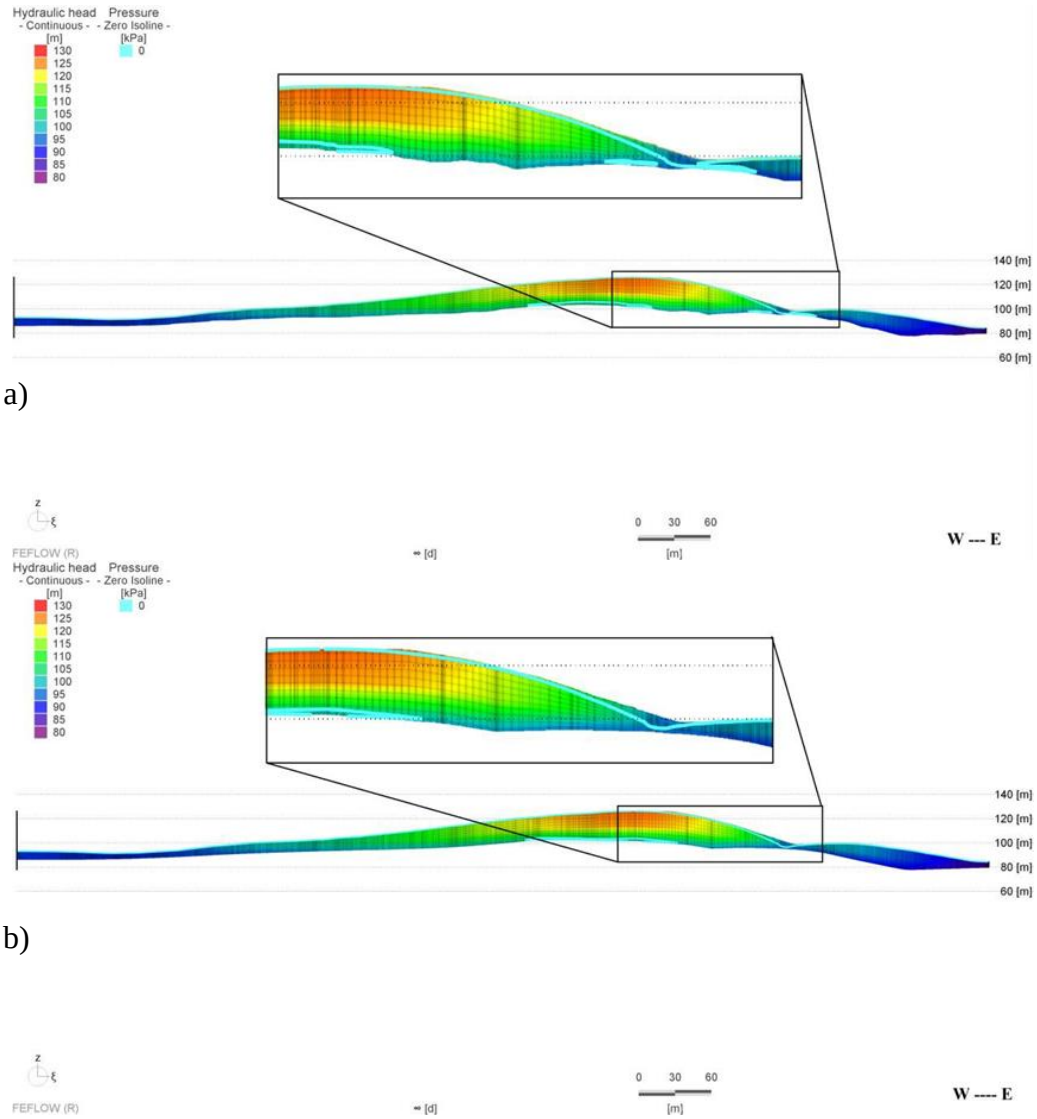

Figure 5.46 Hydraulic head distributions simulated along the cross-section of the three-dimensional Loughbrickland model for the a) "rough" and b) "smooth" scenarios.

The resultant overall recharge and discharge rates for each of the three- dimensional models are outlined in Table 5.24. When comparing the "smooth" and "rough" cross-sections, the water balance is very similar in both scenarios. In this case, there was slightly more discharge in the "smooth" scenario, unlike what was observed in the Craigmore simulations. Further analysis into the influence of the Lough and the "marsh" areas on either side of the drumlin should be conducted to ensure that they are represented appropriately in the simulations. These areas may have a large influence of the three-dimensional simulation's ability to accurately model the drumlin's hydrogeology.

Table 5.24 Comparison of applied unit flux rates to obtain similar hydraulic head gradients and resultant total recharge amounts in each of the three-dimensional simulations.

Simulation (Software)	Total Recharge (mm year^{-1})	Total Discharge (mm year^{-1})	Net (mm year^{-1})
"Smooth" (Entire domain)	80.2	80.2	0
"Smooth" (Cross-section)	79.5	60.8	+18.7
"Rough" (Entire Domain)	80.2	80.2	0
"Rough" (Cross-section)	79.5	60.4	+19.1

5.3 Modeling Summary

The water balance simulations for both of the study sites gave recharge estimates of similar ranges, with 21 to 31 mm year^{-1} at the Craigmore site and 23 to 31 mm year^{-1} at the Loughbrickland site. This recharge rate is considered realistic for both sites, given that properties of the glacial till are similar at both locations. The Craigmore two- and three-dimensional steady state simulations both had best fit recharge rates of approximately 60 mm year^{-1}. This may be an artifact of calibrating the groundwater models to 'average' head conditions. When compared to the annual low hydraulic heads measured in the boreholes, values closer to 40 mm year^{-1} would be more realistic and closer to the water balance estimates. It was noted, however, that research conducted in the area indicated a large range in potential recharge for aquifers underlying glacial till. Robins and Misstear (2000) recommend a general rule of 30% of rainfall is contributed to recharge, while McConville et al. (2001) calculated recharge through glacial till to be 22 mm year^{-1}. Similar hydraulic head distributions were obtained in both of the dimensions, although the total discharge along the cross-section was greatly reduced in the three-dimensional simulation. This is likely influenced by the ability of water to move perpendicular to the cross section in preferential flow paths.

It is understood that the 'best' recharge rates within the model is directly related to the assumed hydraulic conductivity values within the model and that similar hydraulic head distributions could be developed for lower recharge rates as long as the hydraulic conductivity

values were decreased in proportion. When studying the impact of the individual material properties on the Craigmore simulations, it was seen that the hydraulic conductivity of the lower till had a dominant influence on the "best-fit" recharge rate. Increasing the hydraulic conductivity of this unit resulted in a greater downward flow to the bedrock surface, leading to a decrease in the hydraulic head profile in both the upper and lower tills and an increase in the weathered bedrock zone. As the upper till hydraulic conductivity was manipulated, changes between lateral and vertical flows caused the hydraulic head distributions to decrease with an increase in the conductivity and increase with a decrease in the conductivity.

The analyses of the slug tests within the weathered bedrock zone produced similar values to those used in the hydrogeological models. In the transmissivity sensitivity analysis, the hydraulic conductivity of this unit could not be decreased beyond a limit without large shifts in the overall hydraulic head distribution within the till well above realistic values. The upper till hydraulic head distributions were less sensitive to the weathered bedrock transmissivity values. Increasing the transmissivity values of the bedrock led to convergence problems associated with the development of unsaturated conditions and consequently the maximum value of transmissivity analyzed was that associated with saturated conditions within this unit.

When conducting the "smooth" bedrock analysis at Craigmore, it was seen that the changes in the bedrock surface "roughness" had little impact on the simulation results. It is important to note, however, that detailed profiling of the bedrock surface along the modeled cross-section could not be completed and consequently only a 'smooth' interpretation for the bedrock surface could be developed for the region closest to the monitoring wells. Further analysis of the bedrock topography near the cross section is recommended if possible in the future to help determine a more appropriate representation of the system.

The "best-fit" recharge rates for the Lougbrickland simulations were around 80 mm year^{-1}, with an increase in recharge causing very minor changes in hydraulic head distributions. The three- and two-dimensional simulations were able to reach similar head distributions for this applied recharge rate. The main difference between simulations was the total discharge from the two dimensional section. Since the three-dimensional simulation allowed flow outside of the cross-section, less discharge was experienced from the section.

The relationship between applied recharge rate and hydraulic conductivity also applies at Loughbrickland as it did at Craigmore, highlighting the sensitivity of the 'best' recharge rate to the hydraulic conductivity values. It was also determined that the upper till layer has less influence on the overall head distributions and recharge at the Loughbrickland cross-section. As the hydraulic conductivity of the upper layer was increased, there was a decrease in vertical water movement into the lower till, thus causing an increase in the upper till hydraulic heads. The lower till layer appears to be the dominant controlling layer in the hydraulic head distribution of the drumlin, as any manipulation of that layer caused significant changes in all heads within the drumlin. As the lower till hydraulic conductivity was increased, more vertical flow occurred causing a decrease in the hydraulic had distribution with the glacial till layers but an increase in the heads within the weathered bedrock.

Similar to Craigmore, the simulations at Loughbrickland would not converge with increasing the bedrock transmissivity significantly. Lowering of the transmissivity of this zone resulted in a dramatic increase in heads within most of the borehole locations. The weathered bedrock standpipes of BH5 and BH3A were the least influenced by the change in transmissivity because of the near proximity of these locations to the drains installed along the excavation. The upper till hydraulic heads also did not show as significant of a change in heads as the lower till and other weathered bedrock standpipe because of the lower till acting as a confining layer between the two.

There was much more data on the bedrock topography at Lougbrickland than there was at Craigmore. This resulted in greater roughness in the bedrock topography which in turn created more change in the "smooth" dimensional simulation along the weathered bedrock zone. The greatest change was the presence of zero pressure zones along the weathered bedrock below the crest, bench and toe of the excavation. The zone below the bench did not develop at all in the "smooth" simulation, and did not extend as significantly below the crest or toe of the slope. This would indicate that the "roughness" increased the drainage from the weathered bedrock zone, creating zones of zero pressure. As there were no reliable monitoring data available below the crest and only some monitoring data available below the bench and toe, it is unknown which simulation would be considered more accurate at producing realistic bedrock saturation levels.

Further monitoring should be installed and completed within the weathered bedrock zone at this location to determine which simulation is more representative of the natural condition, as well as the overall effect of the weathered bedrock "roughness" and thickness on the overall flow system.

6.0 SUMMARY AND CONCLUSIONS

The potential impact of climate change is becoming increasingly important to the management of civil infrastructure. One of the tools that can be used to anticipate the potential impact of climate cycles are numerical modeling tools such as surface water balance and groundwater models. The design of engineered cuttings through natural landscapes, such as drumlins, will rely on the use of these numerical models to replicate critical processes within the hydrogeological system. These processes include seasonally elevated pore-pressures due to high recharge rates and the pore-pressure cycling that occurs as a result of seasonal variability in the surface water balance. Another important aspect of these models that will also need to be understood and considered in every design is the dimensionality requirements of the model to accurately represent the system in question.

In this research, the main goal was to determine the influence of dimensionality (two- or three-dimensions) on the steady state groundwater flow simulations along engineered cuttings in glacial till drumlins in Northern Ireland. Given the high precipitation and low potential evapotranspiration of the area, the groundwater tables remain relatively near the surface and saturated conditions exist along many soil surfaces intermittently throughout the year.

The simulations conducted at the two sites highlighted that both dimensions were able to produce similar hydraulic head distributions and a similar match to the monitoring data using the same parameterization. The best fit groundwater model at the Craigmore site required an annual recharge rate of 60 mm $year^{-1}$ while it was 80 mm $year^{-1}$ or higher at Loughbrickland. The Loughbrickland simulation indicated more differences between the “rough” and “smooth” scenarios when compared to Craigmore. This was a result of more data being available at the Loughbrickland location directly across the cross-section of interest. However, monitoring data was limited at Loughbrickland when compared to Craigmore, as the conditions along the weathered bedrock zone along the back of the drumlin were not known. The overall discharge from the three-dimensional cross-sections was also much larger at the Craigmore site when

compared to the Loughbrickland location, resulting in a smaller net recharge. This could be a result of increased flow in the third dimension for the Loughbrickland scenario or an influence of the drains creating a constant head along the cross-section, decreasing the water table level along the slope of the cutting. The two-dimensional simulation also showed less discharge than the Loughbrickland scenario, which would be a result of the seepage face along the upper layer where the bedrock outcrops were located at Craigmore.

Given the lack of bedrock elevation data for Craigmore and the inability to access all of the boreholes, a very simplified conceptual model of the Craigmore cross- section was created. This level of simplification; however, is likely not atypical of geotechnical practice where data collection is often limited by time and cost. This may have decreased the overall sensitivity of the simulations to dimensionality effects, as the model created was more symmetrical with less divergence of water flow in the third dimension. The increased number of boreholes and the availability of more seismic transects resulted in increased complexity for the Loughbrickland model. This resulted in more pathways for water release from the drumlin in the third dimension and consequently a smaller rate of discharge and more overall recharge was required in the three-dimensional analyses in order to replicate the observed head distribution. Since these pathways were unavailable in the two-dimensional simulation, more discharge was required to replicate the head distribution. Similar sensitivities to material properties were experienced at each of the sites, indicating that the lower till was the primary material to influence the overall hydraulic head distribution.

It was determined that the complexity required for the third dimension to become more important was not reached at either of the sites. As described above, the data limitations could be the reason for the ability of the three- and two-dimensional models to create representative distributions of the overall hydraulic head at each site. If more data was available for the weathered bedrock zone and other locations along the drumlin, the third dimension may have become more important in simulating the pore pressure cycles accurately. By introducing the transient pore pressure cycles into the simulation scenarios may have also increased the complexity, indicating the requirement for the third dimension. The research study scope, however, did not allow the transient simulations to be included in the inter-site and inter-

dimensional comparison; however, it is recommended that further analysis be conducted to include this comparison in the future. Since the time of this study there is now much more temporal and spatial available including site meteorological data. This expanded data set should be used to extend the models to include the time-dependent effects of the seasonal variations in recharge rates associated with the site water balance.

The results of this research indicate the importance of gathering appropriate data prior to conducting any development of conceptual models for the study of hydrogeological systems. As more data becomes available, the complexity of a system can be more readily understood. Once the complexity of the system is clarified, the analysis of potential dimensionality effects on the outcome of any simulations can be analyzed. If the overall system is fairly simple and symmetrical in nature, the requirement of a third dimension is less important, especially if time and cost are a contributing factor. However, as the system becomes more complex and less symmetrical, the importance of including the third dimension in the analysis is increased drastically. This is especially important when the results are taken into account of a public safety analysis, such as those completed on engineering infrastructures around the world.

7.0 LIST OF REFERENCES

Aimrun, W., M. S. M. Amin, S. M. Eltaib. 2004. Effective porosity of paddy soils as an estimation of its saturated hydraulic conductivity. Geoderma 121 (3-4): 197- 203.

Allen, R. G., L. S. Pereira, D. Raes, and M. Smith. 1998. Crop evapotranspiration: Guidelines for computing crop water requirements. Fand Agricultural Organization's Irrigation and Drainage Paper 56. UN-FAO, Rome, Italy.

Andrei, A. 2000. Embankment stabilization works between Rayners Lane and South Harrow Underground stations. Ground Engineering 33 (1): 37-46.

ASTM Standard D2487, 2000. Classification of Soils for Engineering Purposes (Unified Soil Classification System). ASTM International, West Conshohocken, PA.

Bakr, A. A., L. W. Gelhar, A. L. Gutjahr and R. R. MacMillan. 1978. Stochastic analysis of spatial variability in subsurface flows: 1. Comparison of one- and three-dimensional flow. Water Resources Research 14 (2): 263-271.

Baxter, S. 2008. A geological field guide to Cooley, Gullion, Mourne and Slieve Croob. Louth County Council. Available at [Online]: http://www.louthcoco.ie/en/Publications/General/A_Geological_Field_Guide_to_Cooley,_Gullion,_Mourne_Slieve_Croob_.pdf (February 2011).

Beamish, D., G. S. Kimbell, P. Stone and T. B. Anderson. 2010. Regional conductivity data used to reassess Early Palaeozoic structure in the Northern Ireland sector of the Southern Uplands Down Longford terrane. Journal of the Geological Society 167: 649-657.

Bell, F. G. 2002. The geotechnical properties of some till deposits occurring along the coastal areas of eastern England. Engineering Geology 63: 49-68.

Bonnell, M. 1972. An assessment of possible factors contributing to well level fluctuations in Holderness boulder clay, East Yorkshire. Journal of Hydrology 16: 361-368.

Cai, F. and K. Ugai. 2004. Numerical analysis of rainfall effects on slope stability. International Journal of Geomechanics 4 (2): 69 – 78.

Carse, L. 2014. The geomechanical response of cut slopes in glacial till to climatically driven pore-pressure cycling and hydrogeology. PhD dissertation. Queen's University Belfast, Belfast, Northern Ireland.

Carse, L., M. McLernon, D. Hughes, V. Sirakumar and S. L. Barbour. 2009. The magnitude and variation of pore pressures in glacial till slopes and their effect on slope stability. GeoHalifax Proceedings, Halifax, Nova Scotia.

Clarke, G., 2007. The impact of climate on the hydrogeology and stability of a large excavation in a glacial till. PhD Thesis Dissertation, Queen's University Belfast, Northern Ireland.

Cooper, H.H., J.D. Bredehoeft and I.S. Papadopulos. 1967. Response of a finite diameter well to an instantaneous charge of water. Water Resources Research 3: 263-269.

Cruickshank, J. G. 1997. Soil and Environment: Northern Ireland. Agricultural and Environmental Science Division, DANI and the Agricultural and Environmental Science Department, The Queen's University of Belfast.

Cuthbert, M. O., R. Mackay, J. H. Tellam and K. E. Thatcher. 2010. Combining unsaturated and saturated hydraulic observations to understand and estimate groundwater recharge through glacial till. Journal of Hydrology 391: 263-276.

Dardis, G. F. and A. M. McCabe. 1983. Facies of subglacial channel sedimentation in late-Pleistocene drumlins, Northern Ireland. Boreas 12: 263-278.

Davis, L. A. and G. Segol. 1985. Documentation and user's guide: GS2 & GS3s – variably saturated flow and mass transport models. Rep. NUREG/CR-3901, U.S. Nuclear Regul. Comm., Washington, D.C.

Davies, O., M. Rouainia, S. Glendinning and S. J. Birkinshaw. 2008. Assessing the influence of climate change on the progressive failure of a railway embankment. The 12th International Conference of International Association for Computer Methods and Advances in Geomechanics (IACMAG), Goa, India.

Devito, K., I. Creed, T. Gan, C. Mendoza, R. Petrone, U. Silins and B. Smerdon. 2005. A framework for broad-scale classification of hydrologic response units on the Boreal Plain: is topography the last thing to consider? Hydrological Processes 19: 1705-1714.

DHI-WASY, 2012. Feflow 6.1: Finite Element Subsurface Flow and Transport Simulation System User Manual. DHI-WASY GmbH Berlin, Germany. Available at [Online] http://www.feflow.com/uploads/media/users_manual.pdf (Accessed April 8, 2013).

Dingman, S. L. 2002. Physical Hydrology, Second Edition. Prentice Hall, Upper Saddle River, NJ.

Dixon, N. and E. Brook. 2007. Impact of predicted climate change on landslide reactivation: case study of Mam Tor, UK. Landslides 4: 137 – 147.

Doran, I. G. 1992. The subsoils of Northern Ireland. The Structural Engineer 70 (7): 135 – 138.

Elrick, D.E. and W.D. Reynolds. 1986. An analysis of the percolation test based on three-dimensional, saturated-unsaturated flow from a cylindrical test hole. Soil Science 142: 308-321.

Elrick, D.E., W.D. Reynolds and K.A. Tan. 1989. Hydraulic conductivity measurements in the unsaturated zone using improved well analyses. Groundwater Monitoring and Remediation 9 (3): 184-193.

Eyles, N. and J. A. Sladen. 1981. Stratigraphy and geotechnical properties of weathered lodgement till in Northumberland, England. Quarterly Journal of Engineering Geology London 14: 129-142.

Fetter, C. W. 2001. Applied Hydrogeology (4th ed), Prentice-Hall, Inc. Upper Saddle River, New Jersey.

Fitzsimmons, V. P. And B. D. R. Misstear. 2006. Estimating groundwater recharge through tills: a sensitivity analysis of soil moisture budgets and till properties in Ireland. Hydrogeology Journal 14: 548 – 561.

Freeze, R. A. 1971. Three-dimensional, transient, saturated-unsaturated flow in a groundwater basin. Water Resource Research 7 (2): 347-366.

Freeze, R. A. and P. A. Witherspoon. 1967. Theoretical analysis of regional groundwater flow. 2. Effect of water-table configuration and sub-surface permeability variation. Water Resources Research 3 (2): 623-634.

Frind, E. O. and M. J. Verge. 1978. Three-dimensional modeling of groundwater flow systems. Water Resource Research 14 (5): 844-856.

Ganjian, N., Y. P. Pisheh and S. M. M. M. Hosseini. 2007. Prediction of soil-water characteristic curve based on soil index properties. In Schanz, T. (ed) Experimental Unsaturated Soil Mechanics. Springer Proceedings in Physics, Vol. 112. Springer Berlin Heidelberg: pp 355-367.

Gleeson, T. and A.H. Manning. 2008. Regional groundwater flow in mountainous terrain: three-dimensional simulations of topographic and hydrogeologic controls. Water Resources Research 44 (10): W10403, doi: 10.1029/2008WR006848.

Gleeson, T., L. Marklund, L. Smith and A.H. Manning. 2011. Classifying water table at regional to continental scales. Geophysical Research Letters 38 (5): L05401, doi: 10.1029/2010GL046427.

Google Maps, 2011. Northern Ireland map. [Online] Available at http://maps.google.ca/maps?client=firefox-a&rls=org.mozilla:en-US:official&channel=s&hl=en&source=hp&q=northern%20ireland&um=1&ie= UTF-8&sa=N&tab=wl (obtained January 2013).

Graham, D. J. and N. G. Midgley. 2000. Graphical respresenation of particle shape using triangular diagrams: an Excel spreadsheet method. Earth Surface Processes and Landforms 25: 1473-1477.

Griffiths, D. V. and R. M. Marquez. 2007. Three-dimensional slope stability analysis by elasto-plastic finite elements. Géotechnique 57 (6): 537-546.

Grisak, G. E. and J. A. Cherry. 1975. Hydrologic characteristics and response of fractured till and clay confining a shallow aquifer. Canadian Geotechnical Journal 12: 23-43.

Haitjema, H.M. and S. Mitchell-Bruker. 2005. Are water tables a subdued replica of the topography? Ground Water 43 (6): 781-786.

Hambrey, M. J. 1994. Glacial Environment. University of College Press, London.

Hubbert, M. K. 1940. The theory of groundwater motion. Journal of Geology 48 (8): 785-944.

Hughes, D., V. Sivakumar, D. Glynn and G. Clarke. 2007. A case study: delayed failure of a deep cutting in lodgement till. Geotechnical Engineering. 160 (GE4): 193-202.

Hughes, D., M. McLernon and L. Carse. 1998. Cutting Stability, Craigmore (initial findings). Internal report. Queen's University Belfast, Belfast, Northern Ireland.

Huyakorn, P. S., E. P. Springer, V. Guvansen and T. D. Wadsworth. 1986. A three- dimensional finite-element model for simulating water flow in variably saturated porous media. Water Resources Research 22 (13): 1790-1808.

Hvorslev, M. J. 1951. Time lag and soil permeability in groundwater observations. Bulletin Number 36, Waterways Experiment Station, Corps. Of Engineers, U. S. Army.

Irfran, T. Y. and W. R. Dearman. 1978. Engineering classification and index properties of a weathered granite. Bulletin of the International Association of Engineering Geology 17 (1): 79-90.

ISEE Systems. 2011. STELLA: Systems thinking for education and research. Available at [Online] http://www.iseesystems.com/softwares/Education/StellaSoftware.aspx (Last obtained April 14, 2013).

Lam, L. and D. G. Fredlund. 1993. A general limit equilibrium model for three- dimensional slope stability analysis. Can. Geotech. Journal 30: 905-919.

Land and Property Services (Northern Ireland). 2012. LPS OSNI 10m Digital Terrain Model DTM. Available at [Online] http://data.gov.uk/dataset/lps-osni-10m- digital-terrain-model-dtm-download (Last obtained April 14, 2013).

Leach, B. and R. Herbert. 1982. The genesis of a numerical model for the study of the hydrogeology of a steep hillside in Hong Kong. Quarterly Journal of Engineering Geology and Hydrogeology 15: 243-259.

McCabe, A. M., J. Knight and S. G. McCarron. 1999. Ice-flow stages and glacial bedforms in north central Ireland: a record of rapid environmental change during the last glacial termination. Journal of the Geological Society of London 156: 63-72.

McConnville, C., R.M. Kalin, H. Johnston and G.W. McNeill. 2001. Evaluation of recharge in a small temperate catchment using natural and applied $\delta^{18}O$ profiles in the unsaturated zone. Ground Water 39 (4): 616-623.

McLernon, M. 2014. Climate driven pore water pressure fluctuations and slope stability within glacial till drumlins in Northern Ireland. PhD dissertation. Queen's University Belfast, Belfast, Northern Ireland.

Met Office. 2011. Regional mapped climate averages. Available at [Online] http://www.metoffice.gov.uk/climate/uk/averages/regmapavge.html#nireland (last obtained April 14, 2013).

Milligan, V. 1976. Geotechnical aspects of glacial till. In Legget, R. F. (ed) Glacial till: an inter-disciplinary study. Royal Society of Canada, Special publications no. 12, Ottawa. Pp 269-291.

Mizell, S.A., A. L. Gutjahr and L. W. Gelhar. 1982. Stochastic analysis of spatial variability in two-dimensional steady groundwater flow assuming stationary and nonstationary heads. Water Resources Research 18 (4): 1053-1067.

Ng, C. W. W. And Q. Shi. 1998. Influence of rain intensity and duration on slope stability in unsaturated soils. Quarterly Journal of Engineering Geology and Hydrogeology. 31: 105-113.

Papadopulas, I.S., J.D. Bredehoeft and H.H. Cooper. 1973. On the analysis of slug test data. Water Resources Research 9: 1087-1089.

Papadopulas, I.S. and H.H. Cooper. 1967. Drawdown in a well of large diameter. Water Resources Research 3: 241-244.

Picarelli, L., G. Uriuoli and C. Russo. 2004. Effect of groundwater regime on the behavior of clayey slopes. Canadian Geotechnical Journal 41: 467-484.

Potts, D. M., N. Kovacevic and P. R. Vaughan. 1997. Delayed collapse of cut slopes in stiff clay. Géotechnique 47 (5): 953-982.

Premchitt, J., E. W. Brand and H. B. Phillipson. 1986. Landslides caused by rapid groundwater changes. In Cripps, J. C., F. G. Bell and M. G. Culshaw (eds). Groundwater in Engineering Geology, Geological Society Engineering Geology Special Publication No. 3, pp. 87 – 94.

Pullammanappallil, S. K. and J. N. Louie. 1994. A generalized simulated-annealing optimization for inversion of first arrival times. Bulletin of the Seismological Society of America 84: 1397-1409.

Reisenauer, A. E., K. T. Key, T. N. Narasimhan and R. W. Nelson. 1982. TRUST: a computer program for variably saturated flow in multidimensional, deformable media. Rep. NUREG/CR-2360, U. S. Nuclear Reg. Comm., Washington, D.C.

Robins, N.S. and B.D.R. Misstear. 2000. Groundwater in the Celtic regions. *In* Robins, N.S. and B.D.R. Misstear (eds). *Groundwater in the Celtic Regions: Studies in Hard Rock and Quaternary Hydrogeology*. The Geological Society of London, London, Special Publications 182: 5-17.

Scotland and Northern Ireland Forum for Environmental Research. 2002. Implications of climate change for Northern Ireland: informing strategy development. SNIFFER, Napier Edinburgh.

Segol, G. 1977. A three-dimensional Galerkin-finite element model for the analysis of contaminant transport in saturated-unsaturated porous media. In W. G. Gray, G.F. Pinder and C. A. Brebbia (eds). Finite Elements in Water Resources. Pentech, London. Pp 2.123-2.144.

Sentek Pty Ltd. 2001. Calibration of Sentek Pty Ltd Soil Moisture Sensors. Sentek Pty Ltd, Stepney, South Australia.

Smethurst, J. A., D. Clarke and W. Powrie. 2006. Seasonal changes in pore water pressure in a grass-covered cut slope in London Clay. Géotechnique 56 (8): 523 – 537.

Soil Moisture Equipment Corporation. 2010. Model 2800K1 Guelph Permeameter Operating Instructions. Soil Moisture Equipment Corp, Santa Barbara, CA.

Toth, J. 1963. A theoretical analysis of groundwater flow in small drainage basins. Journal of Geophysical Research 68 (16): 4795-4812.

Van der Kamp, G. 2001. Methods for determining the in situ hydraulic conductivity of shallow aquitards – an overview. Hydrogeology Journal 9: 5-16.

Winter, T. C. 2001. The concept of hydrologic landscapes. Journal of the American Water Resources Association 37 (2): 335-349.

Xie, M., T. Esaki, C. Qui and C. Wang. 2006. Geographical information system-based computational implementation and application of spatial three-dimensional slope stability analysis. Computers and Geotechnics 33: 260-274.

Younger, P. L. 1993. Simple generalized methods for estimating aquifer storage parameters. Quarterly Journal of Engineering Geology 26: 127-135.

Appendix A

Tomography Results of the Seismic Refraction Surveys

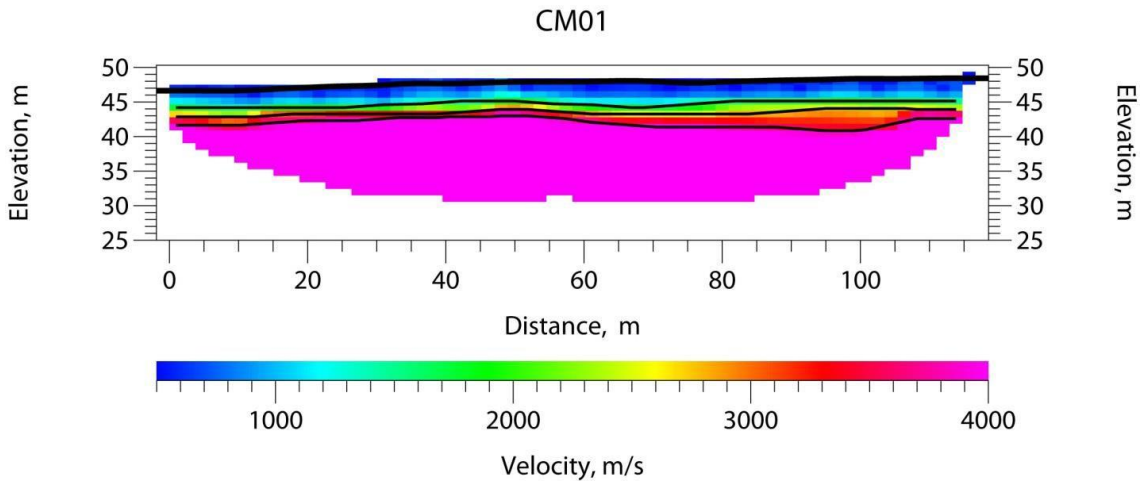

Figure A.1 Tomography results for transcect CM01 at the Craigmore study site.

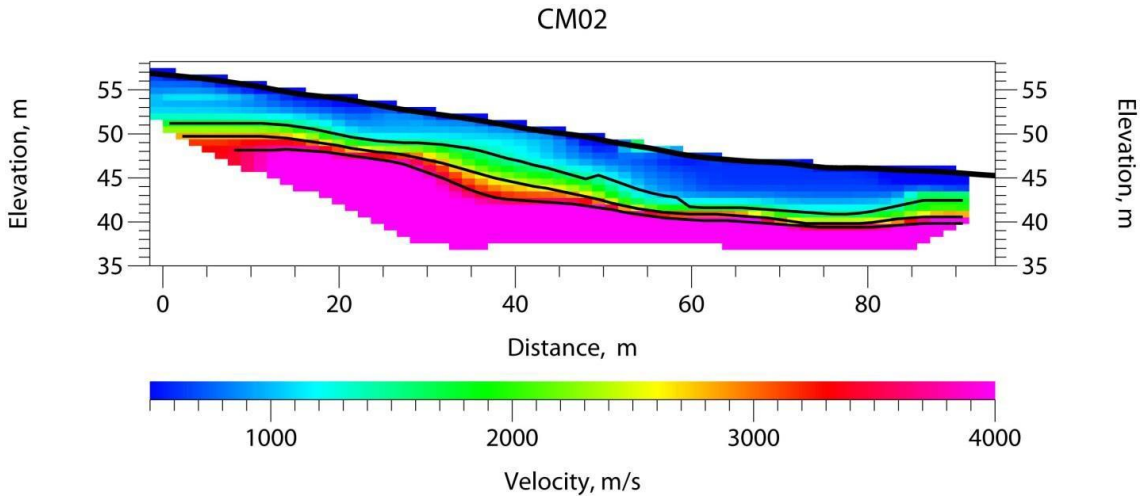

Figure A.2 Tomography results for transcect CM02 at the Craigmore study site.

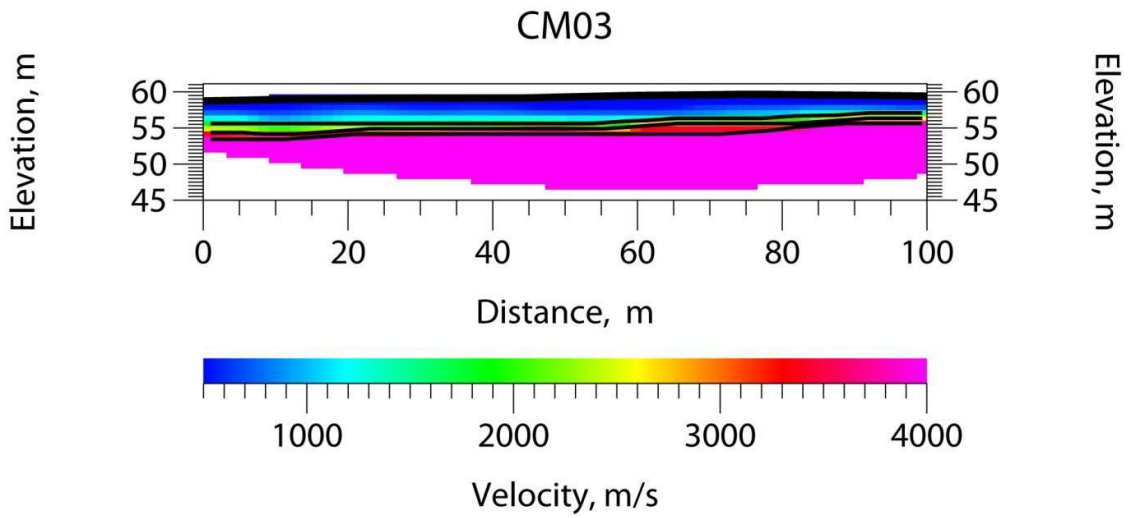

Figure A.3 Tomography results for transcect CM03 at the Craigmore study site.

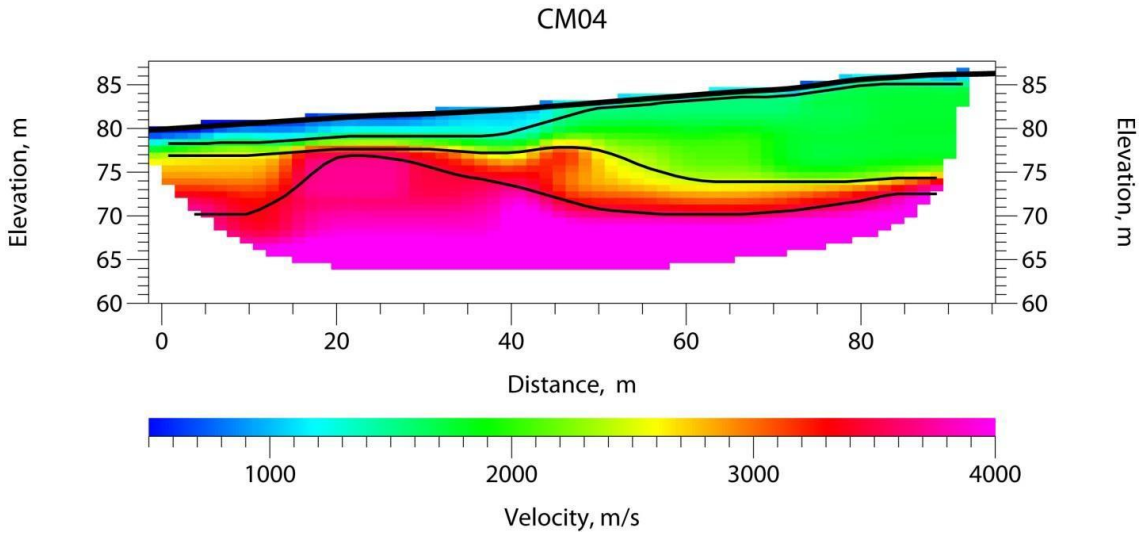

Figure A.4 Tomography results for transcect CM04 at the Craigmore study site.

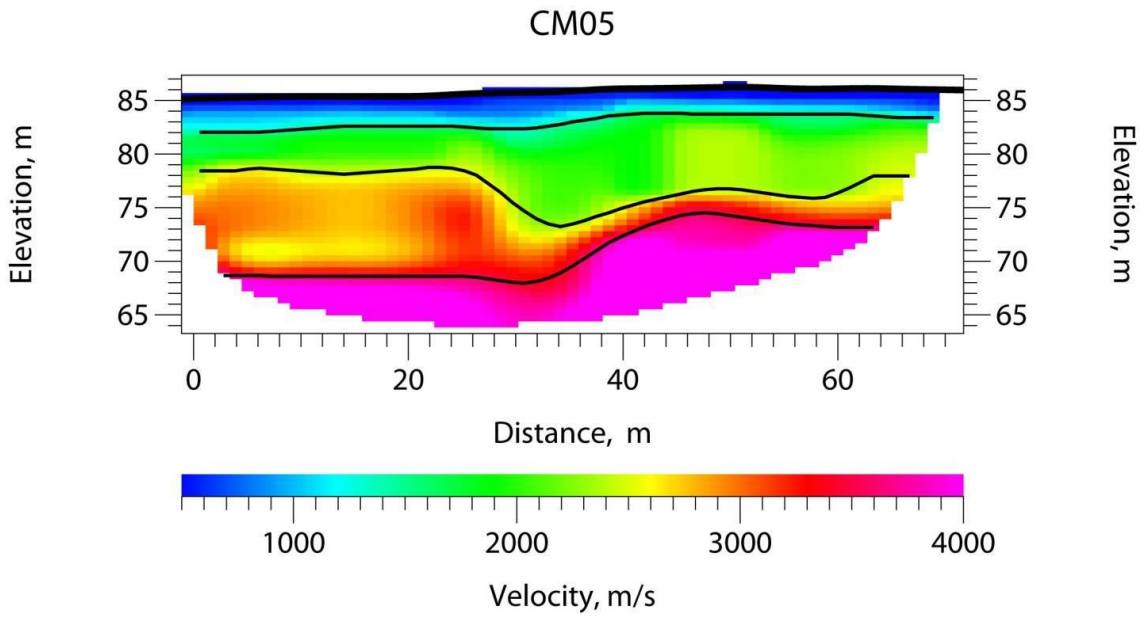

Figure A.5 Tomography results for transcect CM05 at the Craigmore study site.

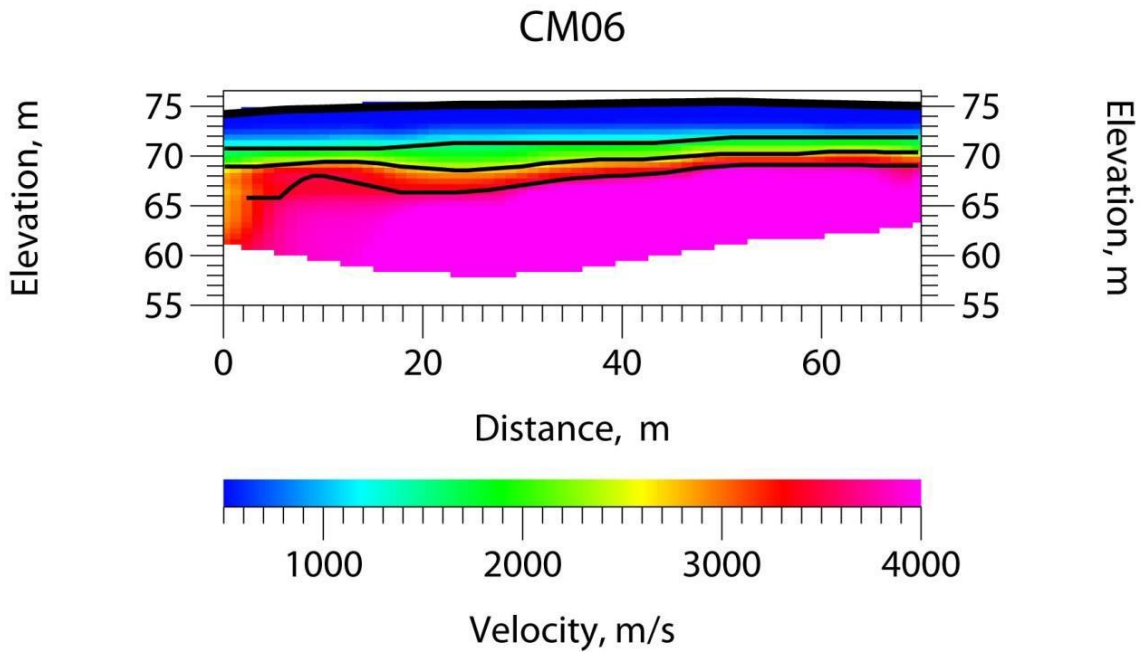

Figure A.6 Tomography results for transcect CM06 at the Craigmore study site.

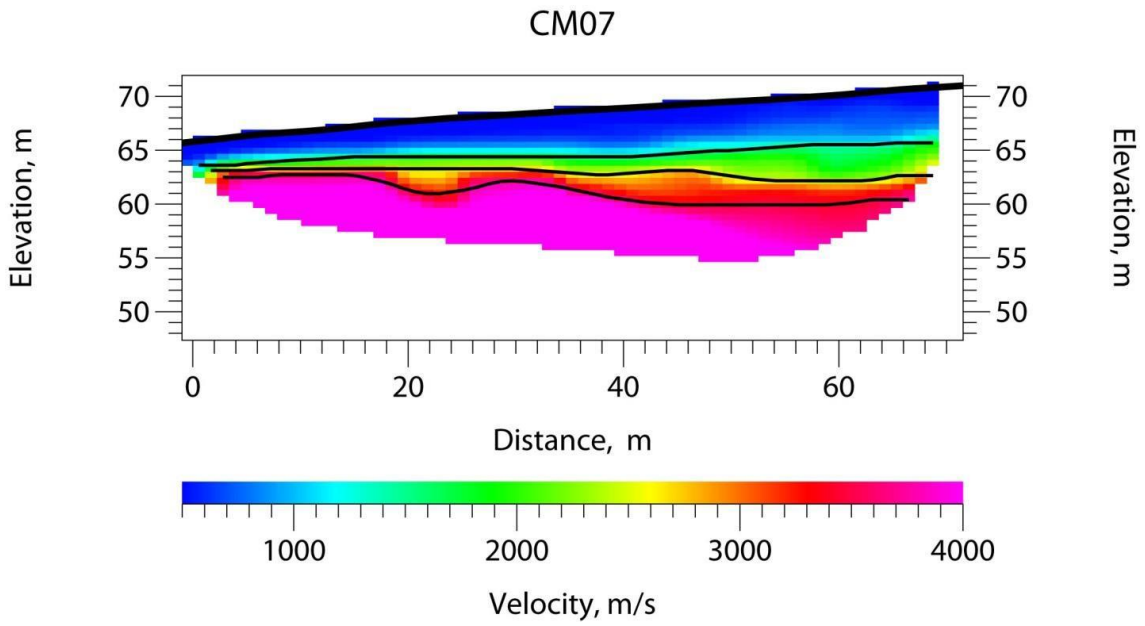

Figure A.7 Tomography results for transcect CM07 at the Craigmore study site.

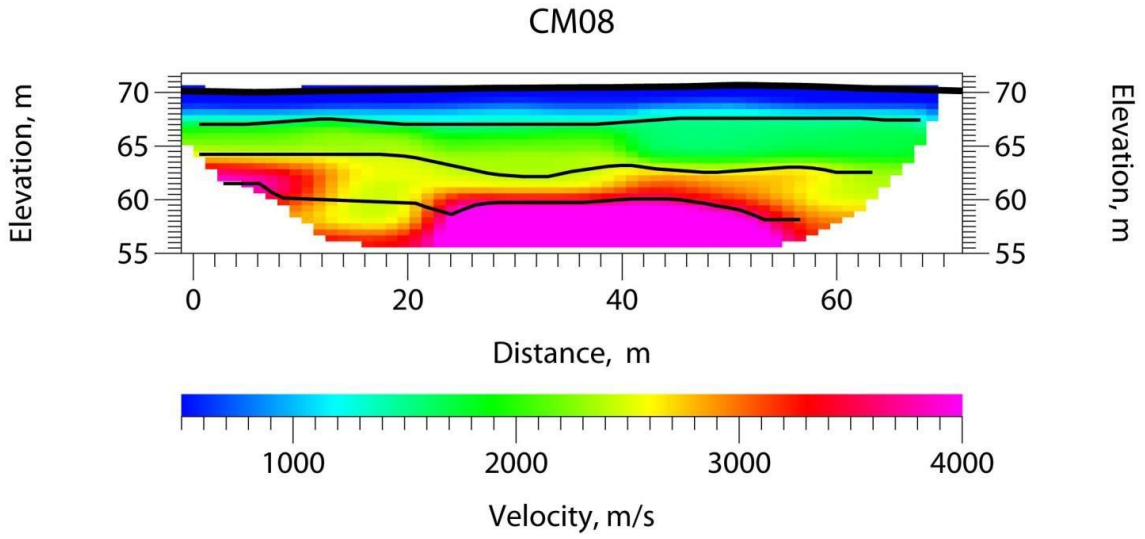

Figure A.8 Tomography results for transect CM08 at the Craigmore study site.

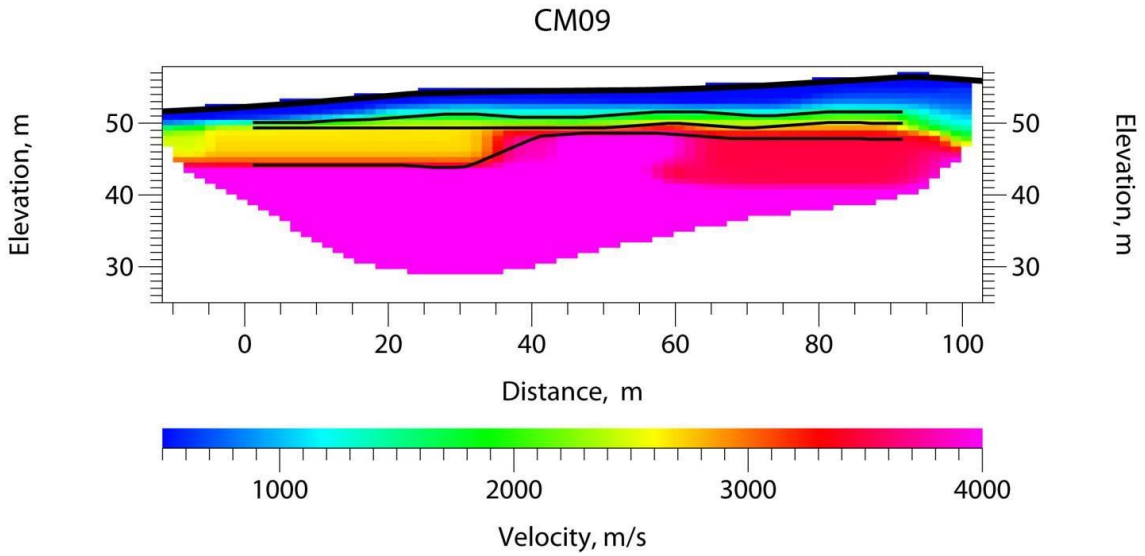

Figure A.9 Tomography results for transect CM09 at the Craigmore study site.

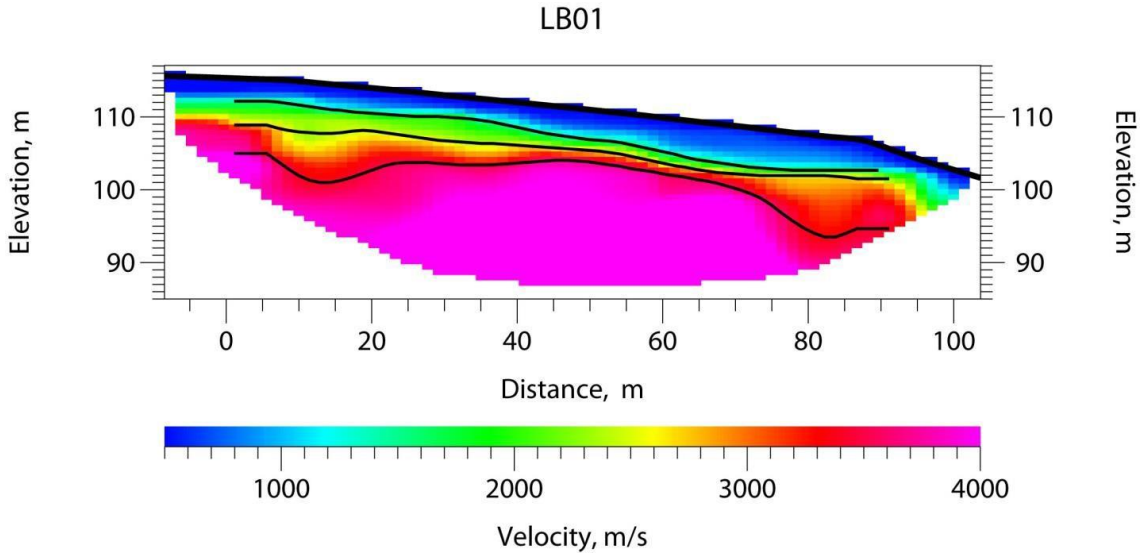

Figure A.10 Tomography results for transect LB01 at the Loughbrickland study site.

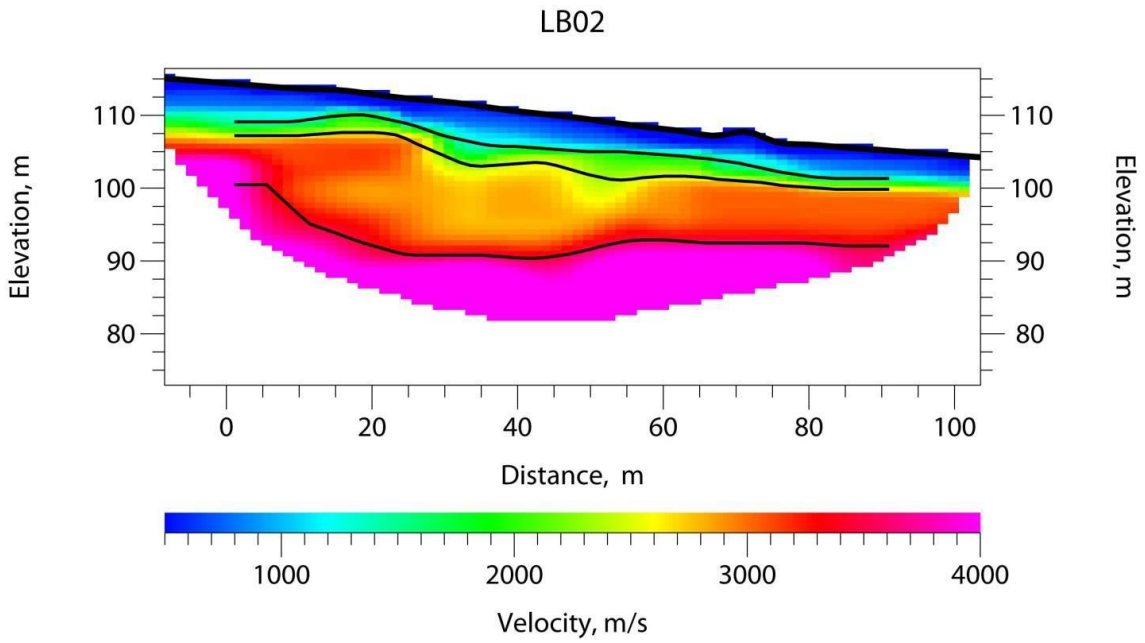

Figure A.11 Tomography results for transcect LB02 at the Loughbrickland study site.

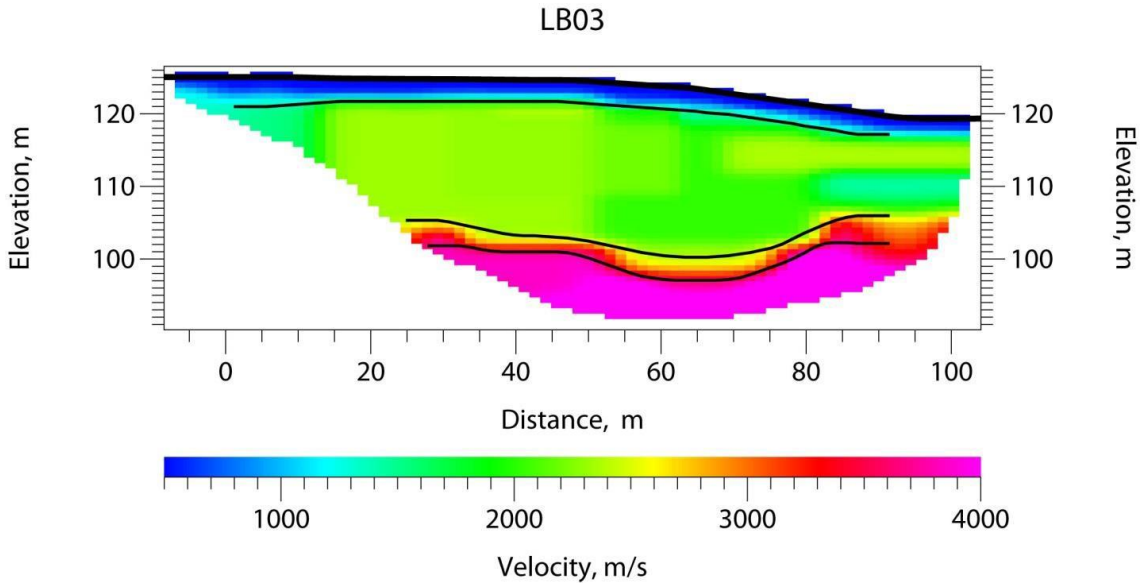

Figure A.12 Tomography results for transect LB03at the Loughbrickland study site.

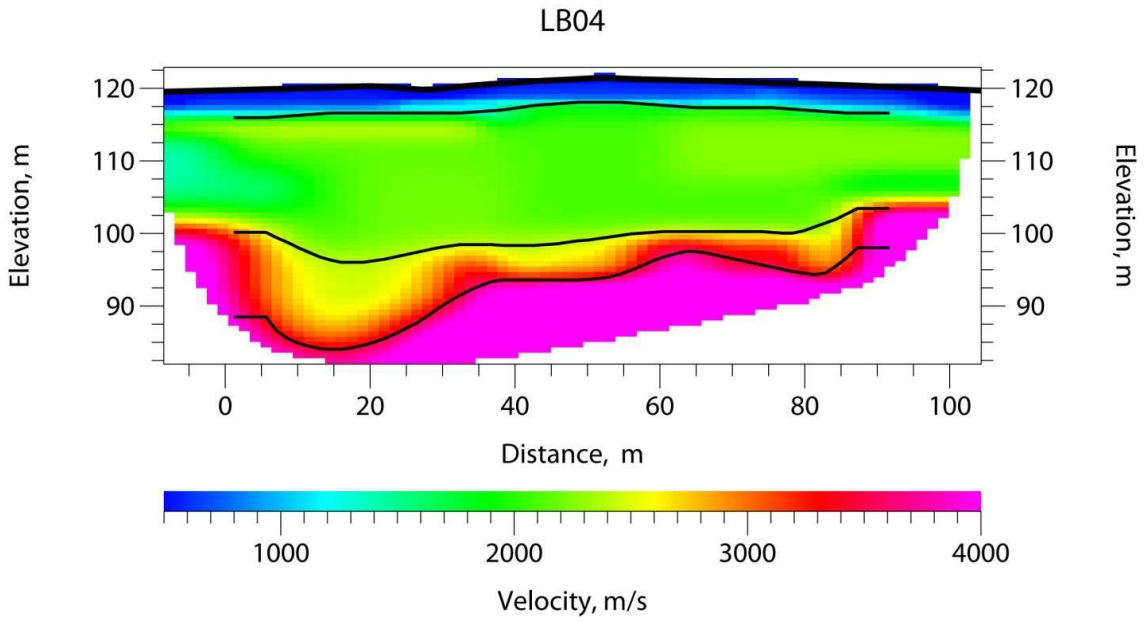

Figure A.13 Tomography results for transect LB04 at the Loughbrickland study site.

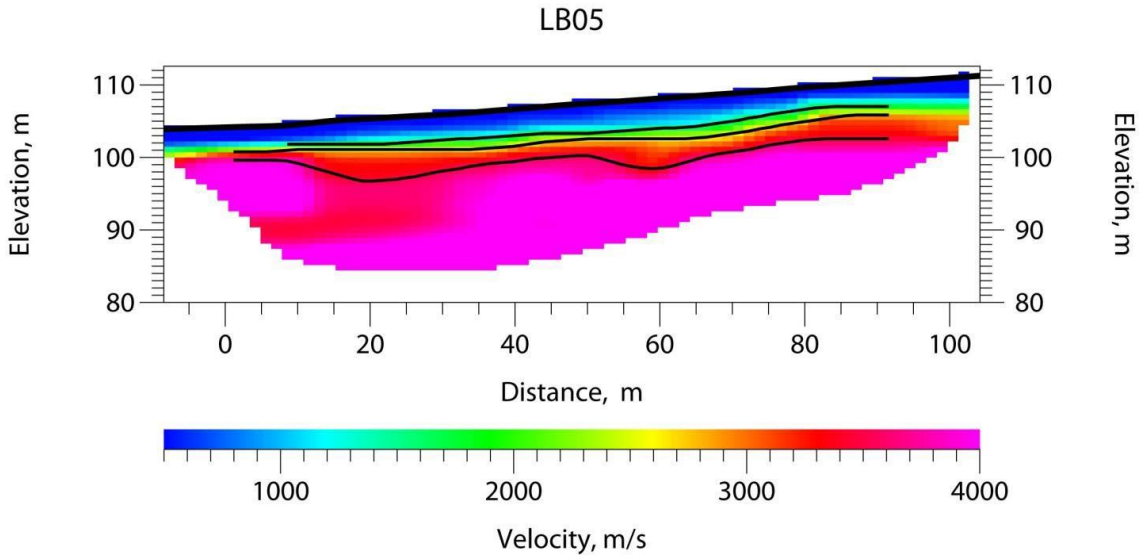

Figure A.14 Tomography results for transect LB05 at the Loughbrickland study site.

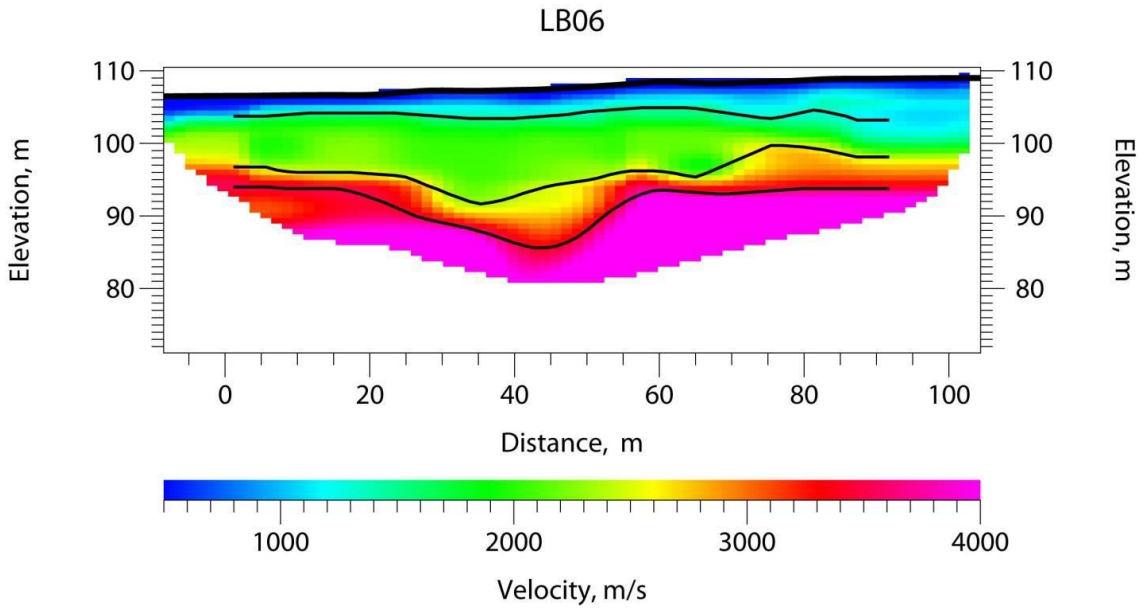

Figure A.15 Tomography results for transcect LB06 at the Loughbrickland study site.

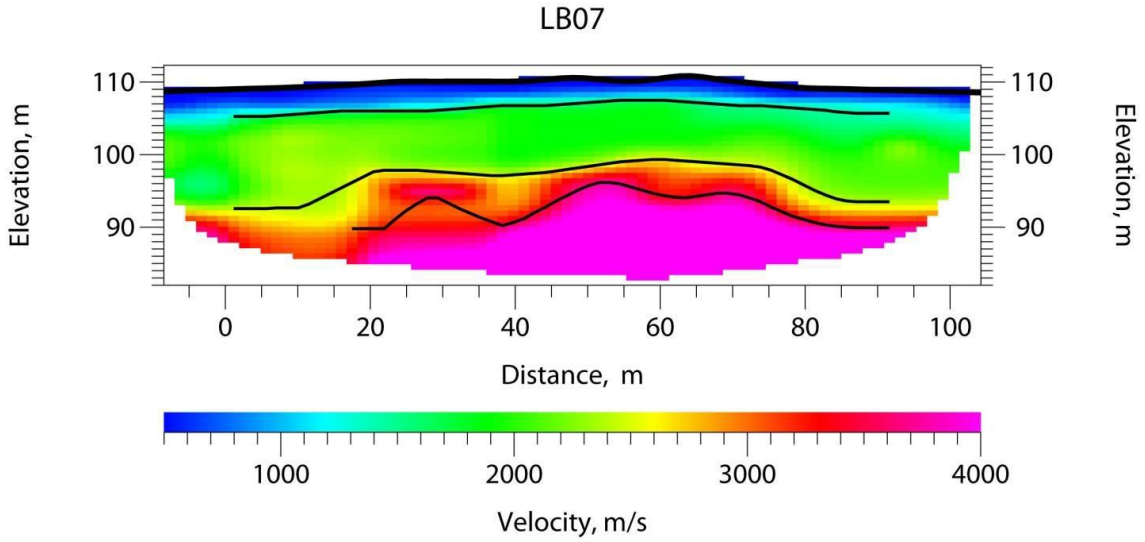

Figure A.16 Tomography results for transcect LB07 at the Loughbrickland study site.

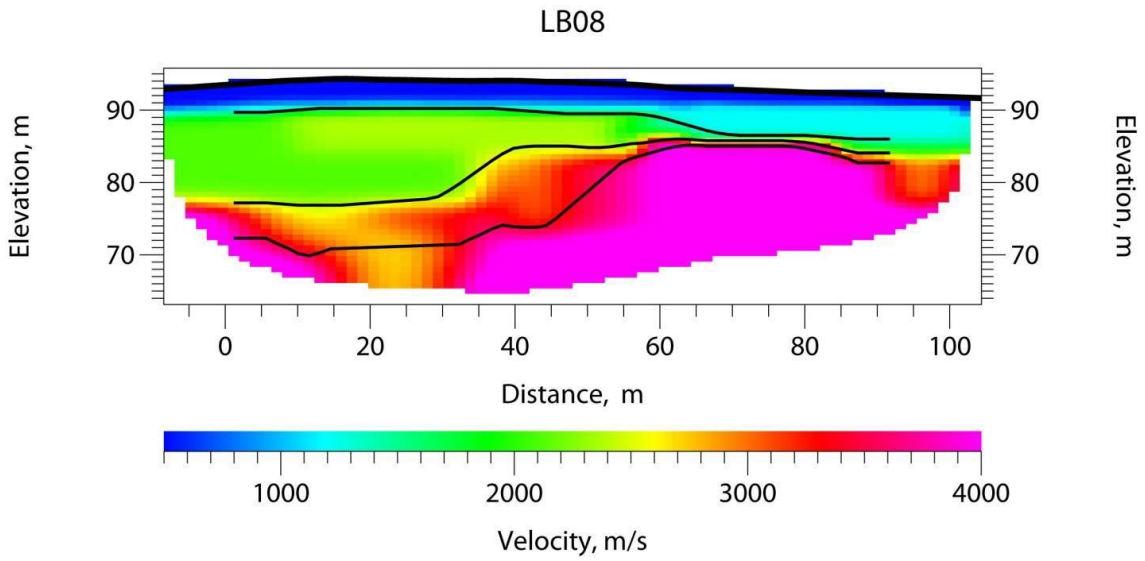

Figure A.17 Tomography results for transect LB08 at the Loughbrickland study site.

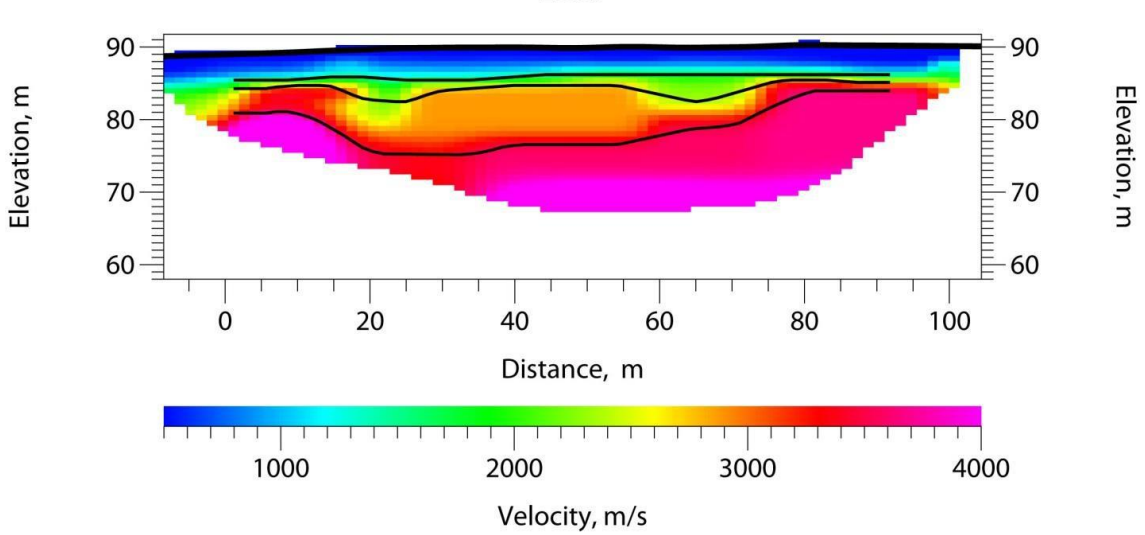

Figure A.18 Tomography results for transect LB09 at the Loughbrickland study site.

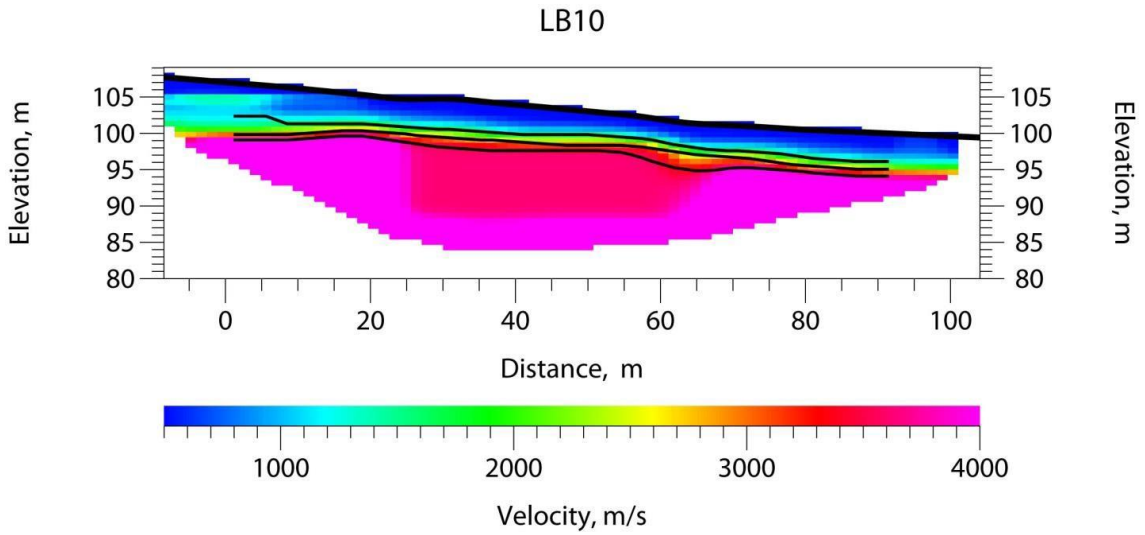

Figure A.19 Tomography results for transect LB10 at the Loughbrickland study site.

Appendix B

EnviroScan Calibration Results

Table B.1 Estimated constants for the calibration curves of the ES01 sensors at Craigmore using the laboratory calibration technique.

Sensor	Depth	Constant		
	(m)	A	B	C
1-1	0.10	0.0095	1	0.4094
1-2	0.30	0.0095	1	0.4205
1-3	0.50	0.0153	1	0.3379
1-4	0.70	0.0140	1	0.3593
1-5	0.90	0.0139	1	0.3523

Table B.2 Estimated constants for the calibration curves of the ES02 sensors at Craigmore using the laboratory calibration technique.

Sensor	Depth	Constant		
	(m)	A	B	C
2-1	0.10	0.0162	1	0.3487
2-2	0.30	0.0160	1	0.3493
2-3	0.50	0.0162	1	0.3487
2-4	0.70	0.0165	1	0.3619
2-5	0.90	0.0162	1	0.3600

Table B.3 Estimated constants for the calibration curves of the Loughbrickland ES01 sensors using the laboratory calibration technique.

Sensor	Depth	Constant		
	(m)	A	B	C
1-6	0.10	0.0090	1	0.4468
1-7	0.30	0.0091	1	0.4364
1-8	0.50	0.0115	1	0.4259
1-9	0.70	0.0116	1	0.4196
1-10	0.80	0.0111	1	0.4396

Table B.4 Estimated constants for the calibration curves of the Loughbrickland ES02 sensors using the laboratory calibration technique.

Sensor	Depth	Constant		
	(m)	A	B	C
2-6	0.10	0.0187	1	0.3230
2-7	0.20	0.0192	1	0.3252
2-8	0.30	0.0090	1	0.3593
2-9	0.50	0.0094	1	0.3796
2-10	0.70	0.0095	1	0.3801